THEILER'S MURINE ENCEPHALOMYELITIS PROTEIN 2C AND ITS EFFECT ON MEMBRANE TRAFFICKING

Elien Moës

A Thesis Submitted for the Degree of PhD
at the
University of St. Andrews

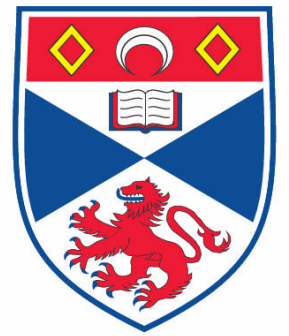

2008

Theiler's murine encephalomyelitis protein 2C and its effect on membrane trafficking

By

Elien Moës B.Sc. (Hons)

Centre for Biomolecular Sciences

University of St. Andrews

A thesis submitted in partial fulfillment
of the requirements for the degree of
Doctor of Philosophy

January, 2008

Declarations

I, Elien Moës, hereby certify that this thesis, which is approximately 56 000 words in length, has been written by me, that it is the record of work carried out by me and that it has not been submitted in any previous application for a higher degree.

Signature:_____ Date:_____

I was admitted as a research student in October 2004 and as a candidate for the degree of Doctor of Philosophy in October 2004; the higher study for which this is a record was carried out in the University of St Andrews between 2004 and 2008.

Signature:_____ Date:_____

I hereby certify that the candidate has fulfilled the conditions of the Resolution and Regulations appropriate for the degree of Doctor of Philosophy in the University of St Andrews and that the candidate is qualified to submit this thesis in application for that degree.

Signature:_____ Date:_____

In submitting this thesis to the University of St Andrews I understand that I am giving permission for it to be made available for use in accordance with the regulations of the University Library for the time being in force, subject to any copyright vested in the work not being affected thereby. I also understand that the title and abstract will be published, and that a copy of the work may be made and supplied to any *bona fide* library or research worker, that my thesis will be electronically accessible for personal or research use, and that the library has the right to migrate my thesis into new electronic forms as required to ensure continued access to the thesis. I have obtained any third-party copyright permissions that may be required in order to allow such access and migration.

Signature:_____ Date:_____

Acknowledgements

"If I have seen farther than other men, it is because I stood on the shoulders of giants."
Sir Isaac Newton

Firstly, I am most grateful to my supervisor, Dr. Martin Ryan, for his guidance, advice and encouragement. Thank you for the many helpful discussions, for sharing your knowledge, and for your consistent support.

I would like to thank my colleagues, who provided me with guidance and useful suggestions and made my time in the lab very enjoyable.

Many thanks to the Biotechnology and Biological Sciences Research Council for funding my work.

I would like to deeply thank my family for their belief and encouragement.
I would like to thank my friends at home for their understanding and for bearing my little availability.
I would also like to thank my friends in St Andrews for making this time, although away from home, very pleasurable. I will miss you!

Last but most importantly, a special thanks to my parents, Paul and Brigitte Moës, whose love, care and consideration made all this possible. Papa en mama, jullie hebben mij steeds gesteund in alles wat ik deed. Ik wil jullie graag danken omdat jullie er steeds voor me zijn. Ik zie jullie graag!

Abstract

Picornaviruses replicate in association with cytoplasmic membranes of infected cells. Poliovirus 2C and 2BC play an important role in the formation of membranous vesicles, and induce dramatic changes in membrane trafficking. Theiler's murine encephalomyelitis virus protein 2C was localized in infected cells using an anti-TMEV-2C antibody. Early upon infection, TMEV 2C was localized in the cytoplasm in an ER-like pattern. At later stages, 2C redistributed to a juxtanuclear site, which represents the viral replication site. Co-localization with the Golgi complex could not be observed. TMEV 2C seems to interact *in vitro* with reticulon 3, a highly conserved ER-associated protein. It was not possible to confirm a previously identified interaction with AKAP10, a protein kinase anchoring protein, presumably reflecting conformational constraints of the interaction. Two mutations in the AKAP10 binding site of TMEV 2C were identified, which inhibit the completion of the infectious cycle of TMEV. The intracellular changes that occur during TMEV infection were observed. Both actin filaments and microtubules may be used at early stages of infection; however both cytoskeleton components accumulate at the periphery of the cell during late stages of infection. A computer-based analysis has demonstrated that TMEV 2C is highly similar to katanin, a microtubule-severing protein, and may play a similar role in the reorganization of microtubules during infection. The Golgi complex turns from a solid, crescent-shaped organelle, into a series of punctuate fluorescent points forming an expanding balloon-like structure surrounding the concomitantly expanding site of virus replication. The remnants of the Golgi complex are finally dispersed throughout the cytoplasm. Live imaging confirmed these findings. It was observed that PKA also undergoes displacement to the cell periphery during infection. However, BIG1 seems to locate to the viral replication site during infection, suggesting it may play a role during viral replication. The localization of PKA and BIG1 in the infected cell may in part explain the observed dispersion of the Golgi complex.

Contents

Figures

Tables

1. Introduction

1.1. Viruses: a general overview

A virus (from the Latin *virus*, meaning toxin or poison) is a sub-microscopic particle that is able to infect cells of a living organism. Viruses have a predatory nature, in that to replicate, they must first infect a cell. A virus particle consists of genetic material contained within a protective protein coat (capsid). Viruses infect a wide variety of organisms; both eu- and prokaryotes, as well as archaea. Many severe human diseases, such as AIDS, influenza and rabies, are caused by viruses. The aim of this introduction is to present a general overview of the characteristics of viruses with the focus on the *Picornaviridae* and the replication of the *Cardiovirus* Theiler's virus.

1.1.1 Discovery of viruses

For many centuries, humans have been affected by viral diseases. There is hieroglyphical evidence of polio in the ancient Egyptian empire. In the late 18th century, Edward Jenner observed and studied Miss Sarah Nelmes, a milkmaid who had previously caught cowpox and was subsequently found to be immune to smallpox.

Adolf Mayer (1843-1942), a German scientist, is considered as a pioneer in the field of modern virology. In 1879, he began his research on diseases of tobacco and named the disease "tobacco mosaic disease" after the pattern of dark and light spots seen on infected leaves. In 1882 he described the first experimental transmission of a viral disease of plants. He inoculated healthy tobacco plants with filtered juice from infected tobacco plants. The plants soon showed the mosaic symptoms characteristic of the disease (reviewed by Levine, 1996). The next step towards the discovery of viruses was taken by a young Russian scientist, Dimitri Ivanovsky (1864-1920), who, in 1892, described a pathogenic agent smaller than any known before. He presented a paper before the Academy of Sciences in St. Petersburg stating that "the sap of leaves infected with tobacco mosaic disease retains its infectious properties even after filtration through Chamberland filter candles" (Ivanovsky, 1892). Similar findings were published in 1898 by Martinus Beijerinck (1851-1931), a

Dutch microbiologist. Unaware of Ivanovsky's work, he demonstrated that the infectious agent causing tobacco mosaic disease was indeed filterable and determined that the agent could reproduce itself within living plants. He observed that the pathogen causing tobacco mosaic virus returned to its original strength after dilution, suggesting that the pathogen is not a chemical substance but an agent that replicates within living cells. The concept of a filterable agent, too small to observe in the light microscope but able to cause disease by reproducing in living cells, was born. Loeffler and Frosh (1898) rapidly described and isolated the first filterable agent from animals, the foot-and-mouth disease virus, and yellow fever virus was the first human virus to be recognized in 1901 by Reed and colleagues (reviewed by: Lustig & Levine, 1992; Levine, 1996).

Since the 19th century virologists have made great progress in unraveling the properties of viruses. Some definite characteristics have been elucidated. Viruses are very small, infectious, obligate intracellular molecular parasites. The viral genome can consist of RNA or DNA. After infection of an appropriate host cell, the viral genome is replicated and the virion components are synthesized. The newly synthesized components are assembled into progeny virions, which are responsible for the transmission of the viral genome to other cells or organisms.

1.1.2 Classification of viruses

The earliest experiments involving viruses were designed to measure a single physiochemical characteristic, that being the small size of viruses as assessed by "filterability". Most studies of viruses were related to their ability to cause infections and diseases. Therefore, the earliest attempts to classify viruses were based on perceived common pathogenic properties, host range, and transmission. When more evidence of the structure and composition of virions became known, a classification based on shared virion properties was suggested. A single universal taxonomic scheme was needed. Therefore, the International Committee on Nomenclature of Viruses (ICNV) was established in 1966, now called the International Committee of Taxonomy of viruses (ICTV). Virion characteristics are considered as criteria to group viruses into orders, families, in some cases subfamilies, and genera (Strauss & Strauss, 1988, Murphy, 1996). The 8th report of the ICTV, published

in 2005, records a taxonomy scheme comprising 3 orders, 73 families, 9 subfamilies, 287 genera, 1938 species and more than 6000 member viruses (Fauquet *et al.*, 2005). However, GenBank contains a staggering additional 3,142 "species" unaccounted for by the ICTV report (Fauquet & Fargette, 2005).

1.1.3 Structure of viruses

A virus particle is a structure that has evolved to transfer nucleic acid from one cell to another. A virion in its most basic form consists of nucleic acid surrounded by a protective coat of many identical proteins encoded by the viral genome, known as the capsid (Crick & Watson, 1956). More complex virus particles include virions that contain several molecules of nucleic acid, express several or many different proteins, and have internal bodies of definite shape and complex envelopes with spikes that usually contain glycoproteins and lipids.

Helical capsids are composed of a single type of subunit stacked around a central axis to form a helical structure which may have a central cavity containing the viral nucleic acid. This arrangement results in filamentous virions. Icosahedral capsid symmetry results in a spherical appearance, but actually consists of capsomers arranged in a regular geometrical pattern. Capsomers are structures constructed from several copies of protomers, which are associated via non-covalent binding to enclose the viral nucleic acid. There is an important distinction between enveloped viruses and non-enveloped viruses. The distinction corresponds to a difference in the way the virus enters and leaves a cell. Enveloped viruses are, in addition to the protein capsid, surrounded with a lipid bilayer membrane. The membrane is studded with proteins, including glycoproteins that can function as receptor molecules, resulting in the uptake of the virion into the cell. Most enveloped viruses depend upon their envelope for infectivity (reviewed by Harrison *et al.*, 1996).

1.1.4 Viral genetic systems

Viruses are mainly concerned with the duplication of their genome and the expression of the information encoded by the genome. All viruses must perform messenger RNA (mRNA) synthesis which will be translated by using cellular ribosomes and soluble factors. The

specific mechanism for mRNA synthesis depends on the structure of the viral genome. The Baltimore Classification describes six basic genetic strategies (figure 1.1, Baltimore, 1971).

Class I consists of viruses which have double-stranded (ds) DNA. They carry out an asymmetric transcription of their DNA to give rise to mRNA. Viruses grouped in Class II contain a single-stranded (ss) DNA genome of the same polarity as mRNA. Class III consists of viruses containing a ds RNA genome. The mRNA for these viruses represents an asymmetric transcript of the genome. The known viruses of this type have multiple segments of ds RNA, each of which express a single protein. Class IV includes ssRNA viruses whose mRNA is identical to the viral RNA. Class V consists of viruses with a ssRNA genome which is complimentary to the mRNA. Class VI contains viruses with a ssRNA genome which have a DNA intermediate in their replication.

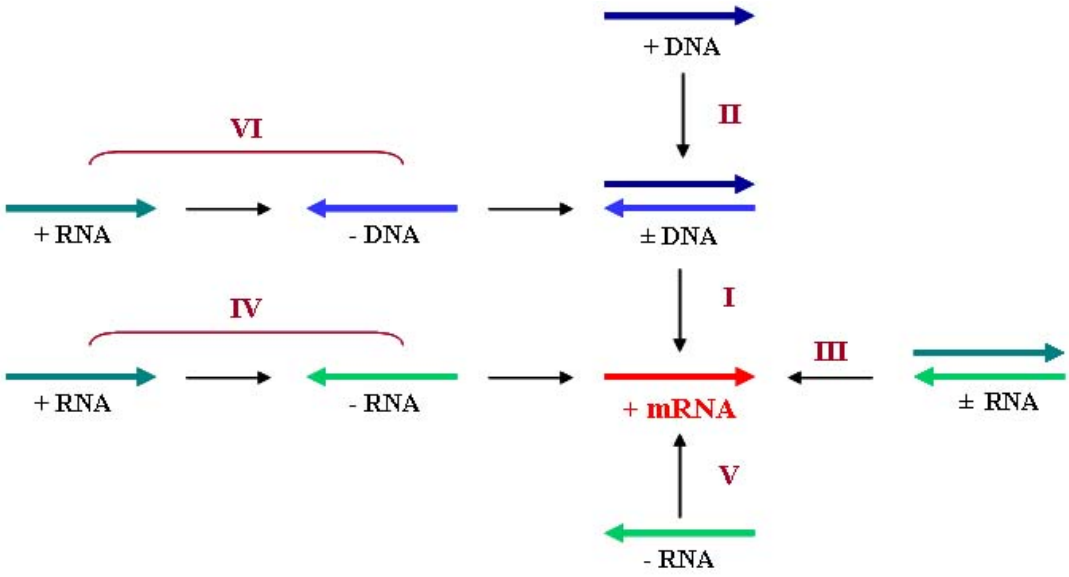

Figure 1.1: The Baltimore classification of viruses, *a classification system which clusters viruses based on their genetic contents and their replication strategies. The central theme in this classification system is that all viruses must generate positive strand mRNA, in order to produce viral proteins and replicate.*

1.1.5 Replication of viruses

The pathological effects of viral diseases result from the toxic effects of viral proteins on the host cell metabolism, the reactions of the host to infected cells expressing viral proteins, and the modifications of host gene expression by interactions with the viral genetic material. The symptoms of acute viral disease are directly related to the destruction of host cells by the infecting virus. A virus must first infect a cell to be able to replicate. At the start of infection, the viral genetic material is introduced into the cell. There is great diversity in sizes, compositions and gene organization of viral genomes. Each type of viral genome requires unique proteins for its replication and must encode one or more of these proteins needed to replicate the viral genome. The strategies used by viruses to ensure replication vary. In some cases, the viral proteins merely assist host proteins to replicate the viral nucleic acid. In most cases, however, the viral proteins replicate the viral genome. In all instances, the viral proteins are responsible for packaging the viral genome into virions (Roizman & Palese, 1996).

1.1.5.1 Lytic or lysogenic cycle

The effects of viral replication may range from cell death to changes in function and antigenic specificity of the infected cell. Viruses that carry out a lytic cycle will induce virus reproduction in the infected cell. After replication and packaging of the viral genome, the virus will cause the cell to lyse in order to release the progeny virus particles, resulting in cell death. Some viruses exit the cell via exocytosis, taking a small portion of the cell membrane with them as a viral envelope. A lysogenic cycle does not result in immediate cell lysis. The viral genome integrates into the host cell genome and is replicated along with it. This allows the host cell to survive and reproduce, and the virus is passed on to the offspring of the host cell. After several replication cycles the virus may become active and will enter the lytic phase (Roizman & Palese, 1996).

1.1.5.2 DNA viruses

Members of the DNA virus families are fully or at least partially double stranded, with the exception of the ssDNA genome of *Parvoviruses* and the circular ssDNA genome of

Circoviruses. Parvovirus virions contain linear ssDNA. *Papovaviruses* have closed circular DNA molecules, whereas the DNA molecules of *Herpesviruses*, *Adenoviruses* and *Poxviruses* are linear. However, *Adenoviruses* contain a protein covalently linked to the 5' end of their DNA strands and the ends of the double stranded poxvirus genome are covalently joined. The DNA of *Hepadnaviruses* is a circular, double stranded molecule in which there are single stranded gaps (figure 1.2; Roizman & Palese, 1996).

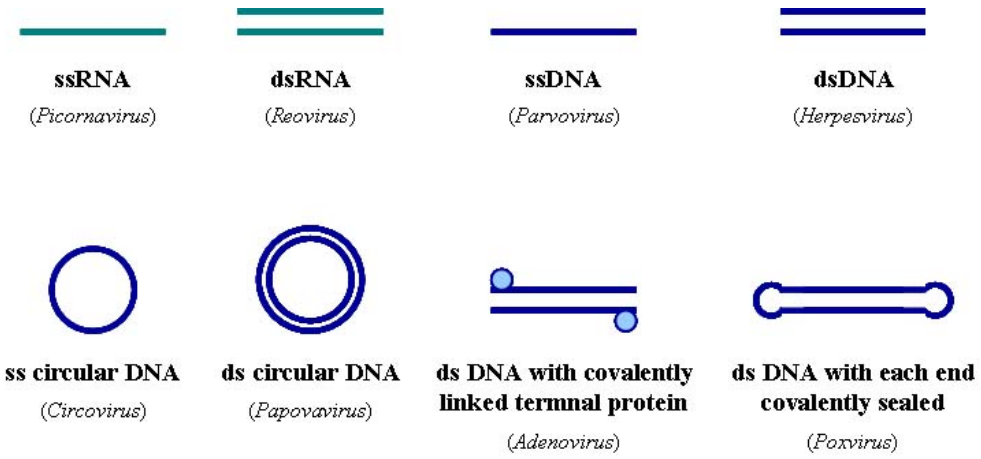

Figure 1.2: Schematic representation of viral genomes. *Examples of viruses containing the different types of genomes are given in between brackets.*

Several dsDNA viruses (*Papovaviruses*, *Adenoviruses*, *Herpesviruses*) replicate in the host cell nucleus and can therefore use the transcriptional enzymes of the host cell for the generation of mRNA. Other dsDNA viruses, such as *Poxviruses*, have been detected in the nucleus but replicate in the cytoplasm. *Poxviruses* evolve all the necessary factors for transcription and replication of the viral genome. *Parvoviruses* are ssDNA viruses, which essentially form two groups. The members of one group are autonomous *Parvoviruses* that are capable of independent replication. The second group contains the Adeno-associated virus, which remains latent by integration at specific sites in the human chromosome. It is capable of independent replication, but only after infection of the cell by a helper virus (*Adenoviruses* or Herpes Simplex viruses). Replication requires the synthesis of a complementary DNA strand in the nucleus and transcription of the genome (Roizman & Palese, 1996).

1.1.5.3 RNA viruses

RNA viruses have mostly single stranded genomes, with the exception of the members of the *Reovirus* family that contain a double stranded genome (figure 1.2). All RNA genomes are linear molecules. Some contain a covalently linked polypeptide at the 5' end of the genome. Positive strand RNA viruses are viruses whose genome serves as mRNA. These positive stranded RNA viruses are divided into viruses coding for a single genome-sized mRNA and viruses that are able to make subgenomic mRNAs. *Picornaviruses* and *Flaviviruses* contain a single genome-sized mRNA that is translated into a single polyprotein, which is proteolytically cleaved during and after translation. The genomic RNA serves as a template for the synthesis of the complementary minus strand by a viral polymerase. The minus strand will serve as a template to make more positive strand RNA. *Togaviruses* are positive strand RNA viruses that code for subgenomic mRNA. At first, only the 5' end of the genomic RNA is available for translation. The function of the encoded proteins is to copy the genomic RNA, after which the complementary minus strand is synthesized. The minus RNA will serve as a template for subgenomic mRNAs. *Retroviruses* are a third group of positive stranded RNA viruses. Their virions uniquely contain two identical copies of genomic RNA (Roizman & Palese, 1996).

Negative strand RNA viruses can be devided into two groups. The first group contains the nonsegmented negative strand RNA viruses, such as *Paramyxo-*, *Rhabdo-* and *Filoviruses*. Their genomes must be transcribed into mRNA, therefore all negative strand RNA viruses package a transcriptase in the virion along with the viral genome. *Bunyaviruses* (3 segments) and *Orthomyxoviruses* (7 to 8 segments) are segmented negative strand RNA viruses. The virion associated polymerase synthesizes mRNA of each segment of the genomic RNA. A unique characteristic of segmented negative strand RNA viruses is their ability to reassort their genes in cells infected by more than one virus of the same family (Roizman & Palese, 1996).

1.2. Positive stranded RNA viruses

All positive stranded RNA viruses, infecting eukaryotic cells, replicate in association with cellular membranes. The RNA replication complex of many virus families is associated with membranes derived from the endoplasmic reticulum (ER). Other organelles of the secretory pathway, mitochondria, endosomes and lysosomes, however, are also used as sites for RNA replication. The membrane association offers protection for the viral RNA against host cell defence mechanisms and it links the RNA replication to a confined space within the infected host cell, increasing concentrations of components necessary for viral RNA replication. The process of membrane binding and targeting to specific intracellular organelles of the replication complexes of different viruses is not yet completely understood. However, extensive studies of viral non-structural proteins have shown that certain non-structural proteins, rather than the viral RNA, are responsible for the association of the replication complex with membranes and the targeting to particular cellular organelles (reviewed by Salonen *et al.*, 2004). *Picornaviruses* comprise a major family of positive stranded RNA viruses, which synthesize their structural and nonstructural proteins in association with cytoplasmic membranes in close vicinity to the RNA replication site. This family of viruses will be discussed in detail in the following section 1.3, and a general overview of membrane trafficking will be included.

1.2.1 Togaviridae

The *Togaviridae* family belongs to the alphavirus-like superfamily, which additionally includes several families of plant RNA viruses. The *Alphaviruses* belong to the *Togaviridae* family together with the *Rubiviruses*. The virus particles are enveloped and the capsid within is icosahedral. The *Togaviridae* belong to group IV of the Baltimore classification of viruses (figure 1.1). The RNA replication of *Alphaviruses* and *Rubiviruses* takes place in association with specific cytopathic vacuoles (reviewed by Salonen *et al.*, 2004).

1.2.1.1 Alphaviruses

Alphaviruses infect a variety of vertebrates such as humans, rodents and birds and infection is usually spread by insect vectors. Semliki Forest virus (SFV) and Sindbis virus are members of

the alphavirus genus and infect birds. Association of SFV-specific RNA synthesis with membranes was demonstrated in the late 1960s. Electron microscopic studies revealed cytoplasmic structures typical for alphavirus-infected cells. These were designated as cytopathic vacuoles (CPVs). Their surface consisted of small vesicular invaginations or spherules and it was suggested they were involved in virus-specific RNA synthesis (Grimley *et al.*, 1968). Froshauer and colleagues (1988) demonstrated that CPVs were modified endosomes and lysosomes with replicase-specific nonstructural proteins (nsP3 and nsP4, figure 1.3) located on their surface. It was suggested that CPVs are not only the site of viral RNA synthesis, but also of translation of structural proteins and the assembly of nucleocapsids (Froshauer *et al.* 1988). However, it has been demonstrated that the endosomal targeting of the replication complexes must be a posttranslational event (Peränen & Kääriäinen, 1991). Alphavirus nonstructural proteins are synthesized as a polyprotein precursor P1234, which is processed into the individual components nsP1-nsP4 (figure 1.3).

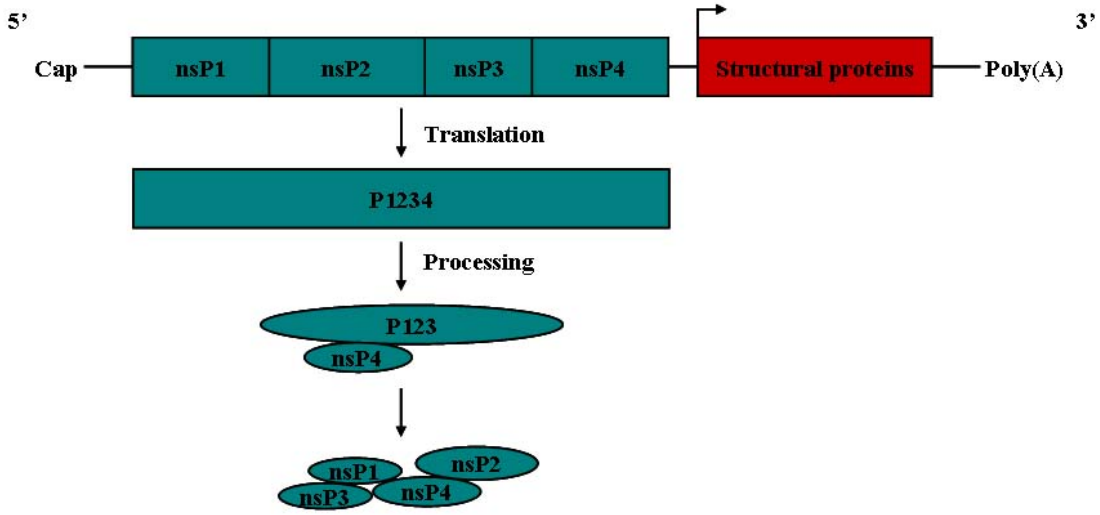

Figure 1.3: The genome organization of *Alphaviruses*. *The translation and processing products relevant for replication are shown.*

Nonstructural protein nsP1 is necessary for the synthesis of the complementary RNA early in infection, nsP2 is involved in the regulation of the subgenomic mRNA coding for the structural proteins of the virion, nsP3 is essential for the formation and the functioning of the replication complex, and nsP4 is the catalytic RNA-dependent RNA polymerase (reviewed by Salonen *et*

al., 2004; Frolova *et al.*, 2006). It has been suggested that all nsPs are associated with CVPs, indicating that these structures are the sites of RNA replication. However, only a fraction of nsPs are present in the replication complexes: nsP2 has been located in the nucleus, nsP1 at the plasma membrane, and nsP3 and nsP4 in the cytoplasm (Kujala *et al.*, 2001). Only nsP1 has a specific association with membranes and was therefore a strong candidate as the membrane anchor of the replication complex. It has been shown that nsP1 was very tightly membrane bound, with a high affinity for endosomes and lysosomes (Peränen *et al.*, 1995).

1.2.1.2 Rubiviruses

Rubella virus is the type species of the *Rubiviruses*, part of the *Togaviridae* family. Rubella virus shares a similar replication strategy with the *Alphaviruses*. During a rubella virus infection, cytoplasmic membrane structures are present that resemble *Alphavirus* replication complexes (Lee *et al.*, 1992). These structures comprise vacuoles which are internally lined with membrane-bound vesicles or spherules. Antibodies against dsRNA have been used to localize dsRNA to these structures suggesting that they function as replication complex (Lee *et al.*, 1994). Magliano and colleagues (1998) have demonstrated that rubella virus replication complexes are virus-modified lysosomes (Magliano *et al.*, 1998). These results where confirmed by Kujala and colleagues (1999), who demonstrated that the rubella virus replicase protein is associated with vesicles and vacuoles of endo-lysosomal origin, and specifically with the spherules lining the interior of these structures, suggesting that these are the sites of viral RNA synthesis (Kujala *et al.*, 1999; reviewed by Salonen *et al.*, 2004).

The alphavirus-like superfamily contains a number of plant viruses that replicate on various intracellular membranes. Brome mosaic virus (BMV) and Tobacco mosaic virus replicate on the ER, Alfalfa Mosaic virus on the vacuolar membrane, and Turnip Yellow Mosaic virus on the chloroplast envelope. The targeting determinant of the replication complex of BMV has been mapped to the 1a protein, and more specifically to the N-terminal domain, part of which is distantly related to the alphavirus nsP1. Structures closely resembling the spherules, described previously for *Alpha*- and *Rubiviruses*, have been detected in BMV-infected cells. It has been shown that BMV protein 1a alone, in the absence of other viral components, can induce spherule formation (reviewed by Salonen *et al.*, 2004).

1.2.2 Flaviviridae

The *Flaviviridae* family contains three genera: the *Flavi-*, the *Hepaci-*, and the *Pestiviruses*. hepatitis C virus (HCV, *Hepaciviruses*) and Kunjin virus (*Flaviviruses*) are the best studied in the context of membrane-associated replication. The positive stranded RNA genome of the *Flaviviridae* is translated to a large polyprotein. The structural proteins consist of a capsid protein and envelope glycoproteins followed by the nonstructural proteins (figure 1.4). The nonstructural proteins of HCV associate to the ER membrane. It has been shown that nonstructural proteins NS2, NS4A, NS4B, NS5A, and NS5B associate with the ER membrane independent of the expression of other HCV proteins. The soluble protease/helicase NS3, however, associates with the ER membrane by interaction with NS4A. When expressed alone, NS3 is found diffusely throughout the cytoplasm and the nucleus, but when co-expressed with NS4A, NS3 is found in association with ER or ER-like membranes. Deletion analysis revealed that the hydrophobic amino-terminal domain of NS4A is necessary for ER targeting of NS3 (Wölk *et al.*, 2000; reviewed by Dubuisson *et al.*, 2002). NS2 is a hydrophobic, polytopic integral membrane protein, which is targeted to the ER membrane by internal signal sequences. The function of NS2 is unclear. Deletion of NS2 did not abolish the replication of HCV RNA, which indicates that NS2 is not essential for viral RNA replication. Before cleavage from the polyprotein, however, NS2 is involved in an autoprotease activity that is responsible for the cleavage between NS2 and NS3 (Yamaga & Ou, 2002; reviewed by Dubuisson *et al.*, 2002). NS4B is a relatively hydrophobic protein of unknown function. It has, however, been demonstrated that the interaction of NS4B with NS3 and NS5B modulates the RNA polymerase activity (Piccininni *et al.*, 2002). NS4B is predicted to be a polytopic membrane protein that is cotranslationally inserted into the ER membrane by internal signal sequences (Hügle *et al.*, 2001). Expression of the HCV polyprotein induces the formation of a special ER-derived membranous web. This membranous web has been proposed as a candidate HCV replication complex. Expression of NS4B alone induced the formation of the web, indicating that NS4B might have a function in inducing a specific membrane alteration necessary for the formation of the replication complex (Egger *et al.*, 2002).

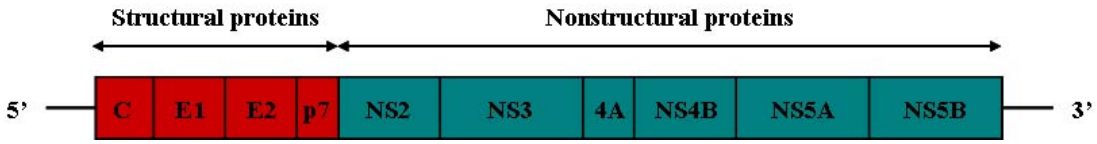

Figure 1.4: The genome organization of hepatitis C virus. *The structural proteins, the capsid protein (C), and the envelope glycoproteins E1 and E2, are present in the N-terminal part of the polyprotein. The function of the p7 polypeptide is still to be determined. The nonstructural proteins NS1, NS2, NS3, NS4A, NS4B, NS5A, and NS5B are involved in the membrane-associated replication.*

The genome organization of Kunjin virus and HCV is similar, but there are some differences as well. Kunjin virus has a nonstructural glycoprotein NS1, which is translocated into the lumen of the ER and transported through the secretory pathway to the exterior of the cell. It also plays an essential role in RNA replication, by recognizing the other replicase proteins associating with the ER membrane. The Kunjin virus polyprotein also contains two small membrane-bound proteins NS2A and NS2B, preceding the NS3 protein. NS2B acts as a cofactor for the NS3 protease (reviewed by Westaway *et al.*, 2002). Kunjin virus nonstructural proteins NS1, NS2A, NS3, NS4A, and NS5 have been associated with dsRNA, which serves as a marker for replication complexes (Westaway *et al.*, 1997). Dramatic changes in the organization of the ER membrane have been observed in Kunjin virus-infected cells. Convoluted membranes, paracrystalline structures and vesicle packets (VP) of smooth membrane appear during infection. The majority of nonstructural proteins and dsRNA have been localized to these VPs, which are derived from trans-Golgi membranes, which suggest that these VPs are sites of replication (Mackenzie *et al.*, 1999; reviewed by Westaway *et al.*, 2002, 2003).

1.2.3 Nidovirales

The *Coronaviridae* and the *Arteriviridae* families are grouped in the order *Nidovirales*. The expression of their replicase-transcriptase genes is mediated by the translation from two large open reading frames; ORF1a and ORF1b (figure 1.5). Initially two large polyproteins pp1a and pp1ab are synthesized. The synthesis of pp1ab involves a programmed ribosomal frame shift during translation of ORF1a. The ORF1a/ORF1b overlap region contains two signals

which are assumed to promote this event: a “slippery” sequence, which is the actual frameshift site, and a downstream RNA pseudoknot structure. Complex proteolytic processing of the polyproteins leads to 12 or more nonstructural proteins. *Coronaviruses* contain 16 nonstructural proteins: nsp1 to nsp11 are encoded in ORF1a, and nsp12 to nsp16 are encoded in ORF1b. *Arteriviruses*, however, only contain 12 nonstructural proteins: nsp1 to nsp8 are encoded in ORF1a, and nsp9 to nsp12 are encoded in ORF1b (reviewed by: Snijder & Meulenberg, 1998, Sawicki *et al.*, 2007).

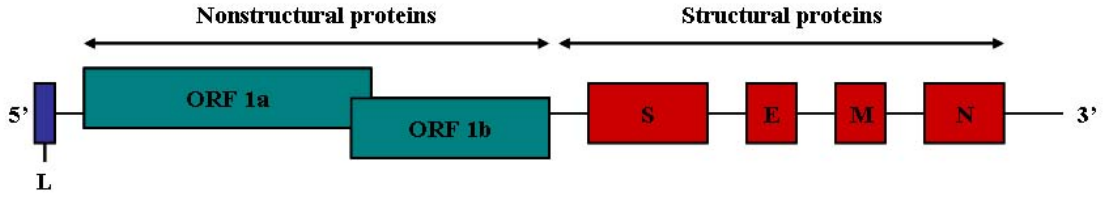

Figure 1.5: The genome organization of *Coronaviruses*. *The nonstructural proteins are encoded in ORF1a and ORF1b and are synthesized initially as two large polyproteins, pp1a and pp1ab. The synthesis of pp1ab involves ribosomal frame shifting during translation of ORF1a. These polyproteins are cleaved in 16 nonstructural proteins. The major structural proteins are the spike glycoprotein (S), the small envelope protein (E), the membrane glycoprotein (M), and the nucleocapsid protein (N). The 5’ end of the genome contains a leader sequence (L).*

The replicase-transcriptase proteins of *Coronaviruses*, together with other viral proteins assemble into replication complexes. These complexes accumulate at the perinuclear regions and are associated with double-membrane vesicles (DMV; Brockway *et al.*, 2003, Snijder *et al.*, 2006). The origin of these DMVs is unclear. The nonstructural proteins and the viral RNA of mouse hepatitis virus, a member of the *Coronaviridae,* have been localized to late endosomal membranes (van der Meer *et al.*, 1999). It has also been shown that the replicase proteins of Equine Arteritis virus (EAV), a member of the *Arteriviridae*, as well as newly synthesized RNA, accumulates in perinuclear vesicles, which are of ER origin (van der Meer *et al.*, 1998). EAV-infected cells revealed DMVs carrying the replication complex, which appear to be derived from paired ER membranes. They are most likely formed by protrusion and detachment of vesicular structures with a double membrane (Pedersen *et al.*, 1999).

Snijder and colleagues (2001) have demonstrated that DMV formation during EAV infection does not depend on RNA synthesis. DMVs resembling those seen in EAV-infected cells can be induced by expression of the nsp2-nsp3 region of the polyprotein, suggesting that nsp2 and nsp3 play a crucial role in the membrane association of the virus replication complex (Snijder *et al.*, 2001). The nsp2 protein contains a long central hydrophobic sequence, which might act as its membrane anchor. Both nsp3 and nsp5 contain several hydrophobic sequences, suggesting that they are polytopic membrane proteins. These nonstructural proteins and their precursors act as integral membrane proteins (van der Meer *et al.*, 1998). Coronavirus nonstructural proteins nsp3, nsp4 and nsp6 contain hydrophobic transmembrane domains, suggesting that they serve to anchor the pp1a/pp1ab polyproteins to membranes during the first step of replication complex formation. All coronavirus nonstructural proteins are associated with the replication complex, however, at later times of infection, the nonstructural proteins encoded in ORF1a remain tightly bound to the replication complex, while proteins encoded in ORF1b detach and diffuse to the cytosol (reviewed by Sawicki *et al.*, 2007).

1.2.4 Caliciviridae

The *Caliciviridae* are a major cause of gastroenteritis in humans and cause a wide variety of other diseases in animals. The *Calicivirus* family contains four genera: the *Lago-*, the *Noro-*, the *Sapo-*, and the *Vesiviruses* (Green *et al.*, 2000). The human enteric *Caliciviruses* (*Noro-* and *Sapoviruses*) have not yet been successfully cultivated. In contrast, Feline Calicivirus (FCV), a virus belonging to the *Vesivirus* genus, and other animal *Caliciviruses* can be propagated in culture, and, as such, provide good model systems for other members of the family *Caliciviridae*. The *Caliciviruses* belong to the picornavirus-like supergroup of the positive-strand RNA viruses, which is characterized by the conservation of three major enzymes: a nucleoside triphosphatase (NTPase; 2C in *Picornaviruses*), a proteinase with a chymotrypsin-like fold (3C), and an RNA-dependent RNA polymerase (3D) (Koonin & Dolja, 1993). All calicivirus genomes are organized with a large nonstructural polyprotein gene (ORF1) that precedes a single structural capsid protein gene. Furthermore, they all contain a small 3’ terminal ORF encoding a basic and hydrophilic protein. In addition, a protein, called VPg, is covalently linked to the 5’ end of the RNA. Two fundamentally

different genome organizations are contained within the four calicivirus genera. ORF1 is either fused to and contiguous with the capsid ORF, forming a single polyprotein, or the capsid gene is encoded in a separate reading frame (ORF2) that overlaps the 3' terminus of ORF1. In both cases, viral replication analysis in infected cells, has demonstrated that the major capsid protein is also encoded by a separate subgenomic RNA molecule (figure 1.6; reviewed in Thiel & Köning, 1999; Clarke & Lamden, 2000).

Studdert and O'Shea, and Love and Sabine (1975) first reported a possible association of FCV replication with cellular membranes. Feline cells infected with FCV showed extensive rearrangements of intracellular membranes (Studdert & O'Shea, 1975, Love & Sabine, 1975). The rearrangements of intracellular membranes were also seen in FCV-infected CRFK cells (Crandell-Rees feline kidney cells). Furthermore, a membranous fraction that could synthesize viral RNA in vitro was isolated from FCV-infected CRFK cells. The enzymatically active component of this membranous fraction was specified as the FCV replication complexes (Green *et al.*, 2002). Analysis of the protein-protein interactions in the FCV replication complex has demonstrated that the p32 protein (picornavirus 2B analogue) interacts with p39 (viral helicase/NTPase, 2C analogue), p30 (3A analogue), and p76 (viral ProPol, 3CD analogue). The FCV protease/RNA polymerase p76 interacts with VPg and ORF2, which encodes the major capsid protein (Kaiser *et al.*, 2006). The Norwalk virus (*Norovirus*) protein p48, a N-terminal nonstructural protein analogue to picornavirus protein 2B, interacts with the Golgi complex, suggesting that it may play a role in the induction of intracellular membrane rearrangements associated with positive-strand RNA replication (Fernandez-Vega *et al.*, 2004). The FCV protein p32, the p48 homologue, however, did not demonstrate an interaction with the Golgi complex (Kaiser *et al.*, 2006). A direct interaction of the Norwalk protein p48 with the SNARE regulator vesicle-associated membrane protein-associated protein A (VAP-A) has also been reported, suggesting that p48 interferes with intracellular protein trafficking (Ettayebi & Hardy, 2003). FCV replication in cells results in changes characteristic of apoptosis, including caspase activation, chromatin condensation and cleavage of poly(ADP-ribose) polymerase. It has been demonstrated that the mitochondrial pathway of apoptosis is triggered during FCV infection (Sosnovtsev *et al.*, 2003, Natoni *et al.*, 2006).

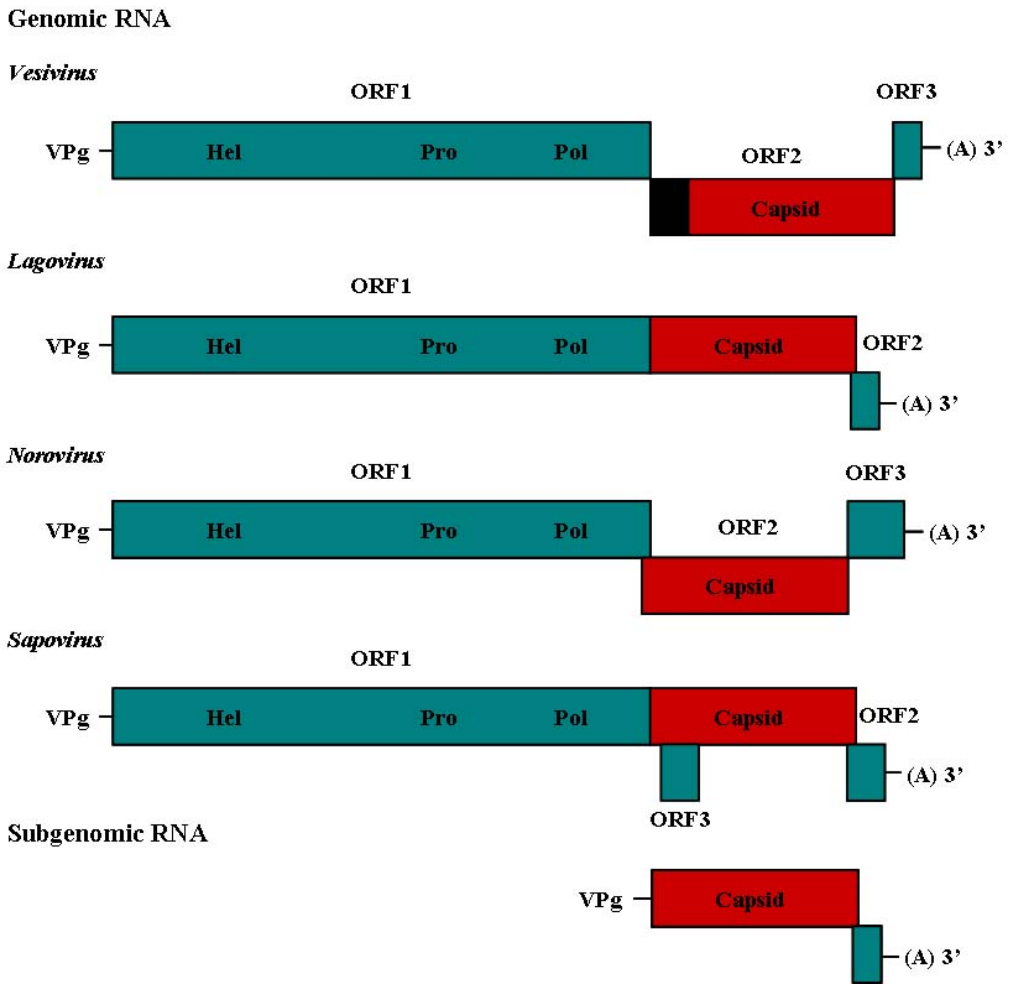

Figure 1.6: The genome organization of *Caliciviruses*. *The genomic organization and reading frame usage are shown for the different Calicivirus genera. The genome size varies between 7.4 and 8.3 kb. The predicted RNA helicase (Hel), protease (Pro), and polymerase (Pol) regions present in all Caliciviruses are indicated. For the genus Vesivirus the black box illustrates the leader sequence of the capsid precursor protein which is post-translationally cleaved off. The subgenomic-sized transcript RNA (2.2 to 2.4 kb), detected in cells infected with animal Caliciviruses, is shown.*

1.3. Picornaviruses

The *Picornaviridae* comprise a significant family of human and agricultural pathogens, such as poliovirus, human hepatitis A virus, foot-and-mouth disease virus (FMDV) and the human *Rhinoviruses*. These viruses are both medically important and economically significant. For example, Human Rhinoviruses are a major cause of the common cold. Foot-and-mouth disease is one of the most infectious pathogens of livestock known and is responsible for worldwide outbreaks of foot-and-mouth disease in cloven-hoofed animals (reviewed by Rueckert, 1996).

1.3.1. Classification

Currently, the *Picornaviridae* family consists of nine genera: *Entero-*, *Rhino-*, *Cardio-*, *Aphtho-*, *Hepato-*, *Parecho-*, *Erbo-*, *Kobu-* and *Teschoviruses*; and three proposed genera provisionally named "*Sapeloviruses*", "*Senecaviruses*", and "*Tremoviruses*". Additionally, the two human rhinovirus species are to be moved to the enterovirus genus, after which the rhinovirus genus will disappear. The classification is based on phylogenetic properties, which reflect evolutionary history. The general hosts of the *Picornaviridae* are vertebrates. Members of the picornavirus family have similar genome organization and are believed to follow a similar replication strategy (King *et al.*, 2000; reviewed by Stanway *et al.*, 2002).

The *Enteroviruses* include not only the *Poliovirus* (PV type 1, 2 and 3), which is the type species, but also the *Coxsackieviruses A* (CVA, 23 serotypes) and *B* (CVB, 6 serotypes), and the *Echoviruses* (28 serotypes). Furthermore, more than 100 serotypes of human enteroviruses have been identified. The enterovirus genus also contains some nonhuman enteric viruses such as bovine enteroviruses (type 1 and 2) and porcine enteroviruses (3 serotypes) (reviewed by Rueckert, 1996; King *et al.*, 2000; Oberste *et al.*, 2001). The *Rhinoviruses* are the most important aetiological agent of the common cold in adults and children and currently 103 serotypes have been identified. They are named *Rhinoviruses* because they replicate in the nasopharynx. This genus includes the species human Rhinovirus A and human Rhinovirus B (reviewed by Racaniello, 2001).

1.3.1.1 Cardioviruses

The *Cardiovirus* genus currently comprises two virus species: *Encephalomyocarditis virus* (EMCV) and *Theilovirus* (ThV). The EMCV species is represented by a single serotype of the same name and furthermore contains the Columbia-SK virus, the Maus-Elberfeld virus, and Mengovirus. EMCV infects many animal species: primarily rodents, cattle, elephants, raccoons, and more rarely primates. The main reservoir host is the rat although mice may also spread the virus, passing it to other species through faecal-oral transmission (Grobler *et al.*, 1995, Knowles *et al.*, 1998, Spyrou *et al.*, 2004, Bakkali Kassimi *et al.*, 2006). The Theilovirus species includes the Theiler's Murine Encephalomyelitis virus (TMEV), Vilyuisk Human Encephalomyelitis virus (VHEV), and Theiler-like virus of rats (King *et al.*, 2000; reviewed by: Rueckert, 1996, Racaniello, 2001; Ohsawa *et al.*, 2003).

Strains of TMEV were first isolated by Max Theiler and early investigations showed that TMEV was a picornavirus causing a subclinical enteric infection in mice. On occasion, TMEV spreads to the central nervous system to cause paralysis and more rarely encephalitis. There are two clusters of TMEV strains based on the differences in biological activities. Strains of the GDVII subgroup, GDVII and FA, are highly virulent and produce an acute and usually fatal encephalomyelitis in mice, which resembles poliomyelitis. The second group, known as Theiler's original (TO), includes the DA, BeAN, WW, and Yale strains (Lipton, 1978). These strains are less virulent and cause a chronic biphasic neurological disease in some mouse strains, which is an animal model of human demyelinating diseases such as multiple sclerosis (Lipton, 1975, Roos, 2002; reviewed by: Racaniello, 2001, Oleszak *et al.*, 2004).

In the late 1950s, an outbreak of degenerative neurological disease occurred within the Yakut population of Siberia. The disease was manifested as either an acute or chronic form of diffuse meningoencephalitis, dementia-schizophrenia, or amyotrophic lateral sclerosis. Autopsy revealed widespread inflammatory-degenerative changes in the nervous system, especially the cerebral cortex and basal ganglia. The suspected etiologic agent, VHEV or Vilyuisk virus, was isolated from the cerebrospinal fluid of a chronic case of encephalomyelitis, and was subsequently characterized as a picornavirus highly similar to TMEV (Lipton *et al.*, 1983, Pritchard *et al.*, 1992). Recently, a novel picornavirus, known

as Saffold virus (SAF-V), has been described. It was isolated in the US (1981) from the stools of an 8-month infant presenting with fever of unknown origin. Molecular evolutionary analysis has demonstrated that SAF-V is a new member of the *Cardiovirus* genus. Phylogenetic analysis of the full length genome sequences has shown that SAF-V is most closely related to Theiler-like virus, followed by TMEV (Jones *et al.*, 2007).

1.3.1.2 Aphthoviruses

Foot-and-mouth disease virus (FMDV) is the type species of the *Aphthoviruses*, which infect cloven-hoofed animals such as cattle, pigs and sheep. Seven FMDV serotypes have been identified: types A, C, O, Asia 1, and the South African Territory types SAT 1, SAT 2, and SAT 3. The *Aphthovirus* genus also includes the Equine Rhinitis A virus (Belsham, 1993; King *et al.*, 2000; reviewed by: Rueckert, 1996; Racaniello, 2001).

FMDV is the causative agent of foot-and-mouth disease (FMD). FMD was first described in Italy in the 1500s. The disease is still prevalent, despite many countries being declared FMD-free. Endemic regions of the disease include areas of Europe (UK), Asia, and South America. Eradication in these areas has been difficult, despite the availability of a vaccine. The cause of FMD was first demonstrated to be viral in 1898 by Loeffler and Frosh. Blood of infected animals was passed through a Chamberland filter, and it was found that the filtered fluid was able to infect healthy animals (reviewed by Levine, 1996). The average incubation period is 3 to 8 days and the disease is characterized by high fever, blisters inside the mouth and on the feet. Most animals recover eventually, but FMD can lead to myocarditis and death. Some animals remain asymptomatic; however, as carriers of the virus they can still transmit the virus to other animals. Humans can be infected with FMDV through contact with infected animals, but this is extremely rare. Symptoms include malaise, fever, vomiting, red ulcerative lesions of the oral tissues, and sometimes vesicular lesions of the skin.

1.3.2. Viral genome

Picornavirus genomes are positive, single-stranded, linear RNA molecules varying in length from 7.1 kilobases (kb) to 8.2 kb. They are composed of three parts: the 5' noncoding region (5'NCR) (600 to 1200 nucleotides [nts]), the coding region (6500 to 7000 nts), and the 3' noncoding region (3'NCR), which contains a heteropolymeric segment (up to 100 nts) and a poly(A) tract (figure 1.7; reviewed by: Rueckert, 1996, Racaniello, 2001, Agol, 2002, Stanway *et al.*, 2002). The genome encodes four major functions: generation of structural and non-structural proteins, RNA replication, virion assembly, and progeny release from the cell (reviewed by Agol, 2002).

The 5'NCRs are long (around 10% of the genome) and highly structured. RNAs possess no cap but instead the 5'NCR is covalently associated with a small virus-specific protein termed VPg, which appears to play an important role in initiation of RNA synthesis. VPg is encoded by a single gene, 3B, in all picornaviruses except the genome of FMDV, which encodes three VPg genes. The 5'NCR contains sequences that control genome replication and translation. It contains a 5'-terminal stem-loop or cloverleaf-structure and it contains the internal ribosome entry site (IRES), which is an element that directs translation of the mRNA by internal ribosome binding. Multiple classes of picornavirus IRES elements have been characterized. The type 1 IRES element is seen only in enteroviruses and rhinoviruses, while aphthoviruses and cardioviruses have a type 2 IRES element (reviewed by: Reuckert, 1996, Racaniello, 2001, Stanway *et al.*, 2002). The Hepatitis A virus IRES is generally considered to represent a third type of IRES. In contrast to other picornavirus IRES elements, it requires the intact translation initiation eIF4F complex. Recently, a new class of picornavirus IRES elements has been identified. This class contains the IRES elements from Porcine Teschoviurs 1 (PTV-1), Simian virus 2 (SV2), Porcine Enterovirus 8 (PEV-8), and Avian Encephalomyelitis virus. These IRES elements show significant similarity to the hepatitis C virus IRES in sequence, function, and predicted secondary structure (Chard *et al.*, 2006, Bakhshesh *et al.*, 2008). The 5'NCR of EMCV contains a poly(C) tract, the 5'NCR of TMEV, however, does not. In poliovirus the cloverleaf binds protein 3CD in the presence of 3AB or in the presence of cellular protein poly(rC) binding protein 2 (PCBP2; Andino *et al.*, 1990, 1993, Harris *et al.*, 1994, Parsley *et al.*, 1997, Gamarnik & Andino, 2000). The J and K stem-loops of the

cardiovirus IRES binds the cellular translation initiation factor 4G (eIF4G), conferring a cap-independent mode of translation (Kolupaeva *et al.*, 1998, 2003, Clark *et al.*, 2003). Other cellular proteins, such as the La autoantigen, pyrimidine tract binding protein (PTB) and PCBP2 have also been shown to bind picornavirus IRESes and enhance translation (Ali & Saddiqui, 1997, Blyn *et al.*, 1997, Hunt *et al.*, 1999). The strongly conserved 3'NCR contains a secondary structure, a pseudoknot, which seems to carry signals for controlling viral RNA synthesis. picornaviruses carry a 3' stretch of poly(A), which has an average length of 35 to 100 nucleotides. Viral RNA from which the poly(A) tract is removed is non-infectious (reviewed by Racaniello, 2001).

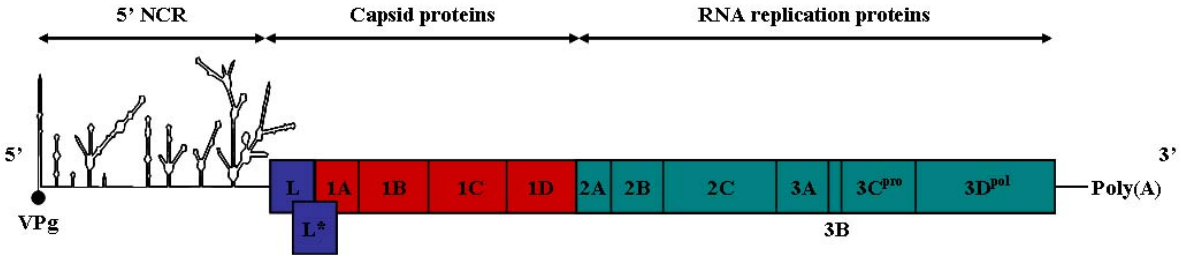

Figure 1.7: The genome organization of *Picornaviruses*. *The RNA secondary structures in the 5' NCR are shown, together with the polyprotein. The polyprotein contains the capsid proteins 1A (VP4), 1B (VP2), 1C (VP3), and 1D (VP1), and the RNA replication proteins 2A to 2C and 3A to 3D. The L protein can only be found in the genome of Aphthoviruses and Cardioviruses. The L* protein is only present in persistent strains of Theiler's virus (DA, BeAn).*

Picornaviruses contain a single, long, open reading frame, which encodes a single polyprotein (around 2200 amino acids [aa]) that is processed to form individual viral proteins. The polyprotein is cleaved during translation, so that the full-length polyprotein is not observed (reviewed by: Racaniello, 2001, Agol, 2002, Stanway *et al.*, 2002). The polyprotein is divided into three regions: P1, P2 and P3 (figure 1.7). The P1 region is the structural region and encodes the viral capsid proteins: VP4 (1A), VP2 (1B), VP3 (1C), and VP1 (1D) (figure 1.7). The P2 and P3 regions encode proteins involved in protein processing and genome replication: P2 contains information for polypeptides 2A, 2B, and 2C; P3 encodes four polypeptides, 3A to 3D (reviewed by: Racaniello, 2001, 2002, Stanway *et al.*, 2002).

1.3.3. Viral polyprotein and proteolytic processing of the polyprotein

Picornavirus proteins are encoded in a single, long, open reading frame (ORF). A single polypeptide, designated the viral polyprotein, is generated from this ORF. Viral replication depends on the activity of proteinases encoded within the polyprotein to process it into the mature viral proteins. The polyprotein corresponding to the complete ORF is never observed in infected cells because virally encoded proteinases initiate polyprotein cleavage cotranslationally. These primary cleavages in *cis* (intramolecular) are followed by secondary reactions in *cis* and *trans* (intermolecular). Picornavirus genomes encode three proteinases: L^{pro}, $2A^{pro}$, and $3C^{pro}$ (reviewed by: Ryan & Flint, 1997, Racaniello, 2001, Leong *et al.*, 2002, Skern *et al.*, 2002).

1.3.3.1 Proteolytic processing of the viral polyprotein

Several picornavirus genera encode a 2A protein with proteolytic activity that is responsible for carrying out the initial cleavage between the capsid precursor P1 and the precursor of the non-structural proteins, P2-P3. In cells infected with rhino- or enteroviruses $2A^{pro}$ cleaves their respective polyproteins between the C terminus of VP1 and their own N terminus. In contrast, 2A of cardio- and aphthoviruses performs the primary cleavage between the C terminus of 2A and the N terminus of 2B, generating a P1-2A precursor. The 2A protein of hepato- and parechoviruses does not have proteolytic activity. They encode only a single proteolytic enzyme, $3C^{pro}$, which carries out both primary cleavage events. The initial cleavage occurs between the P2 proteins 2A and 2B and the second between 2C and 3A. The aphtho- and cardioviruses encode an L protein at the N terminus of their polyprotein. The L^{pro} of FMDV is a proteinase that releases itself from the polyprotein by cleaving between its own C terminus and the N terminus of VP4. In cardioviruses, however, the L protein does not possess any detectable proteolytic activity and cleavage between its C terminus and the P1 precursor is mediated by $3C^{pro}$ in a secondary cleavage (figure 1.8; reviewed by: Ryan & Flint, 1997, Racaniello, 2001, Leong *et al.*, 2002, Skern *et al.*, 2002).

The majority of the secondary processing steps on the polyprotein are performed by $3C^{pro}$. This proteolytic enzyme carries out a primary cleavage between 2C and 3A and it also carries out secondary cleavages of the P1 and P2 precursors. In poliovirus, however, two

cleavages are carried out by the precursor of $3C^{pro}$, $3CD^{pro}$, which is released from the P3 precursor by autocatalytic cleavage. These are between the capsid proteins VP0 (precursor of VP2 and VP4) and VP3 and between VP3 and VP1. Both $3C^{pro}$ and $3CD^{pro}$ can process proteins of the P3 region. The final cleavage to take place is that between the capsid proteins VP4 and VP2. The precursor VP0 is assembled into new viral particles and during maturation of these viral particles, a yet unknown proteolytic activity carries out the cleavage of VP0 (reviewed by: Racaniello, 2001, Leong *et al.*, 2002, Skern *et al.*, 2002).

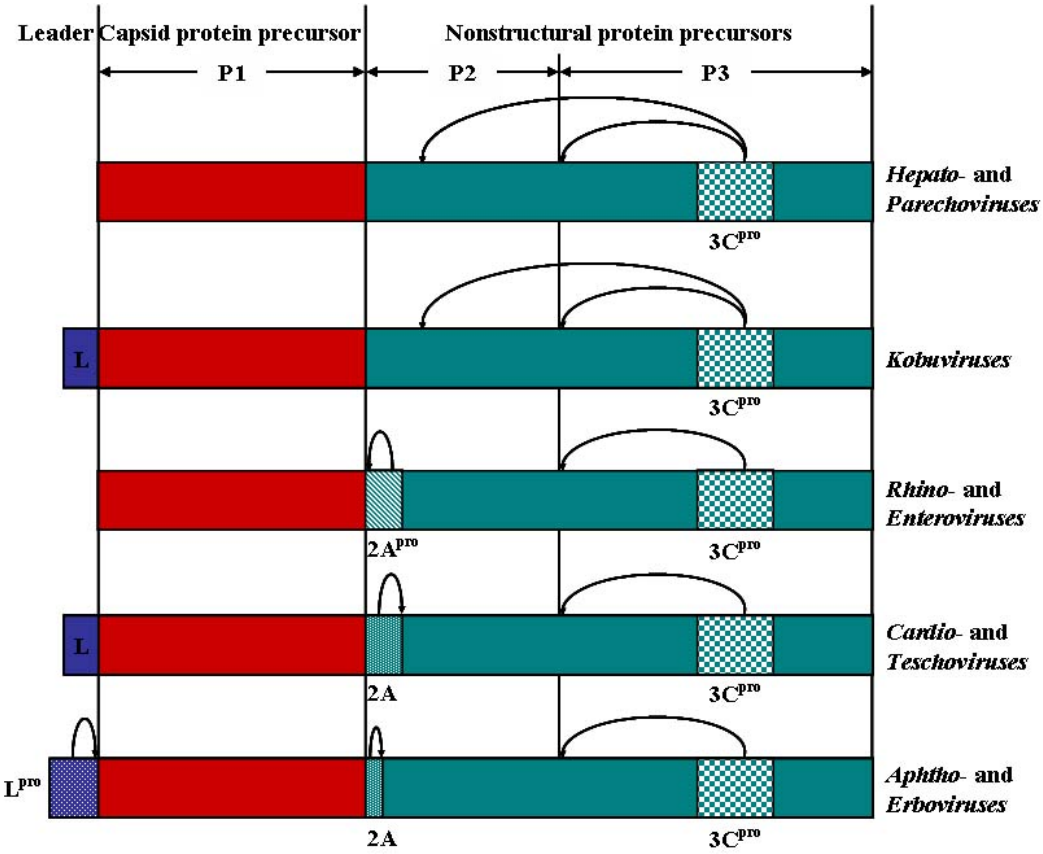

Figure 1.8: *Picornavirus* polyprotein primary cleavages. *The single open reading frame for the different Picornavirus genera is shown and the primary cleavages are indicated. The L protein of Aphthoviruses is a protease, the L protein of Cardioviruses, however, does not show proteolytic activity. Furthermore, the 2A protein of Hepato- and Parechoviruses does not possess proteolytic activity. The shading of the 2A protein of the other Picornavirus genera reflects the differences in mechanism of cleavage.*

1.3.3.2 L protein

Some picornaviruses, such as aphthoviruses and cardioviruses, encode a leader (L) protein at the N terminus of their polyprotein (figure 1.7, 1.8). The aphthovirus L protein (173 to 201 aa) is an autocatalytic protease (explained in more detail in section 1.3.4.1). The cardiovirus L protein (67 to 76 aa) is a much shorter protein without any recognizable proteolytic motifs and no protease activity. It contains sequences consistent with N-terminal zinc-binding motifs, centrally located tyrosine kinase phosphorylation sites, and C-terminal acid-rich domains. The L protein is phosphorylated during viral infection by casein kinase II (CK-2), suggesting that the L protein may play a role in regulation of viral genome translation through a triggering phosphorylation event (Dvorak *et al.*, 2001). It has been demonstrated that the L protein of Theiler's virus plays an important role in blocking the production of alpha/beta interferon by infected cells, and that the zinc-finger motif plays a crucial part in this function (van Pesch *et al.*, 2001, van Pesch & Michiels, 2003). Theiler's L protein also interferes with trafficking of the cytoplasmic interferon regulatory factor 3 (IRF-3), a factor critical for transcriptional activation of alpha/beta interferon genes (Delhaye *et al.*, 2004). Furthermore, it interacts with Ran-GTPase and disrupts nucleocytoplasmic transport (Porter *et al.*, 2006). The L protein is dispensable for virus replication in vitro, but crucial for long-term persistence of the virus in the central nervous system of the mouse (Paul & Michiels, 2006). The L* protein is a unique feature amongst picornaviruses (figure 1.7). It is only present in persistent forms of Theiler's virus (DA, BeAn). The ORF initiates 13 nt downstream of the AUF initiating the polyprotein (Kong & Roos, 1991, Yamasaki *et al.*, 1999). The L* ORF facilitates the infection of macrophage cell lines. This effect is due to the L* protein itself, rather than to competition for the translation of the two overlapping ORFs (van Eyll & Michiels, 2000).

1.3.3.3 Capsid proteins

The capsid proteins 1A-D comprise an icosahedral, non-enveloped particle, approximately 30 nm in diameter. The virion is assembled from 60 protomers arranged as 12 pentamers to form the icosahedral protein shell. Each protomer is composed of four structural proteins: viral protein 1 (VP1 or 1D), VP2 (1B), VP3 (1C) and VP4 (1A). VP1 to VP3 are the major structural components of the virion and have a molecular weight of around 30 kDa. They form an eight-stranded antiparallel β-barrel (made up of two antiparallel β-sheets). VP4 is much smaller and

forms, in conjunction with the amino terminal ends of VP1 and VP2, an interface between the capsid and the internal RNA genome. The surface of the virions consists of a prominent star-shaped plateau (mesa), surrounded by a deep depression (canyon). The canyon may act as a receptor binding site; however, not all picornaviruses have canyons. The capsid serves several key functions such as protecting the viral RNA genome from nucleases, binding receptors in the plasma membrane, avoiding cellular immune response, providing a proteinase involved in the maturation of the virion, and delivering the RNA genome through the cell membrane into the cytosol of susceptible host cells (reviewed by: Hellen & Wimmer, 1995, Rueckert, 1996, Racaniello, 2001, Rossmann, 2002).

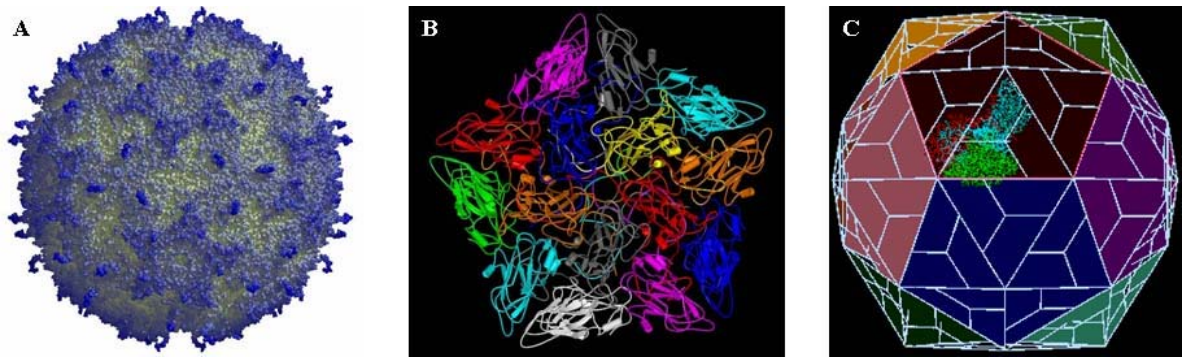

Figure 1.9: Illustration of picornavirus virion structure. *(A) Depth-cued image of TMEV strain BeAn showing the surface topography (Luo et al., 1992); (B) Atomic structure of TMEV strain DA showing the 5-fold axis; (C) Organization of the FMDV external capsid proteins in an icosahedron.*

1.3.3.4 Protein 2A

Early work on poliovirus polyprotein processing revealed that the primary cleavage separating the capsid protein region (P1) from the replicative protein domain (P2) is mediated by the 2A proteinase cleaving at its own N terminus (as described in section 1.3.4.1). Sequence analysis of the 2A region of different picornaviruses showed that the entero- and rhinoviruses possessed highly similar 2A proteinases. The cardiovirus 2A proteins are similar in size to that of entero- and Rhinoviruses, but show no apparent sequence similarity. The 2A region of aphthoviruses is extremely short but does, however, demonstrate sequence similarity with the C-terminal region of the longer cardiovirus 2A proteins. The cardio- and aphthovirus 2A proteins are associated

with an unusual processing activity involving an NPGP motif. The importance of the conservation of the sequence of the cleavage site, and the cleavage site itself (NPG|P) was demonstrated (reviewed by Ryan *et al.*, 2002). The C-terminal region of TMEV-2A is responsible for mediating a primary polyprotein cleavage at its own C-terminus (Donnelly *et al.*, 2001). This apparent cleavage is not proteolysis, but a translational effect involving the NPGP motif (reviewed by Ryan *et al.*, 2002). Host-cell translation is stopped during cardiovirus infection and this is correlated with activation of translation initiation factor 4E binding protein 1 (4E-BP1), which is a repressor of cap-dependent translation (Gingras *et al.*, 1996, Svitkin *et al.*, 2005). In the case of EMCV this activity has been mapped to protein 2A (Aminev *et al.*, 2003). Protein 2A of hepato- and parechoviruses is not believed to be involved in processing. Cleavage of the 2A/2B junction in hepato- and parechoviruses is carried out by $3C^{pro}$ (Gosert *et al.*, 1996). Parechovirus 2A proteins are homologous to 2A of kobuviruses and moreover related to the H-rev107 family of proteins possibly involved in the control of cell proliferation (Hughes & Stanway, 2000). It has also been demonstrated that protein 2A of hepatitis A virus participates in virion morphogenesis (Cohen *et al.*, 2002). The 2A proteins of erbo- and teschoviruses contain the NPGP motif, which suggest that they function like the "translational-type" 2A of aphtho- and cardioviruses.

1.3.3.5 Protein 2B

Picornavirus protein 2B is a rather small protein of about 100 amino acids (AA). It contains two hydrophobic regions, one amphipatic α-helix and a potential transmembrane domain with a β-sheet configuration (figure 1.14). The sequence of protein 2B is one of the least conserved among picornaviruses. The precise function of 2B in the picornavirus replication is not yet defined. PV with mutations in the 2B gene is defective in genome replication. It has also been reported that PV 2B is located mainly in the central portion of the cytoplasm, associated with the membranous vesicles that surround the replication complexes. The expression of PV 2B showed a disassembly of the Golgi complex (reviewed by: Racaniello, 2001, Carrasco *et al.*, 2002, Leong *et al.*, 2002). Furthermore it has been demonstrated that expression of PV protein 2B inhibits vesicular protein transport (Doedens & Kirkegaard, 1995). Protein 2B of enteroviruses has been shown to be a "viroporin". Viroporins are hydrophobic proteins encoded by animal viruses that are able to disturb membrane integrity,

favoring the release of viral progeny. The presence of amphipatic α-helices is a general feature of these membrane-disturbing proteins. Protein 2B of enteroviruses forms pores in ER and Golgi membranes, which results in a decrease of ER and Golgi Ca^{2+} content, which in turn reduces the Ca^{2+} accumulation in the neighboring mitochondria. It has been suggested that this might interfere with Ca^{2+}-dependent vesicular fusion events, which in turn might contribute to the accumulation of the membrane vesicles required for viral RNA replication. Enterovirus protein 2B is involved in suppressing apoptosis of the infected cells. The disturbance of the intracellular Ca^{2+} homeostasis is probably involved in this anti-apoptotic function, as it has been shown that Ca^{2+} fluxes between ER and mitochondria play an important role in ER-dependent apoptosis (Campanella *et al.*, 2004, reviewed by van Kuppeveld *et al.*, 2005).

1.3.3.6 Protein 2C

Protein 2C (~36 kDa) is one of the most conserved picornavirus proteins. Based on sequence alignments it was proposed that protein 2C contained NTP binding motifs and could also be a helicase. The helicase activity has not been demonstrated, but protein 2C does have ATPase/GTPase activities (Rodriguez & Carrasco, 1993, Mirzayan & Wimmer, 1994). Expression of 2C induces membrane proliferation and blocks the exocytic pathway (Barco & Carrasco, 1995, 1998). Protein 2C and its effect on membranes and membrane trafficking during infection will be discussed in detail in section 1.3.7.

1.3.3.7 Protein 3A

The small hydrophobic protein 3A associates with intracellular membranes, and is also observed in its precursor form 3AB. The genome-linked protein VPg (3B) is covalently linked to the 5' end of both plus and minus RNA strands, and is essential for viral genome replication. Precursor 3AB plays a role in delivering VPg to the RNA replication complexes. Protein 3AB interacts with membranes both *in vivo* and *in vitro* and behaves as an integral membrane protein. Protein 3A contains a conserved hydrophobic region of 22 AA near the C-terminus, which is responsible for association with membranes. The introduction of charged residues into this hydrophobic sequence disrupts the 3AB membrane interaction. Thus, the hydrophobic region might serve to anchor 3AB to the membrane replication complex. Heterologous

expression of 3A in *E. coli* showed that 3A affected membrane permeability and proliferation (Lama & Carrasco, 1992, Weber *et al.*, 1996, reviewed by: Carrasco *et al.*, 2002, Leong *et al.*, 2002). Protein 3A is also a potent and specific inhibitor of protein secretion, blocking anterograde protein traffic from the ER to the Golgi complex. This function of 3A is extremely sensitive to mutations near the N-terminus of the protein (Doedens & Kirkegaard, 1995, Doedens *et al.*, 1997, Dodd *et al.*, 2001, Neznanov *et al.*, 2001). Furthermore, it has been demonstrated that protein 3A affects MHC I-dependent antigen presentation (Deitz *et al.*, 2000). FMDV protein 3A, however, does not seem to interfere with ER to Golgi traffic (Moffat *et al.*, 2005). Expression of poliovirus 3A revealed a possible function of 3A as a co-factor for 3D polymerase activity (Lama *et al.*, 1994). Richards and Ehrenfeld (1998) proposed that this activity of 3A is required for stabilizing weak interactions that occur during initiation events in the viral RNA replication complex (Richards & Ehrenfeld, 1998). Sequence analysis of wild-type (wt) and attenuated strains of FMDV revealed nucleotide deletions in the 3A coding region, suggesting that protein 3A may contribute to virulence in cattle (Giraudo *et al.*, 1990). This was subsequently confirmed by analysis of FMDV strains, similarly attenuated, from Asian outbreaks (Beard & Mason, 2000, Knowles *et al.*, 2001, Pacheco *et al.*, 2003). A single mutation within 3A mediated adaptation of FMDV to guinea pigs, whilst mutations within PV 3A also affected host-range (Lama *et al.*, 1998, Nunez *et al.*, 2001).

1.3.3.8 Protein 3B

Protein 3B, also known as VPg, is covalently linked to the 5' end of the genome. A precise function is not yet known, but it has been demonstrated that protein 3B is not required for viral RNA infectivity. It has been shown that VPg can be uridylylated by the viral polymerase 3D, and that this uridylylated VPg can serve as a primer for RNA replication by the RNA-dependent RNA polymerase (reviewed by Leong *et al.*, 2002). An essential RNA structure known as the *cis*-acting replicative element (*cre*) has been identified within the protein-coding region of several picornaviruses. The *cre* is a short hairpin loop which contains a conserved AAACA motif and functions as a template for uridylylation of protein 3B. These *cre* elements are located in different regions of the genomes of several picornaviruses: 1B for cardioviruses, 5' UTR for FMDV, 2C for poliovirus, P1 for HRV-14, and 2A for HRV-2 (Lobert *et al.*, 1999, Rieder *et al.*, 2000, Mason *et al.*, 2002, Yang *et al.*, 2002).

1.3.3.9 Proteinase 3C

Protein 3C is the virus-encoded proteinase responsible for the majority of the processing of the picornavirus polyprotein (reviewed by Ryan & Flint, 1997). All precursors containing 3C (3ABCD, 3BCD, 3CD) are active as proteinases. Protein 3C also has an RNA-binding domain and precursor 3CD binds the 5' RNA cloverleaf structure, which is an essential step during replication. Atomic structures are available for poliovirus, hepatitis A virus, human rhinovirus 2, and FMDV 3Cproteinases (figure 1.10).

Figure 1.10: Atomic structure of FMDV 3C proteinase. *The N- and C-terminal α-helices (red) and several β-sheets (blue) are indicated. This structural figure was prepared using WebLab Viewer Lite (Accelrys, Cambridge, UK).*

1.3.3.10 Polymerase 3D

Protein 3D (~52 kDa) is highly conserved amongst picornaviruses. It serves as the RNA-dependent RNA polymerase, and is responsible for the synthesis of positive and negative strand RNAs. It has been demonstrated that the polymerase activity of protein 3D is positively influenced by the viral protein 3AB. Interactions between 3D and 3AB may facilitate localization of the polymerase to replication complexes. Protein 3D also catalyzes the VPg uridylylation reaction essential for RNA replication (reviewed by Leong *et al.*, 2002). The polymerase has no proof-reading activity and in the absence of any post-replicative mismatch repair, the error-rate of transcription is ~10^{-4}. The protein architecture contains the classical "fingers", "palm", and "thumb" domains. Atomic structures are available for poliovirus polymerase (with a 68aa N-terminal truncation), poliovirus 3CD, and FMDV polymerase in complex with an RNA primer or VPg (figure 1.11).

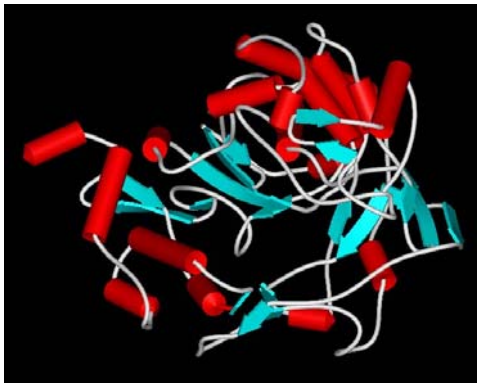

Figure 1.11: Atomic structure of FMDV 3D polymerase. *Several α-helices (red) and β-sheets (blue) are indicated. The protein architecture contains the classical "fingers", "palm", and "thumb" domains. This structural figure was prepared using WebLab Viewer Lite (Accelrys, Cambridge, UK).*

1.3.4. Replication cycle

1.3.4.1 Attachment and entry into the cell

Replication of picornaviruses takes place entirely in the cell cytoplasm. They initiate infection of cells by first attaching to the host cell membrane through a cell receptor. A wide variety of cell surface molecules are used by picornaviruses as cellular receptors. For some picornaviruses, such as polioviruses and rhinoviruses, a single type of receptor is sufficient for entry into cells. Other picornaviruses need a co-receptor for entry into cells (reviewed by Racaniello, 2001).

The receptor of EMCV has been identified as the murine vascular cell adhesion molecule (VCAM-1). Monoclonal antibodies to VCAM-1 inhibited infection and lysis of endothelial cells with the D variant of EMCV (EMCV-D). CHO cells (Chinese hamster ovary cells) transfected with VCAM-1 were susceptible to EMCV-D lysis, while control CHO cells, not expressing VCAM-1, were resistant (Huber, 1994). The TMEV receptor is not known but radio-labelled TMEV (both BeAn and GDVII) bound predominantly to a 34 kDa glycoprotein, and to a lesser extent to 100 and 18 kDa membrane proteins (Kilpatrick & Lipton, 1991). Sialic acid is a (co-) receptor moiety only for the persistent TMEV strains and not for the non-persistent strains. Structural studies have demonstrated that sialyl-lactose binds to a pocket on the viral surface, composed mainly of the amino acid residues from

capsid protein VP2 puff B, in the vicinity of the VP1 CD loop and the C-terminus of VP3 (Zhou *et al.*, 2000). A persistent strain of DA produces a prominent cytopathic effect (CPE) in BHK-21 cells (baby hamster kidney cells) but is much less efficient at infecting L929 cells (mouse fibroblast cells). Adaptation of this DA strain to produce a rapid CPE in L929 cells involved mutations in amino acid residues in the CD loop of VP1, and the EF loop of VP2, which are both exposed at the surface of the capsid, suggesting that these amino acid residues could be involved in receptor recognition. These two clusters of amino acids are part of neutralization epitopes and differentiate persistent from neurovirulent strains of Theiler's virus (Jnaoui & Michiels, 1998, 1999). Infectivity of both TMEV groups requires UDP-galactose transporter (UGT), which belongs to a family of nucleotide-sugar transporter proteins involved in the biosynthesis of complex carbohydrate structures in the trans-Golgi network. UGT most likely mediates TMEV entry and infection by adding galactose to another receptor protein (Hertzler *et al.*, 2001, Shah & Lipton, 2002, Reddi *et al.*, 2003).

Once picornaviruses have attached to their cellular receptor, the viral capsid must dissociate to release the RNA genome into the cell cytoplasm. For some picornaviruses, such as FMDV and rhinovirus, interaction with a cell receptor serves only to concentrate virus on the cell surface. These picornaviruses enter cells by receptor-mediated endocytosis. For other picornaviruses, such as Poliovirus, the cell receptor is also an unzipper and initiates conformational changes in the virus that lead to formation of a pore in the cell membrane through which the viral RNA can be released into the cytoplasm (reviewed by Racaniello, 2001).

1.3.4.2 Translation of viral RNA

Once the positive-stranded viral RNA is released into the cell cytoplasm, it must be translated because it cannot be copied by any cellular RNA polymerase. The viral protein VPg is removed by a cellular unlinking enzyme on entry of the RNA into the cell. Translation initiation is accomplished through a cap-independent mechanism involving an RNA segment called the IRES. The picornavirus IRES is a sequence that promotes translation initiation by internal ribosome binding and contains extensive regions of RNA secondary structure that is conserved within the type I and type II IRES (reviewed by: Racaniello, 2001, Agol, 2002).

The full-length polyprotein is not observed due to rapid primary, co-translational cleavages producing [L-P1-2A], [2BC], and [P3] precursor forms. Precursors are subsequently processed by the virus encoded proteinase 3C (discussed in detail in section 1.3.4.1, reviewed by Ryan & Flint, 1997). Picornavirus proteinases also carry out cleavage of host cell proteins to inhibit non-essential cap-dependent cellular translation. The viral proteinase 2A of entero- and rhinoviruses carries out the cleavage of the eukaryotic initiation factor (eIF) 4GI and its homologue eIF4GII, which are essential components of the host cap-dependent complex. This cleavage results in total shutoff of host protein synthesis. The FMDV L^{pro} protein also cleaves eIF4G during an infection. In both cases the cleavage leads to the inability of the host cell to initiate protein synthesis on its own capped mRNA. This is known as the host-cell protein shutoff (Gradi *et al.*, 1998, Svitkin *et al.*, 1999, reviewed by: Leong *et al.*, 2002, Skern *et al.*, 2002). It has been demonstrated that eIF4G interacts with the IRES for cap-independent translation. The 2A and L^{pro} protein induce cleavage of eIF4G on the C-terminal side of the binding site on eIF4G for eIF4E (the cap-binding protein) and hence, separated the IRES-binding region from the eIF4E interaction site (Clark *et al.*, 2003).

Two proteins are directly involved in the synthesis of viral RNA: the RNA-dependent RNA polymerase $3D^{pol}$ and VPg. VPg serves, after being uridylylated by $3D^{pol}$, as a primer for the initiation of both positive and negative RNA strands. The synthesis of messenger RNA and genome occurs in the cell cytoplasm. The viral RNA polymerase is associated with a cellular membrane fraction, which was called the RNA replication complex. The RNA replication complex consists of small membranous vesicles and several other viral proteins, such as 2BC, 2C, 3AB and $3C^{pro}$, were detected in the RNA replication complexes (reviewed by: Racaniello, 2001, Agol, 2002).

In picornavirus-infected cells, the positive stranded genome is amplified through a negative stranded intermediate. The genomic RNA serves as the template for synthesis of negative-stranded RNA. Initiation of the negative strand demands positioning of $3D^{pol}$ in close proximity to the 3' end of the positive strand, represented by a poly(A) tract. The negative stranded intermediate then serves as a template for the synthesis of positive-stranded genomic RNA, which also serves as mRNA (reviewed by: Racaniello, 2001, Agol, 2002).

1.3.4.3 Virion assembly and release

Once the capsid protein precursor is synthesized and released from the polyprotein by primary cleavage, the precursor will be cleaved into VP0, VP3 and VP1, which remain in a noncovalent complex, the protomer. Five protomers then assemble to form a pentamer. Pentamers can self-assemble into the icosahedral empty capsid. The final steps in the virion assembly are the packaging of the viral RNA into the empty particle followed by the maturation cleavage of VP0 into VP4 and VP2. The picornavirus encapsidation process is highly specific, resulting in packaging of only positive-stranded RNA. The capsid protein signals responsible for the recognition of the viral genome are not yet defined. Evidence exists that each component of a pentamer can be linked with the viral RNA in the replication complex, which means that encapsidation may already start at the pentamer level (reviewed by: Racaniello, 2001, Agol, 2002).

The picornavirus RNA encodes functions ensuring the release of the mature virions. Many picornaviruses have the capacity to lyse the cell. The characteristic morphologic changes known as the cytopathic effects are: condensation of chromatin, nuclear blebbing, proliferation of membranous vesicles, changes in membrane permeability, leakage of intracellular components, and shrivelling of the entire cell. However, little is known about viral mechanisms involved in the cell lysis. Proteins involved in the shutoff of host protein synthesis are likely to be involved, as well as viral proteins responsible for the rearrangement of the cellular infrastructure and permeability changes. The exit of mature virions from the cell may also be accomplished by other mechanisms, such as vesicular transport and a kind of exocytosis. Picornavirus-infected cells may also die of apoptosis, which serves as a host defence to the virus-induced stress. The biological role of apoptosis perhaps consists of limiting virus spread by preventing the completion of the reproduction cycle and isolation of at least a portion of the mature virions within the apoptotic bodies. Picornaviruses possess anti-apoptotic functions to counteract this host cell defense. Several nonstructural proteins, such as 2B/2BC and 3A, appear to interfere with distinct apoptotic pathways. It has been demonstrated that poliovirus protein 3A inhibits tumor necrosis factor (TNF)-induced apoptosis by eliminating the TNF receptor from the cell surface. The depletion of this receptor appeared to result from the lack of its replenishment caused by the disruptions of the

Golgi-mediated trafficking. Poliovirus 2B/2BC and 2C exhibit suppressive anti-apoptotic activity, most likely due to the involvement of these proteins in the rearrangement of the intracellular membranes (Neznanov *et al.*, 2001, reviewed by: Racaniello, 2001, Agol, 2002). The TMEV L* protein exhibits an anti-apoptotic effect in macrophages, and thereby suppressing apoptosis in response to viral infection (Ghadge *et al.*, 1998).

1.3.5. Picornavirus infection

Picornavirus infection leads to profound alterations in the morphology and functioning of cellular membranes. These alterations occur at two well-defined moments during the replication cycle: at early times, when virus particles penetrate the cell, and at late times, when most of the viral proteins are being synthesized. At this late stage of infection several types of changes are observed: enhanced membrane permeability, proliferation of intracellular membranous vesicles, and inhibition of vesicular trafficking with blockage of protein glycosylation. Proliferation of cytoplasmic membrane vesicles is usually observed during the replication of picornaviruses. Viral genome replication depends on the synthesis of these membranous vesicles. Inhibition of membrane proliferation blocks the viral genome replication. Not only the synthesis of several viral nonstructural proteins, but also the formation of new cytoplasmic membranes, are involved in the appearance of picornavirus replication complexes. This also involves drastic changes in vesicular traffic (reviewed by Carrasco *et al.*, 2002).

Dales *et al.* showed the existence of a large number of membrane vesicles in the perinuclear region of poliovirus infected cells. These structures appear 3 hours post infection (p.i.) and proliferate extensively, occupying most of the cytoplasm by 7h p.i. (Dales *et al.*, 1965). The proliferation of these membranous structures is now considered as a common morphological change induced by picornaviruses. The virus-induced vesicles vary in size: their diameters range from 50 to 400 nm. At the beginning of poliovirus infection small vesicles accumulate in the central part of the cytoplasm, while at the end of the replication cycle the vesicles are bigger, resembling autolytic vacuoles. The vesicles have a double lipid bilayer (Schlegel *et al.*, 1996). It has been considered for some time that these vesicles originate by budding from the ER (Bienz *et al.*, 1987). Now, however, it has been suggested that the ER is not the sole source

of the intracellular membranes. Also the Golgi complex and lysosomes are involved in the generation of these membranes and it requires at least in part *de novo* synthesis of phospholipids (Guinea & Carrasco, 1990, Schlegel *et al.*, 1996, reviewed by Carrasco *et al.*, 2002). After infection with PV, the stimulation of phospholipid synthesis leads to proliferation of membrane structures. PV infected cells synthesize smooth membranes that are not present in uninfected cells and PV RNA replication is associated with these smooth membranes. This has also been shown for other picornaviruses such as EMCV, FMDV, and Mengovirus. Protein 2BC seems to play an important part in the mechanisms used by picornaviruses to generate these membrane vesicles (Polatnick & Wool, 1982, reviewed by Carrasco *et al.*, 2002).

Concomitant with the synthesis of new vesicles, there is also an important rearrangement of the intracellular membranous organelles of the secretory pathway, the disappearance of the Golgi complex, and a swelling of the ER together with a reorganization of the cytoskeletal framework (Lenk & Penman, 1979, Joachims & Etchison, 1992). Poliovirus infection causes the disassembly of the Golgi complex. This effect has been attributed to the expression of protein 2B (Sandoval & Carrasco, 1997). Proteins 2B, 2BC and 3A seem to cause a block in the secretion and transport of glycoproteins. 3A seems to block transport from the ER to the Golgi complex, while 2B and 2BC appear to act on a later stage in the exocytic pathway (Doedens & Kirkegaard, 1995, Sandoval & Carrasco, 1997, reviewed by Carrasco *et al.*, 2002). A detailed analysis of this process in yeast revealed that 2BC interferes with vesicular system trafficking at the level of the vesicles that arise from the ER and fuse with the Golgi complex (Barco & Carrasco, 1998).

Picornaviruses synthesize their genomes in association with newly generated membranous vesicles that proliferate from the mid-phase of infection (Caliguiri & Tamm, 1969; 1970a; 1970b). The viral RNA polymerase activity is associated with the smooth membranes of these vesicles and the replication complex was identified on the surface of the membrane structures, which are arranged in a rosette-like fashion (figure 1.12; Bienz *et al.*, 1992, 1994). The vesicles play a structural role in maintaining the replication complexes in the correct configuration for RNA synthesis. The association between the replication complexes and the membranes could be mediated by proteins 2B, 2C and 3AB (Bienz *et al.*, 1987). There is not only a physical connection between membranes and replication.

Cerulenin, an inhibitor of phospholipid metabolism, blocks viral RNA synthesis, which indicates that continuous formation of phospholipids is needed for viral replication to occur (Guinea & Carrasco, 1990). Final evidence for the requirement of a membranous environment for viral RNA synthesis comes from the ability of brefeldin A (BFA), a fungal metabolite that primarily blocks protein transport and vesicular traffic between ER and Golgi apparatus in eukaryotic cells, to potently block PV RNA replication in infected cells. Although the exact mechanism is not understood, the alteration of membrane traffic in cells treated with BFA is thought to inhibit the formation of the virus-induced vesicles, thereby inhibiting viral RNA replication (Irurzun *et al.*, 1992; Maynell *et al.*, 1992; Cho *et al.*, 1994; reviewed by Carrasco *et al.*, 2002).

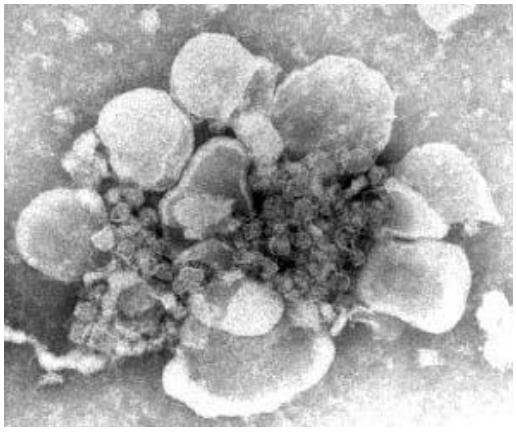

Figure 1.12: Electron micrograph of the *Poliovirus* replication complex. *The PV replication complex surrounded by virus-induced vesicles, which are often arranged in a rosette-like fashion (Bienz et al., 1992).*

1.3.6 Membrane trafficking

Eukaryotic cells have evolved an elaborate internal membrane system consisting of the endoplasmic reticulum (ER), the Golgi complex, endosomes, lysosomes and vacuoles. The secretory pathway allows soluble and membrane proteins to be transported from the ER through the Golgi complex and out to various locations including lysosomes, endosomes, secretory vesicles, and the plasma membrane. The endocytic pathway is used to take up substances from the cell surface into the interior of the cell by way of endosomes and lysosomes. All protein trafficking in the secretory and the endocytic pathways is governed by a

sole principle: transport of membrane and soluble proteins form one membrane-bounded compartment to another is mediated by transport vesicles. These vesicles collect proteins in buds arising from the membrane of a donor compartment and move through the cytoplasm to reach and fuse with the membrane of a target compartment (figure 1.13; reviewed by: Karp, 2005, Lodish *et al.*, 2007).

The ER is divided into two subcompartments, the rough ER (rER) and the smooth ER (sER). They both comprise a system of membranes that enclose a lumen separated from the surrounding cytosol. The rER has ribosomes bound to its cytosolic surface, whereas the sER lacks associated ribosomes. The membranous elements of the sER are typically tubular and form an interconnecting system curving through the cytoplasm. The rER is composed of a network of cisternae and is continuous with the outer membrane of the nuclear envelope. The cisternae of the rER are interconnected, which facilitates the movement of materials from their site of synthesis to sites were they can exit the organelles. The first stage of the secretory pathway takes place in the rER. Newly synthesized soluble and membrane proteins are translocated into the ER, where they are folded into their proper conformation and receive covalent modifications. Secretory proteins are then packaged into anterograde transport vesicles and progress to the second stage of the secretory pathway, the transport through the Golgi. Soon after these vesicles bud from the ER membrane, transport vesicles fuse to form larger vesicles and interconnected tubules in the region between the ER and the Golgi apparatus. This region is known as the ER-to-Golgi intermediate compartment (ERGIC) and the vesicular-tubular clusters are called VTCs. The VTCs move further away from the ER toward the Golgi complex (reviewed by: Klumperman, 2000, Karp, 2005, Lodish *et al.*, 2007).

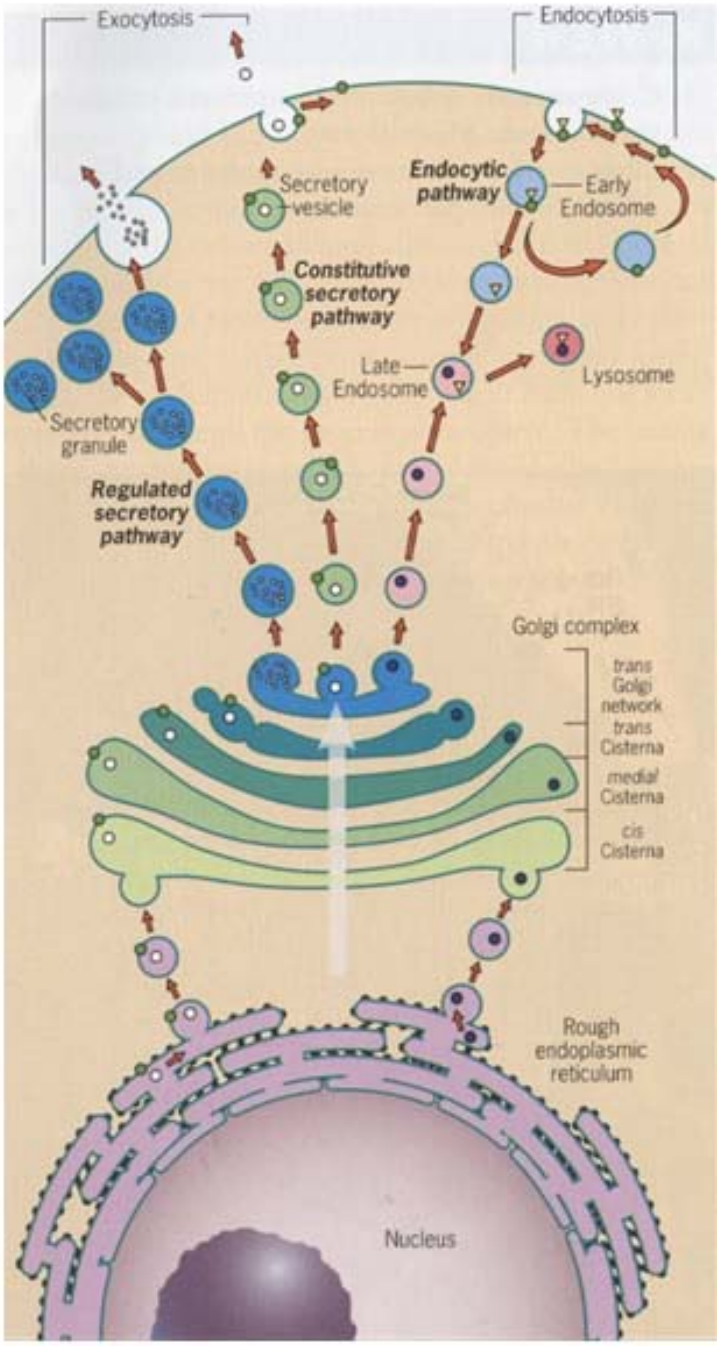

Figure 1.13: An overview of the secretory and endocytic pathways. *Proteins follow the secretory pathway from the ER, through the Golgi complex, out to a variety of intracellular sites such as lysosomes, endosomes, secretory vesicles, vacuoles, and the plasma membrane. Proteins follow the endocytic pathway from the cell surface to endosomes and lysosomes, where they are generally degraded by lysosomal enzymes (reviewed by Karp, 2005).*

The Golgi complex has a characteristic morphology consisting primarily of membranous cisternae, which are arranged in an orderly stack. It is divided into several functionally distinct compartments arranged along an axis from the *cis* or entry face closest to the ER to the *trans* or exit face at the opposite end of the stack. The *cis* face is composed of an interconnected network of tubules referred to as the *cis* Golgi network (CGN), which is thought to function primarily as a sorting station that distinguishes between proteins that have to return to the ER and those that can proceed to the next Golgi station. The major part of the Golgi complex consists of a series of cisternae. The *trans* face contains a distinct network of tubules and vesicles called the *trans* Golgi network (TGN), which is also a sorting station were proteins are segregated into different types of vesicles heading either to the plasma membrane or to various intracellular destinations. Two contrasting views exist concerning the way materials move through the various compartments of the Golgi complex. The vesicular transport model proposes that the cisternae of a Golgi stack remain in place as stable compartments and material is transferred through the Golgi stack in small transport vesicles. Electron microscopy recently revealed many vesicles associated with the Golgi complex, transporting proteins from one Golgi compartment to another. However, these vesicles are most likely involved in retrograde transport, retrieving ER or Golgi proteins from a later compartment and transporting them to an earlier compartment in the secretory pathway. This retrograde pathway may, in addition to the recycling of membrane and proteins back to the ER, play a role in the anterograde cargo concentration (reviewed by Pelham, 2001; Martínez-Menárguez *et al.*, 2001, Mironov *et al.*, 2001). The alternate model, known as the cisternal maturation model, proposes that Golgi cisternae are transient structures which are formed at the *cis* face of the stack by fusion of anterograde transport vesicles from the ER and the ERGIC. Each cisterna moves from the *cis* to the *trans* end of the stack, changing in composition as it progresses. This process does not involve budding off and fusion of anterograde transport vesicles. Each cisterna matures into the next cisterna along the stack (reviewed by: Klumperman, 2000, Pelham, 2001, Karp, 2005, Lodish *et al.*, 2007).

Three types of coated transport vesicles have been identified each with a different type of protein coat. They are named for their primary coat proteins and they transport cargo proteins from specific parent compartments to specific target compartments. COPII-coated vesicles transport proteins from the rER to the ERGIC and the Golgi complex. COPI-coated vesicles

mainly transport proteins in retrograde direction between Golgi cisternae and from the *cis*-Golgi and the ERGIC back to the rER. Clathrin-coated vesicles transport proteins form the plasma membrane and the TGN to late endosomes and lysosomes. All types of coated vesicles are formed by reversible polymerization of a distinct set of protein subunits onto a donor membrane to form vesicle buds that eventually pinch off from the membrane to release a complete vesicle. Shortly after vesicle release, the coat is shed and proteins required for fusion with the target membrane are exposed (reviewed by: Karp, 2005; Lodish *et al.*, 2007).

Although coat proteins differ considerably from one type of vesicle to another, the coats of all three types of vesicles contain a small GTP-binding protein that acts as a regulatory subunit to control coat assembly. Both COPI and clathrin vesicles contain the GTP-binding protein known as ARF protein. The related GTP-binding protein Sar1 is present in the coat of COPII vesicles. ARF and Sar1 are monomeric proteins. They both belong to the GTPase superfamily of proteins that switch between an inactive GDP-bound and an active GTP-bound form. The cycle of GTP binding and hydrolysis by ARF and Sar1 are thought to control the formation and dissociation of vesicle coats. The vesicle coat functions also in selecting specific proteins as cargo by means of direct binding to sorting signals contained within the cytosolic portion of membrane cargo proteins (reviewed by Lodish *et al.*, 2007).

As mentioned previously, shortly after the formation of a vesicle is completed, the coat is shed, exposing vesicle-specific membrane proteins crucial for the docking of the vesicle on its target membrane and the fusion of the vesicle membrane with the correct target membrane. A second set of GTP-binding proteins, the Rab proteins, engage in the targeting of vesicles to the appropriate target membrane. A different type of Rab protein appears to function for each type of vesicle and at every step of the secretory pathway. Each vesicle contains specific membrane proteins, known as v-SNARE proteins, which interact with t-SNAREs in the target membrane. The interaction of cognate SNAREs brings the two membranes into close apposition, allowing the two bilayers to fuse. After the fusion of vesicle and target membrane, the SNARE complexes must dissociate to make the individual SNARE proteins available for additional fusion events. The highly stable SNARE complexes are disassembled in an ATP-dependent reaction mediated by additional cytosolic proteins (reviewed by Lodish *et al.*, 2007).

The endocytic pathway describes the movement of materials from the plasma membrane into the cell interior. All eukaryotic cells continuously engage endocytosis, a process in which a small region of the plasma membrane invaginates to form a membrane-limited vesicle. One type of endocytosis is called pinocytosis, which describes the non-specific uptake of small droplets of extracellular fluids and any material dissolved in it. Receptor-mediated endocytosis brings about the uptake of specific extracellular molecular ligands following their binding to receptors on the external surface of the plasma membrane. The plasma membrane region that contains the receptor-ligand complex then buds inward and pinches off, becoming a transport vesicle (clathrin coated). Following internalization, vesicle-bound materials are transported to endosomes which represent distribution centers along the endocytic pathway. Endosomes are divided into two classes: early endosomes, which are located near the peripheral region of the cell, and late endosomes, which are located closer to the nucleus. Most receptor-ligand complexes dissociate in the late endosome. The receptors are recycled to the plasma membrane, while the ligands are delivered to the lysosomes (reviewed by: Karp, 2005; Lodish *et al.*, 2007).

The major function of lysosomes is to degrade extracellular materials taken up by the cell and certain intracellular components. Materials to be degraded must be delivered to the lumen of the lysosome, where the various degradative enzymes reside. The cell has two specialized pathways for delivery of membrane proteins and cytosolic materials to the lysosomal lumen. The first pathway is used to degrade endocytosed membrane proteins. These endocytosed membrane proteins are incorporated into specialized vesicles that bud into the lumen of the endosome, producing a multivesicular endosome. The surface membrane of a multivesicular endosome will eventually fuse with the membrane of a lysosome, delivering its internal vesicles and the membrane proteins they contain into the lysosomal lumen for degradation. The second pathway, known as autophagy, is employed by cells when they are placed under stress. Cells will recycle macromolecules for use as nutrients by a process of lysosomal degradation. Autophagy involves the formation of double-membraned structures that envelop regions of the cytosol or entire organelles, creating autophagosomes. The outer membrane of an autophagosome can fuse with the membrane of a lysosome, delivering a large vesicle to the interior of the lysosome. Lipases and proteases within the lysosome will degrade the autophagic vesicle and its contents into their molecular components (reviewed by Lodish *et al.*, 2007).

1.3.7. Protein 2C and its effect on membrane trafficking

Poliovirus 2C is a 329aa (~37 kDa) polypeptide and it is the most conserved polypeptide among picornaviruses with respect to amino acid sequence and antigenicity (Argos *et al.*, 1984, Emini *et al.*, 1985, reviewed by Carrasco *et al.*, 2002). 2C-like proteins have been identified in a number of other animal and plant viruses (Gorbalenya & Koonin, 1989). A tentative model of domain organization has been proposed for this protein based on sequence alignments. According to this model, 2C would have three differentiated regions: the central region includes an NTP-binding domain, while the N- and C-terminal parts have a α-helix configuration and might contain amphipathic helices (figure 1.14; Teterina *et al.*, 1997). Near the C-terminus, a cysteine-rich region is located, which displays a zinc finger motif that is conserved in enteroviruses and rhinoviruses and is essential for viral replication (Pfister *et al.*, 2000). The precursor 2BC remains largely uncleaved in picornavirus-infected cells and exerts some of the activities described for the mature proteins 2B and 2C (figure 1.11; reviewed by Carrasco *et al.*, 2002).

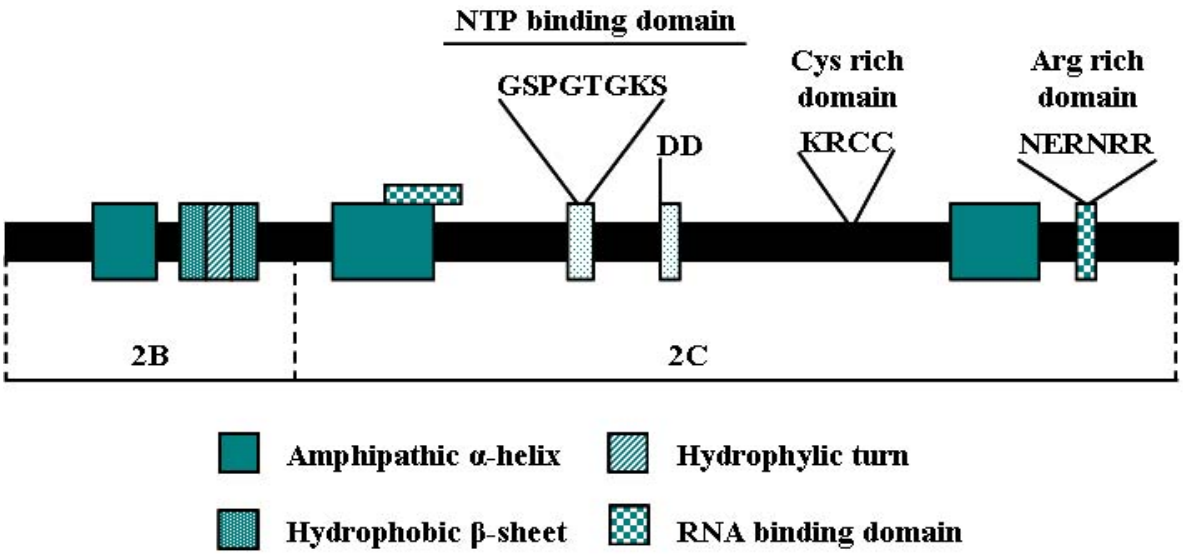

Figure 1.14: Linear map of poliovirus 2BC motifs. *Protein 2B contains 2 hydrophobic regions; one amphipathic α-helix and a potential transmembrane domain with a β-sheet configuration. Protein 2C contains functional domains for RNA and NTP binding.*

1.3.7.1 Membrane proliferation, rearrangement and binding

Several lines of evidence suggest that 2C is involved in membrane proliferation. Bienz and colleagues (1987) were able to follow the location of the proteins of the P2 genomic region in respect to the virus-induced vesicle formation and the viral RNA synthesis during the viral replication cycle. P2 proteins become rER associated soon after their synthesis. At the site of this interaction electron-dense patches appeared which represent the PV replication complex. Simultaneously, vesicles are formed which finally bud off, carrying the patches on their outer surface. Protein 2C is most likely involved in the attachment of the replication complex to the vesicular membranes (Bienz *et al.*, 1987). They were able to confirm these results by isolation of transcriptionally active replication complexes bound to smooth membrane vesicles from PV-infected cells. They demonstrated that the PV replication complex contains the P2 proteins in a membrane-associated form. Their findings allowed them to conclude that 2C or its precursor is responsible for the attachment of the viral RNA to the vesicular membrane and for the spatial organization of the replication complex necessary for its proper functioning in viral transcription (Bienz *et al.*, 1990).

Cho and colleagues (1994) described a system to examine the effects of expression of poliovirus 2C and 2BC in human cells in the absence of other PV proteins. Using a recombinant vaccinia virus system, they expressed 2C and 2BC, as well as the proteins with single point mutations in the NTP-binding motifs which were shown to inactivate viral RNA replication (Teterina *et al.*, 1992, Cho *et al.*, 1994). Both 2C and 2BC were able to induce the reorganization of intracellular membranes and the formation of vesicles, which resembled those found in PV-infected cells. They were both associated with these vesicles. Golgi stacks were absent in cells expressing 2C or 2BC as in PV-infected cells. Mutations in the NTP-binding motifs did not affect vesicle induction by 2C or 2BC (Cho *et al.*, 1994; Aldabe & Carrasco, 1995). Expression of 2BC in yeast cells also induces a number of morphological modifications, one of the most striking being the proliferation of small membranous vesicles (Barco & Carrasco, 1995).

To map the determinants of membrane binding and rearrangement in the 2C protein a computer-assisted analysis of the protein sequence was performed. This led to the prediction that the protein folds into a structure composed of three domains. Expression plasmids that

encode each or combinations of these predicted domains were constructed and the abilities of the expressed partial protein sequences to associate with intracellular membranes and to induce reorganization of these membranes were examined. Sequences from both the N-terminal and the C-terminal portions of the protein, but not the middle region, interact with intracellular membranes. The N-terminal portion of 2C is composed of a number of α-helices. One of these helices is a conserved amphipatic helix (Paul *et al.*, 1994) and is essential for association of the protein with membranes in an *in vitro* membrane binding assay (Echeverri & Dasgupta, 1995). Mutations in the N-terminal sequence, predicted to disrupt the amphipatic helix, were lethal, suggesting that membrane interaction of this region is important for 2C function (Paul *et al.*, 1994). The C-terminal portion of 2C is predicted to include two helices, with one of them also being a conserved amphipatic helix (Teterina *et al.*, 1997).

1.3.7.2 Nucleoside triphosphatase (NTPase) activity

An NTP-motif was identified in nonstructural proteins of several groups of positive-strand RNA-viruses, including picornaviruses. All the NTP-motif-containing proteins comprise several highly conserved sequence stretches. The two most prominent are the A (GXXXXGKS/T) and B (DD/E) motifs. In positive-strand RNA viruses, these proteins are homologous and the A and B sites are highly conserved. Therefore they should play the principal role in the functioning of the proteins (Gorbalenya *et al.*, 1989). Protein 2C is thought to be a member of the AAATPase super-family of proteins. Members of the AAA+ super-family are characterized by the presence of a Conserved ATPase Domain (CAD), containing well-conserved Walker A and B motifs for ATP binding (Walker et al., 1982; Swaffield & Purugganan, 1997). A third conserved C-terminal motif C has been described. Motif C consists of an invariant asparagine (Asn) residue preceded by a stretch of moderately hydrophobic residues. This C motif is common to a large family of NTP-binding pattern containing proteins (helicase superfamily III) encoded by the genomes of small DNA and RNA viruses. A helicase function has therefore been suggested for protein 2C but was not yet confirmed (Gorbalenya *et al.*, 1990, Rodriguez & Carrasco, 1993). All three motifs are required for the functional role of the NTP-binding motif of 2C in RNA replication (Mirzayan & Wimmer, 1992, Pfister & Wimmer, 1999). Analysis of the amino acid sequence of PV protein 2C shows homology to this family of NTP-binding proteins. Point mutations were engineered into the most conserved

residues in the A and B sites. Viral RNA synthesis is greatly reduced in cells transfected with these mutants. This strongly suggests a functional role for the proposed NTP-binding motif of 2C in RNA replication (Mirzayan & Wimmer, 1992).

The first direct evidence for this functional significance of the NTP-binding pattern in PV 2C was given by Teterina and colleagues (1992). They used genetic manipulation of PV cDNA clones, which produce infectious virus upon transfection cells. When conserved aa within the A or B motif of the NTP-binding pattern were replaced, even by similar residues, virus replication could not be detected. In contrast, similar mutations in non-conserved aa within the A motif did not prevent virus replication. These findings suggest that the conservation of the A and B motif within protein 2C may be functionally significant (Teterina *et al.*, 1992). A Baculovirus expression system has also been used to investigate potential enzymatic activities associated with protein 2C. A mutant carrying a lesion in the NTP-binding motif A has been expressed. This mutant is lethal, which suggest an NTPase activity for protein 2C (Mirzayan & Wimmer, 1994). Pfister and Wimmer (1999) demonstrated that the ATPase activity of protein 2C requires all three motifs A, B, and C. Mutations of conserved residues in motif A and B abolished ATPase activity, as did a mutation of the conserved Asn residue in motif C, an observation indicating the involvement of this motif in ATP hydrolysis (Pfister & Wimmer, 1999).

1.3.7.3 Guanidine sensitivity

The growth of many picornaviruses is selectively inhibited by guanidine hydrochloride. Although guanidine inhibits several virus-induced processes, the primary effect appears to be blockage of viral RNA synthesis. Several lines of evidence suggest that protein 2C may be the target for the antiviral action of guanidine. Guanidine-resistant FMDV mutants and poliovirus mutants have been described containing modifications in protein 2C. Pincus and Wimmer (1986) described the cloning of cDNA segments containing either the mutation for guanidine resistance or the mutations responsible for guanidine dependence into the PV wild-type background of an infectious clone. The viruses isolated from the transfected cells were found to express the resistance or dependence phenotypes, demonstrating that mutations in protein 2C are directly responsible for the altered guanidine sensitivity (Pincus & Wimmer,

1986, Baltera & Tershak, 1989). A variety of guanidine-resistant and guanidine-dependent PV strains were selected, and mutations responsible for the phenotypic alterations were mapped to the viral NTP-binding pattern (Tolskaya *et al.*, 1994, Pfister & Wimmer, 1999).

1.3.7.4 RNA binding activity

There is some evidence that protein 2C is an RNA binding protein. Gel retardation experiments indicate that protein 2C interacts with a partial double-stranded RNA molecule. Deletion mutants, which lack different portions of the 2C carboxyl terminus, were constructed and none of these mutants were able to interact with RNA. This indicates that the RNA binding domain lies at the C-terminal end of 2C (Rodriguez & Carrasco, 1993). These preliminary results were confirmed by Rodriguez and Carrasco (1995) by generating 20 variants of 2C and analyzing their RNA binding activities. They were able to indicate two regions in 2C involved in RNA binding: a N-terminal region and a C-terminal region containing an Arg-rich region, a well established RNA-binding motif that is found in several RNA-binding proteins. Deletion of either the N- or C-terminal RNA binding region of protein 2C abolished RNA binding (Rodriguez & Carrasco, 1995). Synthesis of positive-strand RNA is likely to start at the 3' end of the template RNA. Binding of bacterially expressed PV 2C to the 3' end of the negative-strand RNA was examined. It was demonstrated that 2C specifically binds to the 3' cloverleaf structure of the negative-strand RNA. The binding of 2C to the 3' cloverleaf of the negative-strand RNA is, however, greatly affected when the conserved sequence UGUUUU in "stem a" of the cloverleaf is altered. The 2C binding was greatly facilitated when this sequence was present in the context of a double stranded structure (Banerjee *et al.*, 1997). These results were confirmed by Banerjee and Dasgupta (2001) for different picornaviruses, such as HAV and HRV (Banerjee & Dasgupta, 2001). It has also been demonstrated that the 2C precursor, 2BC, also interacts with the 3'-terminal cloverleaf of the negative-strand RNA. Furthermore, it has been shown that the interaction of 2C/2BC with the negative strand 3'-terminal sequence does not only depend on an intact "stem a", but is equally influenced by the presence of an intact "stem b" within the negative-strand cloverleaf structure (Banerjee *et al.*, 2001)

1.4. Aims

* Poliovirus protein 2C has been investigated extensively, including its association with host cell membranes. Therefore, we wish to localize TMEV protein 2C in transfected and TMEV-infected cells.

* Protein 2C has been related to the changes in membrane trafficking in poliovirus infected cells. We therefore wish to identify interactions of TMEV protein 2C with host cell proteins.

* We wish to visualize the effect of TMEV infection on intracellular membranes and membrane trafficking by using cellular markers and live-cell imaging.

* We wish to express and purify TMEV protein 2C in order to produce an anti-TMEV-2C antibody to localize protein 2C in TMEV-infected cells.

2. Materials and methods

2.1. Cloning

2.1.1 Preparative restriction enzyme digests

Typically 2 µg of DNA was digested with 2 units of enzyme, in a final volume of 20 µl containing 2 µl of 10x restriction buffer. The reactions were incubated as per manufacturer's instructions.

2.1.2 Analytical restriction enzyme digests

In general 0.2 µg of DNA was digested with 1 unit of enzyme, in a total volume of 10 µl, including 1 µl of 10x restriction buffer. The reactions were incubated as per manufacturer's instructions.

2.1.3 Polymerase chain reaction

Specific DNA fragments were amplified by Polymerase Chain Reaction (PCR) using BIO-X-ACT™ DNA polymerase (Bioline Ltd, London, UK). BIO-X-ACT™ is a mixture of polymerases that possesses a 5'-3' DNA polymerase activity and 3'-5' proofreading activity which prevents misincorporations during primer extension. BIO-X-ACT™ also leaves an "A" overhang such that the primer extension products are suitable for effective integration in TA cloning vectors. Primers were designed to maintain a single open reading frame (table 2.1).

Primer name	***Primer sequence 5' to 3'***
TMEV-2BC-V5-FW	GGATCCATGCCTGTGCAGTCGGTTTTTCAG
TMEV-2C-V5-FW	GGATCCATGGGGCCTCTACGCGAGGCCAATGAG
TMEV-2C-V5-RV	TCTAGAGACTGGGCAACCAAGCTGTTCATTTTC
TMEV-2Cmut1-FW	GCTGGGCAAGGCCTATCTGTGACC
TMEV-2Cmut1-RV	GGTCACAGAGTTGCCTTGCCCAGC
TMEV-2Cmut2-FW	GTGATTATGAATAATCTACTAGGACAAAATCCC
TMEV-2Cmut2-RV	GGGATTTTGTCCTAGATTATTCATAATCAC

Lenti-TMEV-2BC-FW	GAAATGACTAGTATGCCTGTGCAGTCGGTTTTTCAG
Lenti-TMEV-2C-FW	GTCATGACTAGTATGGGGCCTCTACGCCAGGCCAATGAG
Lenti-TMEV-2C-RV	GTCTGGGGATCCCTGGGCAACCAAGCTGTTCAT
Lenti-FMDV-2B-FW	GACCTCACTAGTATGCCAAATGGAGCGCCCGAAAAGGCG
Lenti-FMDV-2C-FW	GAACTTACTAGTATGGGTGGAAACCATCAACCAGATGC
Lenti-FMDV-2C-RV	CCTGTGGGATCCACCATTTGGGCAAAGTATTTG
TMEV-2C-Pk-FW	GGAAAGCCGATCCCAAACCCTCTATTAGGTCTGGACTCCACCA TGCAACCTCAGGGGCCTCTACGC
TMEV-2C-Pk-RV	GGTGGAGTCCAGACCTAATAGAGGGTTTGGGATCGGCTTTCCA GGTTGCATGACATTGGGGCAAGC
TMEV-3D-RV	GTGGGGACAACTATTCCAACATTGG
TMEV-2B-FW-NheI	GAAATGAACGCTAGCCCTGTGCAGTCGGTT
TMEV-2C-RV-ApaI	GTCTGGTGGGGGCCCGGCAACCAAGCTGTTCATTTTCTT
TMEV-3A-FW-KpnI	AAGAAAGGTACCAGCTTGGTTGCCCAGTCC
TMEV-3D-RV-PmeI	GAATCATAGGTTTAAACAACTATTCCAACATTCCA
2C-Pk-FW-InFusion	CTGTCTACAACCTTCAACAGG
2C-Pk-RV-InFusion	ATAACGGGACAGAACTGCAG
2BC-FW-N-TAP	CATGATGGATCCGATATCATGGGGCCTGTGCAGTCG
2C-FW-N-TAP	CCCAATGGATCCGATATCATGGGGCCTCTACGCGAG
2BC-RV-N-TAP	ATTCTCTCTAGATCACGGGCCCAGCGCTGACTGGGC
C-TAP-FW	GCATCTGGTACCATGGAAAAGAGAAGATGG
C-TAP-RV	GCATCTCTTAAGGGATCCCCGGGAATTCCCCGG
2BC-FW-C-TAP	GATGTAGCGGCCGCTATGGGGCCTGTGCAGTCGGTT
2C-FW-C-TAP	AATGTCGCGGCCGCTATGGGGCCTCTACGCGAGGCC
2BC-RV-C-TAP	CAGTCTGATATCGACTGGCAACCAAGCTGTTCATT
TMEV-2BC-His-FW	GGATCCCCTGTGCAGTCGGTTTTTCAG
TMEV-2C-His-FW	GGATCCGGGCCTCTACGCGAGGCCAAT
TMEV-2C-His-RV	AAGCTTTGACTGGGCAACCAAGCTGTT
TMEV-2BC-bact-FW	GAAATGGGGATCCGACCTGTGCAGTCGGTTTTTCAG
TMEV-2C-bact-FW	GTCATGGGGATCCGAGGGCCTCTACGCGAGGCCAAT
TMEV-2C-bact-RV	CCAGTCGTCGACTCACTGGGCAACCAAGCTGTTCAT
T7	TAATACGACTCACTATAGGG
Tub-RV	GATATCTCTAGAGTATTCCTCTCCTTCTTCCTCACC
Lenti-Cherry-Tub-FW	GGATCCATGGTGAGCAAGGGCGAGGAGG
Lenti-Cherry-Tub-RV	ACTAGTTCATTAGTATTCCTCTCCTTCTTCC

Table 2.1: List of primers used for PCR. *Primers are designed to maintain a single open reading frame. Primer names and sequences are shown. Sequences are presented from 5' to 3' end.*

The PCR was undertaken in a 50 µl reaction mix containing 20ng of template DNA, 5 µl of 10x Optibuffer™ (Bioline Ltd, London, UK), 1 µl PCR nucleotide mix (10 mM of each dNTP, Promega, Southampton, UK), 4 units of BIO-X-ACT™ DNA polymerase (Bioline Ltd, London, UK), 40 pmol of both forward and reverse primer, 2 µl of 50 mM $MgCl_2$, and nuclease-free water up to a final volume of 50 µl. The PCR consists of a series of 35 cycles of amplification. Prior to the first cycle, an initial PCR activation step is carried out at 94°C for 3 min. Following this hold, the three-step cycles begin with a denaturation step at 94°C for 1 min. Denaturation is followed by an annealing step. In this step the reaction temperature is lowered so that the primers can attach to the single-stranded template DNA. The annealing temperature depends on the melting temperature (Tm) of the primers, and is usually between 50°C-64°C for 30 sec. The annealing step is followed by an extension/elongation step at 68°C for 1 min, and a final extension step at 68°C for 10 min. PCRs were performed in a GeneAmp® PCR system 9700 thermal cycler (Applied Biosystems, Foster City, CA, USA).

2.1.4 Agarose gel electrophoresis

Flat bed agarose gels of 1% [w/v] agarose (Biogene, Kimbolton, UK) were prepared with TAE buffer (40 mM tris-acetate, 1 mM EDTA), which contained ethidium bromide at a final concentration of 0.5 µg/ml. DNA samples were loaded onto the gel in agarose loading buffer (50% [v/v] glycerol, 0.005% [w/v] bromophenol blue). Electrophoresis was carried out at 100 to 120 V in TAE buffer and the DNA bands were subsequently visualized by illumination from an UV transilluminator.

2.1.5 Purification of DNA fragments from agarose gels

PCR-products or preparative restriction digests were loaded into preparation wells of flat bed agarose gels (described in section 2.1.4). The band of interest was excised and purified using the QIAquick Gel Extraction Kit (Qiagen, West Sussex, UK), as directed by the manufacturer's instructions.

2.1.6 TOPO® cloning

To facilitate the preparative restriction enzyme digests necessary for further cloning steps, PCR-products were inserted into pcDNA3.1/V5-His-TOPO® (figure 2.1; Invitrogen, Paisley, UK). The TOPO vector is linearized with single 3' thymidine (T) overhangs for TA cloning. The BIO-X-ACT™ DNA polymerase (Bioline Ltd, London, UK) used for the PCRs has a nontemplate-dependent terminal transferase activity that adds a single deoxyadenosine (A) to the 3' ends of PCR products. This allows PCR inserts to ligate efficiently with the TOPO vector. The TOPO cloning reaction was undertaken in a final volume of 6 µl containing 3 µl PCR-product, 1 µl salt solution, 1 µl sterile water, and 1 µl TOPO® vector. After 30 to 60 min incubation at room temperature (RT, 22-23°C), a transformation was carried out using *E. coli* compentent cells (JM109; described in section 2.1.9).

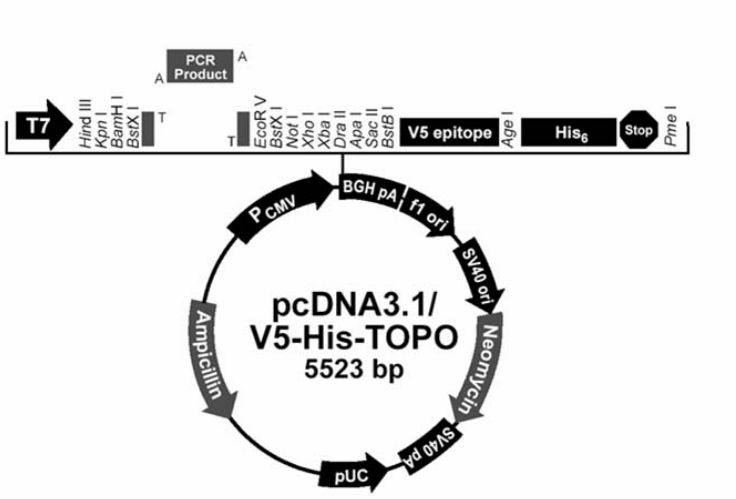

Figure 2.1: pcDNA3.1/V5-His-TOPO vector map: *the map summarizes the features of the pcDNA3.1/V5-His-TOPO© vector (Invitrogen, Paisley, UK).*

2.1.7 Dephosphorylation of linearized plasmid DNA

Calf intestinal alkaline phosphatase (CIAP, Promega, Southampton, UK), catalyzes the hydrolysis of 5'-phosphate groups of DNA. It is used to prevent recircularization and religation of linearized plasmid DNA by removing phosphate groups from both 5'-termini. CIAP is active on 5' overhangs, 5' recessed and blunt ends. Briefly, a reaction containing 40 µl purified DNA (up to 10 pmol of 5'-ends), 5 µl CIAP 10x reaction buffer and up to 5

µl diluted CIAP (0.01 u/µl), was incubated at 37°C for 30 min. The reaction was stopped by adding 0.8 µl of EDTA (0.5 M) and the DNA was subsequently purified using the Wizard® SV gel and PCR clean up kit (Promega, Southampton, UK).

2.1.8 Ligation of DNA

Ligation reactions were set up in 10x T4 DNA ligase buffer (660 mM Tris-HCl, 50 mM $MgCl_2$, 50 mM DTT, 10 mM ATP, pH 7.5) at a final volume of 10 µl. In general the reaction consisted of 1 µl of T4 DNA ligase (Roche Diagnostics Ltd., Burgess Hill, UK), 0.5 µg of plasmid DNA and an equal to 2-fold concentration of insert. The reactions were incubated overnight at 4°C.

2.1.9 In-Fusion PCR cloning

The In-Fusion™ 2.0 Dry-Down PCR Cloning kit (Clontech Laboratories, Inc., Mountain View, USA) was used as an alternative strategy for cloning. The In-Fusion mechanism is ligation-independent and uses the unique properties of the 3'-5' exonuclease activity of the poxvirus DNA polymerase. PCR primers are designed that have at least 15 bases of homology with sequences flanking the desired site of insertion in the cloning vector. The DNA insert is amplified by PCR, as described in section 2.1.3, and subsequently cloned into the cloning vector, as per manufacturer's instructions (figure 2.2). The 3'-5' proofreading activity of the poxvirus DNA polymerase removes nucleotides from the 3' end when incubated with linear duplex DNAs with homologous ends. Complementary regions on the substrate DNAs are therefore exposed that can spontaneously anneal through base pairing. Introduction into *E. coli* repairs the single stranded gaps (Zhu *et al.*, 2007).

In brief, 2 µl of Cloning Enhancer is added to 5 µl of PCR reaction. The mixture is incubated at 37°C for 15 min, and subsequently incubated at 80°C for 15 min. The treated PCR fragment is then mixed with the cloning vector at a 2:1 molar ratio in 10 µl of deionized H_2O, and this mixture is subsequently added to the dried-down In-Fusion enzyme. The In-Fusion reaction mixture is incubated at 37°C for 15 min, followed by 15 min incubation at 50°C. The In-Fusion reaction mixture is subsequently diluted with 40µl TE buffer (10mM Tris pH 7.4, 1 mM EDTA pH 8) and used to transform competent *E. coli* cells (as described below).

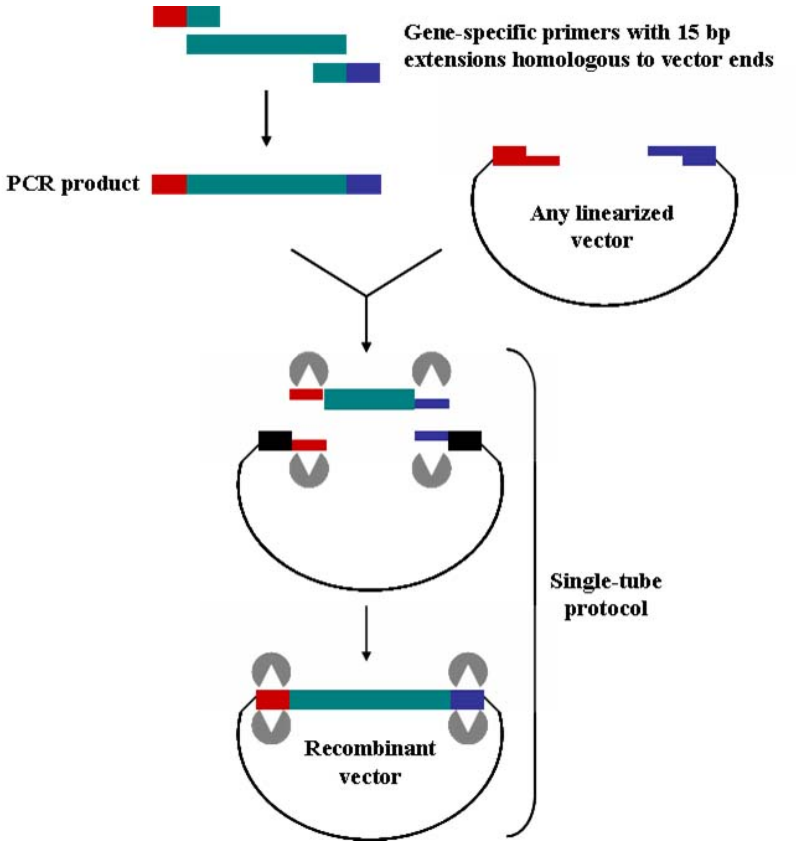

Figure 2.2: The In-Fusion cloning method. *The In-Fusion enzyme produces single-stranded PCR-fragment and vector ends that are fused due to the 15 bp homology.*

2.1.10 Transformation of E. coli competent cells

Competent *E. coli* cells (JM109) were purchased from Promega (Southampton, UK) and transformed using the heat-shock method. In a chilled 1.5 ml microcentrifuge tube, 2 µl of a ligation reaction were added to 50 µl of competent cells. The tubes were flicked gently to mix the contents and placed on ice for 10 minutes. Heat-shock was performed in a water bath at 42°C for 45 seconds. The tubes were immediately returned to ice for 2 minutes. Prior to incubating the transformation reaction for 1 hour at 37°C, 800 µl of Luria Broth (LB; 1% [w/v] bacto-tryptone, 0.5% [w/v] bacto-yeast extract, 1% [w/v] NaCl pH 7.0) was added. The cells were subsequently plate on agar supplemented with 100 µg/ml ampicillin (Amp).

2.1.11 Mini-preparation of plasmid DNA

A single colony was used to inoculate 5 ml of LB medium containing 100 μg/ml Amp and grown overnight at 37°C with moderate shaking. Plasmid DNA was prepared using the QIAprep Miniprep kit (Qiagen, West Sussex, UK), as directed by the manufacturer's protocol.

2.1.12 Maxi-preparation of plasmid DNA

In general, a single colony was used to inoculate an eight hour 5 ml starter culture (5 ml of LB containing 100 μg/ml Amp). An overnight 100 ml culture (100 ml of LB containing 100 μg/ml Amp) was then inoculated with 200 μl starter culture. The plasmid DNA was purified using the Qiafilter Plasmid Maxi kit (Qiagen, West Sussex, UK), following the manufacturer's protocol, and resuspended in water.

2.1.13 DNA sequencing

Double stranded plasmid DNA (300 ng) or PCR product (40 ng), supplemented with 3.2 pmol of sequencing primer was submitted to The Sequencing Service, University of Dundee.

2.2. Analysis of translation profiles

2.2.1 Coupled transcription/translation (T_NT) reaction

Proteins were expressed *in vitro* using the $T_NT^{®}$ Wheat Germ Extract System (Promega, Southampton, UK), following the manufacturer's protocol. In summary, proteins were radiolabelled with [^{35}S]-methionine. T_NT reactions were incubated at 30°C for 60 to 120 min. The reactions were stopped by adding an equal volume of 2x SDS-PAGE sample loading buffer (2% [w/v] SDS, 20% [v/v] glycerol, 2% [v/v] β-mercaptoethanol, 0.2% bromophenol blue, 100 mM Tris, pH 6.8), and analyzed on sodium dodecyl sulfate (SDS) denaturing polyacrylamide gel electrophoresis (PAGE) gels (10% polyacrylamide, described in section 2.2.3).

2.2.2 *Immunoprecipitation with T_NT samples*

Prior to addition to the T_NT samples, the antibody was bound to the affinity media. Protein G Sepharose 4 Fast Flow (GE Healthcare, Chalfont St Giles, UK) was used as affinity media. Prior to the binding of the antibody, the beads were prepared in phosphate-buffered saline (PBS). Three wash steps were carried out with PBS to remove the ethanol in which they were supplied. Between washes the beads were recovered by centrifugation at 10 000 xg for 1 min. A 50% slurry was prepared by adding an equal volume of PBS and the beads were stored at 4°C. To 100 µl of 50% bead solution, 20 µl of antibody was added. The antibody was bound to the beads by rotating for 2 hours at 4°C. After rotation, the bead/antibody complex was washed 4 to 5 times with PBS containing 0.1% [v/v] Nonidet-P40 (N-P40). The complex was recovered between washes by centrifugation at 10 000 xg for 1 min. After the final wash step, the pellet was resuspended in an equal volume of PBS containing 10 mg/ml bovine serum albumin (BSA, Sigma-Aldrich Company Ltd., Dorset, UK) and rotated for 30 min at 4°C. The complex was recovered by centrifugation at 10 000 xg for 1 min, and again resuspended in an equal volume of PBS containing BSA.

For the immunoprecipitation reaction, 1 ml of binding buffer (50 mM Magnesium acetate, 20 mM Tris-HCl pH 7.4, 1mM DTT, 0.05% N-P40, 10 mg/ml BSA) and 10 µl of T_NT sample were added to 50 µl of the 50% solution of antibody/bead complex and rotated for a minimum of 1 hour at 4°C. The precipitated antigen complexes were washed 5 times with wash buffer (50 mM Magnesium acetate, 20 mM Tris-HCl pH 7.4, 1 mM DTT, 0.05% N-P40). The complex was recovered between washes by centrifugation at 10 000 xg for 1 min. After the final wash step, the pellet was resuspended in 10 µl of 2x SDS-PAGE sample loading buffer and the complexes were dissociated at 100°C for 2 min. The beads were pelleted by centrifugation (10 000 xg) for 1 min and the supernatant was analyzed on SDS-PAGE gel (10% polyacrylamide, described in section 2.2.3).

2.2.3 *Denaturing SDS polyacrylamide gel electrophoresis (SDS-PAGE)*

The gels were constructed with a 4% polyacrylamide stacking gel and a 10% polyacrylamide resolving gel. The gel was run using a Hoefer® apparatus (Amersham Biosciences, Buckinghamshire, UK). Electrophoresis was carried out in 1x Tris-Glycine buffer (0.1%

[w/v] SDS, 25 mM Tris, 250 mM Glycine) at a constant current of 40 mA, until the Bromphenol blue dye reached the bottom of the gel. Proteins were stained with Coomassie brilliant blue staining solution (0.2% [w/v] Coomassie brilliant blue (R-250), 20% [v/v] methanol, 20% [v/v] acetic acid). Gels were subsequently destained (20% [v/v] methanol, 10% [v/v] acetic acid) and dried as appropriate.

2.2.4 Visualization of radiolabelled translation products

The distribution of radiolabel between the translation products was visualized by autoradiography on Kodak Biomax MR film (Sigma, Southampton, UK) for preparation of figures.

2.3. Cell culture

2.3.1 Growing cells from liquid nitrogen stock

Aliquots removed from liquid nitrogen storage were defrosted quickly in a water bath. The samples were centrifuged (300 xg) for 3 min and the supernatant was discarded. The cells were resuspended in 1 ml Dulbecco's modified Eagle's medium (DMEM, Sigma-Aldrich Company Ltd., Dorset, UK) containing 10% foetal calf serum (FCS, Invitrogen, Paisley, UK), and added to a 75 cm^2 tissue culture flask (Greiner Bio-One Ltd., Stonehouse, UK) containing DMEM supplemented with 10% FCS. The cells were incubated overnight at 37°C in a 5% CO_2 humidified incubator. The following day the medium was removed, the cells were washed twice with PBS, fresh medium was added and the flasks were returned to the incubator.

2.3.2 Splitting cells

To split cells, the medium was poured off and residual medium was removed by washing quickly with PBS. Trypsin/EDTA (Becton Dickinson, Plymouth, UK), a buffered salt solution containing 0.5% (w/v) trypsin and 0.2% (w/v) EDTA, was added to dissociate the adherent cells. After a short period of time, 10 ml of medium (DMEM containing 10% FCS) was added to the flask to inactivate the trypsin and the cells were subsequently dispersed by agitation. The cell suspension was transferred to a 15 ml tube and a 3 min

centrifugation at 750 xg was carried out, followed by the removal of the supernatant. The cell pellet was resuspended in 10 ml of medium (DMEM containing 10% FCS). To a fresh flask (75 cm²) containing 10 ml of DMEM supplemented with FCS at 10%, 2 ml of cell solution was added. Cells were maintained in 75 cm² flasks at 37°C in a 5% CO_2 humidified incubator.

2.3.3 Freezing cells

Once cells in a 75 cm² flask were 100% confluent (± 8-10x10^6 cells), a cell splitting procedure was carried out as described above until the stage where a pellet is formed. The supernatant was removed and the pellet was resuspended in 1 ml of medium (DMEM containing 10% FCS). Subsequently, 9 ml of medium consisting of 40% DMEM, 40% FCS, and 20% dimethyl sulfoxide (DMSO) was gradually added. The cell suspension was divided into 1 ml aliquots, resulting in ± 500 000 to 1 million cells/ ml. Cells were frozen down slowly overnight in an insulated cell rack at -70°C. After 1 to 2 days cells can be transferred to liquid nitrogen for extended storage.

2.4. TMEV virus stock

2.4.1 Preparation of TMEV virus stock

Monolayers of BHK-21 cells (baby hamster kidney cells) were grown in a 75 cm² tissue culture flask (DMEM supplemented with 10% FCS) until 80% confluence. The medium was removed and the cells were washed twice with serum-free DMEM. Virus stock (0.5 ml; 5x10^8 PFU/ml stock) was added to 2 ml of serum-free DMEM before adding the mixture to the flask containing the cells. The cells were incubated in the presence of the virus for 20 min, at 37°C, with rocking. The medium was removed, replaced with 10 ml DMEM supplemented with 1% FCS and 0.2 ml of 1M HEPES, and the cells were incubated overnight, at 37°C, with rocking. The cells in medium were transferred by pipette into a 50 ml centrifuge tube. Centrifugation (3500 xg) for 5 min pelleted cellular material and the supernatant, containing released virus, was recovered. The cell pellet was resuspended in 5 ml DMEM and any intact cells were lysed by vortexing and freeze/thawing at -80°C.

Aliquots were transferred to microcentrifuge tubes, the cell debris pelleted (14 000 xg, 5 min) and the supernatant recovered. The two supernatants were combined and stored in aliquots at -70°C. Typical virus titres achieved by this method were $5x10^8$ PFU/ml.

2.4.2 Titration of TMEV virus preparation

Monolayers of BHK-21 cells were grown in 6-well plates (Greiner Bio-One Ltd., Stonehouse, UK) until 80 to 90% confluence. The virus preparation was diluted in a series of 10-fold dilutions in DMEM supplemented with 1% FCS. Duplicate wells of cells were set up for each dilution, and cells were inoculated with each virus stock dilution (1ml/well). The cells were incubated with the virus inoculum for 1h (37°C, 5% CO_2) on a rocking platform to allow adsorption of the virus. The virus inoculum was aspirated and 2ml of overlay, consisting of 4% agar (SeaPlaque® agarose, Lonza Ltd., Nottingham, UK) mixed with DMEM (1% FCS) were added to each well. The agar was allowed to set, and an overlay of 2ml DMEM containing 1% FCS was added. The cells were incubated for 2 days (at 37°C, 5% CO_2) without any mechanical action. When plaques were distinctly formed, the medium was aspirated and the monolayers were fixed overnight in 5% formaldehyde. After aspirating the fixative solution, the agar overlay was removed and the fixed cells were washed with PBS. Areas of cell lysis and therefore sites of virus infection or plaques were visualized by Coomassie blue staining (1h). After gently washing the monolayers with water, plaques were observed as unstained areas of the monolayer. Plaques were counted and the titer was estimated (plaque-forming-units per ml of virus preparation, pfu/ml), taking into account the dilutions made.

2.4.3 TMEV production from cDNA clone

2.4.3.1 Plasmid linearization

The plasmid carrying the viral cDNA was linearized using a restriction enzyme cleaving at a unique restriction site after the 3' end of the viral genome. The linearized DNA was purified using the Wizard® PCR preps DNA purification system (Promega, Southampton, UK), following the manufactures guidelines. The DNA was resuspended in RNase free H_2O.

2.4.3.2 In vitro transcription

The linearized plasmid DNA was transcribed *in vitro* using a T7 RNA polymerase (Roche Diagnostics Ltd., Burgess Hill, UK). In summary, the *in vitro* transcription reaction was undertaken in a 25 µl reaction mix containing 400 to 500 ng of linearized plasmid DNA, 10x transcription buffer (supplied with T7 RNA polymerase), ribonucleotides triphosphate (2.5 mM of A, C, G and U; Ribonucleoside triphosphate set, Roche Diagnostics Ltd., Burgess Hill, UK), Protector RNase inhibitor (optional, Roche Diagnostics Ltd., Burgess Hill, UK) and T7 RNA polymerase (Roche Diagnostics Ltd., Burgess Hill, UK). The reaction is incubated for 1 hour at 37°C. The *in vitro* transcribed RNA can be stored at -80°C until needed for cell electroporation. A 5 µl sample was run on a 1% agarose gel to evaluate the quality of the *in vitro* transcribed RNA.

2.4.3.3 Electroporation of BHK-21 cells

For one *in vitro* transcribed viral RNA reaction, two 75 cm² flasks of confluent BHK-21 cells were trypsinized and resuspended in complete medium (DMEM containing 10% FCS). Cells were centrifuged for 5 min at 200 xg. The cell pellet was washed twice with ice-cold sterile PBS and subsequently resuspended in ice-cold sterile PBS (750 µl per electroporation). Electroporation cuvettes and sterile eppendorf tubes containing 10 to 20 µl of in vitro transcribed RNA (2-20 µg) were prepared on ice. Subsequently, 750 µl of cell suspension was transferred to the RNA containing eppendorf tube. The cell and RNA mixture was rapidly transferred to the electroporation cuvette. Electroporation was carried out using the Gene pulser Xcell^{TM} system (Bio-Rad Laboratories Ltd., Hertfordshire, UK, described in section 2.5.3.2). The cells were resuspended in 10 ml DMEM, supplemented with 10% FCS, and transferred to a 75 cm² flask. After 6 to 7 hours, the medium was replaced by 10 ml serum-free medium.

2.4.3.4 Virus harvest

In general, the cells attach and grow normally for 24 hours after electroporation, at which point they nearly reach 100% confluency. The cytopathic effect (CPE) progressively takes place from 24 to 48 hours and becomes complete between 48 and 72 hours after

electroporation. When CPE was complete, the cells were collected with supernatant in a 15 ml Falcon tube, and were frozen at -80°C for at least 8 hours. The tubes were thawed at RT or in a 37°C water bath, mixed vigorously, and centrifuged at 1200 xg for 15 min at 4°C. The supernatant was transferred to a new tube and subsequently aliquoted in cryotubes for storage at -80°C. In general, yields are between $5x10^7$ and $5x10^8$ PFU/ml.

2.4.3.5 RNA extraction and detection of viral RNA

RNA was extracted from the viral preparations by using the QIAamp® Viral RNA mini kit (Qiagen, West Sussex, UK) as per manufacturer's instructions. The extracted RNA was subsequently used as template for one-step PCR assays (QIAGEN® OneStep RNA-PCR kit, Qiagen, West Sussex, UK). The one-step RT-PCRs were undertaken in a 50 µl reaction volume containing 10 µl RNA-extract, 10 µl 5x QIAGEN OneStep RT-PCR Buffer, 2 µl dNTP mix (final concentration of 400 µM of each dNTP), 2 µl QIAGEN OneStep RT-PCR Enzyme Mix (a combination of Omniscript and Sensiscript reverse transcriptase and HotStarTaq DNA polymerase), 1.5 µM of each primer, and RNase-free water to 50 µl. The reaction was carried out with an initial reverse transcription step at 50°C for 30 min, followed by PCR activation at 95°C for 15 min, 35 cycles of amplification (30 sec at 94°C; 30 sec at 56°C; 1 min at 72°C), and a final extension step at 72°C for 10 min.

2.5. Mammalian protein expression

The process of introducing nucleic acids into eukaryotic cells by nonviral methods is defined as "transfection". Using various chemical, lipid or physical methods, this gene transfer technology is a powerful tool for studying gene function in the context of a cell. Essentially, transfection is a method that facilitates the introduction of negatively charged molecules (phosphate backbone of DNA) into cells with negatively charged membranes. The use of viruses as vectors is an alternative method for delivery of genes into cells. lentiviruses (e.g. HIV-1) are of particular interest because they have been well studied and can integrate into the host cell genome to allow stable, long-term expression of the transgene (described in section 2.9; Anson, 2004).

2.5.1 Chemical reagents

A cationic polymer is used to tightly associate with the negatively charged nucleic acids. An excess of positive charge, contributed by the polymer in the DNA/polymer complex, will allow the complex to come into closer association with the negatively charged cell membrane. Uptake of the complex is presumably established by endocytosis.

2.5.1.1. ExGen 500 in vitro transfection reagent

The ExGen 500 *in vitro* transfection reagent (Fermentas, York, UK) is a sterile solution of linear polyethylenimine (PEI, cationic polymer) molecules in water. It is a non-viral, non-liposomal reagent that is capable of transfecting a wide variety of cell types. ExGen 500 has low toxicity and works efficiently in the presence or absence of serum. The efficient gene transfer is related to its capacity for condensing DNA, interacting with the cell membrane, protecting DNA and inducing endosomal swelling and rupture before DNA degradation can occur. ExGen 500 and DNA charge-interact and form small, stable, highly diffusible particles that settle on the cell surface. The ExGen 500/DNA complex is then absorbed into the cell by endocytosis, followed by the release of the complex into the cytoplasm via rupture of the vesicles and the translocation of the DNA to the nucleus.

Prior to transfection, cells were plated to achieve a cell density of 50-70% at the time of transfection. The plasmid DNA was diluted in 150 mM NaCl (see manufacturer's protocol for guidelines), vortexed gently and spun down briefly. ExGen 500 was added and the solution was vortexed immediately for 10 sec after which the ExGen 500/DNA mixture was incubated for 10 min at RT. The ExGen 500/DNA mixture was subsequently added to the cells. The plate was gently rocked to achieve even distribution of the complexes, and centrifuged for 5 min at 300 xg. The plates were then transferred to the incubator for 24 to 48 hours.

2.5.1.2. GeneJuice® transfection reagent

The GeneJuice® transfection reagent (Novagen, Nottingham, UK) is a proprietary formulation optimized for maximal transfection efficiency, ease of use, and minimal cytotoxicity. It is composed of a nontoxic cellular protein and a small amount of a novel polyamine. The

unique chemistry provides the advantage of compatibility with both serum-containing and serum-free media, and makes media changes unnecessary.

Prior to transfection cells were seeded to achieve a cell density of 50-80% at the time of transfection. Initially a GeneJuice®:DNA ratio of 3:1 was used. Different ratios can be used for optimalization (see manufacturer's protocol for guidelines). GeneJuice® transfection reagent was diluted with serum-free medium. GeneJuice® was added drop-wise to the serum-free medium and mixed thoroughly by vortexing. The GeneJuice®/serum-free medium mixture was incubated at RT for 5 min. DNA was added to the GeneJuice®/serum-free medium mixture and mixed gently by pipetting. The GeneJuice®/DNA mixture was incubated at room temperature for 5-15 min. The entire GeneJuice®/DNA mixture was added in a drop-wise manner to the cells in complete growth medium. The dish was gently rocked to ensure even distribution. The cells were incubated for 24 to 72 hours at 37°C (5% CO_2).

2.5.2 Cationic lipids

Liposome-mediated transfection offers advantages such as relatively high efficiency of gene transfer, and ability to transfect certain resistant cell types. Synthetic cationic lipids are used to deliver DNA into cells. The cationic head group of the lipid compound associates with the negatively charged nucleic acids, resulting in an overall positively charged liposome/nucleic acid complex. Closer association of the complex with the negatively charged cell membrane will occur, producing a higher transfer efficiency. Entry of the liposome complex into the cell may occur by endocytosis or fusion with the plasma membrane (Gao & Huang, 1995). Following cellular internalization, the complexes appear in the endosomes, will be released from the endosomes by a so far unclear mechanism, and will later appear in the nucleus.

2.5.2.1. FuGENE 6 transfection reagent

The FuGENE 6 transfection reagent (Roche Diagnostics Ltd., Burgess Hill, UK) is a proprietary blend of lipids and other components that forms a complex with DNA, and then transports it into animal cells. Transfections can be carried out in serum-containing media.

One day before the transfection experiment, cells were plated so that overnight incubation achieved the desired density of 50 to 80% confluency. Initially a FuGENE 6:DNA ratio of 3:1 was used. Different ratios can be used for optimalization (see manufacturer's protocol for guidelines). FuGENE 6 reagent was diluted with serum-free medium. The order and manner of addition is critical. Serum-free medium must be pipetted first, followed by the addition of FuGENE 6 directly into the medium without allowing contact with the walls of the plastic tubes. The tube was flicked to mix and subsequently incubated for 5 minutes at room temperature. DNA was added to the diluted FuGENE 6, the tube was tapped to mix the contents and the transfection reagent/DNA complex was incubated for 15 to 45 min. The complex was then added to the cells in a drop-wise manner. The wells or flasks were swirled to ensure distribution over the entire plate surface, and finally returned to the incubator for 24 to 48 hours to allow gene-expression.

2.5.2.2. Trans IT®-LT1 transfection reagent

The *Trans* IT®-LT1 transfection reagent (Mirus, Cambridge BioScience, Cambridge, UK), a broad spectrum protein/polyamine based reagent that contains histone and a unique lipid, provides high efficiency and cell viability. Transfections do not require media changes and can be carried out in serum-containing media.

Approximately 24 hours prior to transfection, cells were plated so that overnight incubation resulted in 50 to 70% confluency. In a sterile plastic tube, the *Trans* IT®-LT1 reagent (2-8 µl per 1 µg DNA, see manufacturer's protocol for guidelines) was added directly into 250 µl of serum-free medium, and mixed by gentle pipetting. The mixture was incubated at room temperature for 5 to 20 min. The plasmid DNA was added to the diluted *Trans* IT®-LT1 reagent, mixed by gentle pipetting, and incubated at room temperature for 15 to 30 min. The *Trans* IT®-LT1 reagent/DNA complex was added to the cells in a drop-wise manner. The plate was gently rocked to distribute the complexes evenly and returned to the incubator for 24 to 48 hours.

2.5.3 Transfection by electroporation

The mechanism for entry into the cell by electroporation is based upon perturbing the cell membrane by an electrical pulse, which forms pores that allow the passage of nucleic acids into the cell. The technique requires fine-tuning and optimization for duration and strength of the pulse for different cell types. Electroporation also requires more cells than chemical methods because of substantial cell death, and extensive optimization is often required to balance transfection efficiency against cell viability.

2.5.3.1. Cell line nucleofector® kit L

The Nucleofector technology (Amaxa GmbH, Koeln, Germany) is a highly efficient non-viral method for transfection. It is based on two components: the Nucleofector device that delivers unique electrical parameters, and Nucleofector Kits that contain cell-type-specific Nucleofector Solutions. The electrical parameters for particular cell types are pre-programmed into the Nucleofector so that optimization of the electrical parameters is not necessary.

The cell line nucleofector® kit L (Amaxa GmbH, Koeln, Germany) provides a protocol optimized for BHK-21 cells. Monolayers of BHK-21 cells were cultured one day prior to nucleofection with a subcultivation ratio of 1:2. Cells were used at 90% confluency. The cells, $1x10^6$ cells/100 µl of Nucleofector solution, were combined with the plasmid DNA (2µg) and then transferred to an Amaxa certified cuvette, following the manufacturer's optimized protocol. The cell-specific program was chosen and the cuvette was inserted into the Nucleofector and the program was started. The cuvette was rinsed with culture medium and the cells were transferred into a culture dish (75 cm² flask), which was incubated for 24 hours in a humidified 37°C/5% CO_2 incubator.

2.5.3.2. Gene pulser Xcell™ system

The Gene pulser Xcell™ system (Bio-Rad Laboratories Ltd., Hertfordshire, UK) is a flexible, modular pulse delivery system that uses exponential or square-wave pulses to deliver the pulses optimal for different cell types. It presents specific pre-tested parameters for the most frequently used cell lines, including BHK-21 cells. Electroporation was carried out following the manufacturer's protocol. Briefly, one day before electroporation, cells were cultured to

achieve 50 to 70% confluency at the time of the experiment. Cells were harvested and resuspended in electroporation buffer (Opti-MEM® I Reduced Serum Medium (1X), liquid- with GlutaMAX™ I; Invitrogen, Paisley, UK). The required plasmid DNA (10-50 µg/ml) was added to Bio-Rad's high-quality electroporation cuvettes, and the cells were added subsequently. The cuvette was placed in the ShockPod and the cells were pulsed using the pre-set protocol for BHK-21 cells. Immediately after the pulse, the cells were transferred to a 75 cm² flask. The 75 cm² flasks were rocked to assure even distribution of the cells over the surface of the plate and then incubated for 24 to 48 hours at 37°C in a humidified atmosphere.

2.6. Analyses of proteins expressed in mammalian cells

2.6.1 Lysis of cells and purification of proteins

Cells were harvested 24 to 48 hours after transfection. The medium was removed; the cells were washed with chilled PBS and harvested in 5ml PBS. The cells were transferred to a 15 ml centrifugation tube and centrifuged at 400 xg for 5 to 10 min. The supernatant was removed and the pellet was resuspended in 750 µl chilled lysis buffer (20 mM Tris pH 7.8, 650 mM NaCl, 5 mM EDTA, 0.5% N-P40, protease inhibitor cocktail tablet [Complete, Mini, EDTA-free; Roche Diagnostics Ltd., Burgess Hill, UK]). After sonication, the cell debris was pelleted by centrifugation at 10 000 xg for 40 min, and the supernatant was thereafter transferred to a fresh 1.5 ml tube.

2.6.2 Western blotting

Immediately after SDS-PAGE electrophoresis (as described in section 2.2.3), polypeptides were transferred to PVDF membranes (Immobilon™-P Transfer membranes, Millipore Corporation, UK). The membrane was methanol-activated during 10 to 15 min, rinsed with dH_2O and washed in transfer buffer (2.9 g glycine, 5.8 g Tris base, 0.37 g SDS, 200 ml methanol in 1 liter dH_2O). A blotting sandwich was prepared as follows: 1 fiber pad, 1 Whatmann 3MM paper, membrane, protein gel (all air bubbles must be removed), 1 Whatmann 3MM paper, 1 fiber pad. Both fiber pad and Whatmann 3MM paper were pretreated by soaking in transfer buffer. The blotting sandwich was placed in the blotting

apparatus and a constant current was applied (30 mA overnight or 400 mA for 1 hour). Following electroblotting, the membrane was incubated in blocking buffer (5% [w/v] skimmed milk powder, 0.1% [v/v] Tween 20 in PBS) for 1 hour. The proteins of interest were detected by incubating the membrane with an appropriately diluted primary antibody (in blocking buffer, 1:1000) for at least 1 hour. The membrane was washed three times with blocking buffer for 10 to 15 min. In order to detect bound primary antibodies, the membrane was incubated with the appropriate secondary HRP-conjugated antibody (in blocking buffer, 1:3000). After 45 min the membrane was rinsed (briefly) with wash buffer (0.1% [v/v] Tween 20 in PBS), incubated for 15 min in wash buffer, and subsequently washed twice for 10 min with wash buffer. The bound HRP-conjugated secondary antibodies were detected by enhanced chemiluminescence (ECL plus Western Blotting Detection System, Amersham Biosciences, Buckinghamshire, UK), following the manufacturer's instructions, and visualized on Kodak Biomax MR film (Sigma, Southampton, UK).

2.6.3 Fixing cells

Cells grown in DMEM medium supplemented with 10% FCS on coverslips (10mm in diameter; General Scientific Co. Ltd., Redhill, UK) were washed with PBS, and subsequently fixed with 4% paraformaldehyde (PFA) for 30 min. The fixed cells were then washed twice with PBS before they were mounted using mowiol mounting solution (2.4 g Mowiol 4-88 [Calbiochem, San Diego, USA], 6 g glycerol, 6 ml H_2O, 0.2 M Tris pH 8.5, 12 ml 1,4-diazabicyclo[2.2.2]octane [DABCO, Sigma-Aldrich Company Ltd., Dorset, UK]) supplemented with diamino phenylindole (DAPI; 0.5µg/ml; Sigma-Aldrich Company Ltd., Dorset, UK) for nuclear staining.

2.6.4 Immunofluorescence

Cells were grown in DMEM medium supplemented with FCS at 10%. For imaging, cells were seeded onto glass coverslips in a 6 well plate and incubated overnight before being transfected, essentially as described above. After 36 to 48 hours, cells were fixed with 4% PFA for 30 min. The fixed cells were washed with PBS before incubation with permeabilization buffer (500 ml PBS, 10% sucrose, 0.5% N-P40) for 20 min. The cells

were subsequently blocked with blocking buffer (permeabilization buffer containing 30% goat serum; Sigma-Aldrich Company Ltd., Dorset, UK) for 10 to 15 min. The proteins of interest were then detected by incubating the cells with an appropriately diluted primary antibody (in blocking buffer, 1:500) for at least 45 min. The cells were washed three times with wash buffer (0.1% [v/v] Tween 20 in PBS) for 5 min. In order to detect bound primary antibodies, the cells were incubated with the fluorochrome-conjugated secondary antibody (in blocking buffer, 1:500). Coverslips are kept in the dark to reduce photo-bleaching of the fluorescent probe. After 30 min the cells were washed three times (briefly) with wash buffer. The coverslips were subsequently mounted in mowiol mounting solution containing DAPI for nuclear staining.

2.6.5 Imaging

Images were acquired using a DeltaVision® microscope system (Applied Precision, Marlborough, UK), consisting of an inverted microscope (Olympus 1x70, Olympus, Tokyo, Japan) with a 1.40 NA 100x or 60x oil immersion objective and Photometric CH300 CCD camera. Images were processed with the softWoRx® Imaging software package (Applied Precision, Marlborough, UK).

For live imaging cells were grown on WILLCO thin “glass bottomed” microwell dishes (dish 35 mm diameter, glass 12 mm diameter; Intracel Ltd., Royston, UK).

2.7 Bacterial protein expression and purification

To purify a single protein for further study, affinity purification tags can be fused to any recombinant protein of interest, allowing fast and easy purification using the affinity properties of the tag. Fusion tags are polypeptides, small proteins or enzymes added to the N- or C-terminus of a recombinant protein. The biochemical features of different tags influence the stability, solubility and expression of the proteins to which they are attached (Nilsson *et al.*, 1997).

2.7.1 Polyhistidine tagging of proteins

The most commonly used tag for purification and detection of recombinant proteins is the polyhistidine tag (His-tag). Protein purification using the His-tag relies on the affinity of histidine residues for immobilized metal such as nickel, which allows selective purification of proteins (Yip *et al.*, 1989). The His-tag offers several advantages for protein purification. The tag usually does not need to be removed for downstream applications following purification as its small size renders it less immunogenic than other larger tags. It may be placed on either N- or C-terminus of the protein of interest. The interaction of the His-tag does not depend on the tertiary structure of the tag, making it possible to purify otherwise insoluble proteins using denaturing conditions.

The protein of interest was inserted into the peHisTev vector (figure 2.3). A transformation was carried out (as described in section 2.1.9) using BL21(DE3)pLysS competent cells (Promega, Southampton, UK). A single colony of *E. coli* transformed with the peHis-Tev recombinant was used to inoculate 2 ml of LB medium containing the 30 µg/ml of kanamycin (Kan) and grown overnight at 37°C with moderate shaking. This starter culture was diluted 1:10 and grown at 37°C with moderate shaking to an A_{600} of 0.6. Protein expression was initially induced by adding isopronyl β-D thiogalactoside (IPTG) to a final concentration of 0.5 mM after which incubation was continued for a further 2 to 6 hours. Bacterial cells were pelleted by centrifugation at 4000 xg for 10 min. The bacterial cells were lysed by resuspending the pellet in 500 µl of sample buffer (PBS containing 0.3 M NaCl, 10 mM imidazol, protease inhibitor protease inhibitor cocktail tablet [Complete,

Mini, EDTA-free; Roche Diagnostics Ltd., Burgess Hill, UK]), followed by sonication. The lysate was centrifuged for 10 min at 12 000 xg at 4°C. The supernatant was transferred to a fresh tube and 100 µl of a 50% slurry of ProBond^{TM} Nickel-Chelating Resin (PBS equilibrated; Invitrogen, Paisley, UK) was added. Samples were gently mixed and rotated for 1 hour at 4°C. After rotation, the bead/fusion protein complex was washed 3 times with 0.5 ml of washing buffer (PBS containing 0.3 M NaCl, 30 mM imidazol and 1 mM PMSF). The complex was recovered between washes by centrifugation at 12 000 xg for 1 min. After the final wash step, 50 µl of elution buffer (PBS containing 0.3 M NaCl, 500 mM imidazol, 1 mM PMSF) was added to the bead/fusion protein complex and incubated for 2 min. After centrifugation at 12 000 xg for 1 min, the pellet was resuspended in 2x SDS-PAGE sample loading buffer, the complexes were dissociated at 100°C for 2 min and analyzed on SDS-PAGE gel (10% polyacrylamide, described in section 2.2.3).

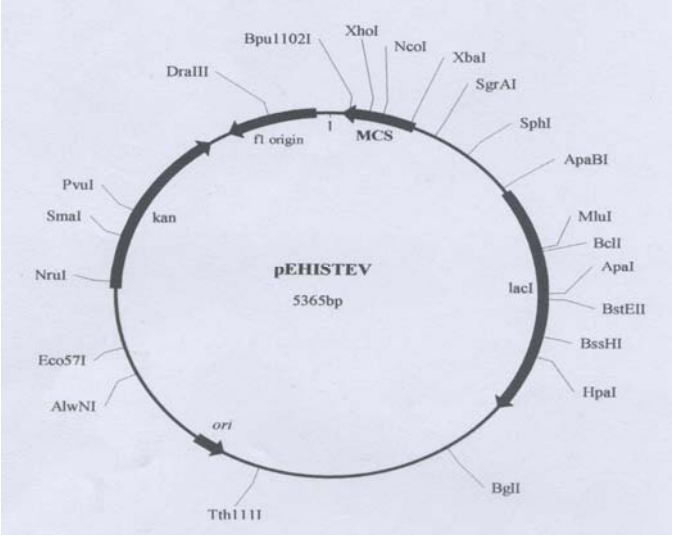

Figure 2.3: peHisTev vector map: *the map summarizes the features of the peHis-Tev vector used for polyhistidine tagging of proteins.*

2.7.2 Glutathione-S-Transferase tagging of proteins

The glutathione-S-transferase (GST) tag has a strong affinity for immobilized glutathione-covered matrices (Smith & Johnson, 1988). Glutathione-S-transferases are a family of cytosolic proteins with multiple functions that are present in eukaryotic organisms (Armstrong, 1997). GST isoforms are not produced in bacteria, thus endogenous proteins do not compete with the GST-fusion proteins for binding to the purification resin. The GST-tag (M_r 26 000) enhances the solubility of many eukaryotic proteins expressed in bacteria.

The GST Gene Fusion System (Amersham Biosciences, Buckinghamshire, UK) was used to express, purify and detect fusion proteins produced in *E. coli*. The system is based on inducible, high-level expression of proteins as fusions with *Schistosoma japonicum* GST (pGEX plasmid; Smith & Johnson, 1988). Expression in *E. coli* generates fusion proteins with the GST moiety at the amino-terminus and the protein of interest at the carboxyl terminus. GST fusion proteins are purified from bacterial lysates by affinity chromatography using immobilized glutathione. GST fusion proteins are captured by the affinity medium, impurities are removed by washing, and the fusion proteins are eluted under mild, non-denaturing conditions using reduced glutathione. Cleavage of the protein from GST can be achieved using a site-specific protease whose recognition site is located immediately upstream from the multiple cloning site of the pGEX vector.

The protein of interest was inserted into the multiple cloning site of vector pGEX-5X-3 (figure 2.4). Expression is under the control of the *tac* promoter, which is induced by IPTG. Expression is prevented until IPTG induction by the *lac*I^q gene product, a repressor protein that binds to the operator region of the *tac* promoter. A transformation was carried out (as described in section 2.1.9) using BL21(DE3)pLysS competent cells (Promega, Southampton, UK). A single colony of *E. coli* transformed with the pGEX recombinant was used to inoculate 2 ml of LB medium containing 100 µg/ml Amp and grown overnight at 37°C with moderate shaking. This starter culture was diluted 1:10 and grown at 37°C with moderate shaking to an A_{600} of 0.6-0.8. Fusion protein expression was induced by adding IPTG to a final concentration of 0.5 mM, after which incubation was continued for a further 2 to 6 hours. Bacterial cells were pelleted by centrifugation at maximum speed for 4 min. The bacterial cells were lysed by resuspending the pellet in 500 µl PBS containing 0.1% N-

P40, 2 mM Benzamidine, 1 mM PMSF and 1 mM DTT, followed by sonication. The lysate was centrifuged for 10 min at maximum speed at 4°C. The supernatant was transferred to fresh tubes and 20 µl of a 50% slurry of Glutathione Sepharose™ 4B (PBS equilibrated; GE Healthcare, Chalfont St Giles, UK) was added. Samples were gently mixed and rotated for 30 min at 4°C. After rotation, the bead/fusion protein complex was washed 4 to 5 times with PBS containing 0.1% [v/v] N-P40. The complex was recovered between washes by centrifugation at 10 000 xg for 1 min. After the final wash step, the pellet was resuspended in 2x SDS-PAGE sample loading buffer, the complexes were dissociated at 100°C for 2 min and analyzed on SDS-PAGE gel (10% polyacrylamide, described in section 2.2.3).

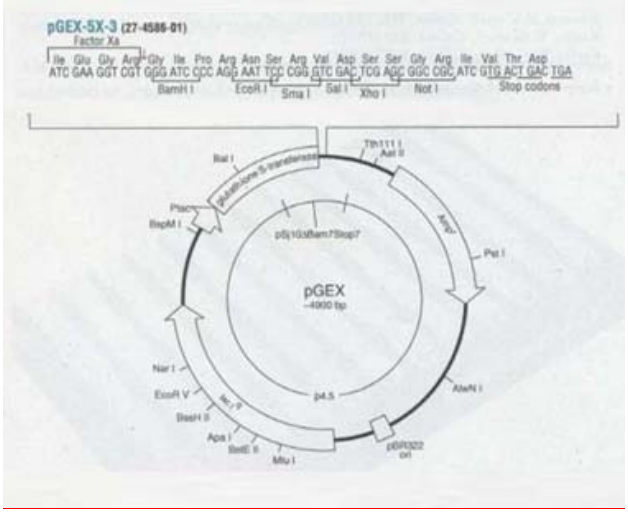

Figure 2.4: pGEX-5x-3 vector map: *the map summarizes the features of the pGEX-5x-3 vector used for Glutathione-S-transferase tagging of proteins.*

2.7.3 Maltose binding protein tagging of proteins

The pMAL™ Protein Fusion and Purification System (pMAL™-2 vectors; New England BioLabs Ltd., Herts, UK) provides a method for expressing and purifying proteins. The protein of interest is inserted downstream of the *malE* gene of *E. coli*, which encodes maltose binding protein (MBP), resulting in the expression of an MBP fusion protein. High-level expression of the fusion protein is achieved by using the strong "tac"-promotor and the *malE* translation initiation signals. The pMAL™-2 vectors carry the *lacI*^{q} gene, which codes for the Lac repressor. This will keep expression of the fusion protein low in the absence of IPTG induction.

The protein of interest was inserted in pMAL-C2E (figure 2.5) and subsequently a transformation was carried out (as described in section 2.1.9) using *E. coli* K12 TB1 competent cells (New England BioLabs Ltd., Herts, UK). Rich broth (80 ml; 1% [w/v] tryptone, 0.5% [w/v] yeast extract, 0.5% [w/v] NaCl pH 7.0, 0.2 % [w/v] glucose) containing 100 µg/ml Amp, was inoculated with 0.8 ml of an overnight culture of cells containing the fusion plasmid. This culture was grown at 37°C with moderate shaking to an A_{600} of 0.5, after which IPTG was added to the culture to a final concentration of 0.3 mM to induce expression of the fusion protein. Incubation was continued at 37°C for 2 hours. The cells were harvested by centrifugation at 4000 xg for 10 min. The supernatant was discarded and the pellet was resuspended in 5 ml of column buffer (20 mM Tris HCl pH 7.4, 200 mM NaCl, 1 mM EDTA). The cells, resuspended in column buffer, were stored overnight at -20°C and thawed in cold water. The cells were lysed by sonication and the lysate was centrifuged for 20 min at 9000 xg at 4°C. The supernatant was transferred to fresh tubes and subsequently 50 µl of the supernatant was mixed with 50 µl amylose resin (New England BioLabs Ltd., Herts, UK) slurry. The amylose resin slurry was prepared by transferring 200 µl amylose resin to a microcentrifuge tube, after which a brief centrifugation was carried out. The supernatant was removed by aspiration and discarded. The resin was washed twice with 1.5 ml column buffer and finally resuspended in 200 µl column buffer resulting in a 50% amylose resin slurry. The resin/ fusion protein complex was incubated for 15 min on ice, followed by centrifugation for 1 min. The supernatant was removed and the pellet was washed with 1 ml column buffer. After centrifugation for 1 min and removal of the supernatant, the resin was resuspended in 2x SDS-PAGE sample loading buffer, the complexes were dissociated at 100°C for 2 min and analyzed on SDS-PAGE gel (10% polyacrylamide, described in section 2.2.3).

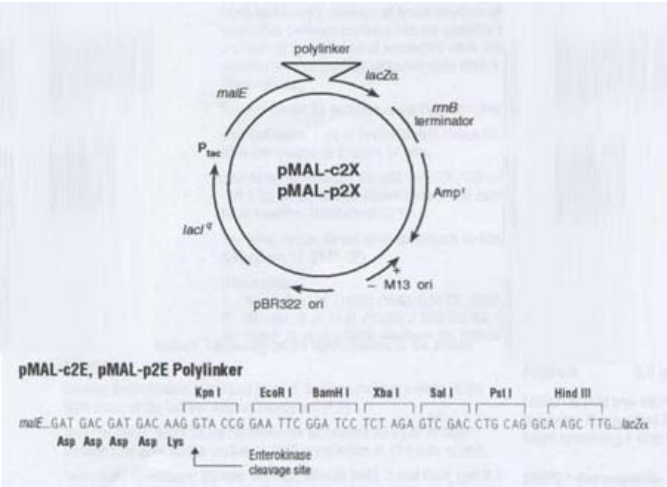

Figure 2.5: pMAL-c2E vector map: *the map summarizes the features of the pMAL-c2E vector used for maltose binding protein tagging of proteins.*

2.8. *In vitro* binding assay

2.8.1 In vitro binding assay of cellular proteins

The GST-tagged protein of interest was expressed and bound to Glutathione Sepharose™ 4B beads, essentially as described above. Furthermore, BHK-21 cells were grown to 100% confluency and then harvested. Cells were lysed by adding 1 ml of lysis buffer (650 mM NaCl, 5 mM EDTA, 0.5% N-P40, protease inhibitor cocktail tablet [Complete, Mini, EDTA-free; Roche Diagnostics Ltd., Burgess Hill, UK]). The lysate was vortexed for 10 seconds and freeze/thawed. The lysate was then clarified by centrifugation (14 000 xg) at 4°C for 10 minutes. The supernatant was recovered, added to the GST-fusion protein/bead complex and rotated for a minimum of 1 hour at 4°C. After rotation, the bead/fusion protein complex was washed 4 to 5 times with PBS. The complex was recovered between washes by centrifugation at 12 000 rpm for 1 min. After the final wash step, the pellet was resuspended in 2x SDS-PAGE sample loading buffer, the complexes were dissociated at 100°C for 2 min and analyzed on SDS-PAGE gel (10% polyacrylamide, described in section 2.2.3).

2.8.2 In vitro binding assay of T_NT samples

The GST-tagged protein of interest was expressed and bound to Protein Glutathione Sepharose™ 4B beads, essentially as described above. Furthermore, the relevant proteins were expressed *in vitro* using the $T_NT^®$ Wheat Germ Extract System (Promega, Southampton, UK), following the manufacturer's protocol. A typical binding reaction consisted of *in vitro* translation reaction (50 µl) added to the GST-fusion protein/bead complex and rotated for a minimum of 1 hour at 4°C in the presence of 1 ml binding buffer (50 mM Magnesium acetate, 20 mM Tris-HCl pH 7.4, 1 mM DTT, 0.05%-0.1% N-P40, 10 mg/ml BSA). After rotation, the bead/fusion protein complex was washed 4 to 5 times with binding buffer without BSA. The complex was recovered between washes by centrifugation at 12 000 rpm for 1 min. After the final wash step, the pellet was resuspended in 2x SDS-PAGE sample loading buffer, the complexes were dissociated at 100°C for 2 min and analyzed on SDS-PAGE gel (10% polyacrylamide, described above).

2.9. Generating lentiviruses and establishing stable cell lines

2.9.1 Generating lentiviruses

A lentivirus is generated by cotransfecting HEK-293T cells (human embryonic kidney cells) with three plasmids: CMV, VSV/G and pdlNotI'MCS'F (figure 2.6; a kind gift from Prof. Rick Randall). The first plasmid CMV (pCMVR8.91) encodes most of the HIV-1 viral proteins, including Gag, Pro-Poly, Rev and Tat which are driven by the CMV promoter. The second plasmid VSV/G (pMD-G) uses the CMV promoter to drive the expression of the viral envelope glycoprotein of vesicular stomatitis virus. The third plasmid pdlNotI carries the protein of interest and the puromycin gene, which are driven by the SFFV promoter. Only the pdlNotI plasmid contains the viral packaging signal sequence. lentiviral particles generated by cotransfection of these three plasmids will carry the gene of interest and the puromycin gene but none of the HIV-1 viral protein genes. The generated lentiviral particles can infect the target cell by using the VSV envelope glycoprotein, but no new viral particles will be produced after infection.

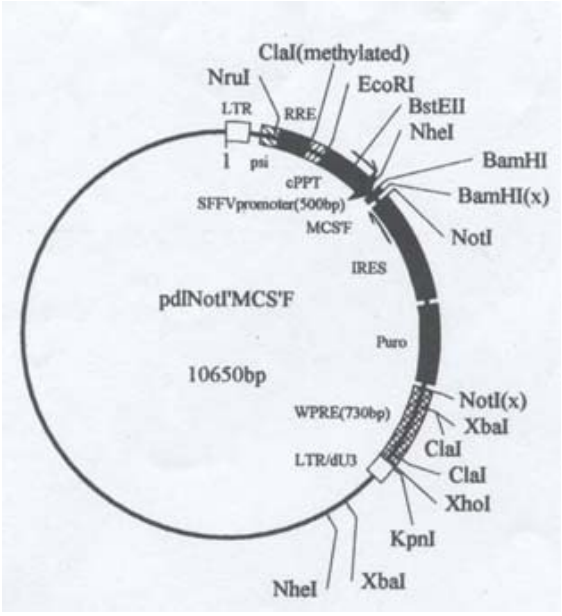

Figure 2.6: pdlNotI'MCS'F vector map: *the map summarizes the features of the pdlNotI'MCS'F vector used for cotransfecting HEK-293 cells, combined with the CMV and VSV/G plasmids, to generate a Lentivirus that carries the gene of interest.*

To generate lentivirus, 70% confluent HEK-293T cells (75 cm² flask containing DMEM supplemented with 10% FCS) were transfected with 3 µg VSV/G, 3 µg CMV and 4.5 µg pdlNotI using the FuGENE 6 transfection reagent (Roche Diagnostics Ltd., Burgess Hill, UK), essentially as described above. Virus was harvested 48 hours and 72 hours after transfection, filtered through a 0.45 µm filter (Millipore, Billerica, USA), aliquoted (1 ml/vial) and stored at -70°C. Following this procedure, generally, the titre of virus will be 10 000 pfu/ml.

2.9.2 Establishing stable cell lines

To establish a stable cell line expressing the protein of interest using the recombinant lentivirus, the cell line of interest was grown in a 25 cm² flask to 50% confluency. The cells were infected with lentivirus (1 ml of virus stock [10 000 pfu/ml]) combined with serum-free DMEM (1 ml) and polybrene (4 mg/ml stock; 1:500 final dilution) and subsequently centrifuged at 300 xg for 30 min. After infection, the inoculum was topped up to 5 ml with DMEM supplemented with 10% FCS, and cells were incubated for 48 hours. After incubation, infected cells were selected

with puromycin. The toxicity of the selection agent on the cell line determines the appropriate concentration (described in section 2.9.3). Cell death should occur within 24 hours. If massive cell death occurs, it is advisable to change the medium immediately; otherwise the selection medium should be replaced every 3 to 4 days. After replacing the medium twice or more, expression of the protein of interest can be examined.

2.9.3 Puromycin titration

Cell types of interest were plated (2 x 10^4 cells) into each well of a 24-well plate containing 1 ml of DMEM supplemented with 10% FCS. After 24 hours, the culture medium was discarded and 1 ml of fresh DMEM (containing 10% FCS) was added. Puromycin was also added in concentrations varying from 1-24 µg/ml. The cells were cultured for 3 to 5 days, replacing the puromycin containing medium every three days. The dishes were examined every day for viable cells. The lowest concentration of puromycin that causes massive cell death within 3 to 5 days was identified.

3. Results

3.1. Localization of TMEV protein 2C in cells

Poliovirus protein 2C and its precursor 2BC have been associated with the membranous vesicles comprising the PV replication complex. The P2 proteins are rER associated soon after synthesis. At the site of protein-ER interaction, the PV replication complexes appear. Replication occurs on the cystosolic surface of membranous vesicles. These vesicles, containing the replication complexes, move away from the rER to form a growing vesiculated area in the center of infected cells. Protein 2C and its precursor 2BC seem to be responsible for the attachment of viral RNA to the vesicular membranes and for the spatial organization of the replication complexes (Dales *et al.*, 1965, Bienz *et al.*, 1987, 1990, Egger & Bienz, 2005).

To elucidate the localization of TMEV protein 2C and its precursor 2BC in the cell, constructs were made containing protein-complex 2BC and protein 2C tagged with the V5 epitope. Mutations were introduced within the Walker A and B motifs. It was intended to express the V5-tagged proteins in mammalian cells and to determine the localization of the proteins by means of the anti-V5 antibody. The anti-V5 antibody is a high affinity monoclonal antibody raised against a linear 14aa epitope (GKPIPNPLLGLDST) found on the paramyxovirus SV5 P/V common N-terminal domain (produced from a mouse hybridoma cell-line). Moreover, it was intended to construct a full length infectious copy of TMEV containing the V5-epitope at the C-terminal end of protein 2C, in order to determine the localization of TMEV protein 2C in the cell in the context of other viral proteins. Furthermore, we wished to observe the localization of TMEV-protein 2C in TMEV-infected cells by use of anti-FMDV-2C and anti-TMEV-2C antibodies. The anti-TMEV-2C antibody will also be used for co-localization of TMEV protein 2C with the Golgi complex in TMEV-infected cells.

3.1.1 Preparation of TMEV-2BC and TMEV-2C constructs tagged with the V5 epitope

3.1.1.1 Construction of V5-tagged TMEV-2BC and TMEV-2C using the TOPO vector

Sequences encoding protein-complex 2BC and protein 2C of the *wt* TMEV strain GDVII were amplified by PCR using primers TMEV-2BC-V5-FW/TMEV-2C-V5-FW and TMEV-2C-V5-RV. Primers used for PCR amplification are outlined in table 2.1, section 2.1.3. PCR fragments of the correct length (2BC: 1386 bp; 2C: 978 bp) were purified by agarose gel electrophoresis. The PCR fragments were cleaved with *BamHI* and *XbaI* and the restriction fragments were subsequently gel purified. The purified restriction fragments were ligated into pcDNA3.1/V5-His-TOPO®, similarly restricted, to form TMEV-2BC-V5 and TMEV-2C-V5. Furthermore, the constructs were checked by sequencing.

3.1.1.2 Overlap PCR introducing mutations in highly conserved regions of TMEV-2C

Mutations in the highly conserved Walker A and B motifs have been introduced using site-directed mutagenesis by overlap extension PCR (figure 3.1). Three rounds of PCR reactions have been carried out to produce protein-complex 2BC and protein 2C with the two desired mutations. The highly conserved lysine (K) in the A motif (GSPGTGKS) has been changed to asparagine (N). Additionally, the conserved pair of aspartic acids in the B motif (DD) has been altered to asparagines (NN). The first two PCR assays were performed essentially as described in section 2.1.3. The first PCR was performed using the following primers: TMEV-2BC-V5-FW/TMEV-2C-V5-FW and TMEV-2Cmut1-RV/TMEV-2Cmut2-RV. The second PCR was carried out using TMEV-2Cmut1-FW/TMEV-2Cmut2-FW and TMEV-2BC-V5-RV as primers. The gel-purified PCR products from round I were used as template for the final PCR amplification, with TMEV-2BC-V5-FW/TMEV-2C-V5-FW and TMEV-2BC-V5-RV as primers (figure 3.1). The final PCR products were purified by agarose gel electrophoresis. The PCR fragments were cleaved with *BamHI* and *XbaI* and the restriction fragments were subsequently gel purified. The purified restriction fragments were ligated into pcDNA3.1/V5-His-TOPO®, similarly restricted, to form TMEV-2BC/2Cmut1-V5 and TMEV-2BC/2Cmut2-V5. The presence of the desired mutations was confirmed by sequencing.

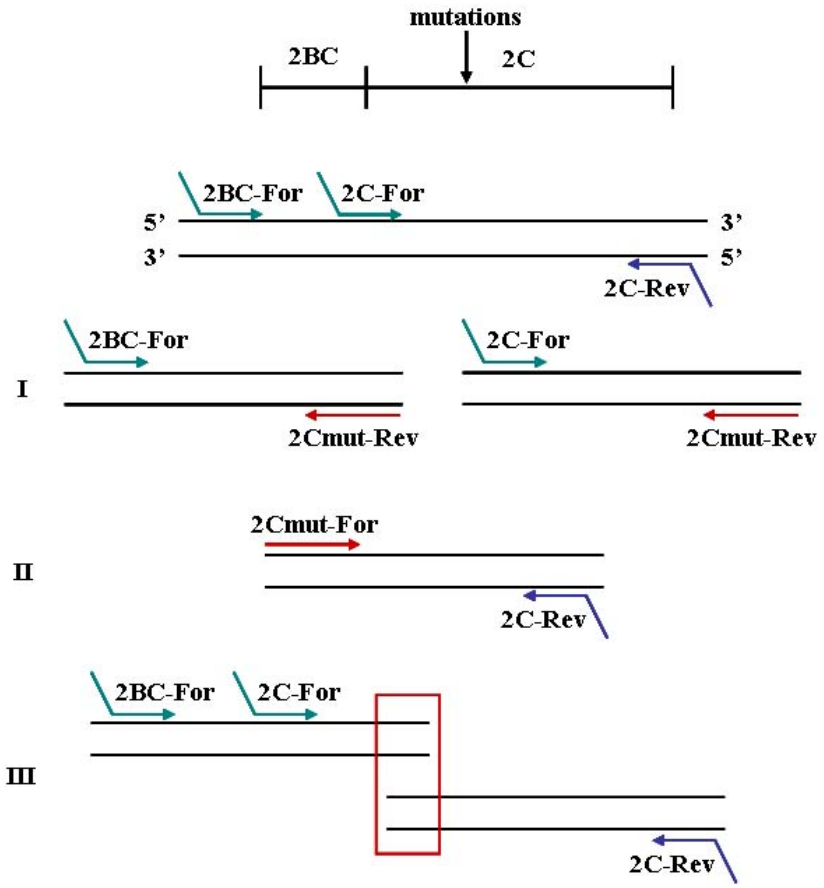

Figure 3.1: Overview of an overlap extension PCR utilized for site-directed mutagenesis. *Three rounds of PCR reactions are carried out to produce protein-complex 2BC and protein 2C with the two desired mutations. PCR I is carried out using a reverse primer containing the desired mutation. PCR II is performed using a forward primer containing the same mutation. The final PCR is carried out using PCR-product I and II, which overlap in the region (boxed area) containing the desired mutation, as templates.*

3.1.1.3 Construction of V5-tagged TMEV-2BC, TMEV-2C, FMDV-2BC, and FMDV-2C using a lentiviral vector

Sequences encoding protein-complex 2BC and protein 2C of the *wt* TMEV strain GDVII were amplified by PCR using Lenti-TMEV-2BC-FW/Lenti-TMEV-2C-FW and Lenti-2C-RV. Additionally, the FMDV-2BC-V5 plasmid, previously constructed, was used as template to generate FMDV-2BC and FMDV-2C PCR fragments. The primers used for these PCRs were Lenti-FMDV-2BC-FW/Lenti-FMDV-2C-FW and Lenti-FMDV-2C-RV.

PCR fragments were purified by agarose gel electrophoresis. The PCR fragments were cleaved with *SpeI* and *BamHI* and the restriction fragments were subsequently gel purified. The purified restriction fragments were ligated into pdlNotI'MCS'R'Pk, similarly restricted, to form Lenti-TMEV-2BC, Lenti-TMEV-2C, Lenti-FMDV-2BC, and Lenti-FMDV-2C. The pdlNotI'MCS'R'Pk plasmid is a lentiviral vector containing the V5 (Pk) epitope (figure 3.2, a kind gift from Prof. Rick Randall).

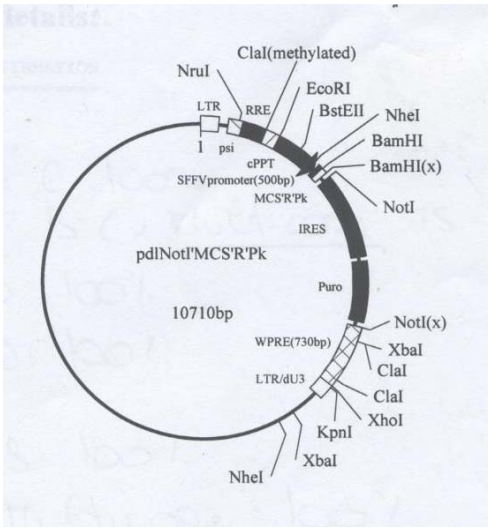

Figure 3.2: pdlNotI'MCS'R'Pk vector map: *the map summarizes the features of the lentiviral vector pdlNotI'MCS'R'Pk vector used for V5 tagging of TMEV-2BC, TMEV-2C, FMDV-2BC, and FMDV-2C. The vector contains the SFFV promoter for mammalian expression of the V5-tagged proteins.*

3.1.2 In vitro expression of V5-tagged proteins and detection of expressed proteins using the anti-V5 antibody

The TOPO vector system contains a T7 promotor which can be used for *in vitro* expression of proteins. Proteins can be expressed as a fusion with the V5 epitope, and the fusion proteins can be subsequently detected by using an antibody to the V5 epitope. The V5-tagged TMEV constructs were used for *in vitro* expression, as well as the V5-tagged FMDV constructs that already existed in our laboratory.

3.1.2.1 In vitro expression of TMEV-2BC-V5, TMEV-2C-V5, and TMEV-2C-V5 mutants and detection of the expressed proteins using the anti-V5 antibody

The TMEV-2BC-V5, TMEV-2C-V5, TMEV-2Cmut1-V5, and TMEV-2Cmut2-V5 plasmids were expressed *in vitro* using a wheat germ extract coupled transcription/translation system. The radiolabelled translation products were separated by 10% SDS-PAGE. The distribution of radiolabel was visualized by autoradiography. The gel profiles of the V5-tagged TMEV proteins are shown in figure 3.3. Furthermore, an immunoprecipitation experiment was performed. The *in vitro* translated radiolabelled proteins were incubated with protein G Sepharose beads containing the anti-V5 antibody. The proteins associated with the anti-V5 antibody were eluted from the beads by boiling in SDS gel-loading buffer and analyzed by SDS-PAGE (figure 3.3). The anti-V5 antibody binds TMEV-2BC-V5, TMEV-2C-V5 and both mutants of TMEV-2C. It is generally accepted that the extra bands seen on the gel are a result from internal initiation. Several internal in-frame methionines (Met; M) have been identified in the TMEV protein 2B and 2C amino acid sequences that could result in the protein size of the extra bands. The extra band observed for TMEV-2BC (figure 3.3, *) may result from internal initiation at an in-frame Met identified in protein 2B at position 99. The extra band observed for TMEV-2C and mutants (figure 3.3, **) may also result from internal initiation from in-frame Met. Three possible in-frame Met have been identified in protein 2C at position 50, 60, and 62.

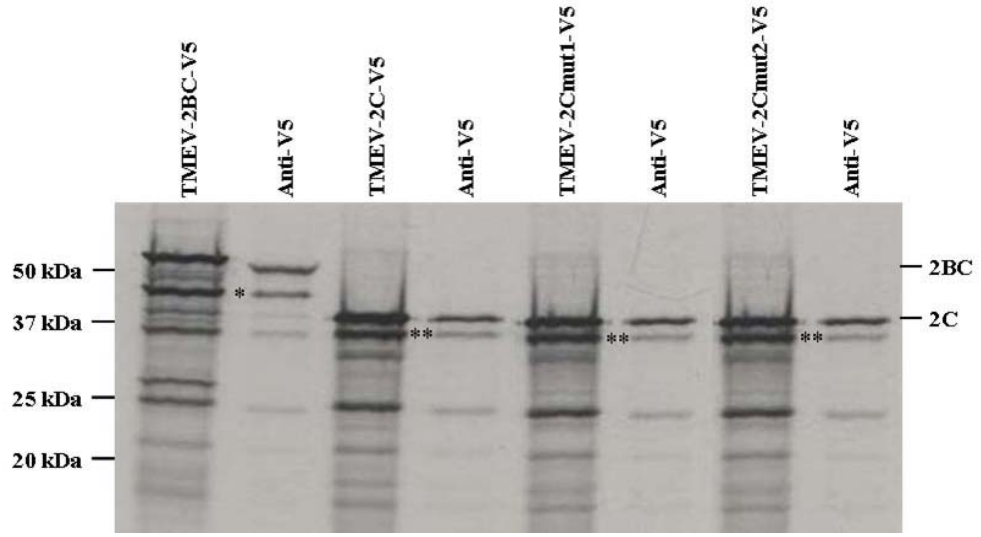

Figure 3.3: Gel profiles of *in vitro* coupled transcription/translation reactions and subsequent immunoprecipitation reactions. *The lanes are labelled with the constructs used for the transcription/translation reactions and the antibody used for the immunoprecipitation reactions. The positions of the protein size markers are indicated.*

3.1.2.2 In vitro expression of FMDV-2BC-V5, FMDV-2B-V5, and FMDV-2C-V5 and detection of the expressed proteins using the anti-V5 antibody

Previously in our laboratory constructs were made containing V5-tagged FMDV-2BC, FMDV-2B, and FMDV-2C. These plasmids were expressed *in vitro* using a wheat germ extract coupled transcription/translation system. The *in vitro* translated radiolabelled proteins were subjected to immunoprecipitation with the anti-V5 antibody. The radiolabelled translation products, together with the proteins associated with the anti-V5 antibody were separated by 10% SDS-PAGE. The distribution of radiolabel was visualized by autoradiography. The gel profiles of the *in vitro* expressed proteins and the result of the subsequent immunoprecipitation reactions are shown in figure 3.4. The anti-V5 antibody binds FMDV-2BC-V5, FMDV-2B-V5, and FMDV-2C-V5. The extra bands observed on the gel profile are the result of initiation at internal Met identified in the FMDV protein 2B and 2C amino acid sequences. The extra band observed for FMDV protein 2C has been identified to be the result of internal initiation at an in-frame Met in FMDV protein 2C at position 43 (figure 3.4, *).

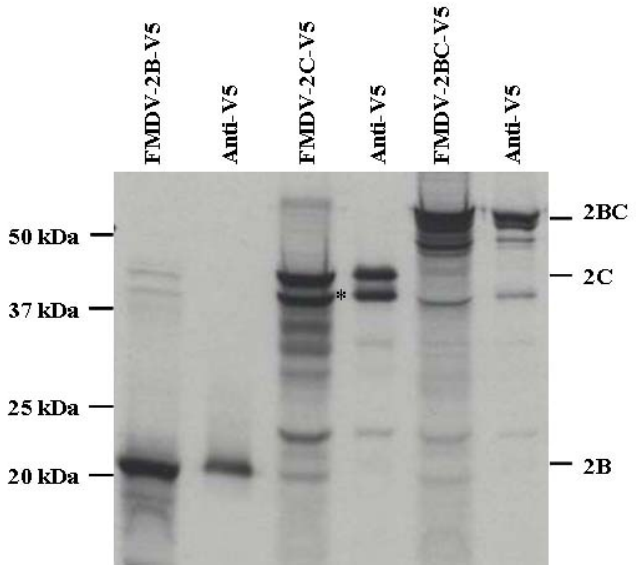

Figure 3.4: Gel profiles of *in vitro* coupled transcription/translation reactions and subsequent immunoprecipitation reactions. *The lanes are labelled with the constructs used for the transcription/translation reactions and the antibody used for the immunoprecipitation reactions. The positions of the protein size markers are indicated.*

3.1.3 Intracellular localization of V5-tagged TMEV-2BC and TMEV-2C

It was intended to localize V5-tagged TMEV protein-complex 2BC and protein 2C in the cell. BHK-21 cells were transfected with the constructs encoding the V5-tagged proteins, described above. Different transfection methods were employed (section 2.5). To localize the V5-tagged proteins, immunofluorescence was carried out as described in section 2.6.4. For detection of the V5-tagged proteins, the anti-V5 antibody was used and, for visualization, a rabbit anti-mouse antibody coupled to TexasRed (Abcam, Cambridge, UK) was used. It was not possible to detect an immunofluorescent signal for neither TMEV-2BC nor TMEV-2C. Furthermore, both mutants of TMEV-2C (section 3.1.1.2) were used for transfection. It was, however, not possible to detect a higher immunofluorescent signal. However, when the constructs encoding V5-tagged FMDV-2BC and FMDV-2C were used for transfection, we were able to detect an immunofluorescent signal (data not shown). The distribution of V5-tagged FMDV-2BC and FMDV-2C observed upon transfection resembled the distribution previously seen by Moffat and colleagues (2005). It has to be noted, however, that both

TMEV and FMDV constructs encoding the V5-tagged 2BC and 2C could be detected after *in vitro* expression using the anti-V5-antibody (section 3.1.2.1; section 3.1.2.2).

3.1.4 Construction of an infectious TMEV clone expressing protein 2C tagged with the V5 epitope

To localize TMEV protein 2C in cells in the presence of all TMEV proteins, it was intended to construct a full-length infectious TMEV cDNA expressing protein 2C fused with the V5 epitope. This construct would subsequently be used for *in vitro* transcription and the resulting RNA would be utilized for transfection of mammalian cells. To investigate the localization of protein 2C, HEK-293 cells would be transfected with RNA by electroporation using the Gene pulser Xcell^{TM} system. Furthermore it was intended to transfect BHK-21 cells in the same manner to see if virus particles containing a V5-tagged genome could be rescued. Several strategies were applied to prepare this construct (see below), but all were unsuccessful. This work was therefore not pursued any further.

3.1.4.1 Construction of an infectious TMEV clone expressing protein 2C tagged with the V5 epitope by overlap PCR

Primers were designed to insert the V5 epitope (Pk) at the C-terminus of TMEV protein 2C by overlap PCR (figure 3.1). Both TMEV-2C-Pk-FW and TMEV-2C-Pk-RV contained the V5 epitope followed by a repeat of the last four amino acids of protein 2C (MQP-V5-MQPQ) in order to keep the proteolytic cleavage site between proteins 2C and 3A intact. It was intended to amplify by PCR two fragments containing the V5 epitope, using TMEV-2BC-V5-FW/TMEV-2C-Pk-RV and TMEV-2C-Pk-FW/TMEV-3D-RV as primer pairs. These two fragments, which share the V5 epitope, would then be used as template for a final PCR using primers TMEV-2BC-V5-FW and TMEV-3D-RV resulting in PCR fragment 2BC-V5-P3. The PCR fragment would subsequently be cleaved with *EcoNI* and *PstI* and ligated into a similarly cleaved TMEV cDNA to form a full-length infectious TMEV cDNA expressing protein 2C fused with the V5 epitope. The overlap PCR, however, was unsuccessful. The primers TMEV-2C-Pk-FW and TMEV-2C-Pk-RV were first acquired from Eurogentec (Eurogentec Ltd., Hampshire, UK). As the accuracy of the

primer sequence was questioned, a second set of overlap primers was obtained from MWG (MWG-Biotech, Ebersberg, Germany). Both primer sets, however, were found to be inadequate to amplify the desired PCR fragments.

3.1.4.2 Construction of an infectious TMEV clone expressing protein 2C tagged with the V5 epitope using construct pLH135

The second strategy applied to construct a full-length infectious TMEV cDNA expressing protein 2C fused with the V5 epitope, makes use of the construct pLH135 previously made in our laboratory (figure 3.5). TMEV-2BC was amplified by PCR using TMEV-2B-FW-NheI and TMEV-2C-RV-ApaI as primers. Furthermore, a PCR was carried out to amplify TMEV-P3 using TMEV-3A-FW-KpnI and TMEV-3D-RV-PmeI as primers. Both PCR fragments were purified by agarose gel electrophoresis. In order to construct plasmid p2BC-V5-P3, the V5CFP2A fragment in pLH135 was excised with *NheI* and *ApaI*, and replaced with a similarly restricted TMEV-2BC. The Pac fragment was subsequently removed with restriction enzymes *KpnI* and *PmeI* and substituted with a similarly restricted TMEV-P3 to form p2BC-V5-P3 (figure 3.5). It was intended to excise protein 2C-V5 with EcoNI and PstI, and subsequently ligate this fragment into a similarly cleaved TMEV cDNA to form a full-length infectious TMEV cDNA expressing protein 2C fused with the V5 epitope. However, restriction analysis revealed an *EcoNI* restriction site within the V5 epitope, and no other single restriction sites within TMEV protein 2C were available. Therefore, a different strategy was applied to transfer the V5-tagged protein 2C into the full-length TMEV cDNA clone (explained in section 3.1.4.3).

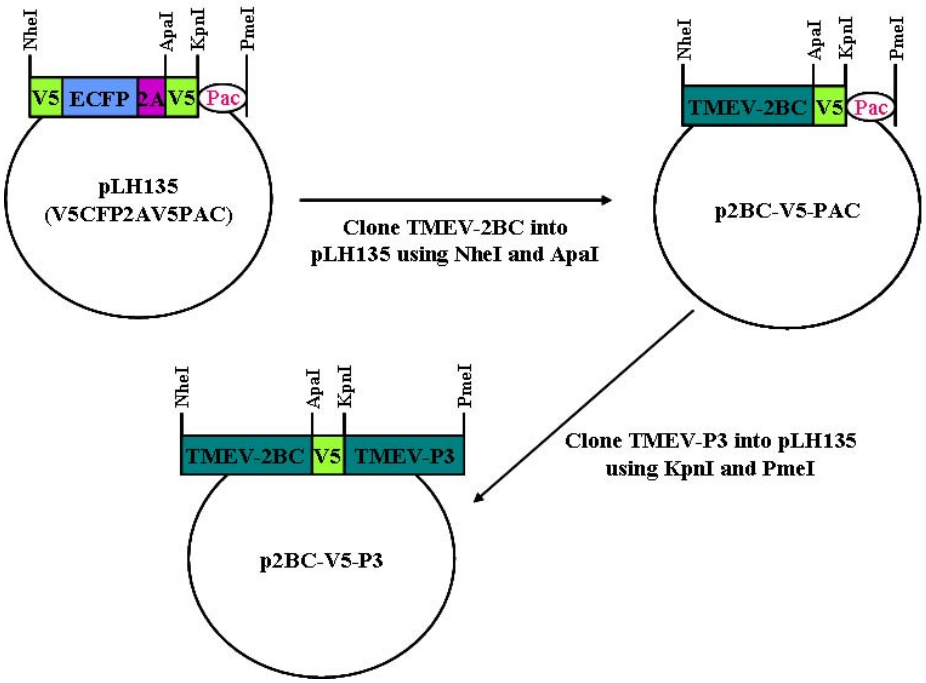

Figure 3.5: Overview of the cloning strategy utilized for the formation of p2BC-V5-P3. *The V5CFP2A fragment in pLH135 was excised with NheI and ApaI and replaced with a similarly restricted TMEV-2BC. The Pac fragment was subsequently excised with KpnI and PmeI and replaced with a similarly restricted TMEV-P3 to form p2BC-V5-P3.*

3.1.4.3 Construction of an infectious TMEV clone expressing protein 2C tagged with the V5 epitope by In-Fusion PCR cloning

The In-Fusion™ PCR Cloning kit (section 2.1.9) was employed, unsuccessfully, to insert the V5-tagged protein 2C into the full-length TMEV cDNA clone. Primers with 15 bases of homology with sequences flanking the desired site of insertion in the TMEV cDNA clone were designed to amplify 2C-V5. The TMEV cDNA clone was cleaved with *EcoNI* and *PstI* to create the insertion site. The plasmid p2BC-V5-P3 (section 3.1.4.3) was used as template to amplify the 2C-V5 fragment with 2C-Pk-FW-InFusion and 2C-Pk-RV-InFusion as primers. The PCR fragment was purified by agarose gel electrophoresis and subsequently used for In-Fusion PCR cloning. It was not possible to construct the desired full-length infectious TMEV cDNA expressing a V5-tagged protein 2C.

3.1.5 Intracellular localization of TMEV-2C after TMEV infection detected with anti-2C antibody

3.1.5.1 Localization of protein 2C in TMEV-infected BHK-21 cells detected by anti-FMDV-2C

We wished to determine if the intracellular localization of protein 2C in TMEV-infected cells could be determined using anti-FMDV-2C antibodies, available in our laboratory. DM10 is a rabbit polyclonal antibody raised against the full length FMDV protein 2C. The 4E3 antibody is a mouse monoclonal antibody raised against the full length FMDV protein 2C. To demonstrate that these antibodies could be used to detect TMEV protein 2C, BHK-21 cells were infected with TMEV-GDVII. Subsequently, western blot analysis, using both DM10 and 4E3, was carried on the cell extracts. Mock-infected BHK-21 cells were used as a negative control. Western blot analysis suggests that both DM10 and 4E3 can detect TMEV-2C; however, the results are not conclusive. The binding of the anti-FMDV-2C antibodies seems to be non-specific as demonstrated by the bands seen in the mock-infected cell extracts. Interestingly an extra band, not present in TMEV-infected cell extracts, can be observed in mock-infected cell extracts. The nature of this band has yet to be determined (figure 3.6).

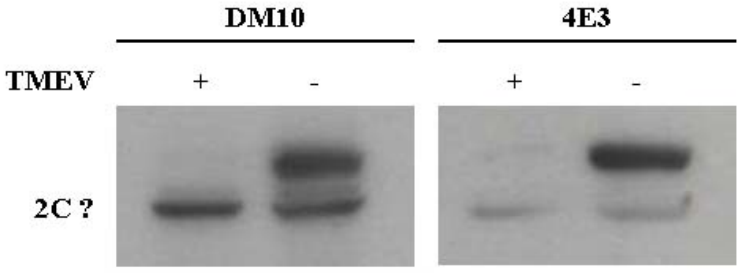

Figure 3.6: Western blot analysis of TMEV-infected and mock-infected BHK-21 cells using anti-FMDV-2C antibodies. *DM10 (left panel) and 4E3 (right panel) antibodies were used to detect TMEV protein 2C in TMEV-infected BHK-21 cells. TMEV-infected (+) and mock-infected (-) cell extracts are indicated. The binding of the anti-FMDV-2C antibodies is non-specific as demonstrated by the bands identified in the mock-infected extracts.*

The previously described constructs TMEV-2BC-V5, TMEV-2C-V5, FMDV-2BC, and FMDV-2C (section 3.1.1; section 3.1.2.2) were expressed *in vitro* using a wheat germ extract coupled transcription/translation system. The *in vitro* translated radiolabelled proteins were subjected to immunoprecipitation with the anti-FMDV-2C antibody DM10. The radiolabelled translation products, together with the proteins associated with DM10 were separated by 10% SDS-PAGE. The distribution of radiolabel was visualized by autoradiography. The gel profiles of the *in vitro* expressed proteins and the result of the subsequent immunoprecipitation reactions are shown in figure 3.7. DM10 associates with both FMDV-2BC and FMDV-2C as expected. Moreover, a very weak association of DM10 with TMEV-2BC-V5 and TMEV-2C-V5 can also be observed.

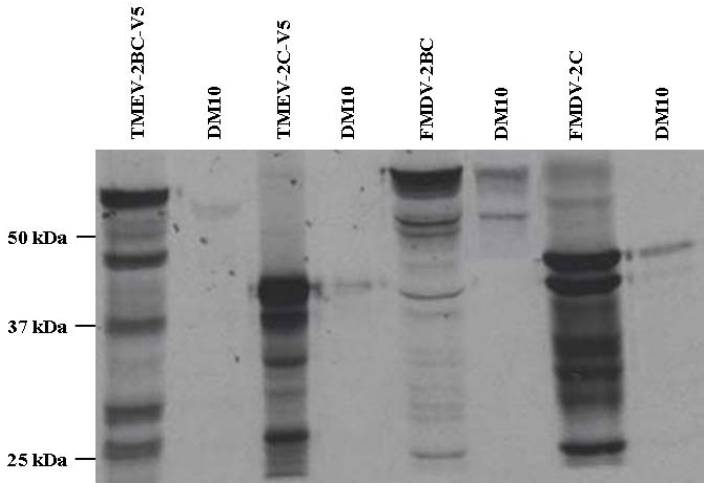

Figure 3.7: Gel profiles of *in vitro* coupled transcription/translation reactions and subsequent immunoprecipitation reactions. *The lanes are labelled with the constructs used for the transcription/translation reactions and the antibody used for the immunoprecipitation reactions. The positions of the protein size markers are indicated.*

DM10 was furthermore used to localize TMEV protein 2C in TMEV-infected BHK-21 cells. TMEV GDVII virus stocks were prepared as described in section 2.4.1, and virus titers were determined by standard plaque assay on BHK-21 cells (section 2.4.2). The titer of the viral stock used was 5 x 10^8 plaque forming units (PFU). BHK-21 cells were grown to semi-confluence (1-4 x 10^4 cells/cm^2) on 10 mm diameter coverslips. Cell cultures were

infected with TMEV GDVII at a multiplicity of infection (MOI) of 100. Cell cultures were washed twice to remove serum components and 0.2 ml of virus stock was added. After adsorption of the virus for 3 hours at 37°C, cells were fixed and immunofluorescence was carried out (section 2.6.4). TMEV protein 2C was detected with DM10 and visualized with a sheep anti-rabbit antibody coupled to TexasRed (Abcam, Cambridge, UK). At 3 hours post infection (p.i.), TMEV protein 2C seems to be spread out in the cytoplasm, showing a typical ER-like pattern (figure 3.8).

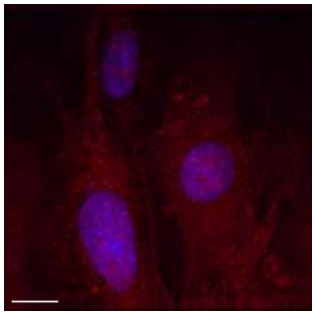

Figure 3.8: Localization of TMEV protein 2C in TMEV-infected cells. *TMEV protein 2C was localized in TMEV-infected BHK-21 cells at 3 hours p.i. using DM10, an anti-FMDV-2C antibody. TMEV protein 2C showed an ER-like pattern. DAPI (blue) was used for nuclear staining. Bar, 5 µm.*

3.1.5.2 Localization of protein 2C in TMEV-infected BHK-21 cells detected by anti-TMEV-2C

The anti-TMEV-2C antibody, described in section 3.3.2, was used to localize TMEV protein 2C in TMEV-infected BHK-21 cells. Cell cultures were prepared and infected as described above (section 3.1.5.1). The virus was adsorbed at 37°C, cells were fixed at hourly time points (1-8 h p.i.), and immunofluorescence was carried out (section 2.6.4). TMEV protein 2C was detected with anti-TMEV-2C antibody and visualized with a sheep anti-rabbit antibody coupled to TexasRed. At 1 hour p.i., tiny dots spread out in the cytoplasm can be seen, which represent newly synthesized protein 2C. At 2 to 3 hours p.i., a typical ER-like pattern can be observed; including small granules intermixed with the ER-like pattern. Protein 2C seems to accumulate in a peri- and juxtanuclear area from 4 to 6 hours p.i. This pattern can still be observed at 7 and 8 hours p.i., however, protein 2C seems to spread out in the cytoplasm as well (figure 3.9).

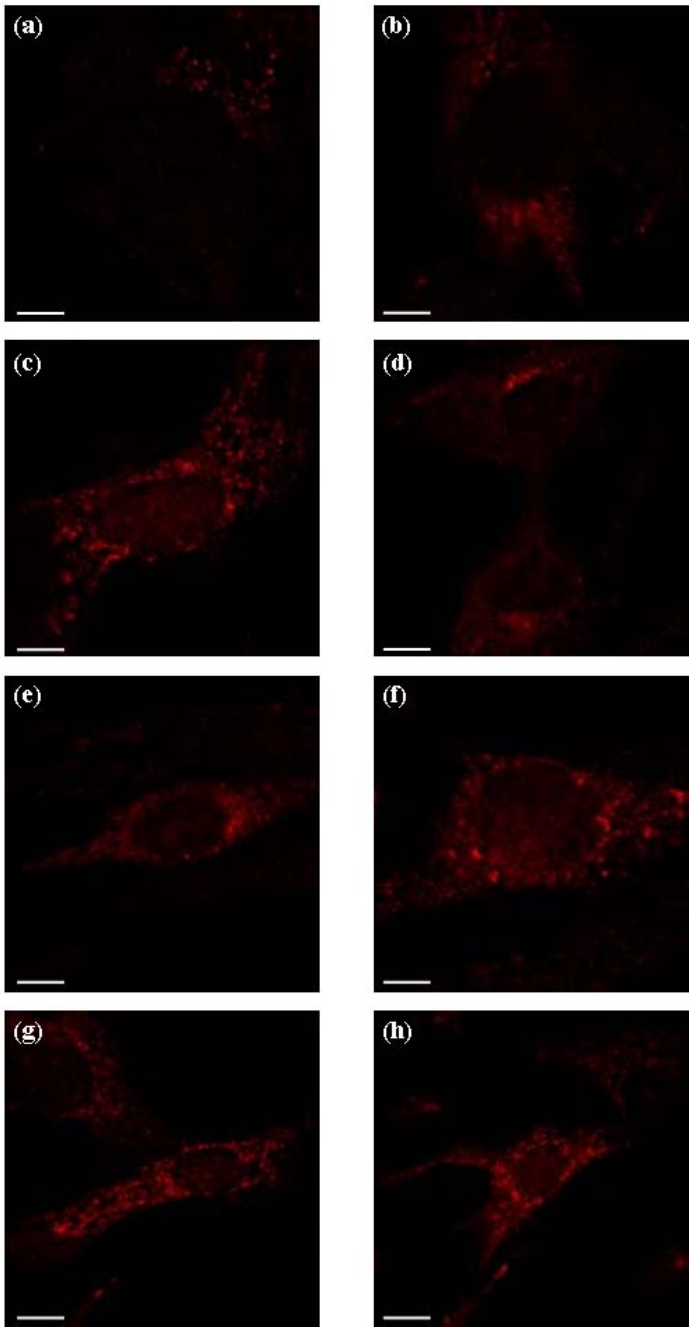

Figure 3.9: Localization of TMEV protein 2C in TMEV-infected BHK-21 cells. *TMEV protein 2C was localized in TMEV-infected BHK-21 cells using the anti-TMEV-2C antibody. Newly synthesized protein 2C can be observed as tiny dots spread out in the cytoplasm at 1h p.i. (a). At 2h (b) and 3h p.i. (c), protein 2C seems to form an ER-like pattern. Accumulation of protein 2C in a peri- and juxtanuclear region can be observed after 4h (d), 5h (e), and 6h p.i. (f). At 7h (g) and 8h p.i. (h), protein 2C seems to start to spread out more in the cytoplasm. Bar, 5 µm.*

3.1.5.3 Localization of protein 2C in TMEV-infected BHK-PDF18 cells detected by anti-TMEV-2C

BHK-PDF18 is a stable cell line which contains a yellow fluorescent Golgi complex and a cyan fluorescent ER. The PDF18 construct, previously made in our laboratory, was used to establish this stable cell line. The PDF18 construct contains the enhanced yellow fluorescent protein (EYFP) preceded by galactosyltransferase (GT), and followed by the self-cleaving FMDV-2A. It also contains the enhanced cyan fluorescent protein (ECFP) followed by FMDV-2A and the puromycin resistance gene (Pac). GT is a type II signal-anchor sequence that will target YFP to the Golgi complex. The PDF18 construct does not contain a signal sequence targeting ECFP to the ER, but it has been demonstrated that ECFP co-localizes with ER markers in transfected cells (Dr. Pablo de Felipe, personal communication). Pac will act as selection agent (figure 3.10).

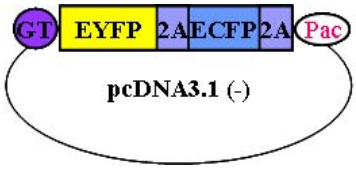

Figure 3.10: Diagram of the construct pPDF18 employed to establish the BHK-PDF18 stable cell line. *The construct contains yellow fluorescent protein (YFP), preceded by galactosyltransferase (GT), and followed by protein 2A, cyan fluorescent protein (CFP) and a second protein 2A. The construct also contains a puromycin resistance gene (Pac).*

The anti-TMEV-2C antibody, described in section 3.3.2, was used to localize TMEV protein 2C in TMEV-infected BHK-PDF18 cells. Cell cultures were prepared and infected as described in section 3.1.5.1. The virus was adsorbed at 37°C, cells were fixed at hourly time points (1-8 h p.i.), and immunofluorescence was carried out as described in section 2.6.4. TMEV protein 2C was detected and visualized as described above (section 3.1.5.2). At 1 hour p.i. (figure 3.11-a), little newly synthesized protein 2C can be observed, and the Golgi complex is intact. At 5 hours p.i., protein 2C is accumulated in the perinuclear region. The Golgi complex has changed from a solid, crescent-shaped organelle into a series of punctuate fluorescent points forming a balloon-like structure. Some overlap between protein 2C and Golgi complex can be observed (figure 3.11-b). After 8 hours of infection, the remnants of the Golgi complex are dispersed throughout the cytoplasm, overlapping with

protein 2C (figure 3.11-c). There is no co-localization between the Golgi complex and TMEV protein 2C, as both red and green signal can be observed separately in the merged image.

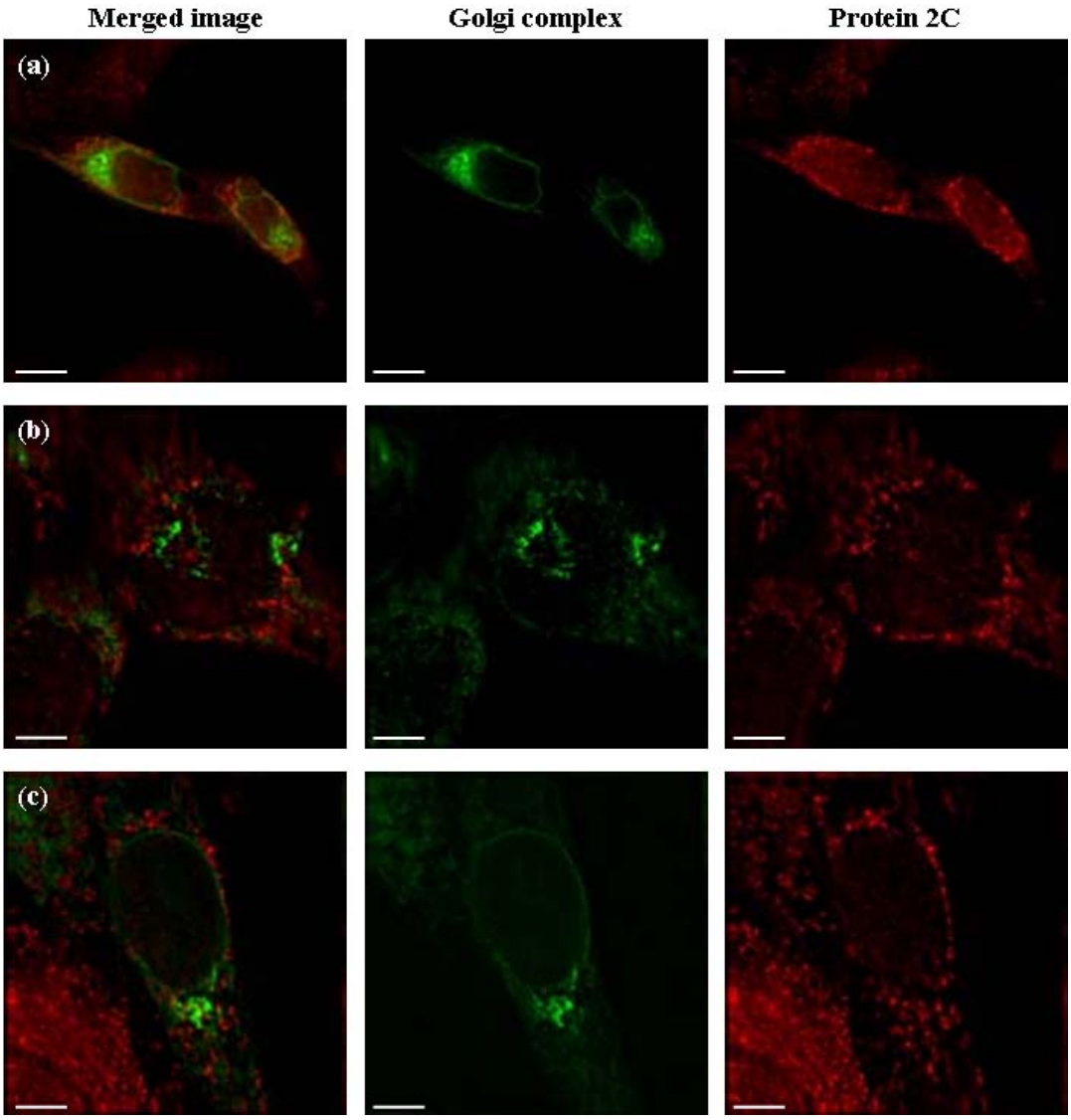

Figure 3.11: Localization of TMEV protein 2C in TMEV-infected BHK-PDF18 cells. *TMEV protein 2C was localized in TMEV-infected BHK-PDF18 cells using the anti-TMEV-2C antibody. The merged image is shown, followed by the Golgi complex (green) and protein 2C (red). Newly synthesized protein 2C can be observed as tiny dots spread out in the cytoplasm at 1h p.i., and the Golgi complex is intact (a). At 5h p.i., the Golgi complex is changed into a balloon-like structure, overlapping with a perinuclear accumulated protein 2C (b). At 8h p.i., protein 2C starts to spread out more in the cytoplasm, overlapping with the dispersed remnants of the Golgi complex (c). Bar, 5 µm.*

3.2. Interaction of TMEV protein 2C with host cell proteins

3.2.1 Transfection of mammalian cells with V5-tagged TMEV protein 2C

The V5-tagged TMEV constructs (described in section 3.1.1) were used for transient transfection of mammalian cells. As discussed previously in section 3.1.3, very low transfection efficiencies were observed. Therefore, different cell lines were used, and furthermore different transfection methods were applied (section 2.5) in order to express the V5-tagged TMEV proteins. It was intended to express TMEV protein 2C in mammalian cells, and to identify cellular proteins that interact with TMEV protein 2C. A transient transfection was to be carried out, after which the cells were to be radiolabelled. X-linked anti-V5 beads were to be used to pull down any cellular proteins interacting with TMEV protein 2C. This work was, however, not pursued further due to low transfection efficiency.

3.2.1.1 Transfection of different cell lines with TMEV-2BC-V5, TMEV-2C-V5, and TMEV-2Cmut1-V5

The TOPO vector system, used to construct plasmids TMEV-2BC-V5, TMEV-2C-V5, and TMEV-2Cmut1-V5, contains a CMV promotor for mammalian expression. Proteins can be expressed as a fusion with the V5 epitope in transiently transfected cells, and the fusion proteins can be subsequently analyzed by western blot using the anti-V5 antibody. Different cell lines were used for transient transfection: Balb/c cells (mouse fibroblast cell line), HeLa cells (immortal cell line derived from cervical cancer cells), HEK-293 cells (human embryonic kidney cell line), and BHK-21 cells (baby hamster kidney cell line). Furthermore, several transfection methods were applied (section 2.5). For the initial experiments, the transfection reagent FuGENE 6 was used. The low transfection efficiency of the V5-tagged TMEV proteins, as discussed previously in section 3.1.3, was confirmed by western blot analysis of the transfected cell extracts (figure 3.12). Western blot analysis demonstrated no expression of TMEV-2BC-V5, TMEV-2C-V5, or TMEV-2Cmut1-V5. However, the transient transfection of a V5-tagged Influenza NS1 protein was successful (figure 3.12).

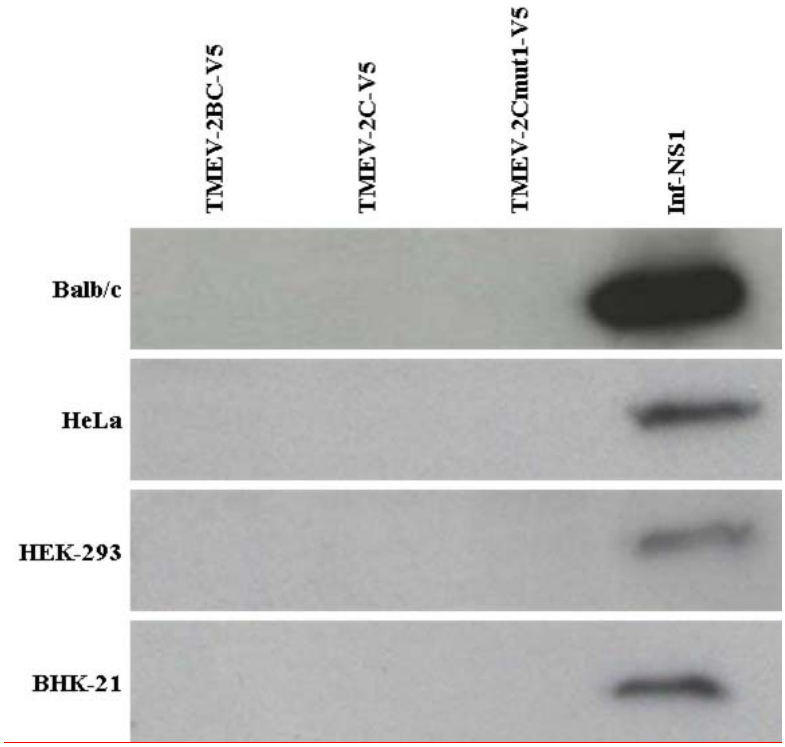

Figure 3.12: Western blot analysis of transfected cell extracts. *Several mammalian cell lines (Balb/c, HeLa, HEK-293, BHK-21) were transiently transfected with TMEV-2BC-V5, TMEV-2C-V5, TMEV-2Cmut1-V5, and a V5-tagged Influenza NS1 protein. Transfected cell extracts were subsequently analyzed by western blot using the anti-V5 antibody.*

In section 3.1.2.1, it was demonstrated that TMEV-2BC-V5, TMEV-2C-V5, and TMEV-2Cmut1-V5 can be expressed *in vitro* by using the T7 promoter provided within the TOPO vector system. Therefore, BSR-T7 cells were used for transient transfection. The BSR-T7 cell line is a BHK cell line constitutively expressing a T7 RNA polymerase (a kind gift from Prof. R. Elliot). Western blot analysis of the transfected cell extracts demonstrated no expression of TMEV-2BC-V5, TMEV-2C-V5, or TMEV-2Cmut1-V5. A negative control confirmed that the observed bands are non-specific (figure 3.13).

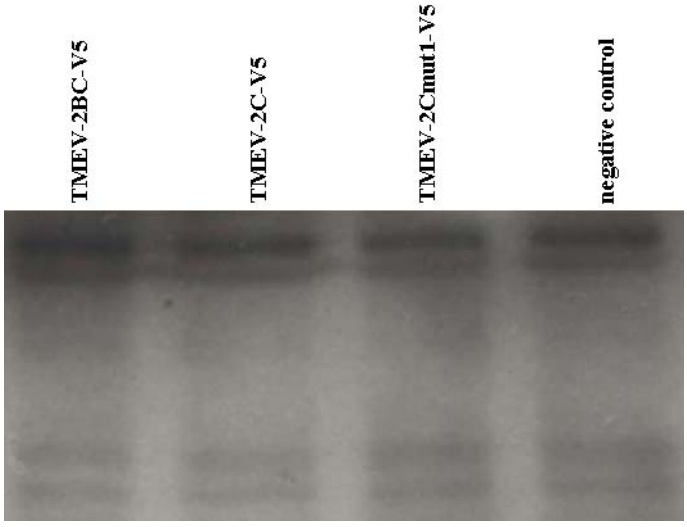

Figure 3.13: Western blot analysis of transfected cell extracts. *BSR-T7 cells were transiently transfected with TMEV-2BC-V5, TMEV-2C-V5, and TMEV-2Cmut1-V5. Transfected cell extracts were subsequently analyzed by western blot using the anti-V5 antibody.*

3.2.1.2 Transfection of BHK-21 cells with Lenti-TMEV-2BC and Lenti-TMEV-2C

The plasmids Lenti-TMEV-2BC and Lenti-TMEV-2C (section 3.1.1.3) were used to transiently transfect BHK-21 cells. The transfection was carried out using the GeneJuice® transfection reagent (section 2.5.1.2). Western blot analysis of the transfected cell extracts demonstrated no expression of Lenti-TMEV-2BC. Lenti-TMEV-2C was expressed. However, after repeating the experiment, expression of Lenti-TMEV-2C could not be confirmed (figure 3.14).

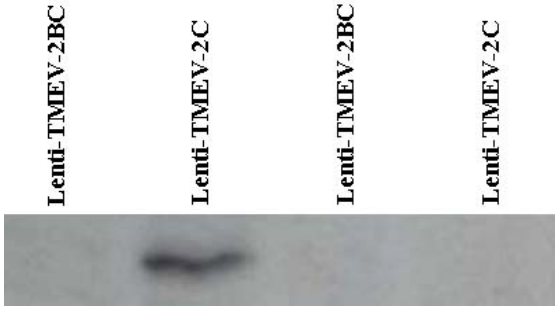

Figure 3.14: Western blot analysis of transfected cell extracts. *BHK-21 cells were transiently transfected with Lenti-TMEV-2BC, and Lenti-TMEV-2C. Transfected cell extracts were subsequently analyzed by western blot using the anti-V5 antibody.*

3.2.2 Transfection of mammalian cells with TAP-tagged TMEV proteins

It was intended to apply the TAP-tag system to identify cellular proteins interacting with TMEV protein 2C. Proteins can be fused with a TAP-tag at both N- and C-terminus. The TAP-tag consists of two IgG binding domains of *Staphylococcus Aureus* protein A (prot A) and a calmodulin binding protein (CBP) separated by a Tobacco Etch virus (TEV) protease cleavage site. The N-terminal TAP-tag contains an additional cleavage site, an enterokinase (EK) (figure 3.15). However, as for the V5-tagged TMEV proteins, the transfection efficiency of the TAP-tagged TMEV proteins was very low, and could therefore not be used to identify cellular proteins interacting with TMEV-2C.

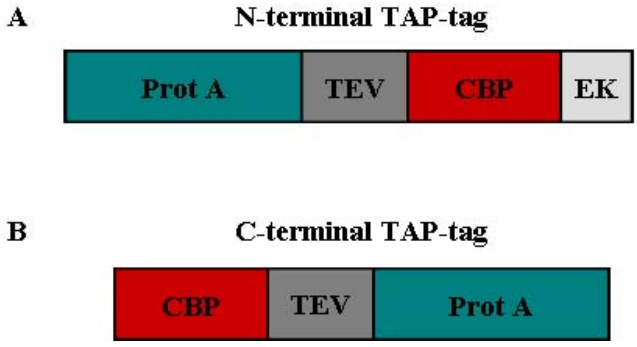

Figure 3.15: The TAP-tag system. *The TAP-tag can be fused to a protein at the N- or C-terminus. Both N-terminal (A) and C-terminal (B) TAP-tag consists of two IgG binding domains of Staphylococcus Aureus protein A, and a CBP, separated by a TEV protease cleavage site. The N-terminal TAP tag also contains an EK cleavage site.*

3.2.2.1 Construction of N-TAP-tagged TMEV-2BC, TMEV-2C, TMEV-2C mut1/mut2

Protein-complex 2BC, protein 2C, and both 2C mutants were amplified by PCR using 2BC-FW-N-TAP/2C-FW-N-TAP and 2C-RV-N-TAP. PCR fragments were purified by agarose gel electrophoresis. The PCR fragments were cleaved with *BamHI* and *XbaI* and the restriction fragments were subsequently gel purified. The purified restriction fragments were ligated into a similarly restricted N-TAP-tag vector to form TMEV-2BC-N-TAP, TMEV-2C-N-TAP, TMEV-2Cmu1-N-TAP, and TMEV-2Cmut2-N-TAP (figure 3.16). The N-TAP-tag is provided in the pCMV5 vector which contains a CMV promotor for expression in mammalian cells.

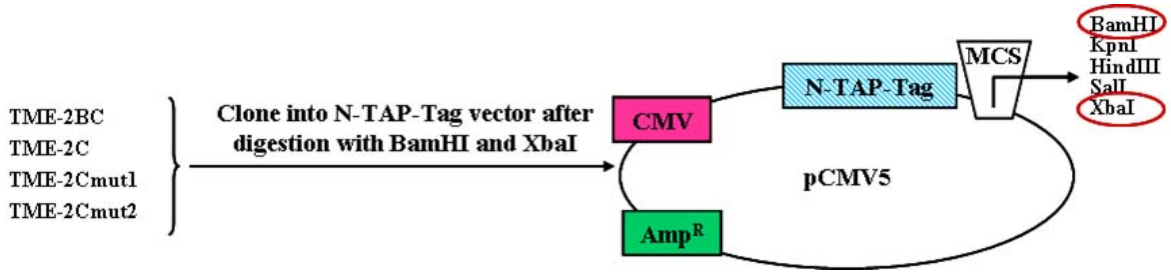

Figure 3.16: Illustration of the cloning strategy utilized for the formation of N-TAP-tagged TMEV proteins. *PCR-amplified TMEV-2BC, TMEV-2C, TMEV-2Cmut1, and TMEV-2Cmut were cleaved with BamHI and XbaI and ligated into a similarly restricted N-TAP-tag vector.*

3.2.2.2 Construction of C-TAP-tagged TMEV-2BC, TMEV-2C, TMEV-2C mut1/mut2

The C-TAP-Tag is provided in the pIRESpuro2 vector. However, the remaining restriction sites in the multi cloning site (MCS) were not suitable for cloning. Therefore, the C-TAP-Tag was amplified by PCR using primer set: C-TAP-FW and C-TAP-RV. The PCR product was gel purified, and subsequently digested with restriction enzymes *KpnI* and *AflII*. The restriction fragment was gel purified and ligated into a similarly digested pcDNA3.1(-) vector to form pcDNA/C-TAP. Protein-complex 2BC, protein 2C, and both 2C mutants were amplified by PCR using 2BC-FW-C-TAP/2C-FW-C-TAP and 2C-RV-C-TAP. PCR fragments were purified by agarose gel electrophoresis. The PCR fragments were cleaved with *NotI* and *EcoRV* and the restriction fragments were subsequently gel purified. The purified restriction fragments were ligated into a similarly restricted pcDNA/C-TAP to form TMEV-2BC-C-TAP, TMEV-2C-C-TAP, TMEV-2Cmu1-C-TAP, and TMEV-2Cmut2-C-TAP (figure 3.17).

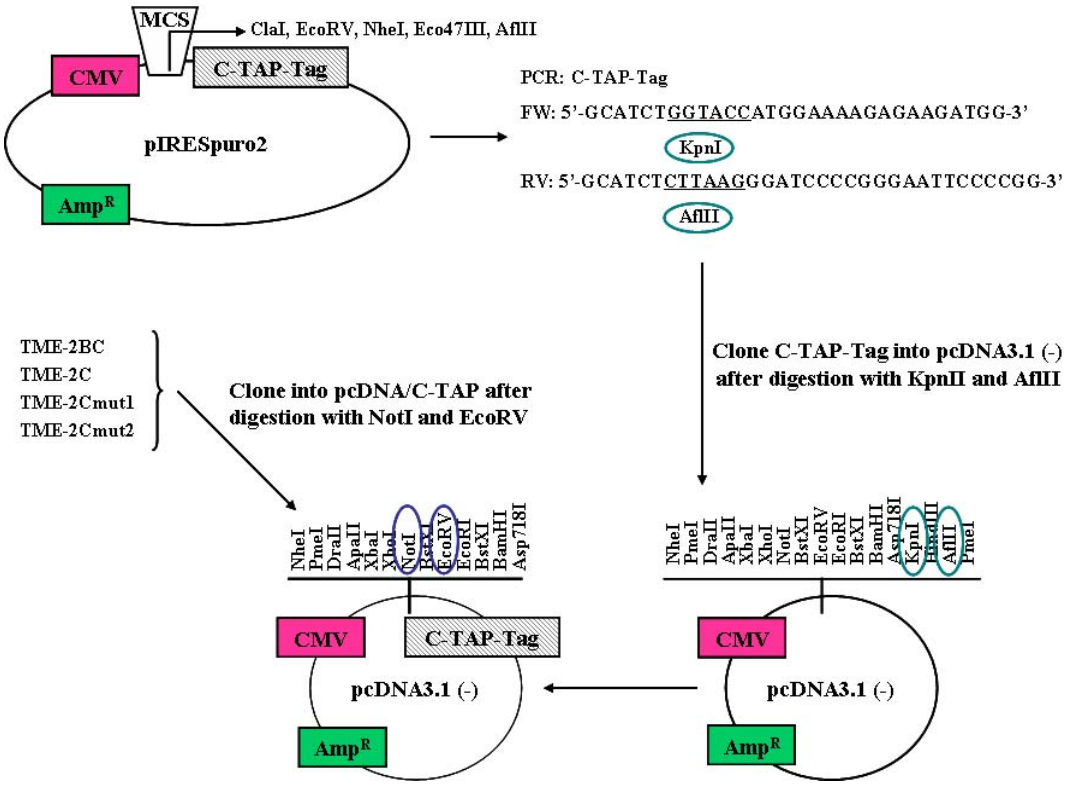

Figure 3.17: Illustration of the cloning strategy utilized for the formation of C-TAP-tagged TMEV proteins. *The C-TAP-tag was amplified by PCR, cleaved by KpnI and AflIII, and finally ligated into a similarly restricted pcDNA3.1(-) vector. PCR-amplified TMEV-2BC, TMEV-2C, TMEV-2Cmut1, and TMEV-2Cmut were cleaved with NotI and EcoRV and ligated into a similarly restricted pcDNA/C-TAP vector.*

3.2.2.3 Intracellular localization of TAP-tagged TMEV-2BC and TMEV-2C

It was intended to localize TAP-tagged TMEV protein-complex 2BC and protein 2C in the cell. BHK-21 cells were transfected with the constructs containing the TAP-tagged proteins, described above. Different transfection methods were employed (section 2.5). To localize the TAP-tagged proteins, immunofluorescence was carried out essentially as described in section 2.6.4. Weser and colleagues (2006) have described that the highly specific interaction of the ZZ-domain of Protein A, which constitutes part of the TAP-tag, to rabbit IgGs can be used to detect TAP-tagged proteins in fixed cells by use of labelled secondary antibodies (Weser *et al.*, 2006). For detection and visualization of the TAP-tagged proteins, a sheep anti-rabbit antibody coupled to TexasRed was used. It was not possible to detect an immunofluorescent signal for TAP-tagged TMEV-2BC or TMEV-2C.

3.2.3 In vitro binding assay of cellular proteins using a total cell extract

It was intended to identify cellular proteins that interact with TMEV protein 2C by using a total cell extract (section 2.8.1). Therefore a total cell extract of a BHK-21 monolayer was prepared. Furthermore, a GST-2C fusion protein was expressed in bacterial cells, and subsequently bound to glutathione sepharose beads (section 2.7.2, 3.3.1.2). The total cell extract was added to the GST-2C/bead complex to "pull down" cellular proteins associated with TMEV-2C. The gel profile obtained from SDS-PAGE shows the expression of GST-2C, the vast pool of proteins present in the total cell extract, and the recovered protein/bead complex (figure 3.18). It was not possible to identify cellular proteins interacting with TMEV-2C. This work was not pursued further due to time constraints.

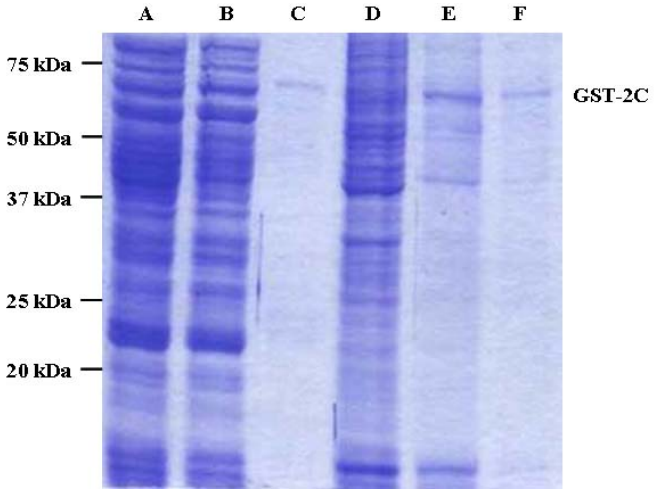

Figure 3.18: Gel profile of an *in vitro* binding assay of total cell extract using GST-2C. *Protein complex GST-2C was expressed in BL21 bacterial cells (A: uninduced; B: induced), and subsequently bound to glutathione sepharose beads (C). A total cell extract of BHK-21 cells was prepared (D), and added to the GST-2C/bead complex. After rotation, the supernatant (E) was aspirated, the protein/bead complex was washed, and analyzed on SDS-PAGE (F). The band corresponding to GST-2C is indicated. Furthermore, the positions of the size markers are shown.*

3.2.4 Binding of in vitro translated reticulon 3 and AKAP10 to TMEV-2C

It has been shown that the N-terminus of FMDV protein 2C binds to the C-terminal region of a protein kinase A (PKA) anchoring protein, AKAP10, and competes with the RII regulatory subunit of PKA (Knox *et al.*, submitted). PKA activity is known to play a number of key roles in the regulation of cellular membrane traffic. The binding to AKAP10 was also observed for 2C proteins derived from viruses of other genera within the *Picornaviridae*: the *Entero*-, *Rhino*-, *Cardio*-, *Parecho*-, and *Hepatoviruses*. In all cases specific binding, but with different affinities, was observed (Knox *et al.*, submitted). It was intended to confirm the binding of TMEV protein 2C to AKAP10. Furthermore, it has been demonstrated that the host cell protein reticulon 3 (RTN3) associates with the viral replication complex through direct interaction with the N-terminus of the enterovirus 71-encoded protein 2C (Tang *et al.*, 2007; section 4.2.1). The possible binding of TMEV protein 2C to RTN3 was investigated.

To confirm the interaction between TMEV-2C and AKAP10, protein 2C was expressed as a GST-fusion protein (GST-2C), and as a MBP-fusion protein (MBP-2C). GST-2C and GST alone were purified on glutathione sepharose beads. MBP-2C and MBP alone were immobilized on amylose resin. Both GST-2C and MBP-2C were tested for their ability to interact with an *in vitro* translated AKAP10. A full length mouse AKAP10 clone was purchased from RZPD Deutches (clone: IRAKp961M07111Q; Ressourcenzentrum für Genomforschung GmbH, Berlin, Germany). Moreover, both GST-2C and MBP-2C were analyzed for their ability to bind an *in vitro* translated RTN3. A full length mouse RTN3 was also purchased from RZPD (clone: IRAVp968C0112D). The gel profiles demonstrate that RTN3 associates *in vitro* with GST-2C and MBP-2C (figure 3.19). They also show some non-specific binding to GST and MBP alone. However, it can be observed that the association to GST-2C and MBP-2C is stronger as suggested by the intensity of the bands. This *in vitro* binding assay did not show an interaction between TMEV-2C and AKAP10. The gel profiles show no association with GST-2C or MBP-2C (figure 3.19). This is in contrast to previously obtained results that demonstrated an interaction between protein 2C and GST-IAP3. IAP3 consists of the C-terminal 52 amino acids of AKAP10 (Knox *et al.*, submitted). Several internal initiation sites have been identified within the RTN3 and AKAP10 amino acid sequences, which can explain the extra bands observed on the gel.

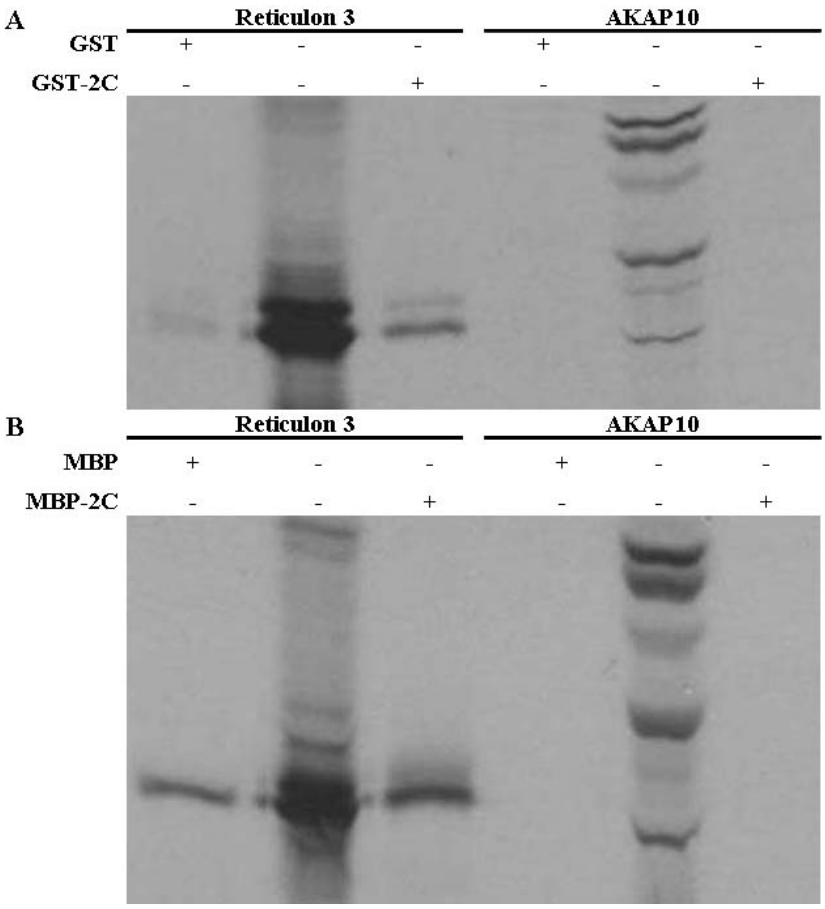

Figure 3.19: Binding of *in vitro* translated reticulon 3 and AKAP10 to TMEV protein 2C. *In vitro translated RTN3 and AKAP10 were incubated with glutathione sepharose beads containing either GST or GST-2C (A), or MBP or MBP-2C (B). RTN3 associates with TMEV protein 2C. However, some non-specific binding to GST and MBP can be observed. AKAP10 does not interact with TMEV-2C.*

3.2.5 Transfection and infection of cells with TMEV containing mutations within the N-terminal part of protein 2C

It has been demonstrated that the N-terminal part of TMEV-2C binds to the C-terminal part of AKAP10 (Knox *et al.*, submitted). Constructs encoding specific point mutations in the N-terminal part of the coding region of the 2C protein in the TMEV cDNA have previously been made in our laboratory. The point mutations cause amino acid substitutions in the 2C coding sequence (table 3.1).

Construct	*Position of amino acid substitution mutation in 2C coding sequence*	*Amino acid substitution mutation*
pGDVII-wt	none	none
pGDVII-mt4	4	Arginine → Alanine
pGDVII-mt8	8	Glutamate → Alanine
pGDVII-mt14	14	Lysine → Alanine
pGDVII-mt18	18	Tryptophan → Alanine
pGDVII-mt23	23	Isoleucine → Alanine

Table 3.1: Constructs encoding specific point mutations in the coding region of the 2C protein in the cDNA of TMEV. *The positions of the amino acid substitutions in the 2C coding region are shown. The amino acids have all been substituted by an alanine.*

It was intended to investigate the effect of the amino acid substitutions on virus replication. Therefore, wild type and mutant TMEV cDNAs were used to prepare virus stocks as described in section 2.4.3. The wild type and mutant TMEV cDNAs are provided in the pBluescript II SK (+) vector (Fermentas, York, UK). The cDNA was linearized using *BamHI*. The linearized plasmid DNA was subsequently purified and transcribed *in vitro* using a T7 RNA polymerase. The RNA was used for transfection of BHK-21 cells by electroporation. After 6 hours, growth medium was changed to serum-free medium and cells were examined for the appearance of CPE at different time points over a period of 120 hours. Cells were harvested when 100% CPE was displayed or at 120 hours post infection. CPE is characterized by the rounding up and detaching of the cells. Wild type and mutant 14 TMEV showed 100% CPE at 72 hours post infection, and mutant 18 TMEV displayed 100% CPE at 96 hours post infection. However, mutant 4, mutant 8, and mutant 23 TMEV showed some cell death that resembled the cell death observed in the negative control. BHK-21 cells were used for transfection by electroporation without adding RNA. These cells showed cell death, which is most likely due to serum-starvation. The proportion of BHK-21 cells showing CPE at different time points after transfection, are displayed in table 3.2.

Transfected	***Approximate % CPE***					
TMEV RNA	**6 hours**	**24 hours**	**48 hours**	**72 hours**	**96 hours**	**120 hours**
Wild type	10	50	90	100		
Mutant 4	10	20	40	60	70	80
Mutant 8	10	40	40	60	70	80
Mutant 14	10	50	80	100		
Mutant 18	10	50	70	80	100	
Mutant 23	10	20	60	80	90	80
No RNA	10	20	40	60	70	80

Table 3.2: The proportion of BHK-21 cells displaying CPE subsequent to transfection with RNA encoding wild type or mutant TMEV RNA. *CPE was first observed in cells transfected with wild type and mutant 14 TMEV RNA, followed by mutant 18 TMEV. Cell death observed in cells transfected with mutant 4, mutant 8, and mutant 23 TMEV RNA resembled cell death seen in the negative control (no RNA).*

BHK-21 cells were infected with wild type and mutant TME viruses obtained from the growth medium covering BHK-21 cells previously transfected with wild type and mutant TMEV RNA. At 24 hours post infection, a characteristic CPE was seen for wild type (95%), mutant 14 (90%) and mutant 18 TMEV (85%). Mutant 4, mutant 8 and mutant 23 displayed some cell death after 24 hours, which resembled cell death seen in the negative control (table 3.2; figure 3.20), suggesting that no viral particles were rescued after transfection. This was confirmed by titration of the wild type and mutant TME virus preparations as described in section 2.4.2. The titration results are shown in table 3.3. No plaques could be observed for mutant 4, mutant 8, and mutant 23 TMEV mutants. Viral RNA was extracted from the virus preparations and detected by PCR (section 2.4.3.5). It was possible to rescue viral RNA from wild type and mutant TMEV virus preparations, suggesting that mutant 4, mutant 8, and mutant 23 are still able to replicate the viral RNA but are not capable of forming new virus particles. The presence of the expected mutations was checked by sequencing. The sequencing results confirmed the presence of mutant 4 and mutant 8. However, mutant 14, mutant 18, and mutant 23 TMEV seemed to have back-mutated to the original wild type sequence. After sequencing the original constructs, previously made in our laboratory, it was demonstrated that mutant 14 was not present in the original construct. Mutant 18 and mutant 23, however, were present in the original constructs.

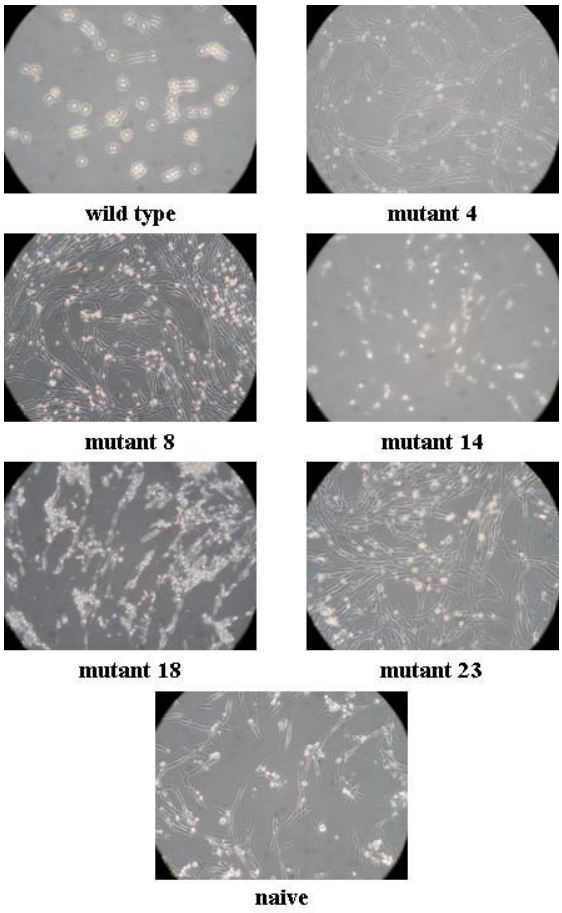

Figure 3.20: CPE observed 24 hours after infection with wild type and mutant TME viruses. *A typical CPE can be observed in cells infected with wild type, mutant 14 and mutant 18 TME viruses. Most cells have rounded up and detached. Cells infected with mutant 4, 8, and 23 resemble those of the negative control (naive). Some cell death can be observed.*

TMEV virus	*Approximate % CPE*	*Titration of virus preparation*
	24 hours	
Wild type	95	8×10^6 pfu
Mutant 4	20	no plaques
Mutant 8	20	no plaques
Mutant 14	90	4×10^5 pfu
Mutant 18	85	3×10^5 pfu
Mutant 23	20	no plaques
naive	20	/

Table 3.3: The proportion of BHK-21 cells showing CPE 24 hours after infection with wild type or mutant TME viruses and titer of the viral preparations. *BHK-21-cells were infected with wild type and mutant TME viruses obtained from growth medium covering BHK-21 cells previously transfected with wild type and mutant TMEV RNA. CPE was observed in cells 24 hours after infection with wild type (95%), mutant 14 (90%) and mutant 18 (85%) TMEV. Cell death observed in cells infected with mutant 4, mutant 8, and mutant 23 TMEV resembled cell death seen in the negative control (naive). Furthermore, the titer of the viral preparations is estimated. Mutant 4, mutant 8, and mutant 23 TMEV displayed no plaques.*

3.2.6 Expression of GFP-IAP3

A discrepancy was observed concerning the binding of TMEV protein 2C to AKAP10. Therefore, we wished to locate AKAP10 in mammalian cells and explore the possible interaction with TMEV-2C. It has been demonstrated that the N-terminal part of protein 2C associates with the C-terminal part of AKAP10 (Knox *et al.*, submitted). IAP3 consists of the C-terminal 52 amino acids of AKAP10. Therefore it was intended to construct a plasmid containing IAP3 fused to enhanced green fluorescent protein (EGFP), which can be used for *in vitro* expression and for expression in mammalian cells.

3.2.6.1 Construction of pGFP-IAP3

The IAP3 fragment was excised from a plasmid, pGST-IAP3, previously made in our laboratory, using *BamHI* and *EcoRI* restriction enzymes. The gel purified IAP3 fragment was subsequently ligated into pEGFP-C1, which was previously restricted with *BglII* and *EcoRI*,

to form pGFP-IAP3. This plasmid can be used for expression in mammalian cells. It was intended to construct a plasmid which could also be used for *in vitro* translation. Therefore, the GFP-IAP3 fragment was excised from pGFP-IAP3 with *NheI* and *EcoRV* restriction enzymes, and ligated into a similarly restricted pcDNA3.1(-) vector to form pcDNA-GFP-IAP3 (figure 3.21). This construct can be used for *in vitro* translation, as well as expression in mammalian cells.

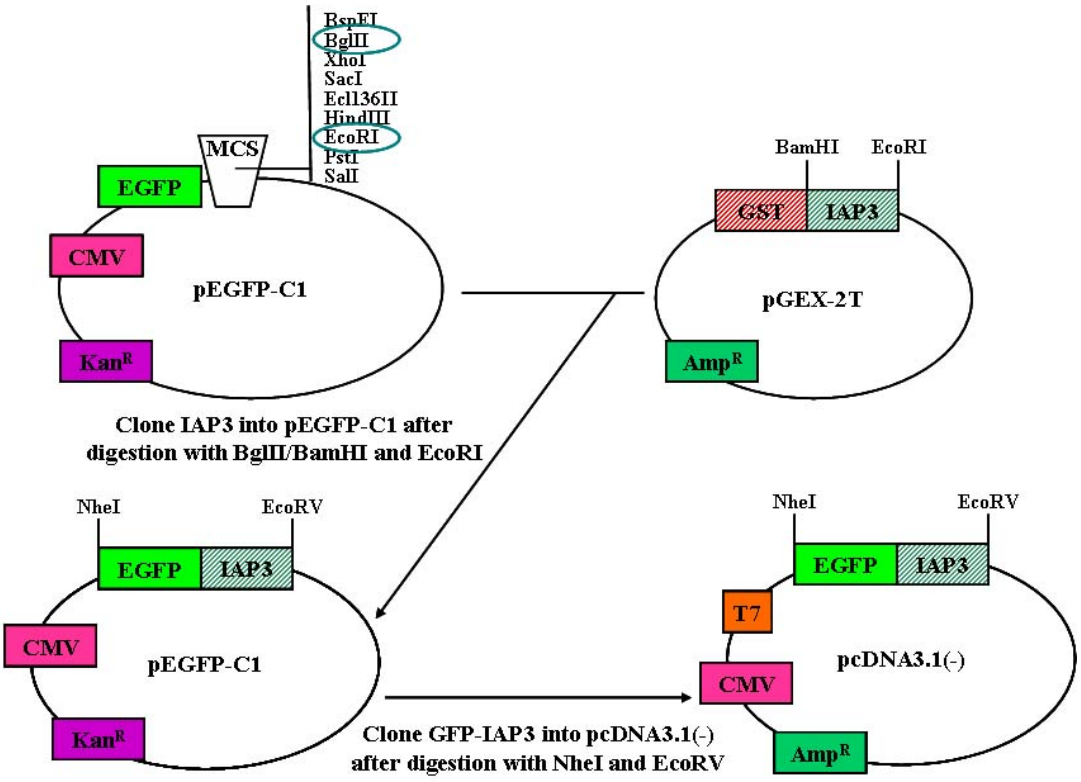

Figure 3.21: Overview of the cloning strategy utilized for the formation of the GFP-IAP3 construct. *The IAP3 fragment was excised from a construct containing GST-IAP3 with BamHI and EcoRI. IAP3 was subsequently ligated into pEGFP-C1, previously restricted with BglII and EcoRI to form pGFP-IAP3. The GFP-IAP3 fragment was subsequently excised from pGFP-IAP3 sing NheI and EcoRV and ligated into a similarly restricted pcDNA3.1(-) vector to form pcDNA-GFP-IAP3.*

3.2.6.2 In vitro translation of pcDNA-GFP-IAP3

The pcDNA-GFP-IAP3 construct was used to program a wheat germ extract coupled transcription/translation reaction. Furthermore, the GFP-2A-GUS and GUS-2A-GFP constructs, previously made in our laboratory, have been used as control reactions. The radiolabelled translation products were separated by 10% SDS-PAGE and visualized by autoradiography. The gel profiles of the *in vitro* coupled transcription/translation reactions show translation of GFP-IAP3, and moreover the expected translation products of GFP-2A-GUS and GUS-2A-GFP can be observed (figure 3.22).

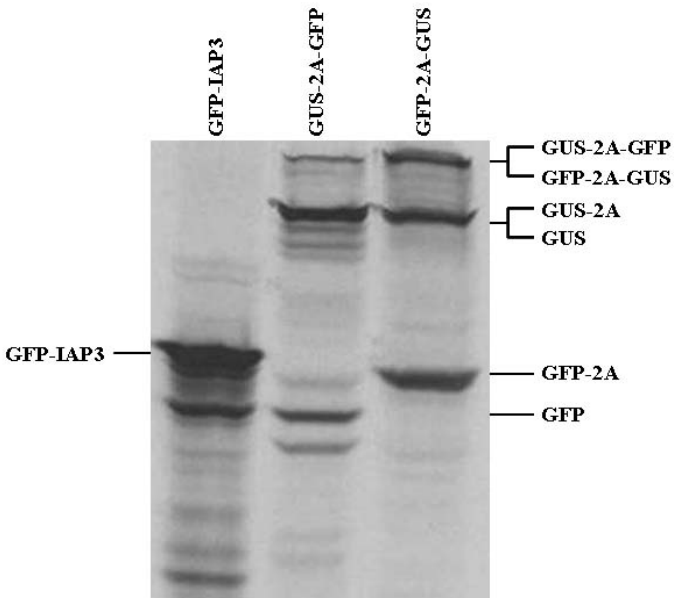

Figure 3.22: Gel profiles of *in vitro* coupled transcription/translation reactions. *The lanes are labelled with the constructs used for the transcription/translation reactions. In vitro translation of GFP-IAP3 can be observed. Furthermore, the full length and processed translation products of GFP-2A-GUS and GUS-2A-GFP are indicated.*

3.2.6.3 Intracellular localization of GFP-IAP3

The pGFP-IAP3 construct, described in section 3.2.6.1, was used to transfect BHK-21 cells using the FuGENE 6 transfection reagent (section 2.5.2.1). Cells were fixed 24 hours after transfection, as detailed in section 2.6.3. Images were acquired using the DeltaVision® microscope system (section 2.6.5). IAP3 seems to form a granular pattern spread out in the

cytoplasm (figure 3.23). It was intended to co-transfect cells with pGFP-IAP3 and V5-tagged TMEV-2C to investigate the possible co-localization of IAP3 and protein 2C. However, this was not possible due to very low transfection efficiencies observed for TMEV protein 2C. Furthermore, it was aspired to transfect BHK-21 cells with the pGFP-IAP3, followed by an infection with TMEV GDVII, in order to investigate the co-localization of IAP3 and protein 2C, visualized using anti-TMEV-2C antibody (section 3.3.2). This work was not pursued due to time constraints.

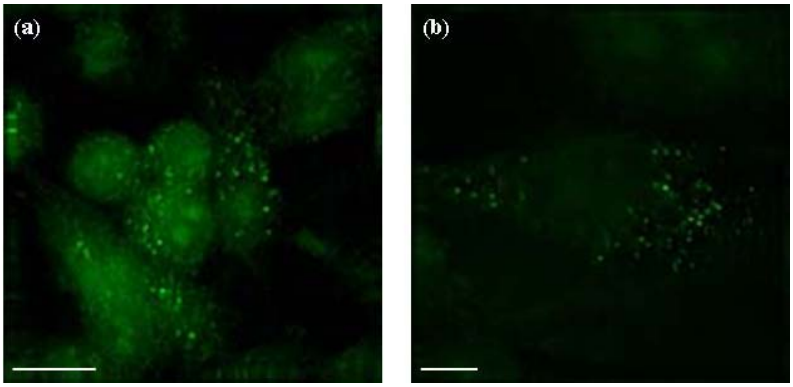

Figure 3.23: Intracellular localization of IAP3. *The pGFP-IAP3 construct was used to transfect BHK-21 cells. A granular pattern, spread out in the cytoplasm, can be observed for IAP3. Bar (a), 15 µm; bar (b), 5 µm.*

3.3. TMEV protein 2C antibody production

3.3.1 Bacterial expression of TMEV protein 2C

3.3.1.1 Polyhistidine tagging of TMEV-2BC and TMEV-2C

Protein-complex 2BC and protein 2C of the *wt* GDVII TMEV strain were amplified by PCR using TMEV-2BC-His-FW/TMEV-2C-His-FW and TMEV-2C-His-RV. PCR fragments were purified by agarose gel electrophoresis. The PCR fragments were cleaved with *BamHI* and *HindIII* and the restriction fragments were subsequently gel purified. The purified restriction fragments were ligated into a similarly restricted peHisTev vector to form TMEV-2BC-His and TMEV-2C-His (figure 3.24).

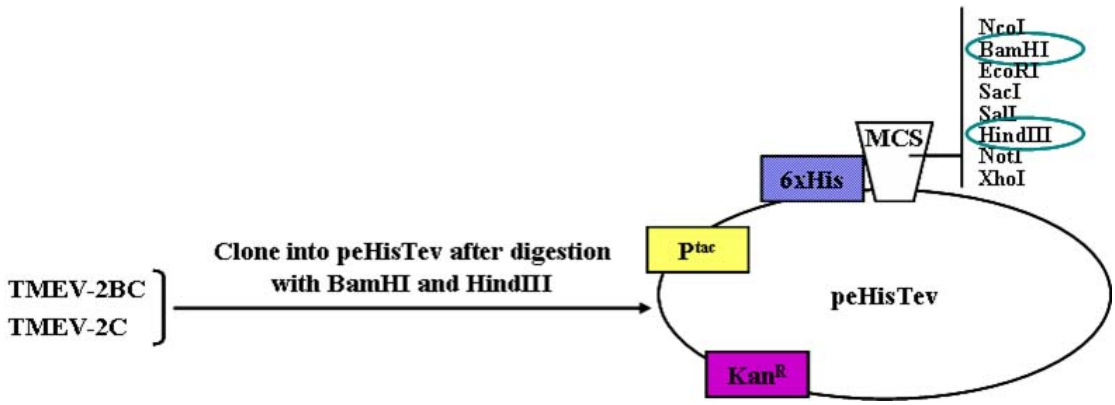

Figure 3.24: Illustration of the cloning strategy utilized for the formation of His-tagged TMEV proteins. *TMEV-2BC and TMEV-2C were amplified by PCR. The purified PCR-products were restricted with BamHI and HindIII and ligated into a similarly restricted peHisTev vector.*

TMEV-2BC-His and TMEV-2C-His were expressed essentially as described in section 2.7.1. BL21(DE3)pLysS competent cells were initially used for transformation. Expression of TMEV-2BC-His and TMEV-2C-His was induced at 37°C using 0.5 mM IPTG (final concentration), and the induced cell extract was subsequently used for binding to nickel beads. No expression could be observed. Therefore, different final IPTG concentrations were employed to induce expression of the His-tagged proteins. Figure 3.25 shows the gel profiles of TMEV-2BC-His and TMEV-2BC-His expressed at 37°C using 0.1 mM, 0.5 mM or 1 mM IPTG (final concentration). No expression could be observed under these conditions. Induction of expression of the His-tagged proteins was also carried out at RT using different IPTG concentrations. However, no expression could be detected at RT. Therefore, a different strain of bacterial cells, called Rosetta(DE3)pLysS competent cells, was used for transformation of the TMEV-2BC-His and TMEV-2C-His constructs. Rosetta(DE3)pLysS competent cells are a derivative of BL21(DE3)pLysS which supply the tRNAs for six codons that are used infrequently in *E. coli*. Expression was induced at 37°C and at RT using 0.1 mM, 0.5 mM, and 1 mM IPTG (final concentration). However, expression could still not be observed.

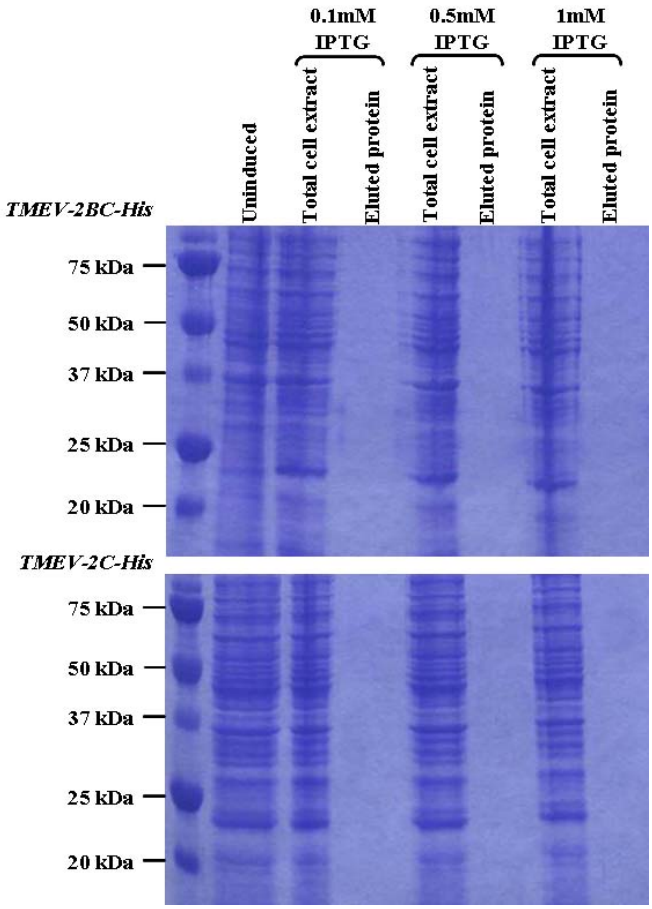

Figure 3.25: Gel profiles of His-tagged TMEV-2BC and TMEV-2C. *BL21(DE3)pLysS competent cells were used for transformation of TMEV-2BC-His (top) and TMEV-2C-His (bottom). Expression of the His-tagged proteins was induced at 37°C using different final IPTG concentrations as indicated. The uninduced cell extract, the induced cell extract, and the protein/nickel bead complex (eluted protein) are shown. The positions of the protein size markers are indicated.*

3.3.1.2 Glutathione-S-transferase tagging of TMEV-2BC and TMEV-2C

Protein-complex 2BC and protein 2C of the *wt* GDVII TMEV strain were amplified by PCR using TMEV-2BC-bact-FW/TMEV-2C-bact-FW and TMEV-2C-bact-RV. The purified PCR fragments were cleaved with *BamHI* and *SalI* and the restriction fragments were subsequently gel purified. The purified restriction fragments were ligated into a similarly restricted pGEX-5V-3 vector to form TMEV-2BC-GST and TMEV-2C-GST (figure 3.26).

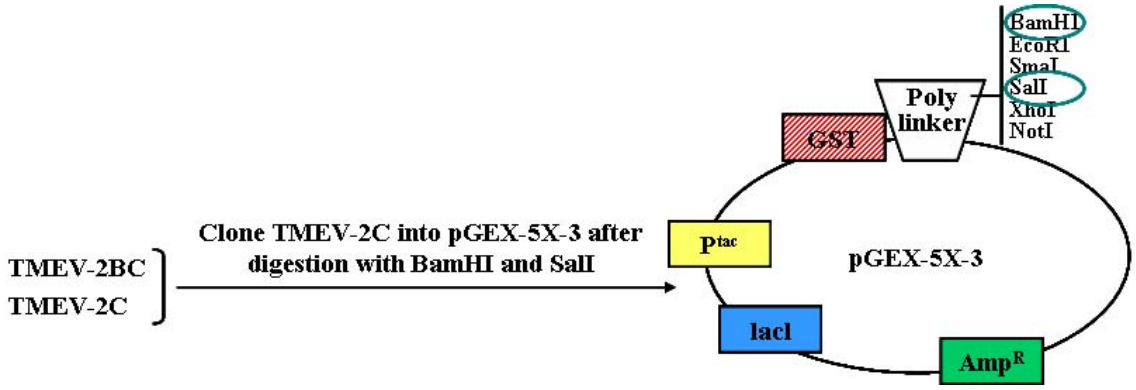

Figure 3.26: Overview of the cloning strategy utilized for the formation of GST-tagged TMEV proteins. *TMEV-2BC and TMEV-2C were amplified by PCR. The purified PCR-products were restricted with BamHI and SalI and ligated into a similarly restricted pGEX-5X-3 vector.*

TMEV-2BC-GST and TMEV-2C-GST were expressed essentially as described in section 2.7.2. BL21(DE3)pLysS competent cells were used for transformation. Expression of TMEV-2BC-GST and TMEV-2C-GST was induced at 37°C using 0.5 mM IPTG (final concentration), and the induced cell extract was subsequently used for binding to glutathione sepharose beads. It was not possible to detect expression of TMEV-2BC-GST. However, expression of TMEV-2C-GST was observed (figure 3.27).

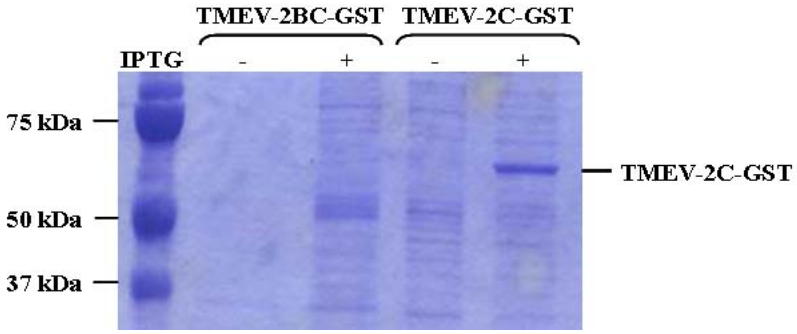

Figure 3.27: Gel profiles of GST-tagged TMEV-2BC and TMEV-2C. *BL21(DE3)pLysS competent cells were used for transformation of TMEV-2BC-GST and TMEV-2C-GST. Expression of the GST-tagged proteins was induced at 37°C using a 0.5 mM final IPTG concentration. The expressed TMEV-2C-GST bound to glutathione sepharose beads is shown. The positions of the protein size markers are indicated.*

3.3.1.3 Maltose binding protein tagging of TMEV-2BC and TMEV-2C

Protein-complex 2BC and protein 2C of the *wt* GDVII TMEV strain were amplified by PCR using TMEV-2BC-bact-FW/TMEV-2C-bact-FW and TMEV-2C-bact-RV. The PCR fragments were purified by agarose electrophoresis. The purified PCR fragments were cleaved with *BamHI* and *SalI* and the restriction fragments were subsequently gel purified. The IAP3 fragment in the pMAL-IAP3 construct, previously made in our laboratory, was excised using *BamHI* and *SalI*, and replaced with the similarly restricted PCR-fragments to form TMEV-2BC-MBP and TMEV-2C-MBP (figure 3.28).

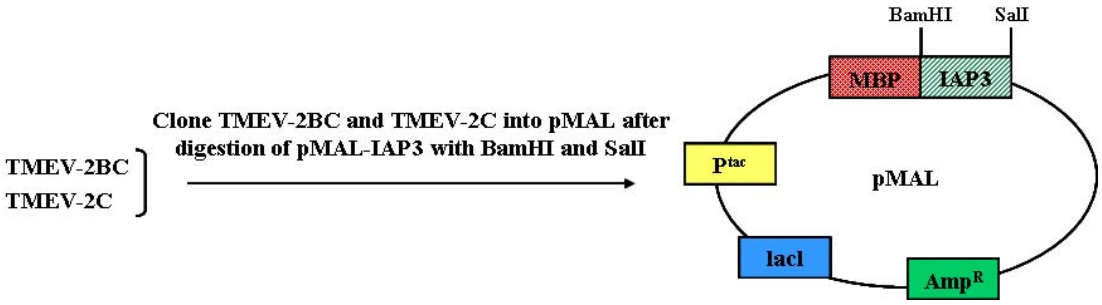

Figure 3.28: Illustration of the cloning strategy employed for the formation of MBP-tagged TMEV proteins. *The IAP3 fragment was excised from pMAL-IAP3 with restriction enzymes BamHI and SalI, and replaced by similarly restricted TMEV-2BC and TMEV-2C PCR-fragments.*

TMEV-2BC-MBP and TMEV-2C-MBP were expressed essentially as described in section 2.7.3. BL21(DE3)pLysS competent cells were used for transformation, and expression of TMEV-2BC-GST and TMEV-2C-GST was induced at 37°C using 0.3 mM IPTG (final concentration). The induced cell extract was subsequently used for binding to amylase resin. It was not possible to observe expression of TMEV-2BC-MBP. However, expression of TMEV-2C-MBP was detected (figure 3.29).

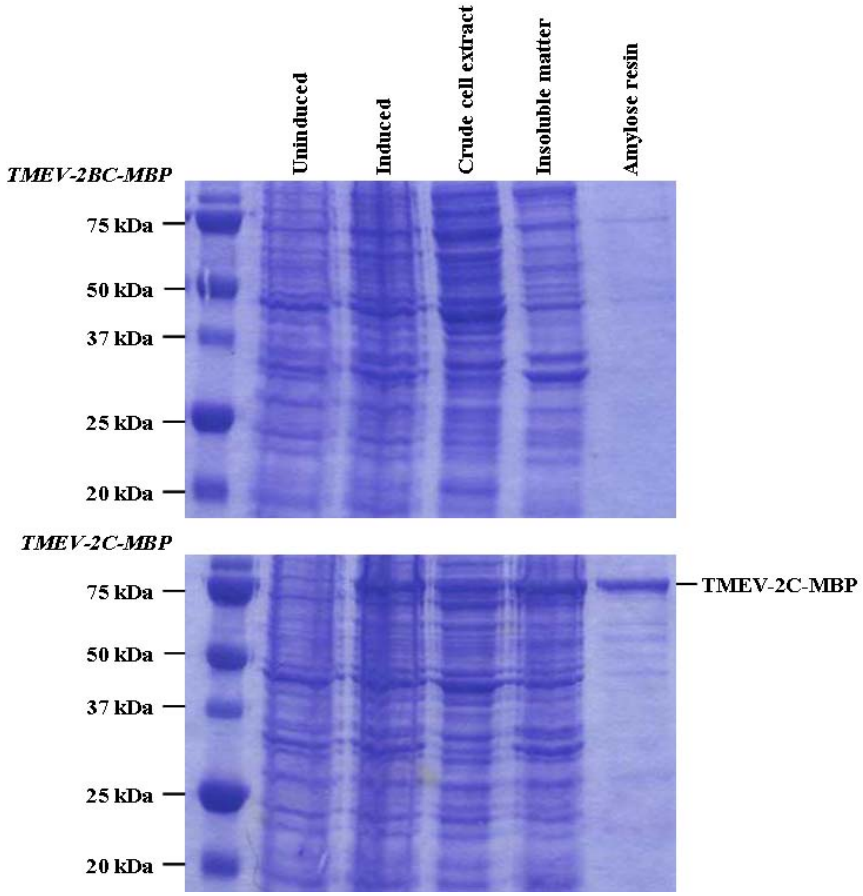

Figure 3.29: Gel profiles of MBP-tagged TMEV-2BC and TMEV-2C. *BL21(DE3)pLysS competent cells were used for transformation of TMEV-2BC-MBP (top) and TMEV-2C-MBP (bottom). Expression of the MBP-tagged proteins was induced at 37°C using a 0.3 mM final IPTG concentration. The expressed TMEV-2C-MBP bound to amylose resin is shown. The positions of the protein size markers are indicated.*

3.3.2 Development of an anti-TMEV-2C antibody

The bacterial expression of TMEV-2C allowed us to have an anti-TMEV-2C antibody developed. TMEV-2C-MBP was purified by John Nicholson. In brief, a 100 ml overnight culture was prepared, as described in section 2.7.3, and incubated at 37°C. After incubation, 50 ml of overnight culture was transferred into 2x1 L culture and incubated at 37°C until an OD (600 nm) of 0.6 was reached. IPTG was added to a final concentration of 0.5 mM, and incubation was continued for 3 hours. Cells are centrifuged at 6000 rpm for 20 min, and subsequently resuspended in column buffer and sonicated. The lysed cells are centrifuged

for 15 min at 10 000 rpm to remove the cell debris. An amylase resin column (New England BioLabs Ltd., Herts, UK) was used to purify TMEV-2C-MBP. The polyclonal anti-TMEV-2C antibody was developed by Diagnostics Scotland (Edinburgh, Scotland). The purified TMEV-2C-MBP was used for immunization of rabbits. Serum was collected at 1, 2, and 3 months after immunization. It was intended to purify the anti-TMEV-2C-antibody using TMEV-2C-GST. However, due to time constraints, the purification was not carried out. Therefore, the whole antiserum was used for preliminary experiments.

The TMEV-2BC-V5 and TMEV-2C-V5 constructs, discussed in section 3.1.1.1, were expressed *in vitro* using a wheat germ extract coupled transcription/translation system. Furthermore, an immunoprecipitation experiment was performed. The *in vitro* translated radiolabelled proteins were incubated with protein G Sepharose beads containing the anti-TMEV-2C antibody. The proteins associated with the anti-TMEV-2C antibody were eluted from the beads by boiling in SDS gel-loading buffer and analyzed by 10 % SDS-PAGE. The distribution of radiolabel was visualized by autoradiography (figure 3.30). The anti-TMEV-2C antibody binds TMEV-2BC-V5 and TMEV-2C-V5.

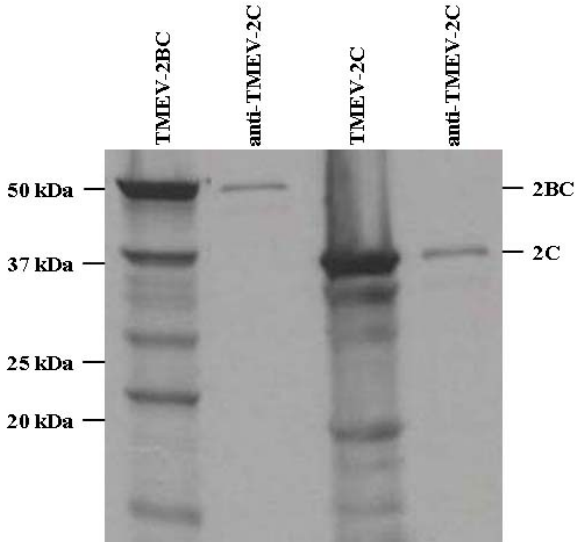

Figure 3.30: Gel profiles of *in vitro* coupled transcription/translation reactions and subsequent immunoprecipitation reactions. *The lanes are labelled with the constructs used for the transcription/translation reactions and the antibody used for the immunoprecipitation reactions. The positions of the protein size markers are indicated.*

TMEV-2C-GST and GST alone were expressed essentially as described in section 2.7.2. The cell extracts were analyzed by western blot using the anti-TMEV-2C antibody. TMEV-2C-GST was detected by the anti-TMEV-2C antibody, as shown in figure 3.31. However, some non-specific bands can be observed for both TMEV-2C-GST and GST alone. Purification of the anti-TMEV-2C antibody might result in a more specific binding.

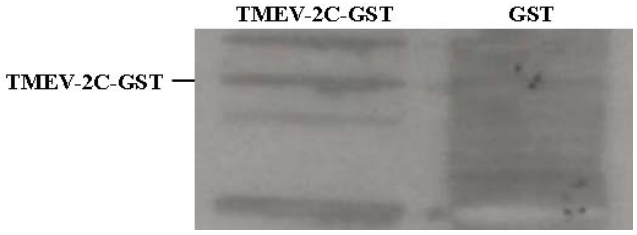

Figure 3.31: Western blot analysis of TMEV-2C-GST using anti-TMEV-2C. *TMEV-2C-GST and GST alone were expressed, and cell extracts were subsequently analyzed by western blot using the anti-TMEV-2C antibody. TMEV-2C-GST is indicated.*

The anti-TMEV-2C antibody was also used for immunofluorescence experiments described in section 3.1.5. Protein 2C can be localized in TMEV-infected cells by using the anti-TMEV-2C antibody. Furthermore, protein 2C was localized in TMEV-infected BHK-PDF18 cells, showing overlap with the dispersed remnants of the Golgi complex at late stages of infection.

3.4. TMEV infection

3.4.1 Creation of a stable cell line constitutively expressing fluorescent microtubules

A computer-based analysis has demonstrated that TMEV protein 2C is highly similar to three members of the AAA ATPase superfamily: (1) lipotransin: a hormone-sensitive lipase (HSL)-interacting protein that appears to translocate HSL to the lipid droplet; (2) VPS4: a protein required for endosomal transport; and (3) p60 katanin: the katanin subunit responsible for microtubule severing (figure 3.32). It was intended to investigate the similarity between TMEV protein 2C and the p60 subunit of katanin.

Katanin is a heterodimeric, ATP-dependent, microtubule-severing protein first purified from sea urchin eggs (*Strongylocentrotus purpuratus*). It has a microtubule-stimulated ATPase activity and hydrolysis of ATP is required for the microtubule-severing reaction. Katanin is also known to disassemble stable microtubules (MTs) to form polymerisation-competent tubulin subunits (McNally & Vale, 1993). It is a heterodimer of 60 and 80 kDa subunits, which is highly concentrated at centrosomes throughout the cell cycle (McNally *et al.*, 1996).

TMEV protein 2C might exhibit a similar function to the p60 subunit of katanin in infected cells. Therefore, it was aspired to produce a stable cell line constitutively expressing fluorescent MTs. The stable cell line would then be infected with TMEV and the effect of TMEV on MTs would be investigated. The anti-TMEV-2C antibody would be used to link TMEV protein 2C to the possible effect of TMEV on MTs.

MTs and the Golgi complex are closely related in the cytoplasm of the cell. The Golgi complex is composed of cisternal stacks, usually arranged around the centrosome, which is the major organizing center for MTs. Golgi stacks are broken up and dispersed in the cytoplasm upon drug-induced disruption of MTs. Furthermore, MT-dependent motor proteins dynein and kinesin bind to the Golgi membrane and seem to play a role in transport to and from the Golgi complex. The Golgi complex undergoes fragmentation during mitosis. MTs depolymerize during prophase resulting in the extensive reorganization of the Golgi stacks (reviewed by Thyberg & Moskalewski, 1999).

Figure 3.32: Alignment showing similarity with TMEV protein 2C. *A computer based analysis showed that TMEV protein 2C is highly similar to lipotransin, VPS4, and p60-katanin. The conserved Walker A, B and C motifs are indicated in red. The additional conserved residues (*) are indicated in blue.*

3.4.1.1 Creation of a stable cell line constitutively expressing YFP-tubulin

It was intended to produce a stable cell line constitutively expressing YFP-tubulin. Poliovirus protein 2C and its precursor 2BC have been associated with the membrane rearrangements, the disappearance of the Golgi complex, and the vesicle formation observed in infected cells. Therefore, it was intended to also induce CFP-Golgi or CFP-ER in the stable cell line expressing YFP-tubulin.

A construct was generated containing α-tubulin preceded by EYFP and followed by the self-cleaving FMDV 2A protein. Moreover, the construct contained ECFP preceded by GT or calreticulin (CR), and followed by a second FMDV 2A protein and Pac. GT is a type II signal-anchor sequence that will target CFP to the Golgi complex. CR, however, is a type I signal sequence that will transport CFP to the ER. Pac will act as selection agent.

EYFP-α-tubulin was amplified by PCR using T7 and Tub-RV. The pIRES-EYFP-tubulin plasmid, available in our laboratory, was used as template. It contains a fusion protein of EYFP and human α-tubulin. The purified PCR product was cleaved with *NheI* and *XbaI*, and subsequently purified by agarose gel electrophoresis. Furthermore, the constructs pEYFP-2A-GT-ECFP-2A-Pac and pEYFP-2A-CR-ECFP-2A-Pac, previously made in our laboratory, were cleaved with *NheI* and *XbaI*, creating three fragments: (1) pcDNA3.1(-)-2A-Pac; (2) 2A-GT/CR-CFP; and (3) EYFP. EYFP-α-tubulin was ligated into pcDNA3.1(-)-2A-Pac, forming pEYFP-α-tubulin-2A-Pac. The 2A-GT/CR-ECFP fragment was subsequently ligated into pEYFP-α-tubulin-2A-Pac, previously cleaved with *XbaI*, to form pEYFP-α-tubulin-2A-GT-ECFP-2A-Pac and pEYFP-α-tubulin-2A-CR-ECFP-2A-Pac (figure 3.33).

The constructs were used to transfect BHK-21 cells using the FuGENE 6 transfection reagent, as described in section 2.5.2.1. Puromycin was used as a dominant selectable marker to permit isolation of stable transfectants. Therefore, the overlaying growth medium was replaced 24 hours post transfection with growth medium supplemented with 10μg/ml puromycin. Cells were grown for 14 days with a change of medium supplemented with puromycin after 7 days. After 14 days, the plates were inspected for the presence of colonies. It was, however, not possible to isolate healthy colonies.

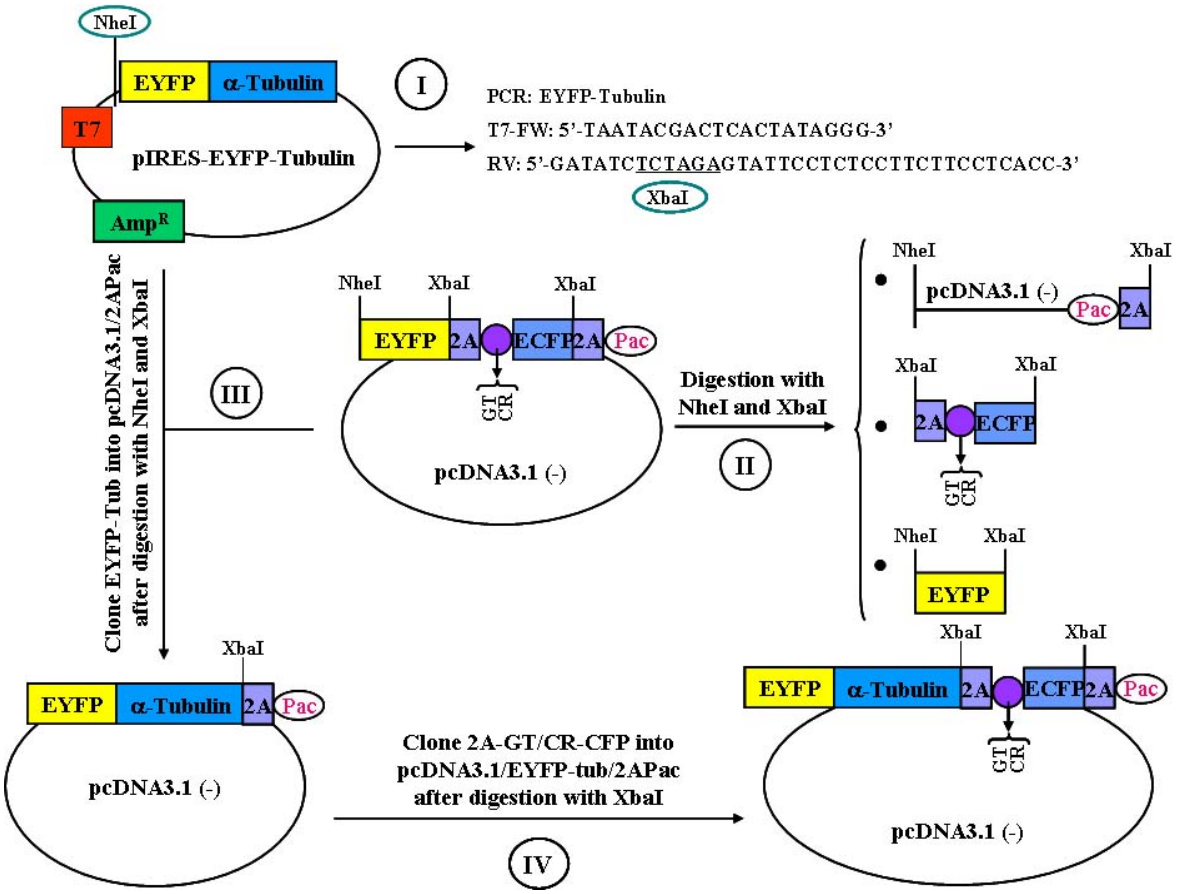

Figure 3.33: Overview of the cloning strategy used for the creation of a stable cell line constitutively expressing YFP-tubulin. *EYFP-α-tubulin was amplified by PCR and cleaved with NheI and XbaI. The pEYFP-2A-GT/CR-ECFP-2A-Pac construct was similarly restricted, creating the following fragments: pcDNA3.1(-)-2A-Pac, 2A-GT/CR-ECFP, and EYFP. EYFP-α-tubulin ligated into pcDNA3.1(-)-2A-Pac. Subsequently, 2A-GT/CR-ECFP was ligated into pEYFP-2A-Pac, previously restricted with XbaI.*

3.4.1.2 Creation of a stable cell line constitutively expressing cherry-tubulin using the lentivirus system

Cherry-tubulin was amplified by PCR using Lenti-cherry-Tub-FW and Lenti-cherry-Tub-RV. A vector containing cherry-tubulin, available in our laboratory, was used as template. The purified PCR product was cleaved with *BamHI* and *SpeI* and subsequently gel purified. cherry-tubulin was then ligated into the similarly restricted pdlNotl'MCS'F vector (figure 2.5, section 2.9.1), to form Lenti-cherry-Tubulin (figure 3.34).

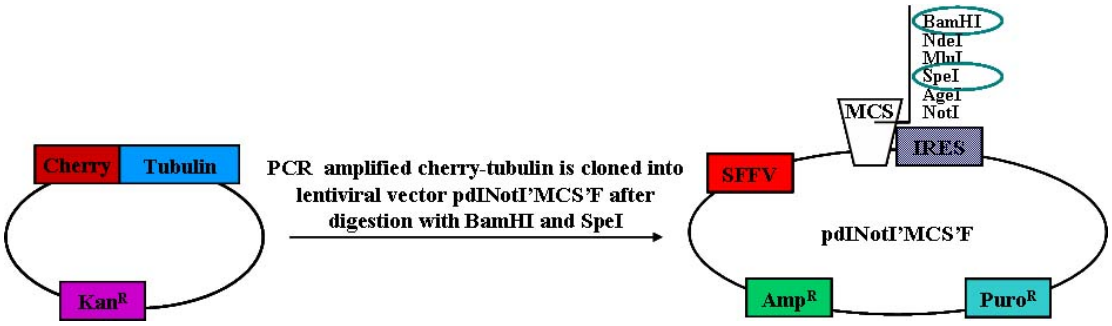

Figure 3.34: Overview of the cloning strategy employed for the creation of a stable cell line constitutively expressing cherry-tubulin. *Cherry-tubulin was amplified by PCR. The purified PCR-product was cleaved with BamHI and SpeI, and subsequently ligated into a similarly restricted pdlNotl'MCS'F vector.*

The Lenti-cherry-tubulin construct was used to generate lentivirus particles that carry the cherry-tubulin fusion protein (as described in section 2.9.1). These lentivirus particles were subsequently used to infect BHK-21 cells, as described in section 2.9.2; and infected cells were selected with puromycin. The lowest concentration of puromycin that causes massive cell death of BHK-21 cells was identified as 10µg/ml (section 2.9.3). It was intended to use the lentiviral particles containing cherry-tubulin to establish a stable cell constitutively expressing cherry-tubulin. However, it was not possible to create this stable cell line. Colleagues have encountered extensive problems with creating a stable cell line constitutively expressing fluorescent microtubules (Tony Vaughn, personal communication).

3.4.2 Observation of intracellular changes during TMEV infection by means of various cellular markers

Various cellular markers were used to observe intracellular changes in TMEV-infected BHK-21 cells. Different compartments and proteins that serve a function in membrane trafficking were targeted. Most cellular markers showed similar changes in the infected cells as a result of infection. Infection causes a decentralization of the monitored organelles and proteins, which results in an accumulation of the organelles and proteins at the periphery of the cell. The different organelles and proteins seem to surround the expanding site of virus replication. One exception was identified; BIGI is localized at the Golgi complex in mock-infected cells, and is spread out in the cytoplasm during TMEV infection (section 3.4.2.6).

3.4.2.1 Changes in the intracellular structure of actin caused by TMEV infection

Actin is a highly conserved globular, structural protein (G-actin). The individual G-actin subunits assemble into long filamentous polymers called F-actin. Two parallel F-actin strands interact in a helical formation, giving rise to microfilaments, a major component of the cytoskeleton. Actin participates in many important cellular functions, including vesicle and organelle movement and the maintenance of cell shape. Furthermore, actin is the monomeric subunit of thin filaments, which are part of the contractile apparatus in muscle cells. It was intended to investigate the changes in the intracellular structure of actin caused by TMEV infection.

BHK-21 cell cultures were prepared and infected as described in section 3.1.5.1. The virus was adsorbed at 37°C, cells were fixed at hourly time points (1-8 h p.i.), and immunofluorescence was carried out (section 2.6.4). Actin was detected with a monoclonal anti-actin antibody using a 1:200 dilution (Sigma-Aldrich Company Ltd., Dorset, UK), and visualized with a rabbit anti-mouse antibody coupled to TexasRed. Figure 3.35 shows a mock infection of BHK-21 cells (a), and BHK-cells at 5 hours and 7 hours post infection. Preliminary results suggest that the filamentous structure of actin disappears during infection. Actin appears to accumulate at the cellular membrane, creating an area devoid of actin, which is thought to be the viral replication site. These results have to be confirmed by further experiments.

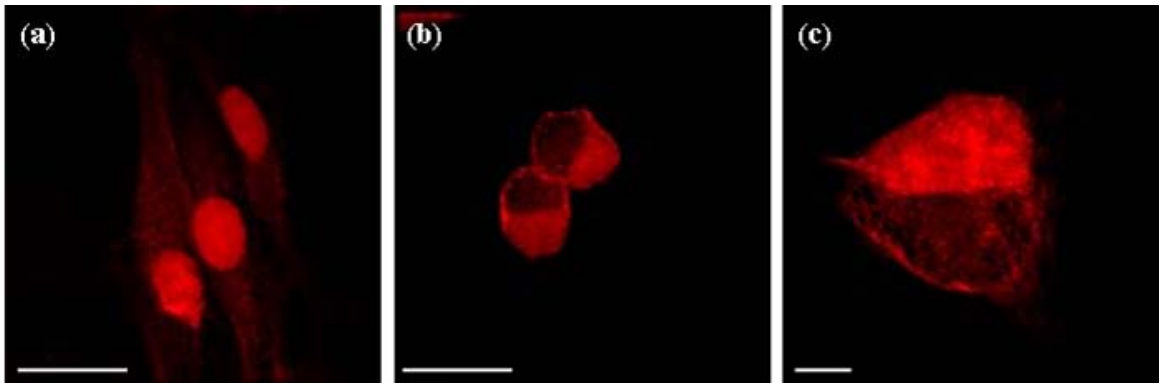

Figure 3.35: Immunofluorescent staining of BHK-21 cells using anti-actin. *Mock-infected cells show an actin organization (a). Actin appears to accumulate at the periphery of the cell during infection as shown at 5 hours (b) and 7 hours p.i. (c). Nuclear staining is due to the secondary antibody. Bar (a-b), 15 µm; bar (c), 5 µm.*

3.4.2.2 Changes in the intracellular organization of tubulin caused by TMEV infection

As it was not possible to establish a stable cell line constitutively expressing fluorescent microtubules (section 3.4.1), it was intended to determine the effect of TMEV-infection on microtubules by means of a cellular marker for tubulin.

Cultures of BHK-21 cells were prepared and infected as described previously (section 3.1.5.1). The virus was adsorbed at 37°C, cells were fixed at hourly time points (1-8 h p.i.), and immunofluorescence was carried out (section 2.6.4). Tubulin was detected with an anti-tubulin antibody using a 1:80 dilution (Sigma-Aldrich Company Ltd., Dorset, UK), and visualized with a sheep anti-rabbit antibody coupled to TexasRed. Preliminary results suggest that TMEV-infection causes a redistribution of tubulin. At 7 hours post infection, tubulin seems to cluster at the periphery of the cell, surrounding the viral replication complexes (figure 3.36). Further experiments are required to confirm these results.

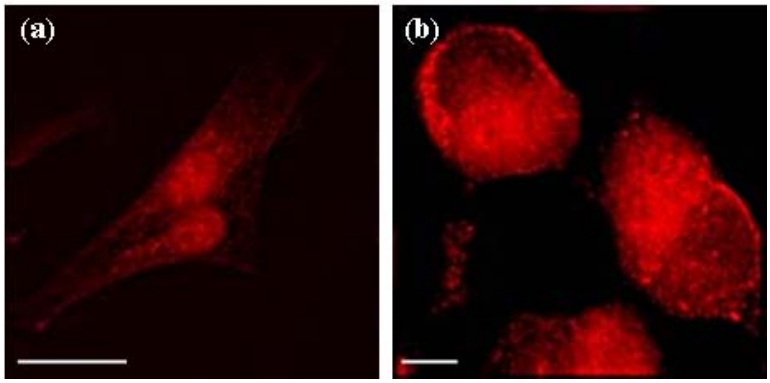

Figure 3.36: Immunofluorescent staining of BHK-21 cells using anti-tubulin. *The normal intracellular tubulin organization can be seen in image (a). At 7h p.i. (b), it can be observed that tubulin is concentrated near the cellular membrane, surrounding the site of viral replication. Nuclear staining is due to the secondary antibody. Bar a, 15 µm; bar b, 5 µm.*

3.4.2.3 Disassembly of the Golgi complex caused by TMEV infection

It has been demonstrated that membranous vesicles arise in the perinuclear region of PV-infected cells. These vesicles proliferate extensively, and spread out in the cytoplasm. The Golgi complex is involved in the generation of these membranous vesicles. Furthermore, PV infection results in the disassembly and disappearance of the Golgi complex. It was, therefore, aspired to observe the changes in the Golgi complex, occurring during TMEV-infection. The observations made, are confirmed by live imaging of TMEV-infected BHK-PDF18 cells as described in section 3.4.3.

BHK-21 cell cultures were prepared and infected as described in section 3.1.5.1. TMEV GDVII was adsorbed, cells were fixed at hourly time points (1-8 h p.i.), and immunofluorescence was carried out (section 2.6.4). Two antibodies were used to localize the Golgi complex in the TMEV-infected cells: (i) anti-GM130 antibody (Sigma-Aldrich), an antibody raised against the 130 kDa Golgi matrix protein (1:500 dilution); and (ii) a monoclonal anti-Golgi 58K protein antibody (anti-Golgi; Sigma-Aldrich), which recognizes an epitope on the microtubule-binding peripheral 58 kDa Golgi membrane protein (1:100 dilution). Anti-GM130 was visualized with a sheep anti-rabbit antibody coupled to TexasRed, whilst anti-Golgi was visualized using a rabbit anti-mouse antibody coupled to TexasRed. A mock infection of BHK-21 cells shows the typical crescent-shaped Golgi complex. This shape remains at 1 hour and 2 hours post infection. At 3 hours p.i., the solid, crescent-shaped organelle has changed into a series of punctuate fluorescent points spread out in the cytoplasm. At 5 and 7 hours p.i., the Golgi complex has disassembled and the remnants form a balloon-like structure, surrounding the viral replication site (Figure 3.37).

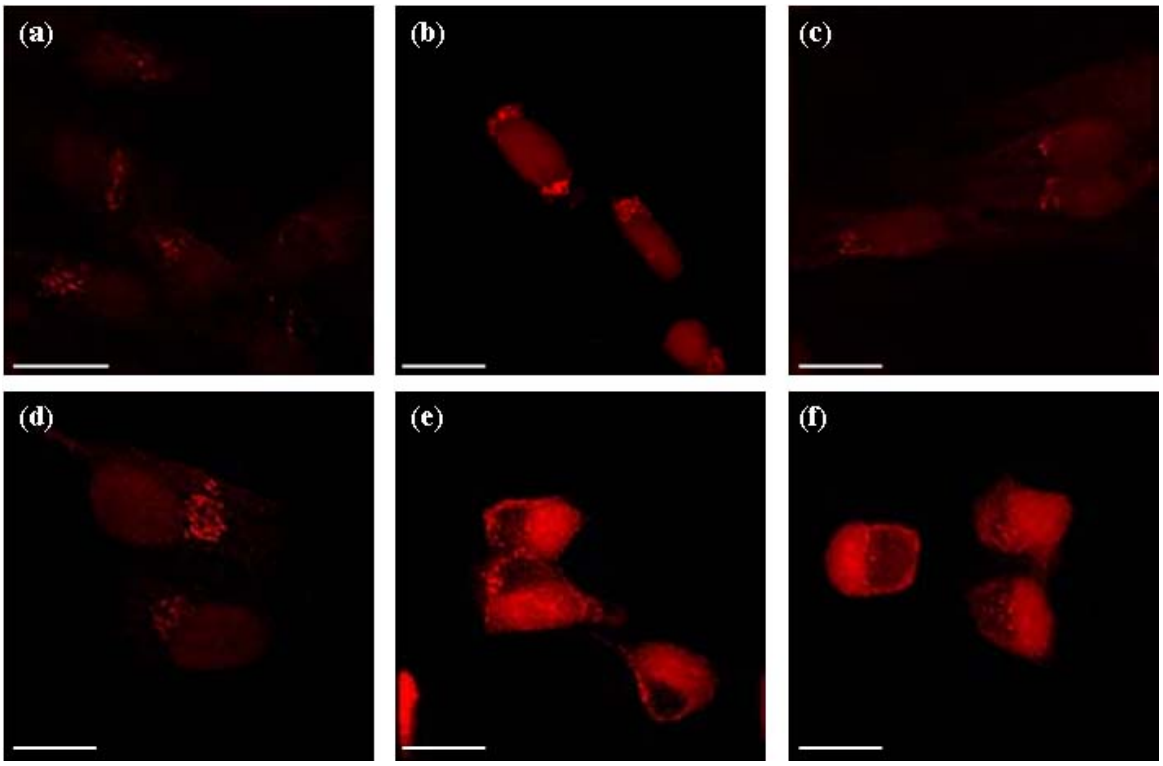

Figure 3.37: Immunofluorescent staining of BHK-21 cells using anti-GM130/Golgi. *A mock infection (a; anti-GM130) shows a crescent-shaped Golgi-complex, which remains at 1h (b, anti-GM130) and 2h p.i. (c; anti-Golgi). At 3h p.i. (d; anti-Golgi), the Golgi complex is dispersed over the cytoplasm. At 5h and 7h p.i. (e-f; anti-Golgi), the remnants are accumulated at the cellular membrane. Bar (a), 30 µm; bar (b-f), 15 µm.*

3.4.2.4 Relocalization of PKA caused by TMEV infection

Protein kinase A (PKA) activity is known to play a number of key roles in the regulation of cellular membrane traffic. It has been shown that the N-terminus of TMEV protein 2C binds to the C-terminal region of a PKA anchoring protein, AKAP10 and competes with the RII regulatory subunit of PKA (Knox *et al.*, submitted). This may serve to displace PKA from the Golgi complex. It has been shown that PKA is involved in various aspects of vesicle-mediated protein transport processes: (1) protein transport from the ER to the Golgi complex (Muniz *et al.*, 1997); (2) budding of constitutive transport vesicles from the trans-Golgi network (Muniz *et al.*, 1997); (3) endosome-to-Golgi and Golgi-to-ER transport (Lee & Linstedt, 2000); (4) endosome fusion, exo-, endo-, and transcytosis (Hansen & Casanova, 1994, Takuma & Ichida,

1994a, Muniz *et al.*, 1996;, Rapacciuolo *et al.*, 2003, Kim *et al.*, 2005); and (5) stimulation of the binding of ADP-ribosylation factor 1 (Arf1) to the Golgi membranes. PKA seems to play an important role in membrane trafficking (Martin *et al.*, 2000).

It was intended to localize PKA in TMEV-infected BHK-21 cells. Cell cultures were prepared and infected as described previously (section 3.1.5.1). The virus was adsorbed at 37°C, cells were fixed at hourly time points (1-8 h p.i.), and immunofluorescence was carried out (section 2.6.4). Three antibodies were used to localize PKA: (i) polyclonal to protein kinase A regulatory subunit I alpha (anti-PKAI; Abcam); (ii) polyclonal to cAMP-dependent protein kinase type II-alpha regulatory subunit (anti-PKAII; Abcam); and (iii) PKA antibody, which is raised against the catalytic subunit (anti-PKA-CAT; Abcam). The three primary antibodies were used at a 1:500 dilution. Anti-PKAI and anti-PKAII were visualized with a sheep anti-rabbit antibody coupled to TexasRed, whilst anti-PKA-CAT was visualized using a rabbit anti-mouse antibody coupled to TexasRed. Preliminary results suggest that TMEV infection alters the intracellular distribution of PKA. At 7 hours post infection, PKA appears to cluster near the cellular membrane, creating a region devoid of PKA within the cell were viral replication takes place (figure 3.38). Confirmation of these results by further experiments is required.

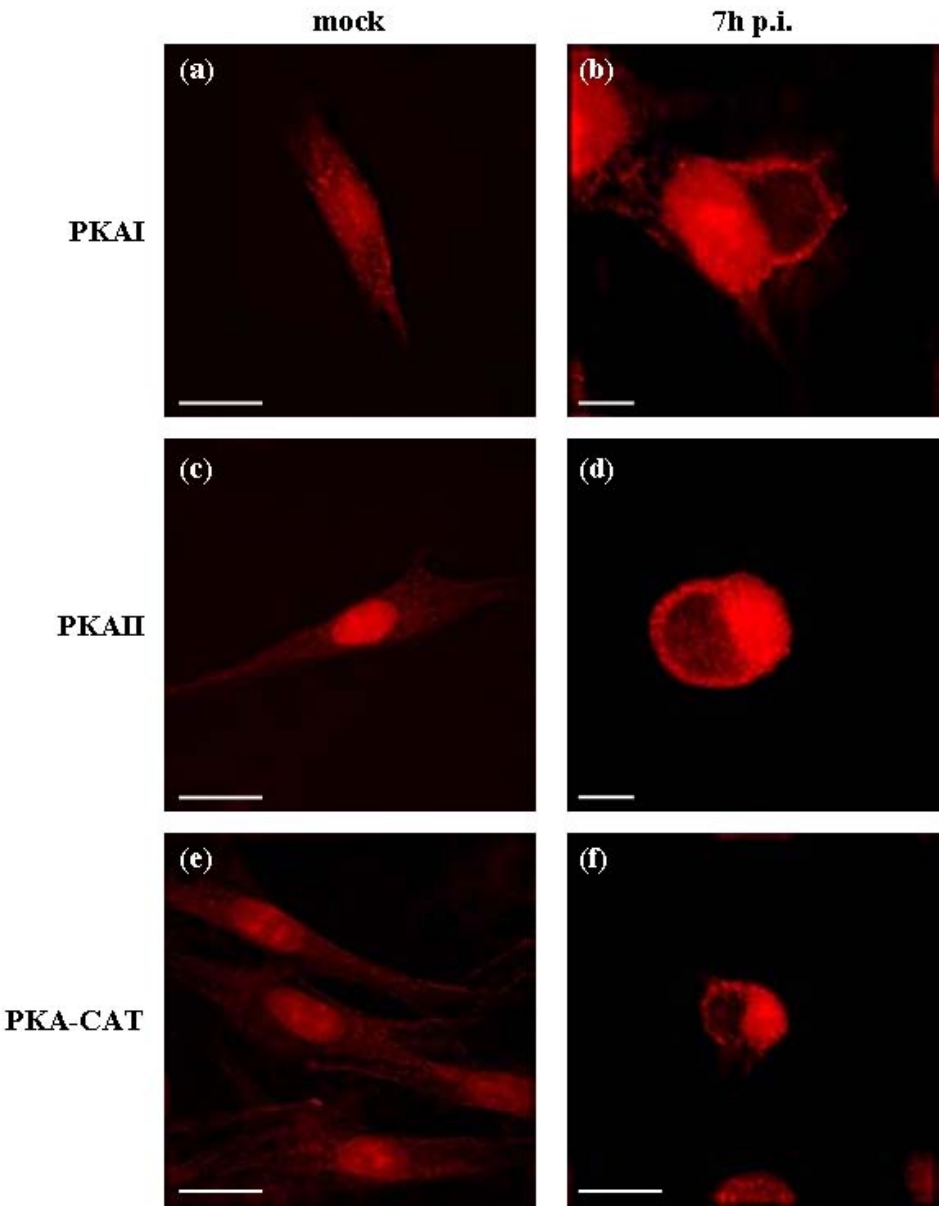

Figure 3.38: Relocalization of PKA in BHK-21 cells upon TMEV infection. *Mock-infected cells stained with anti-PKAI/PKAII/PKA-CAT, show the intracellular localization of PKA. At 7h p.i., PKA appears to have accumulated at the periphery of the cell. Nuclear staining is due to the secondary antibody. Bar (a,c,e,f), 15 µm; bar (b,d), 5 µm.*

3.4.2.5 Changes in the localization of endosomes caused by TMEV infection

Endosomes are membrane-bound compartments within the cell. They are part of both the secretory and the endocytic pathway of membrane trafficking. The secretory pathway allows soluble and membrane proteins to be transported from the ER through the Golgi complex and out to various locations including endosomes. The endocytic pathway is used to take up substances from the cell surface into the interior of the cell by way of endosomes. It was aspired to investigate the effect of TMEV-infection on the localization of early endosomes (EE).

BHK-21 cell cultures were prepared and infected as described in section 3.1.5.1. TMEV GDVII was adsorbed, cells were fixed at hourly time points (1-8 h p.i.), and immunofluorescence was carried out (section 2.6.4). Early endosomes were detected with a polyclonal anti-EEA1 antibody, an early endosome marker, using a 1:500 dilution (anti-EE; Abcam), and visualized with a sheep anti-rabbit antibody coupled to TexasRed. A mock infection shows an even distribution of the EE in the cytoplasm. At 6 hours post infection, early endosomes have accumulated at the periphery of the cell, surrounding the viral replication site (figure 3.39).

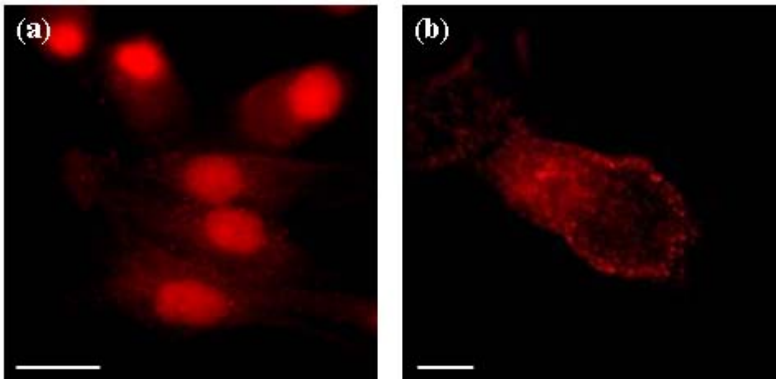

Figure 3.39: Immunofluorescent staining of BHK-21 cells using anti-EE. *A mock infection (a) shows EE spread out in the cytoplasm. At 6h p.i. (b), early endosomes are concentrated at the cell membrane. Bar (a), 15 µm, bar (b) 5 µm.*

3.4.2.6 Redistribution of BIGI caused by TMEV infection

BIGI, also called ADP-ribosylation factor guanine nucleotide-exchange factor I (Arf-GEFI), activates ADP-ribosylation factor I (ArfI) by catalyzing the replacement of Arf-bound GDP with GTP to regulate Golgi vesicular transport. It has recently been observed that some members of the Arf family of small GTPases (ArfI), which control secretory trafficking, associate with newly formed membranous RNA replication complexes in PV-infected cells (Belov *et al.*, 2005). Two PV proteins 3A and 3CD, recruit different Arf-GEFs, including BIGI, to the membranous vesicles that arise during PV infection. These are responsible for Arf activation and translocation to these membranes (Belov *et al.*, 2007).

It was intended to localize BIGI in TMEV-infected BHK-21 cells. Cell cultures were prepared and infected as described previously (section 3.1.5.1). The virus was adsorbed, cells were fixed at hourly time points (1-8 h p.i.), and immunofluorescence was carried out (section 2.6.4). BIGI was localized using a polyclonal anti-BIGI/ARFGEFI antibody at a 1:500 dilution (anti-BIGI; Bethyl Laboratories Inc., Cambridge BioScience, Cambridge, UK), and visualized with a sheep anti-rabbit antibody coupled to TexasRed. Mock-infected cells show a typical localization to the Golgi area. At 3 hours post infection, BIGI has been redistributed to the perinuclear region, where the replication vesicles are located. At 5 and 7 hours post infection, BIGI can be observed spread out in the cytoplasm at the viral replication site (figure 3.40).

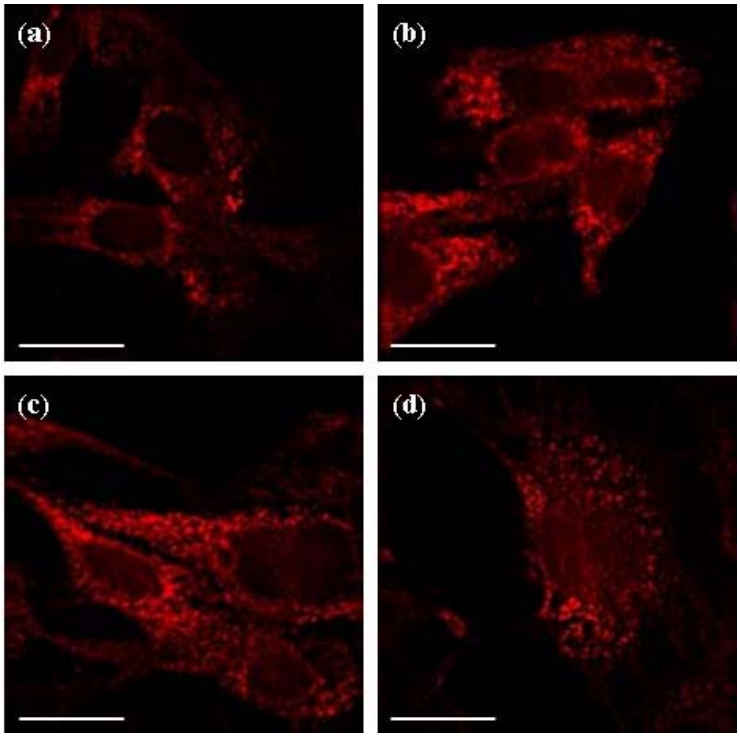

Figure 3.40: Relocalization of BIGI in BHK-21 cells upon TMEV infection. *Mock-infected cells stained with anti-BIGI localize BIGI to the Golgi area (a). TMEV-infected cells stained with anti-BIGI at 3h p.i. (b), show redistribution to the perinuclear area. At 5h and 7h p.i. (c,d), BIGI is localized in the cytoplasm. Bar, 15 µm.*

3.4.3 Live imaging of TMEV-infected BHK-PDF18 cells

BHK-PDF18 cells (section 3.1.5.3) were infected with TMEV GDVII and monitored every 10 minutes for 24 hours. It can be observed that the Golgi complex turns from a solid, crescent-shaped organelle at the start of infection, into a series of punctuate fluorescent points (4h p.i.) forming an expanding balloon-like structure, surrounding the concomitantly expanding site of virus replication. The remnants of the Golgi complex are finally dispersed throughout the cytoplasm (6-8h p.i.). No rapid collapse of the Golgi complex back onto the ER can be observed (figure 3.41, supplementary material). The movie, provided on CD-ROM, shows the complete sequence of the images.

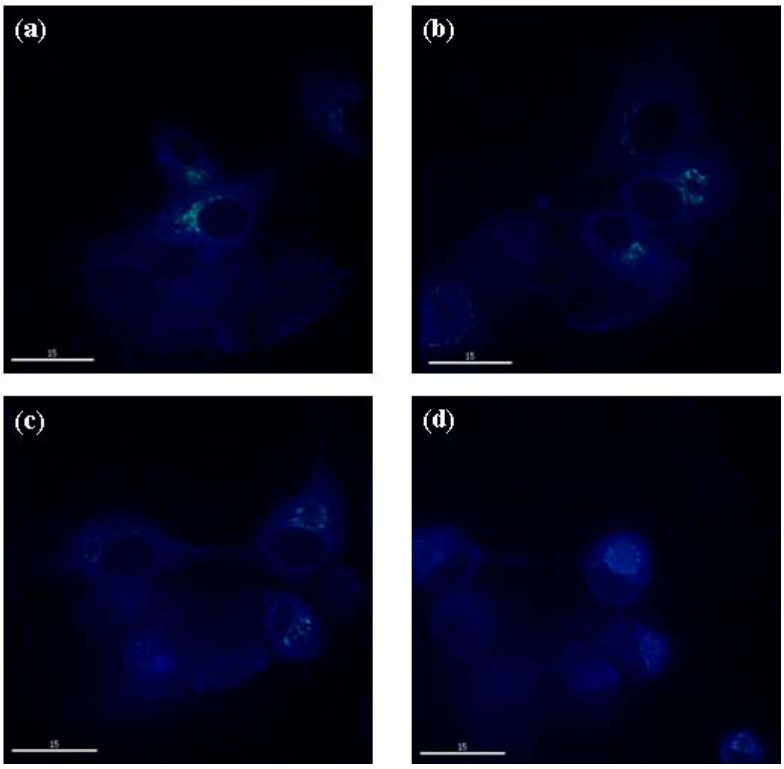

Figure 3.41: Disassembly of the Golgi complex upon TMEV infection. *BHK-PDF18 cells were infected with TMEV and images were taken every 10 minutes for 24 hours. The figure shows selected images taken at the start of infection (a), 4h p.i. (b), 6 h p.i. (c), and 8 h p.i. (d). For the complete sequence, see the movie. Bar, 15µm.*

4. Discussion

"The very essence of the virus is its fundamental entanglement with the genetic and metabolic machinery of the host."
American Nobel laureate Joshua Lederberg, 1993

In the introduction, several examples of how positive stranded RNA viruses replicate in association with cytoplasmic membranes of infected cells were presented. Poliovirus protein 2C and its precursor 2BC seem to play an important role in the formation of membranous vesicles and therefore have a considerable effect on membrane trafficking in infected cells. I will describe the intracellular localization of TMEV protein 2C and the intracellular changes seen in TMEV infected cells. Furthermore, I suggest that the observed interactions of TMEV protein 2C with cellular proteins may cause some of the effects on membrane trafficking seen in infected cells.

4.1. Intracellular localization of TMEV protein 2C

4.1.1 Expression of TMEV protein 2C

Localization of transiently expressed protein 2C tagged with the V5 epitope was not possible. The lack of detection of protein 2C is likely to result from either low levels of protein expression, suggesting expression of protein 2C may have a detrimental effect on cells, or rapid degradation of protein 2C after expression. It was demonstrated that the expression level of protein 2C was not altered by introducing mutations in the highly conserved Walker A and B motifs. Use of the lentivector, containing a different promoter for mammalian expression, also did not change transfection efficiency. Transient expression analysis of FMDV protein 2B and 2C also resulted in very low expression levels. FMDV-2B could not be detected due to low levels of expression, probably due to cell toxicity (Garciá-Briones *et al.*, 2006). Transfection efficiency improved when a modified FMDV protein 2B, including a tag was used (Moffat *et al.*, 2005). FMDV-2C could be detected by western blotting and a typical 2C fluorescence signal could be observed in cells. However, the rate of expressing cells was very low, and the intensity of the fluorescence signal in positive cells was faint. Cells also showed an elongated morphology, suggesting that expression of 2C has a toxic effect on cell viability and cell

morphology (Garciá-Briones *et al.*, 2006). An additional explanation for our results could be that the epitopes recognized by the anti-V5 antibody are masked. It is possible that TMEV protein 2C expresses, but that the conformation of the V5-tagged protein prevents the anti-V5 antibody from binding to the V5 epitope. It was, however, demonstrated that *in vitro* coupled transcription/translation of the V5-tagged TMEV protein 2C results in expression of TMEV-2C detectable by using the anti-V5 antibody.

The transfection efficiency of protein 2C is greatly improved when only the N-terminal 60aa of protein 2C tagged with the V5 epitope, are used for transfection (Dr. Caroline Knox, personal communication). It has been shown that the N-terminal region of PV protein 2C (residues 1 to 122) is required for membrane association. It was predicted that the N-terminal region is composed of a number of α-helices, of which one is a conserved amphipathic helix essential for membrane association. The C-terminal region of PV protein 2C (residues 252-329) also seems to include a conserved amphipathic helix, which is possible responsible for the membrane related activities of that part of protein 2C. The central region of PV protein 2C (residues 88 to 274) includes well-conserved NTP-binding motifs (Walker A and B motifs), and does not display any determinants for membrane association. Analysis of the different regions of PV protein 2C showed that the N- and C-terminal region, but not the central region, interact with intracellular membranes and induce major changes in their morphology. However, when the central region was fused to the N-terminal region, the membrane rearrangements induced were most similar to the smooth vesicles that proliferate in PV-infected cells. Mutation analysis has demonstrated that the NTP-binding activity is not required for vesicle induction (Teterina *et al.*, 1997). The higher expression levels of TMEV protein 2C observed when only the N-terminal 60 residues of 2C are used may be explained by the membrane rearrangements caused by the central region of protein 2C. The N-terminal region of protein 2C is required for membrane association; however, the membrane rearrangements induced by only this region may not be as detrimental as the ones induced by the full length protein.

It was not possible to construct a full length infectious copy of TMEV containing the V5 epitope at the C-terminus of protein 2C. Overlap PCR was used to try to introduce the V5-epitope in the full length TMEV cDNA. Primers used for the overlap PCRs were found to be inadequate, possible due to inaccurate primer sequences. It was possible to construct a

2BC-V5-P3 fragment by using the pLH135 construct, previously made in our laboratory. The In-Fusion^{TM} PCR Cloning kit was then used, unsuccessfully, to insert the V5-tagged protein 2C into the full-length TMEV cDNA clone, possible due to using less than optimal conditions. A full length infectious TMEV copy containing the V5 epitope would be a useful tool to localize the V5-tagged protein 2C in the context of the other viral proteins. It would be possible to localize protein 2C and its precursor 2BC in infected cells, in association with the replication complex. The localization of TMEV protein 2C may differ in the context of other viral proteins compared to the localization of transiently expressed protein 2C. The effect of introducing the V5 epitope in the genomic cDNA on viral viability could also be ascertained.

4.1.2 Localization of protein 2C upon TMEV infection

4.1.2.1 Highly conserved protein 2C

Protein 2C is the most conserved protein in the *Picornavirus* family and it was postulated that TMEV protein 2C may exhibit similar antigenic determinants to FMDV protein 2C. Therefore, anti-FMDV-2C antibodies were employed for detection and localization of TMEV protein 2C. The results demonstrated that TMEV-2C can be detected by anti-FMDV-2C antibodies; however, the interaction is highly non-specific. Furthermore, our results showed that the extra band observed in the gel profile of FMDV-2C, which is a result of internal initiation, is not detected by the DM10 antibody (figure 3.7, section 3.1.5.1). This suggests that the N-terminal region may contain an immuno-dominant epitope. It has been demonstrated that protein 2C is highly conserved across the *Picornavirus* family (Mirzayan & Wimmer, 1992). Protein 2C is completely conserved among the 3 serotypes of PV (Toyoda *et al.*, 1984). Comparison of the amino acid sequence also demonstrated a high degree of homology over a region of 115 residues between other *Picornaviruses*, such as EMCV, PV, FMDV, RV-14 and RV-12 (Argos *et al.*, 1984, Franssen *et al.*, 1984, Pincus *et al.*, 1986). Furthermore, it was observed that protein 2C contains an NTP-binding pattern, which is evolutionary conserved and can be found in several viral proteins (Gorbalenya & Koonin, 1989, Klein *et al.*, 1999). Comparative sequence analysis has identified 2C-like proteins in several virus families (figure 4.1). Analysis of the amino acid sequence of several animal *Picornaviruses* and Cowpea Mosaic virus (CPMV), a member of the *Comoviruses*, shows a

strong homology in the 2C region. CPMV contains a two-part genome consisting of an M-RNA (middle component) and a larger B-RNA (bottom component), which are separately encapsidated. The B-RNA part encodes the viral non-structural proteins, including the 2C-like protein p58 (Argos *et al.*, 1984, Franssen *et al.*, 1984). *Potyviruses* contain a 2C-like protein, the CI protein, which contains the conserved NTP-binding pattern (Lain *et al.*, 1991). Furthermore, *Caliciviruses* contain a 2C-like protein with NTPase activity (Koonin & Dolja, 1993, Kaiser *et al.*, 2006). Several insect viruses, including Drosophila C virus, contain 2C-like regions (Johnson & Christian, 1998, Sasaki *et al.*, 1998, Nakashima *et al.*, 1999).

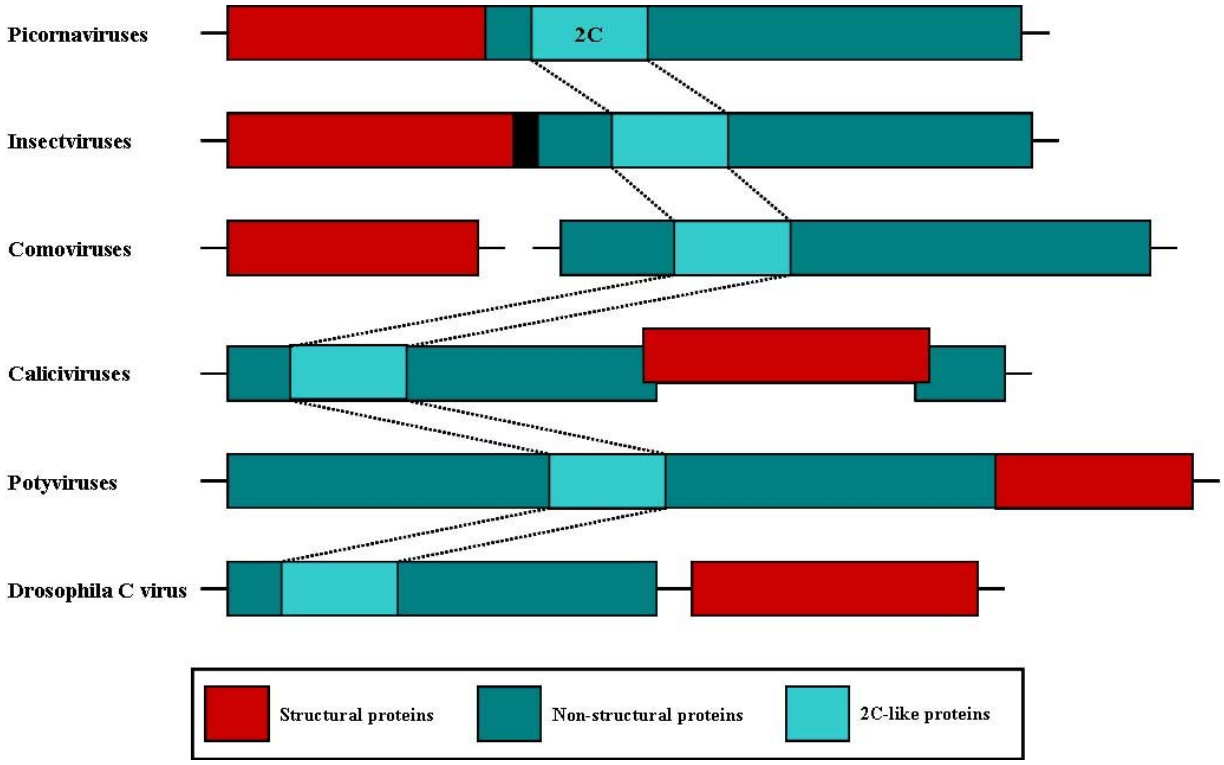

Figure 4.1: The 2C-like proteins. *Protein 2C is highly conserved across the Picornavirus superfamily. The structural and non-structural protein regions of picornavirus-like viruses are shown. The 2C-like protein is indicated.*

4.1.2.2 Localization of TMEV protein 2C

TMEV infection of BHK-21 cells resulted in a typical distribution of protein 2C detected with the anti-TMEV-2C antibody. At 1 hour post infection, newly synthesized protein 2C can be observed as tiny dots spread out in the cytoplasm. After 2 to 3 hours, a typical ER-

like pattern can be seen, suggesting that viral protein synthesis occurs at the ER. Protein 2C then redistributes to accumulate in a juxtanuclear site, possible the Golgi complex area, suggesting that this may be the viral replication site. After 7 to 8 hours, this pattern can still be observed, but protein 2C also seems to spread out in the cytoplasm, suggesting a rapidly expanding viral replication site. During PV infection, no newly synthesized proteins could be observed 1 hour upon infection. After 1.5 hours, protein 2B could be observed spread out in the cytoplasm and 3 hours upon infection a feathery ER-like pattern could be seen, possible indicating viral translation at the ER. After 4 hours, vesicles containing viral proteins and negative stranded RNA arose that moved rapidly towards the nucleus to accumulate in a perinuclear area. These vesicles represent viral replication complexes, and migrate eventually to the microtubule organizing centre (MTOC), which contains the Golgi complex (Egger & Bienz, 2005). Furthermore, FMDV infection in BHK-21 cells resulted in a similar distribution for protein 2C. At 2 to 2.5 hours upon infection, protein 2C exhibited a punctuated, scattered pattern. After 3 hours, protein 2C appeared to concentrate at one side of the nucleus, which has been associated with the viral replication site (Moffat *et al.*, 2005, Garciá-Briones *et al.*, 2006). Transfection with FMDV-2C resulted in a perinuclear distribution close to the Golgi complex, similar to that observed at early times upon infection (Knox *et al.*, 2005, Garciá-Briones *et al.*, 2006). Moreover, Human Parechovirus-1 (HPEV-1) infection also showed a comparable localization of protein 2C. Early upon infection (4h p.i.), protein 2C was found in numerous small granules in the cytoplasm. After 6 hours, the pattern of protein 2C was changed drastically into dot- and stick-like formations concentrating in a perinuclear area or accumulating on one side of the cell. At 8 hours p.i., protein 2C was still presented in long stick-like structures, and after 10 hours as irregular bodies (Krogerus *et al.*, 2003).

TMEV infection of the BHK-PDF18 stable cell line resulted in a typical disassembly of the Golgi complex and localization of protein 2C showed an overlap with the Golgi complex. At 1 hour upon infection, little newly synthesized protein 2C was observed scattered throughout the cytoplasm and an intact Golgi complex is seen. After 5 hours, protein 2C is accumulated at one side of the nucleus, near a dispersed Golgi complex, which has changed from a solid crescent shape into a series of punctuate dots forming a balloon-like structure. At 8 hours p.i., the remnants of the Golgi complex are dispersed throughout the cytoplasm.

Some overlap between protein 2C and the Golgi complex can be observed, however the superimposed images show two separate signals for protein 2C and the Golgi complex. This suggests that protein 2C may play a role in the viral replication complexes that form near the Golgi complex. However, the source of the membranous vesicles, which contain the replication complexes, may not be the Golgi complex. Similar observations were made for FMDV protein 2C. FMDV protein 2C is membrane-associated but does not fractionate with Golgi markers on density gradients, suggesting that the Golgi complex is not a source for the structures containing protein 2C, or, that the used Golgi markers are excluded. Furthermore, FMDV protein 2C did not co-localize with marker proteins for the Golgi complex, the ER, the ERGIC, endo- and lysosomes. Golgi markers and protein 2C largely overlap but merged immunofluorescence images show no co-localization. This suggests that the juxtanuclear distribution of protein 2C is not maintained by association with the Golgi complex (Knox *et al.*, 2005, Garciá-Briones *et al.*, 2006). Poliovirus replication complexes contain all viral structural and non-structural proteins, including protein 2C (Girard *et al.*, 1967, Takegami *et al.*, 1983, Takeda *et al.*, 1986, Bienz *et al.*, 1992, Pfister *et al.*, 1992, Egger *et al.*, 1996, 2000). PV induced membranous vesicles are initially formed from ER membranes (Bienz *et al.*, 1987). At later times in infection, PV proteins co-localize with Golgi markers (Bolten *et al.*, 1998). Furthermore, virus induced membranes isolated from PV-infected cells contained marker proteins for the ER, Golgi, and lysosomes (Schlegel *et al.*, 1996).

4.2. Interaction of TMEV protein 2C with host cell proteins

It was not possible to identify interactions of transiently expressed protein 2C with host cell proteins due to very low transfection efficiency, as measured by expression. Transfection of different mammalian cell lines did not result in expression levels of protein 2C detectable by western blotting. As it was possible to express TMEV protein 2C *in vitro* by using the T7 promoter, BSR-T7 cells, a cell line that constitutively expresses the T7 polymerase, were used to transiently express protein 2C. No expression of protein 2C was detected. Furthermore, introduction of a TAP-tag at the N- or C-terminus of protein 2C does not alter the level of expression, suggesting that protein 2C may be degraded as discussed previously (section 4.1.1).

4.2.1 Interaction of protein 2C with reticulon 3

It was shown that reticulon 3 (RTN3) binds TMEV protein 2C (figure 3.19, section 3.2.4), which suggest a function for RTN3 in viral replication. RTN3 is a member of a widely distributed family of highly conserved ER-associated proteins with a reticular distribution (van de Velde *et al.*, 1994, Oertle *et al.*, 2003a). Reticulon/Nogo was first described as a neuroendocrine-specific protein (Roebroek *et al.*, 1993). Four genes have been identified in mammals: RTN1, 2, 3, and RTN4/Nogo, and each of them can produce multiple N-terminal isoforms as a result of differential promoter usage or alternative splicing (Oertle *et al.*, 2003b). The N-terminal region is highly variable and different in size, whereas the C-terminal region is well conserved among family members. RTN1-4 share an 188aa domain localized in the C-terminal region, called the RTN homology domain (RHD). The RHD contains two potential transmembrane domains and a 66aa hydrophilic loop, which was called Nogo66 for RTN4/Nogo (Oertle *et al.*, 2003a). The functions of RTNs remain largely unknown. It has been demonstrated that RTN4/Nogo exhibits a potent inhibitory effect on neurite outgrowth and is involved in restricting neuronal regeneration in the central nervous system (Chen *et al.*, 2000, GrandPré *et al.*, 2000, Prinjha *et al.*, 2000, reviewed by Oertle & Schwab, 2003). These functions are however not common to other RTNs. They have been linked to a variety of proteins. Nogo-A is expressed in association with α-tubulin and myelin basic protein in mature oligodendrocytes of rat spinal cord (Taketomi *et al.*, 2002). Nogo has also been linked to mitochondrial proteins (Hu *et al.*, 2002). Furthermore, it has been suggested that RTNs can modulate the anti-apoptotic activity of Bcl-XL and Bcl-2 through interaction and relocalization to the ER (Tagami *et al.*, 2000), meaning that RTNs might be involved in the regulation of cell survival. *Caenorhabditis elegans* RTN interacts with RME-1, a protein functioning in the endocytic recycling, during embryogenesis, suggesting that RTN functions in the endocytic pathway (Iwahashi *et al.*, 2002). RTN1-C interacts with SNARE proteins, suggesting that RTNs are involved in membrane trafficking including exocytosis (Steiner *et al.*, 2004). The accumulation of RTNs in the ER suggests an intracellular function related to the ER.

The role of RTN3 in membrane trafficking has been investigated. It has been demonstrated that RTN3 is involved in membrane trafficking in the early secretory pathway. Expression of full-length RTN3 displayed heterogenous patterns: a filamentous/reticular pattern, which substantially overlaps with microtubules, and a granular distribution, which reflects

aggregated ER. The N-terminal cytoplasmic region within the RHD is required for the formation of the filamentous/reticular pattern. However, both the N- and C-terminal cytoplasmic regions within the RHD are necessary for the formation of the granular pattern. Overexpression of full-length RTN3 caused dispersion of Golgi proteins and blockage of antero- and retrograde protein transport between ER and Golgi. ERGIC-53, a marker for the ER-Golgi intermediate compartment, showed a perinuclear accumulation with loss of peripheral ERGIC-53 localization, suggesting an inhibition of retrograde transport from the ER-Golgi intermediate compartment (ERGIC) and *cis*-Golgi to the ER. However, two other recycling proteins, the KDEL-receptor and gp27, were dispersed. Transport of VSVG-GFP from ER to Golgi was also blocked by overexpression of RTN3 (Wakana *et al.*, 2005).

It has recently been demonstrated that RTN3 binds the 2C protein of Enterovirus 71 (EV-71), and is required for viral replication (Tang *et al.*, 2007). The host-encoded RTN3 was found to be associated to the viral replication complex through direct interaction with the EV71 protein 2C. It was observed that the N-terminal region of protein 2C, featuring both RNA- and membrane-binding activity, interacts with RTN3. The region of interaction was mapped to the RHD region of RTN3. However, the N-terminal region of RTN3 might play a role in regulating the interaction. Decreased production of RTN3 reduced the synthesis of EV71-encoded viral proteins and replicative double-stranded RNA. RTN3 seems to play an important role in EV71 replication, through potential modulation of the interaction between viral RNA and replication complex (Tang *et al.*, 2007).

Interaction of RTN3 with the 2C proteins encoded by different *Enteroviruses*, such as EV71, PV, and coxsackievirus A16 (Tang *et al.*, 2007), and TMEV (section 3.2.4), suggest it is a common factor in viral replication of *Picornaviruses*. PV infection involves complex membrane rearrangements and the formation of replication complex-associated vesicles. These vesicles are derived mainly from the ER, but also possibly from the Golgi-complex. Protein 2C can bind to cellular membranes and induce vesicle formation through the N-terminal amphipatic region (Dales *et al.*, 1965, Bienz *et al.*, 1983, 1987, Cho *et al.*, 1994, Suhy *et al.*, 2000). A mutant (I25K) of PV 2C showed a reduction in negative RNA synthesis (Paul *et al.*, 1994). When this mutation was introduced into EV71 2C, no interaction between 2C and RTN3 was detected, suggesting that the decrease in viral RNA synthesis was caused by the loss of the RTN3-2C interaction (Tang *et al.*, 2007). The interaction of protein 2C with

RTN3 is another indication that protein 2C interferes with the membrane trafficking in infected cells. It has been demonstrated that a member of the RTN family interacts with SNARE proteins (Steiner *et al.*, 2004). RTN3 may exhibit similar interactions. SNARE proteins participate in COPII vesicle formation (Springer & Schekman, 1998). Furthermore, it has been shown that PV replication complex-associated vesicles are derived from the ER by the COPII budding mechanism and are similar to the vesicles of the secretory pathway (Rust *et al.*, 2001). The interaction between 2C and RTN3 may be necessary for the formation of vesicles via a COPII-dependent pathway.

4.2.2 Interaction of protein 2C with AKAP10?

4.2.2.1 In vitro interaction of protein 2C and AKAP10?

Knox and colleagues (submitted) demonstrated that the N-terminal part of FMDV protein 2C binds to the C-terminal region of AKAP10, also called D-AKAP2, and competes with the RII regulatory subunit of PKA (figure 4.2). The binding of AKAP10 was also observed for 2C proteins derived from other *Picornaviridae*, including TMEV (Knox *et al.*, submitted). A yeast two-hybrid screen was employed to identify cellular proteins that possible interact with protein 2C. The C-terminal region of AKAP10 was identified by interaction with FMDV protein 2C. To confirm this interaction, the C-terminal 52aa of AKAP10 (IAP3) were expressed as a GST-fusion protein (GST-IAP3), purified onto glutathione sepharose beads and tested for its ability to bind *in vitro* translated FMDV protein 2C. The regulatory subunit type IIα which binds AKAP10, was also tested for binding to GST-IAP3. Both FMDV-2C and RIIα interact *in vitro* with GST-IAP3. Protein 2C and RIIα share an identical 28aa binding domain on GST-IAP3, suggesting that the two proteins compete for binding to AKAP10. This was confirmed using a competition binding assay (Knox *et al.*, submitted). This suggests that protein 2C may exhibit a similar conformation to PKA to bind AKAP10. Figure 4.3 shows a model of the binding of the dimer of regulatory subunits of PKA to AKAP10. The binding site seems to be formed by α-helices within the regulatory subunits of PKA. It has been predicted that the N-terminal region of protein 2C, which has been identified to bind to AKAP10, is composed of a number of α-helices (Teterina *et al.*, 1997), which may contribute to the interaction with AKAP10. As described in section 3.2.4, the interaction between TMEV protein 2C and AKAP10 could not be confirmed. TMEV protein

2C was expressed as a GST-fusion protein, purified on glutathione sepharose beads and tested for its ability to bind *in vitro* translated AKAP10. No *in vitro* interaction between AKAP10 and GST-2C could be observed.

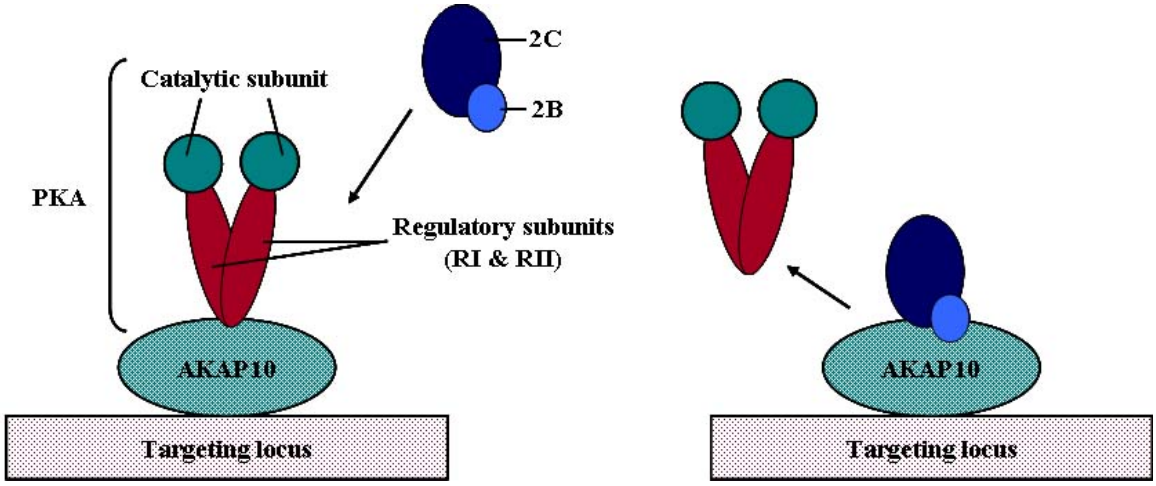

Figure 4.2: Competition between PKA and picornavirus protein 2C for binding to AKAP10. *PKA consists of two regulatory subunits and two catalytic subunits. AKAP10 is a PKA anchoring protein, targeting PKA to intracellular membranes. AKAP10 is known to interact with the RIIα subunit of PKA. Protein 2C competes with this interaction.*

The N-terminus of protein 2C was identified as the binding site of AKAP10 (Knox *et al.*, submitted). The fusion of GST to protein 2C at the N-terminus of 2C might interfere with the interaction. "Unidirectional" interactions have previously been observed and are likely to reflect conformational constraints of the interactions. The polarity of the interaction may be explained by the possibility that the interacting fusion protein is misfolded. The fusion at the N-terminus, which harbors the binding site, may interfere with the overall structural integrity of protein 2C. This "unidirectionality" has been observed for protein interaction mapping of viruses. A unidirectional interaction was seen between calicivirus proteins p76 and p32 (Kaiser *et al.*, 2006). Furthermore, an *in vitro* binding assay using PV P2 nonstructural proteins, identified a 2C/2C association not detected using a yeast two-hybrid system (Cuconati *et al.*, 1998). Various two-hybrid studies demonstrated that the two-hybrid system never detects all physiological interactions, and the failure of an *in vitro* binding assay does not necessarily indicate that the interactions are false, as structural constraints might play a role (reviewed by Uetz *et al.*, 2007). Interestingly, the N-terminal region of protein 2C has also been identified as the binding region of RTN3 (Tang *et al.*,

2007); however, the fusion of GST to the N-terminal part of TMEV protein 2C does not interfere with the interaction with RTN3. To resolve the discrepancy observed for the interaction between TMEV 2C and AKAP10, the binding assay with AKAP10 would have to be repeated in parallel with FMDV-2C expressed as a GST-fusion protein to determine if the polarity of the interaction also interferes with the interaction between FMDV-2C and AKAP10. Furthermore, it would be interesting to carry out competition binding assays with RTN3 and AKAP10 to determine if TMEV protein 2C is most likely to interact with RTN3 or AKAP10 when both proteins are present.

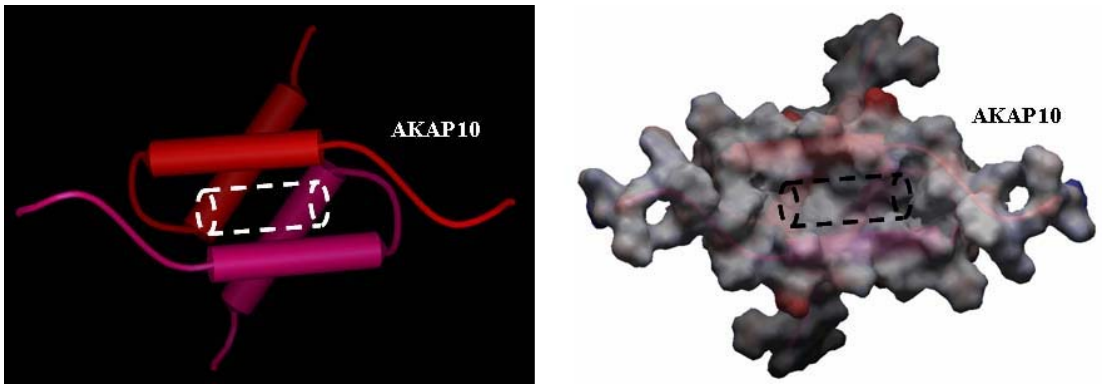

Figure 4.3: Illustration for the interaction between AKAP10 and PKA. *The regulatory subunits of PKA (red and pink) form a dimer and interact with AKAP10 for membrane targeting. The possible interaction site for AKAP10 is indicated.*

A kinase anchoring proteins (AKAPs) are multifunctional proteins that function as targeting units and recruit PKA by binding to a specific docking domain at the N-terminus of the R subunit (Newlon *et al.*, 1997). PKA consists of two regulatory (R) subunits and two catalytic subunits. Two types of R subunits have been identified; RI and RII (figure 4.2). Dual specific AKAPs (D-AKAPs) interact with both RI and RII. The members of the AKAP family have been localized to different subcellular sites such as the plasma membrane, the actin cytoskeleton, the nucleus, the mitochondria and the ER (Huang *et al.*, 1999, reviewed by Colledge & Scott, 1999). Huang and colleagues (1997) identified the mouse D-AKAP2 (AKAP10). It contains a C-terminal PKA binding region that binds RIα, RIIα, RIIβ but not RIβ *in vitro*, and a putative regulator of G protein signaling (RGS) domain (Huang *et al.*, 1997). The human D-AKAP2 contains an additional putative RGS domain (Wang *et al.*, 2001).

The subcellular localization of PKA through AKAPs is believed to be responsible for the specificity of the cAMP signaling pathway. PKA has been localized to ER and Golgi complex (Nigg *et al.*, 1985, Rios *et al.*, 1992, Keryer *et al.*, 1999). Protein phosphorylation by PKA is important for regulating membrane trafficking. Protein transport from ER to Golgi complex is regulated by phosphorylation (Davidson *et al.*, 1992). Furthermore, PKA plays a role in budding and transport of vesicles across the Golgi stacks and from the trans-Golgi-network to the plasma membrane (Ohasi & Huttner, 1994, Muniz *et al.*, 1996, 1997). PKA is moreover involved in exo-, endo-, and transcytosis, and endosome fusion (Woodman *et al.*, 1992, Eker *et al.*, 1994, Hansen & Casanova, 1994, Takuma & Ichida, 1994b). The binding of Arf1, a GTP-binding protein required for the formation of COP-coated vesicles, to Golgi membranes is enhanced by PKA (Martin *et al.*, 2000). It has also been observed that COPII recruitment and export from the ER is initiated by PKA signaling (Aridor & Balch, 2000). Phosphorylation by PKA of specific SNARE proteins may play an important role in exocytosis (Foster *et al.*, 1998, Marash & Gerst, 2001).

PV protein 2C seems to be involved in the perturbation of the host-cell membrane traffic and the formation of virus-induced vesicles (Bienz *et al.*, 1983, 1990, 1992, Cho *et al.*, 1994, Aldabe & Carrasco, 1995, Teterina *et al.*, 1997). Protein 2C binds to membranes and this interaction is mediated through its N-terminus (Echeverri & Dasgupta, 1995, Kusov *et al.*, 1998). The N-terminal part has also been found to be the binding site of the membrane protein AKAP10 (Knox *et al.*, submitted). Protein 2C and PKA RIIα share an identical binding domain on AKAP10. The redistribution of PKA induced by the binding of AKAP10 to protein 2C may explain the effect on membrane trafficking seen during infection.

4.2.2.2 Mutations in the AKAP10 binding region

Mutations have been introduced at several sites within the N-terminal region of TMEV protein 2C, which has been identified as the binding region for AKAP10. The amino acids at position 4, 8, 14, 18, and 23 were changed into alanines. After sequencing it was observed that the original pGDVII-mut14 construct did not contain the desired mutation. Transfection of the TMEV mutant RNAs resulted in dramatic differences in the onset of CPE compared to wild type TMEV. The cell culture supernatants were used for infection and were furthermore examined by plaque assay. TMEV mutant 4, mutant 8, and mutant 23 did not show a typical

CPE after transfection, and no plaques could be observed after titration. TMEV mutant 18 showed typical CPE after transfection, and plaques were observed after titration. Infection of BHK-21 cells using the cell culture supernatants also resulted in CPE as seen in a wild type infection, albeit some retardation in the onset of CPE could be observed.

TMEV mutant 4, 8, and 23 seem to have an important effect on virus replication. Viral RNA can be rescued from the cell culture supernatant after transfection. Sequencing results showed that TMEV mutant 4 and 8 still contained the desired mutation. The mutations introduced in position 4 and 8 of protein 2C might interfere with the binding of AKAP10. It has been shown that the first 20aa are sufficient for binding to IAP3 (Knox *et al.*, submitted). The N-terminal region of protein 2C has been identified to play an important role in membrane binding of protein 2C (Echeverri & Dasgupta, 1995, Kusov *et al.*, 1998). The alanine substitutions may result in a less tightly membrane associated protein 2C, which may have major implications for virus replication. This was also observed for the alphavirus membrane associated protein nsP1. When the cystein residues (418-420), responsible for the very tight binding to membranes of Semliki Forest virus nsP1 protein, were mutated to alanines, nsP1 was still membrane associated, but less tightly (Laakkonen *et al.*, 1996). Furthermore, it has been observed that PV protein 2C may play a role in determining virion structure (Li & Baltimoree, 1990). It has been postulated that viral RNA replication and virion assembly are coupled processes which occur in association with membranes (Calguiri & Compans, 1973). Protein 2C is tightly associated with membranes, suggesting it could function during encapsidation of viral RNA (Vance *et al.*, 1997). As it was possible to rescue viral RNA of TMEV mutant 4 and 8 but no viral particles, these mutants of protein 2C might also interfere with the encapsidation of viral RNA.

TMEV mutant 23 however does not contain the desired mutation after transfection, as confirmed by sequencing. The dramatic effect on the onset of CPE might be caused by second-site mutations that occurred during viral replication. RNA viruses show high mutation rates partly caused by the lack of exonuclease proofreading activity of the virus-encoded RNA polymerases. New viral genetic variants are constantly created to adapt to changing environmental conditions. Beneficial mutations needed for adaptation are quickly identified (reviewed by Holland *et al.*, 1982, Elena & Sanjuán, 2005). This might also explain the disappearance of the introduced mutation in TMEV mutant 18, which acts as wild type TMEV.

4.2.2.3 Intracellular localization of IAP3

Transfection of BHK-21 cells with the pGFP-IAP3 construct resulted in a granular pattern spread out in the cytoplasm, which seems to be similar to the mitochondrial localization previously observed for full length AKAP10 (Wang *et al.*, 2001). IAP3 consists of the C-terminal 52aa of AKAP10. The C-terminal 40 residues of AKAP10 were shown to be responsible for the interaction with the R subunits of PKA. AKAP10 binds to both RI and RII subunits (Huang *et al.*, 1997). Wang and colleagues (2001) have observed that AKAP10 (D-AKAP2) is enriched in mitochondria, together with cytochrome c, a mitochondrial marker. In addition to the mitochondrial staining, subcellular localization of AKAP10 also reveals a low level diffuse background signal and low levels of nuclear staining, suggesting the existence of multiple pools of AKAP10 (Wang *et al.*, 2001). Furthermore, D-AKAP1 has also been localized to mitochondria (Huang *et al.*, 1999). The primary function of AKAPs is to target PKA to specific subcellular locations. PKA protein or enzymatic activity has been associated with mitochondria (Kleitke *et al.*, 1976, Dimino *et al.*, 1981, Burgess & Yamada, 1987, Muller & Bandlow, 1987). Furthermore, it has been demonstrated that cAMP can be transported into mitochondria (Kulinskii *et al.*, 1981, Kulinskii & Zobova, 1985). PKA has moreover been associated with mitochondrial respiration (Papa *et al.*, 1999, Qu *et al.*, 1999). Mitochondria are also involved in triggering the apoptotic pathway (Kroemer, 1999, reviewed by Waterhouse & Green, 1999).

TMEV protein 2C binds AKAP10 and may therefore be localized to the mitochondria in infected cells. PKA, which has been associated with mitochondria, may be redistributed in the cell caused by the interaction of protein 2C and AKAP10. This may have important implications for the mitochondrial pathway of apoptosis. Interaction of protein 2C with AKAP10 may prevent the triggering of the apoptotic pathway. Furthermore, enterovirus protein 2B is involved in suppressing apoptosis of the infected cells. Protein 2B forms pores in ER and Golgi membranes, which results in a decrease of ER and Golgi Ca^{2+} content, which in turn reduces the Ca^{2+} accumulation in the neighboring mitochondria. The disturbance of the intracellular Ca^{2+} homeostasis is probably involved in this anti-apoptotic function, as it has been shown that Ca^{2+} fluxes between ER and mitochondria play an important role in ER-dependent apoptosis (Campanella *et al.*, 2004, reviewed by van Kuppeveld *et al.*, 2005).

4.3. Expression of TMEV protein 2C in *E. coli*

The results demonstrated that we were able to express TMEV protein 2C in *E. coli* as a fusion protein to the GST-tag, as well as the MBP-tag. This allowed us to purify TMEV protein 2C in order to have a polyclonal antibody made against protein 2C. The anti-TMEV-2C antibody has been proven to be adequate for immunoprecipitation and immunofluorescence experiments. However, the anti-TMEV-2C antibody showed some non-specificity when used for western blotting, suggesting that purification of the antibody might be desirable. It was observed that fusion to a His-tag did not result in expression of protein 2C. Furthermore, the precursor 2BC could not be expressed in *E. coli*. It has been demonstrated that TMEV proteins 2B and 2C contain hydrophobic domains and are tightly membrane bound, which can interfere with expression. Protein 2C can be expressed as a fusion to the GST-tag and the MBP-tag, which suggests protein 2C may be less toxic for the *E. coli* cells than protein 2B. However, when fused to the His-tag, protein 2C can not be expressed. This suggests that the size of the tag fused to protein 2C plays a role in the expression. A larger tag may change the structure of the fusion protein, and therefore the effect of expression of the protein on the *E. coli* cells. The lack of expression observed for the precursor 2BC, may be caused by the high toxicity of protein 2B. Previous efforts to express PV protein 2B and 2C at high levels in *E. coli* cells have been proven difficult. It was observed that PV protein 2B is toxic for *E. coli* and lysed the cells upon production. Protein 2B contains two hydrophobic regions: an amphipathic α-helix and a potential transmembrane domain with a β-sheet configuration (Teterina *et al.*, 1997). Expression of protein 2B can only be tolerated for a very limited period of time before drastic changes in membrane permeability eventually cause cell lysis. Protein 2C is also hydrophobic and associated to membranes and therefore toxic; however expression can be tolerated for longer. High levels of expression of protein 2C do not seem to modify membrane permeability and do therefore not cause lysis of *E. coli* cells (Lama & Carrasco, 1992, Lama *et al.*, 1992).

4.4. TMEV infection and its effect on membrane trafficking

4.4.1 Cytoskeleton

The cytoskeleton, contained within the cytoplasm, is a dynamic structure that maintains cell shape, enables cellular motion, and plays important roles in both intracellular trafficking and cellular division. The cytoskeleton consists of three main components: actin filaments, intermediate filaments, and microtubules. The actin and microtubule cytoskeleton play a major role in the entry, replication and egress of viruses. Viruses induce rearrangements of the cytoskeleton by interfering with cellular signaling pathways to support infection. The actin and microtubule transport systems and their motor proteins are employed by viruses to move to different subcellular sites, which provide the optimal molecular environment for uncoating, replicating and packaging of the viral genome. Furthermore, it has been demonstrated that microtubule motors, kinesin and dynein, and the actin filament motor, myosin, cooperate and that their coordinated activity is essential for organelle motility (reviewed by Langford, 1995, Rogers & Gelfand, 1998). The effect of TMEV infection on actin filaments and microtubules was investigated by means of cellular markers for actin and tubulin. The preliminary results suggest that TMEV infection causes both cytoskeleton components to accumulate at the cellular membrane, creating a hollow area which is thought to represent the expanding viral replication site. This suggests that cytoskeletal integrity may not be necessary for TMEV infection, as was previously shown for poliovirus (Doedens *et al.*, 1994).

4.4.1.1 Actin filaments

The actin cytoskeleton plays a critical role in cell migration, and mediates several intracellular transport processes, based on controlled actin polymerization or on myosins, which translocate along actin filaments upon ATP hydrolysis. The actin-myosin system has been implicated in membrane trafficking (reviewed by Goodson *et al.*, 1997). Viruses have evolved the capacity to use the host actin cytoskeleton to promote their own motility during infection. Actin is an ATP-binding protein that exists in two forms, monomers (G-actin) and double helical polymers or filaments (F-actin). Actin filaments are built by head-to-tail assembly of polar monomeric actin. The resulting filaments are characterized by a fast

growing plus-end and a slow growing minus-end. The processes of actin poly- and depolymerization are regulated by numerous actin-binding proteins. They allow the cell to modulate actin assembly based on external and internal stimuli. Actin is present throughout the cytoplasm but the highest concentration of actin is directly underneath the plasma membrane, where it forms the actin cortex. Several viral proteins are known to interact with actin-binding proteins, and are therefore able to control actin poly- and depolymerization to support their own motility (reviewed by: Gouin *et al.*, 2005, Radtke *et al.*, 2006).

The actin-cytoskeleton plays an important role in the life-cycle of a number of viruses. They interact with the actin filaments at various stages during infection, disrupting and rearranging the actin filaments to their own advantage. Furthermore, the infectious particles of several viruses, such as *Retro*-, *Picorna*-, and *Herpesviruses*, contain actin (Grigera *et al.*, 1988, reviewed by Cudmore *et al.*, 1997, Newman & Brown, 1997, Grünewald *et al.*, 2003, Johannsen *et al.*, 2004). The actin cytoskeleton dramatically changes during vaccinia infection. The Vaccinia virus induces disassembly of actin stress fibers and formation of actin tails to allow efficient egress and intracellular spread. The polymerization of actin filaments is promoted by the virus, probably by recruiting host proteins that are associated with the actin cytoskeleton (reviewed by Cudmore *et al.*, 1997, Higley & Way, 1997, Wolffe *et al.*, 1997, Roper *et al.*, 1998). The polymerization of actin filaments is probably used to propel viruses from cell to cell (reviewed by Smith & Enquist, 2002). Retrovirus infection results in a rapid loss of cytoskeletal integrity, and in addition they have been shown to depend on actin filaments for the completion of their infectious life cycle. The budding process may be dependent on actin (reviewed by Cudmore *et al.*, 1997). The HIV Gag protein has been identified as necessary and sufficient for viral budding, and has been associated with the actin cytoskeleton (Rey *et al.*, 1996). Furthermore, the HIV protein Nef has been shown to increase infectivity, probably by interacting with proteins involved in actin cytoskeleton rearrangements (Campbell *et al.*, 2004). It has also been shown that HIV infection is less effective after inhibiting actin polymerization (Komano et *al.*, 2004). Recently, it was observed that rotavirus infection and replication leads to rearrangements of the cytoskeleton with disorganization of cytoskeletal elements, such as actin, through a calcium-dependent process. The NSP4 protein may play a role in these calcium-dependent actin rearrangements (Berkova *et al.*, 2007).

TMEV may use the actin cytoskeleton early in infection for intracellular transport. At later stages of infection actin appears to disappear from the cytoplasm and accumulate at the plasma membrane. This suggests that actin is no longer needed for viral replication. A hollow area is created within the cell, which we believe represents the expanding viral replication site. It is not known in which way TMEV could induce actin rearrangements. Actin reorganizations may be caused by interactions of viral proteins with actin-binding proteins. It has been previously observed that HPEV-1 protein 2C does not co-localize with actin (Krogerus *et al.*, 2003). This suggests that protein 2C does not bind to actin, however it does not rule out a possible function of protein 2C in the actin rearrangements. Protein 2C may interact with actin-binding proteins that regulate the process of actin poly- and depolymerization. Furthermore, it is possible that the actin rearrangements are calcium-dependent. Protein 2B forms pores in ER and Golgi membranes (reviewed by van Kuppeveld *et al.*, 2005), which results in the disturbance of the intracellular Ca^{2+} homeostasis, which may be involved in the redistribution of actin in infected cells.

4.4.1.2 Microtubules

Microtubules are an important component of the cytoskeleton of the cell, and they play a vital role in the control of cell morphology and function. They help to organize membranous organelles during interphase and comprise the mitotic spindle of a dividing cell. They help to maintain the shape and the internal arrangements of the cell, and delineate tracks along which membrane organelles are transported during exo- and endocytosis. Intact microtubules are also required for preservation of the normal structure and function of the Golgi complex. Microtubules are composed of α/β-tubulin dimers and several microtubule-associated proteins (MAPs; reviewed by Thyberg & Moskalewski, 1999). Some of the dynamic properties of microtubules can be accounted for by the intrinsic properties of the α/β-tubulin heterodimer. Microtubules undergo periods of growth and shrinkage and can switch rapidly between these two states (Mitchison & Kirschner, 1984). This dynamic instability is a result of the GTP hydrolysis by tubulin (Caplow & Shanks, 1996, Desai & Mitchison, 1997). A variety of proteins have also been purified that modulate the dynamic behaviour of microtubules. Some of these microtubule-associated proteins stabilize the microtubules, while others promote destabilization. The destabilization and disassembly of microtubules are necessary for cell processes such as mitosis. Microtubules transport membrane bound

organelles and other structures by using motor proteins. Kinesin and dynein are the two main microtubule associated motors. Kinesin serves plus-end directed transport, towards the plasma membrane, while dynein serves minus-end transport, towards the centrosome, which regulates to a large extent the distribution of microtubules. Both motor proteins have been shown to bind to the Golgi complex (reviewed by Thyberg & Moskalewski, 1999).

A computer-based analysis has demonstrated that TMEV protein 2C is highly similar to katanin, a member of the AAA ATPase superfamily (figure 3.32, section 3.4.1). Katanin is a heterodimeric, ATP-dependent, microtubule-severing protein first purified from sea urchin eggs (*Strongylocentrotus purpuratus*; figure 4.4). It has a microtubule-stimulated ATPase activity and hydrolysis of ATP is required for the microtubule-severing reaction. Katanin is also known to disassemble stable microtubules to form polymerisation-competent tubulin subunits (McNally & Vale, 1993). It is a heterodimer of 60 and 80 kDa subunits, which is highly concentrated at centrosomes throughout the cell cycle (McNally *et al.*, 1996). The p60 subunit is a novel member of the AAA ATPase superfamily. Sequence analysis of p60 revealed an ORF that encodes a 516aa polypeptide, which contains a C-terminal domain that is highly conserved in the AAA ATPase superfamily. This region contains the "Walker A" and "Walker B" motifs found in many ATPases. Consistent with the finding of an AAA domain in its sequence, p60 displayed a microtubule-stimulated ATPase activity. Furthermore, p60 exhibits a microtubule-severing activity. Both p60 activities are displayed even in the absence of the p80 subunit (Hartman *et al.*, 1998). It has also been demonstrated that the p60 subunit of katanin oligomerizes in an ATP- and microtubule-dependent manner. Oligomerization increased the affinity of katanin for microtubules and stimulated its ATPase activity. After ATP hydrolysis, microtubule-bound katanin oligomers disassembled microtubules and then dissociated into free katanin monomers (Hartman & Vale, 1999). Sequence analysis of the p80 subunit revealed a predicted 690aa polypeptide that contains six "WD40" repeat motifs. The WD40 repeats in several proteins have been documented to participate in protein-protein binding interactions (Komachi *et al.*, 1994; Wall *et al.*, 1995). Two functional domains of p80 were postulated. It is thought that p80 may be involved in heterodimerization with p60. Furthermore, p80 could contain a domain that interacts with a centrosomal protein. The six WD40 repeats in p80 represent a good candidate domain for participating in either dimerization or

centrosome targeting. Hartman and colleagues showed that the WD40 repeats are not required for dimerizing the two katanin subunits, but they have uncovered a role for the WD40 domain of p80 in targeting katanin to centrosomes *in vivo* (Hartman *et al.*, 1998).

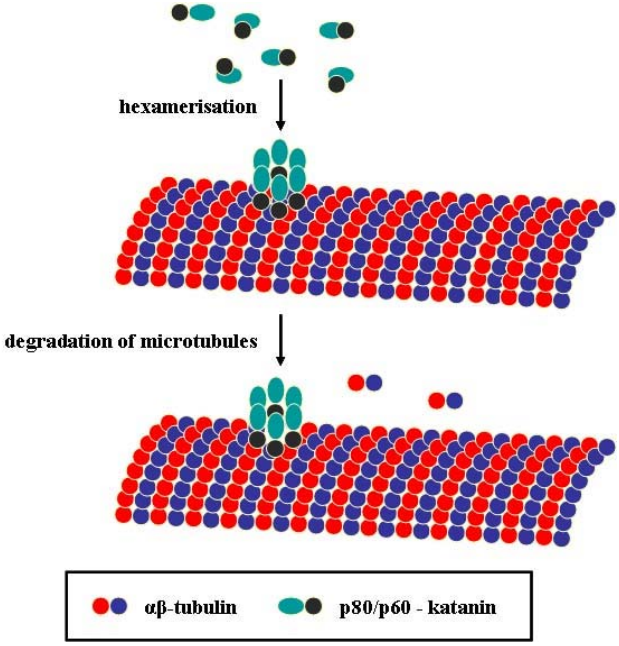

Figure 4.4: Illustration of the microtubule-severing activity of katanin. *The p60 and p80 subunit of katanin oligomerize to form a hexamer, which disassembles microtubules in an ATP-dependent manner.*

We aspired to establish a stable cell line constitutively expressing fluorescent microtubules to observe the effect of TMEV infection and in particular protein 2C on microtubules. We were not able to establish a stable cell line, possibly because polymerization of a tubulin fusion protein into microtubules is not feasible. Therefore we employed a cellular marker for tubulin to determine the effect of TMEV infection on microtubules. Our preliminary results suggest that microtubules, like actin filaments, cluster near the plasma membrane creating a hollow area representing the viral replication site. It is possible that protein 2C exhibits a similar function to katanin. Protein 2C may induce the disassembly of microtubules, resulting in monomeric tubulin, which is redistributed to the verge of the infected cell caused by the expansion of the viral replication site. The dissociation of the microtubules may play a role in the disassembly of the Golgi complex during infection, as discussed in section 4.4.2.

Furthermore, it is possible that other viral proteins interact with microtubules or MAPs, and therefore cause the microtubule rearrangement observed during infection.

Many viruses require microtubules for efficient replication. Microtubules are required during cell entry, for efficient nuclear targeting, and for cytosolic transport of the viral genome-protein complex. Microtubule motors are known to catalyze the intracellular transport of many viral structures. Viruses make use of the cytoplasmic membrane traffic; endocytosis for entry, and exocytosis for egress. Furthermore, it has been demonstrated that depolymerization of microtubules results in reduction of the viral yield, probably because free diffusion in the cytoplasm is then used for viral distribution. Viral proteins also interact directly with the microtubule motors dynein or kinesin. Dynein transports viral particles to the MTOC during virus entry and assembly. Viral proteins interact with kinesin during assembly and egress, and kinesin may also catalyze transport from the MTOC to the nucleus during entry (reviewed by: Döhner *et al.*, 2005, Greber & Way, 2006). Herpes Simplex virus (HSV) infection results in the loss of the radial organization of microtubules. Microtubules are redistributed to the cell periphery and the MTOC disappears. The reorganization of the microtubule network seems to facilitate the nuclear localization of VP22, a major virion phosphoprotein (Kotsakis *et al.*, 2001). Furthermore, it has been demonstrated that axonal HSV progeny capsids colocalize with kinesin-1 (Diefenbach *et al.*, 2002). The Gag polyprotein of many *Retroviruses* contains a matrix protein that has been shown to interact with kinesin-4. This interaction may play a role in the transport of subviral particles to the plasma membrane for virus budding (Tang *et al.*, 1999). *Adenoviruses* deliver their genomes to the nucleus after entry into the cell. They travel along the microtubule cytoskeleton towards the nucleus, using the microtubule motor dynein (Bailey *et al.*, 2003). The microtubule cytoskeleton also plays an important role during influenza infection. Drug-induced microtubule depolymerization results in a random distribution of the nucleoprotein in the cytoplasm, and interferes with the normal polarized delivery and segregation of hemagglutinin to the apical surface (Rindler *et al.*, 1987, Momose *et al.*, 2007). Vaccinia virus infection requires microtubules for efficient formation of intracellular mature virus particles and for the assembly of intracellular enveloped virus particles. Newly assembled virus particles accumulate near the MTOC in a microtubule and dynein-dependent manner. At later stages of the infection, the microtubule cytoskeleton becomes dramatically reorganized, probably caused by the loss of centrosome function. An

accumulation of viral encoded proteins exhibiting MAP-like properties can also be observed, which may play a vital function in the rearrangements of the microtubule cytoskeleton (Ploubidou *et al.*, 2000).

4.4.2 Golgi complex

Picornavirus infection leads to profound alterations in the morphology and functioning of cellular membranes. Proliferation of cytoplasmic membrane vesicles is usually observed during the replication of *Picornaviruses*. Large numbers of membrane vesicles have been observed in the perinuclear region of poliovirus infected cells (Dales *et al.*, 1965). It has been suggested that these vesicles originate from several intracellular membrane structures, such as ER, Golgi complex and lysosomes and it requires at least in part *de novo* synthesis of phospholipids (Bienz *et al.*, 1987, Guinea & Carrasco, 1990, Schlegel *et al.*, 1996). Concomitant with the synthesis of new vesicles, there is also an important rearrangement of the intracellular membranous organelles of the secretory pathway, the disappearance of the Golgi complex, and a swelling of the ER together with a reorganization of the cytoskeletal framework (Lenk & Penman, 1979, Joachims & Etchison, 1992). Poliovirus infection causes the disassembly of the Golgi complex. This effect has been attributed to the expression of protein 2B (Sandoval & Carrasco, 1997). Our results show a redistribution of the Golgi complex during TMEV infection. Cellular markers have been used to determine the effect of TMEV infection on the Golgi complex. We observed that the Golgi complex turns from a solid, crescent-shaped organelle at the start of infection, into a series of punctuate fluorescent points forming an expanding balloon-like structure, surrounding the concomitantly expanding site of virus replication. The remnants of the Golgi complex are finally dispersed throughout the cytoplasm. Live imaging confirmed these findings. The exact mechanism behind the disassembly of the Golgi complex upon TMEV-infection is not known.

The Golgi complex is a membrane-bound organelle that consists of a stack of flattened cisternae connected by tubular bridges into a ribbon structure. It is localized to the perinuclear area, close to the centrosome, which is the major organizing center for microtubules. The Golgi apparatus serves an essential role in secretory trafficking, lipid biosynthesis, protein modifications and the sorting and transport of proteins. Many factors contribute to the formation and the maintenance of the Golgi structure: Golgi matrix

proteins, GTPases, specialized cytoskeleton motors, regulatory kinases, and a constant membrane input from the ER (reviewed by Colanzi & Corda, 2007). The Golgi complex undergoes extensive fragmentation during mitosis which allows its correct partitioning and inheritance by daughter cells. The Golgi ribbon is converted into clusters of vesicles and tubules dispersed throughout the cytoplasm. Membrane trafficking is inhibited during mitosis and occurs when Golgi fragmentation starts, suggesting that the inhibition of vesicular transport is partly responsible for Golgi fragmentation. Furthermore, it has been demonstrated that the Golgi complex is closely related to microtubules. Intact microtubules are required for the maintenance of the normal structure and function of the Golgi apparatus. The Golgi complex is disassembled and dispersed upon drug-induced disruption of microtubules. During prophase microtubules depolymerize resulting in a reorganization of the Golgi complex and eventually the Golgi fragmentation (reviewed by: Lowe *et al.*, 1998, Thyberg & Moskalewski, 1999, Colanzi & Corda, 2007).

Our results showed that microtubules undergo dramatic reorganizations upon TMEV-infection. The microtubule cytoskeleton in the cytoplasm disappears and tubulin accumulates at the periphery of the infected cell. The disassembly of the Golgi complex in TMEV-infected cells may resemble the fragmentation of the Golgi complex during cell division. The reorganization of the microtubules observed in infected cells may in part cause the dispersion of the Golgi complex. Our results showed that TMEV protein 2C does not co-localize with the Golgi complex, however, its possible severing effect on microtubules may indirectly cause the dispersion of the Golgi complex in TMEV-infected cells. However, very recently, it was observed that Golgi fragmentation in PV-infected cells requires intact microtubules (Beske *et al.*, 2007). PV infection induces a dramatic disruption of the Golgi complex. A loss of the cohesive Golgi structure can be observed, accompanied by a dispersion of the remnants throughout the cytoplasm. Similar observations can be made following expression of PV protein 2B in isolation (Sandoval & Carrasco, 1997). Fragmentation of the Golgi complex is prevented by pre-treatment with nocodazole, a drug that induces microtubule depolymerization. This suggests that Golgi fragmentation in PV-infected cells requires intact microtubules (Beske *et al.*, 2007). Perhaps microtubules are also required for Golgi fragmentation in early stages of TMEV-infection. Furthermore, it was recently observed that Arf1 is active during mitosis and that this activity is required for mitotic Golgi fragmentation. Arf1 is a small GTPase required

for COPI vesicle formation from the Golgi membrane, suggesting that Golgi fragmentation during mitosis is mediated by vesicle budding (Xiang *et al.*, 2007). BIG1 activates ArfI to regulate Golgi vesicular transport. It has recently been observed that some members of the Arf family of small GTPases (ArfI), which control secretory trafficking, associate with newly formed membranous RNA replication complexes in PV-infected cells (Belov *et al.*, 2005). Two PV proteins 3A and 3CD, recruit different Arf-GEFs, including BIG1, to the membranous vesicles that arise during PV infection. These are responsible for Arf activation and translocation to these membranes (Belov *et al.*, 2007). Our results showed that BIG1 is located at the viral replication site during TMEV-infection, as discussed in section 4.4.5, suggesting that Arf1 may also be redistributed from the Golgi complex to the viral replication site. This may in part contribute to the Golgi fragmentation seen in TMEV-infected cells.

Recently it was shown that PKA plays a vital role in the assembly and the maintenance of the Golgi complex (Bejarano *et al.*, 2006). PKA is associated with the cytosolic surface of the Golgi membrane through interactions of the RIIα subunits with an anchor protein (Nigg *et al.*, 1985). It was shown that PKA is locked in the Golgi complex, not exchanging rapidly with the cytosolic pool. Down-regulation of RIIα by siRNA resulted in the depletion of the Golgi apparatus. Furthermore, the displacement of PKA from the Golgi complex resulted in the collapse of the organelle, and inhibition of PKA activity caused fragmentation of the Golgi complex (Bejarano *et al.*, 2006). The possible interaction of TMEV protein 2C with AKAP10 may cause a redistribution of PKA, as observed in TMEV-infected cells (discussed in section 4.4.3). The displacement of PKA from the Golgi complex may in part explain the dispersion of the Golgi complex upon infection.

4.4.3 Protein kinase A

Protein kinase A, also known as cyclic-AMP-dependent protein kinase, is an enzyme that is regulated by the fluctuating levels of cyclic AMP within cells. PKA alters the phosphorylation state of cellular target proteins that act through the cAMP signaling pathway. The PKA holoenzyme is a heterotetramer that contains a regulatory (R) subunit dimer that maintains two catalytic (C) subunits in an inactive state. Binding of cAMP to sites in each R subunit results in the dissociation of PKA and the release of the active C subunits. Phosphorylation of substrates occurs at serine (Ser) or threonine (Thr) residues

and the target sequences are Arg-Arg-X-Ser/Thr or Lys-Arg-X-X-Ser/Thr. The intracellular concentration of cAMP controls PKA activity. Low levels of cAMP result in inactive C subunits bound to the R subunit dimer. Increase in cAMP results in binding of cAMP to the R subunits, followed by an allosteric conformational change which causes release of the C subunits. Furthermore, PKA activity is modulated by protein kinase inhibitors that act as pseudo-substrates for the C subunits. The existence of multiple C and R subunit isoforms specifies PKA signaling. Three isoforms of the C subunit have been identified (α, β, and γ). The kinetic characteristics and cAMP sensitivities of Cα- and Cβ-containing PKA show small differences, but substrate specificity and interaction with R subunits are indistinguishable. The R subunits exist in two major isoforms, RI and RII, with two subtypes each, α and β. The dimeric R subunits exhibit distinct cAMP binding affinities and differential localization within the cell. Type I enzymes are predominantly located in the cytoplasm, whereas type II enzymes tend to associate with cellular membranes. Spatial targeting of PKA results from interactions with anchoring proteins (AKAPs). The differences in subcellular targeting of type I and type II PKA contribute to the specificity in cellular responses (reviewed by Dell'Acqua & Scott, 1997).

Protein kinase A (PKA) activity is known to play a number of key roles in the regulation of cellular membrane traffic. PKA has been implicated in protein transport from the ER to the Golgi complex, and in the budding of constitutive transport vesicles from the trans-Golgi network (Muniz *et al.*, 1997). Furthermore, PKA seems to play a role in endosome-to-Golgi and Golgi-to-ER transport (Lee & Linstedt, 2000). In addition PKA activity has also been associated with endosome fusion, exo-, endo-, and transcytosis (Takuma & Ichida, 1994a, Muniz *et al.*, 1996;, Rapacciuolo *et al.*, 2003, Kim *et al.*, 2005, Hansen & Casanova, 1994). Moreover, PKA functions in the stimulation of the binding of Arf1 to the Golgi membrane (Martin *et al.*, 2000).

Our preliminary results suggest that PKA undergoes redistribution upon TMEV infection, and accumulates at the periphery of the cell during late stages of infection. We determined the localization of PKA in infected cells by means of cellular markers for both RIα and RIIα subunits, and the catalytic subunit. Similar redistribution was observed for all cellular markers in TMEV-infected cells. Particular isoforms of PKA are localized to the Golgi complex and protein phosphorylation is an important feature in regulating steps along cellular transport

pathways. Sub-cellular compartmentalization of PKA through the use of AKAPs is now widely believed to be responsible for the specificity of the cAMP signaling pathway. It has been shown that the N-terminus of TMEV protein 2C binds to the C-terminal region of a PKA anchoring protein, AKAP10 and competes with the RII regulatory subunit of PKA (Knox *et al.*, submitted). This may serve to displace PKA from the Golgi complex, resulting in the dispersion of the Golgi complex as observed in TMEV-infected cells (discussed in section 4.4.2). Furthermore, PKA is known to stimulate binding of Arf1 to the Golgi membranes. The changes in PKA localization during TMEV infection may cause a redistribution of Arf1, which may contribute to the Golgi fragmentation observed in TMEV-infected cells.

4.4.4 Endosomes

Internalization of proteins and lipids is mediated by clathrin-coated vesicles and other less characterized pathways. The endocytosed molecules are delivered to the early endosomes. Receptor-mediated endocytosis is an essential process in signal transduction whereby receptor-ligand complexes are internalized and processed. After receptor-ligand uncoupling, receptors are transported along the recycling pathway, whereas ligands follow the degradation route. Early endosomes are generally accepted as the single entry site for internalized molecules and the first sorting station on the endocytic pathway. They are a dynamic compartment with a high homotypic fusion capacity, and exhibit a highly complex organization consisting of cisternal regions of tubular elements and large vesicles. There are two extreme views on the relationship between early and late endosomes. The endosome maturation model states that early endosomes are formed *de novo*, presumably from clathrin-coated vesicles. Late endosomes are formed by fusion of residual components of the early endosomal compartment, once recycling to the plasma membrane has been exhausted. The second model states that early endosomes represent a stable compartment maintained by a balance of incoming and departing material. Endosomal carrier vesicles are formed from early endosomes and fuse with late endosomes in a microtubule-dependent manner. The clathrin-coated vesicle pathway is the best characterized internalization pathway and is cytosol- and ATP-dependent with a requirement for multiple GTP-binding proteins such as the GTPase dynamin. Dynamin is a ~100 kDa protein that facilitates budding of clathrin-coated pits, which leads to the formation of coated vesicles in a GTP-

dependent manner. Other small GTPases, such as Rab4 and Rab5, have been associated with early endosomes. Rab5 plays a role in promoting early endosome fusion and regulates the rate of clathrin-dependent endocytosis at the plasma membrane. Rab4 has been implicated in recycling endosomal material to the plasma membrane. The endocytosis process also seems to require myosin and actin filaments. Furthermore, the dynamics of early endosomes and microtubules are in part coupled. The tubular elements of endsomes overlap with microtubules and transport from early to late endosomes is microtubule-dependent. Moreover, coat proteins have been identified on early endosomes. The COPI coat complex is known to regulate retrograde transport from the Golgi complex to the ER, but there are some indications that an endosomal COPI complex functions in endosomal transport. The endosomal COPI interacts with membranes through interaction with small GTPases, such as Arf1 (reviewed by: Claque, 1998, Battey *et al.*, 1999, Gruenberg, 2001).

The clathrin-dependent endocytic pathway is employed by many viruses for entry into host cells. It is generally accepted that Semliki Forest virus (SFV), an enveloped alphavirus, requires the clathrin-dependent pathway for entry (DeTulleo & Kirchhausen, 1998). Entry of HIV is believed to occur by direct fusion at the plasma membrane; however clathrin-dependent endocytosis has been shown to significantly contribute to productive entry into the host cells, suggesting that the clathrin-dependent pathway is used by some viruses as an alternative entry route (Daecke *et al.*, 2005). Contradictions have been observed for other viruses, such as Sindbis virus and some *Picornaviruses*. Electron microscopy has not been able to resolve the viral entry route. Poliovirus has been found in association with clathrin-coated pits and in completely invaginated coated vesicles (Zeichhardt *et al.*, 1985, Willingmann *et al.*, 1989). However, more recent studies demonstrated that PV does not appear to require the clathrin-dependent endocytic pathway (DeTulleo & Kirchhausen, 1998). Cells expressing dominant-negative forms of dynamin that block clathrin-dependent endocytosis were used to examine the mode of entry of SFV, Sindbis virus, Human Rhinovirus 14 (HRV-14), and PV. It was shown that PV was not prevented from entering cells in which the clathrin-mediated endocytosis was blocked. However, SFK, Sindbis virus and HRV-14 were only able to infect cells were the clathrin-dependent endocytic pathway was active (DeTulleo & Kirchhausen, 1998). Clathrin-coated vesicles are not the sole route of endocytic transport from the plasma membrane to the endosomal compartments,

suggesting that PV employs an alternative non-clathrin-mediated pathway of endocytosis for entry into the cell (Hansen *et al.*, 1993, Damke *et al.*, 1995).

We wanted to determine the effect of TMEV infection on the endocytic pathway using a cellular marker for early endosomes. Our results showed that early endosomes show a punctate staining pattern consistent with the cytoplasmic distribution of endosomes in mock infected cells and at early stages of infection. During late stages of infection, the early endosomes seem to accumulate at the periphery of the cell surrounding the expanding viral replication site. The TMEV-receptor for entry into the cell has not yet been identified. Entry into the cell differs amongst *Picornaviruses*; however it is possible that TMEV employs the clathrin-mediated endocytic pathway for entry into the cell. This may explain the characteristic endosomal staining early upon infection. Actin filaments and microtubules have been associated with early endosomes. The effects observed on these cytoskeleton components during TMEV-infection may partly explain the accumulation of early endosomes at the periphery of the cell at later stages of infection. Furthermore, the involvement of Arf1 in endosomal COPI coated vesicles may also contribute to explaining our results. Arf1 may be displaced from endosomal vesicles by BIG1, as discussed in section 4.4.5, which may account for the redistribution of early endsomes. Our results also showed an interaction between TMEV protein 2C and RTN3. It was suggested that RTNs may play a role in the endocytic pathway (Iwahashi *et al.*, 2002), and a possible interaction with SNARE proteins, which are involved in membrane trafficking including endocytosis, has been proposed (Steiner *et al.*, 2002). The interaction of TMEV protein 2C with RTN3 may play a role in the effect of TMEV infection on endocytosis. Interestingly, a computer-based analysis has demonstrated that TMEV protein 2C is highly similar to vacuolar protein sorting protein 4 (VPS4), an AAA ATPase required for endosomal transport (figure 3.32, section 3.4.1). VPS4 catalyzes the release of an endosomal membrane associated class E protein complex required for normal morphology and sorting activity of the endosome (Babst *et al.*, 1998).

4.4.5 BIG1

BIG1 or Brefeldin A-inhibited guanine nucleotide-exchange protein 1 is a ~200kDa protein that preferentially activates Arf1 and Arf3. BIG1 is mainly cytosolic and Golgi-associated, and is found in the cytosol in a multiprotein complex with a similar Arf-activating protein

BIG2, which also serves as an A-kinase anchoring protein. It has been demonstrated that the N-terminal part of BIG1 is required for Golgi association (Mansour *et al.*, 1999). Recently, BIG1 was also localized to several nuclear sites in serum starved HepG2 cells, which suggests a previously unknown function for BIG1 in nuclear processes (Padilla *et al.*, 2004). BIG1 is a member of the guanidine-exchange protein family (GEPs). GEPs differ in molecular weight, domain structure and sensitivity to inhibition by Brefeldin A (BFA); however all GEPs contain an ~200aa Sec7 domain that is responsible for Arf activation (Franzusoff & Schekman, 1989, Chardin *et al.*, 1996). Arfs are 20 kDa GTPases of the Ras superfamily that regulate vesicular transport. Arfs function in the formation of coated membranous vesicles originating from different intracellular departments. Furthermore, they participate in cytoskeleton remodeling and regulation of phospholipase D activity. Three classes of Arfs have been described. Class I consists of Arf1-3, and functions in ER-Golgi trafficking. The not well-characterized class II contains Arf4 and Arf5, whereas class III contains Arf6 which plays a significant role in endocytic pathways and cytoskeletal remodeling (reviewed by Moss & Vaughan, 1998). They are activated by GEPs, which promote the replacement of bound GDP with GTP, and inactivated by GTPase-activating proteins, which are required to stimulate hydrolysis of bound GTP to generate Arf-GDP (Donaldson, 2000, Jackson & Casanova, 2000). The best characterized member of the Arf family is Arf1, which is vital for retrograde membrane transport from the Golgi complex to the ER and intra-Golgi. Arf1 has also been implicated in membrane transport from the trans-Golgi network, endosomal trafficking and exocytosis of secretory vesicles (reviewed by Nie *et al.*, 2003).

Recently, it was observed that some members of the Arf family of small GTPases (ArfI), which control secretory trafficking, associate with newly formed membranous RNA replication complexes in PV-infected cells. The accumulation of Arfs on membranes does not occur in the presence of BFA, a fungal metabolite that prevents normal function of Arfs and is known to inhibit poliovirus infection. It was also demonstrated that the Arf translocation can be induced independently by synthesis of PV protein 3A or protein-complex 3CD. Arf1-GFP redistributes from the Golgi-complex to a perinuclear site in PV infected cells, which represents the PV replication site. This suggests that Arfs are involved in PV replication. Interestingly PV proteins 2B and 2C and their precursor 2BC, which are

known to bind and remodel membranes, do not seem to have an effect on Arf distribution (Belov *et al.*, 2005). Moreover, it was demonstrated that Coxsackievirus B3 protein 3A inhibits the activation of Arf1, which regulates the recruitment of the COPI coat complex to membranes. Protein 3A is known to inhibit ER-to-Golgi transport, which may be important for viral suppression of immune responses. The underlying mechanism may be that protein 3A specifically inhibits GBF1, a member of the GEP family, by interacting with its N-terminus (Wessels *et al.*, 2006a). It was confirmed that protein 3A of Coxsackievirus B3 inhibits ER-to-Golgi transport by interfering with the Arf1-dependent COPI recruitment to membranes through binding GBF1 and inhibiting its function. It was also shown that PV protein 3A interferes with Arf1 function in the same manner; however no interference with protein transport or COPI-recruitment was observed for protein 3A of several other *Picornaviruses*, such as HRV, ECMV, FMDV and HAV (Wessels *et al.*, 2006b, 2007).

BIG1 activates Arf1 and therefore we aspired to determine the effect of TMEV-infection on BIG1. Our results showed that BIG1 concentrated in a juxtanuclear area, representing the Golgi-complex, in mock-infected cells. Upon infection, BIG1 undergoes redistribution to the perinuclear area, which is the site of viral RNA replication. During the late stages of infection, BIG1 is distributed in a punctate pattern in the cytoplasm, which represents the expanding viral replication site. This is in contrast to our results for the other intracellular components investigated, which all accumulate at the periphery of the cell at late stages of TMEV-infection. This suggests that BIG1 plays a role in the viral replication, probably by displacing Arf1 to the replication vesicles. These results were recently confirmed for PV infected cells by Belov and colleagues (2007). They demonstrated that Arf family members become membrane bound after synthesis of PV proteins 3A and 3CD, and associate with newly formed membrane RNA replication complexes in PV-infected cells. Furthermore, they showed that Arf1 colocalizes with the newly formed replication complexes in PV-infected cells. Protein 3A and 3CD also independently recruit GBF1 and BIG1/2, members of the GEP family, to the newly formed replication complexes. This suggests that the recruitment of these GEPs is responsible for Arf activation and translocation to these membranes (Belov *et al.*, 2007a, 2007b).

4.5. Conclusions

- Protein 2C of several *Picornaviruses*, such as poliovirus and FMDV, has been proven to express to detectable levels for both immunofluorescence and western blot experiments. However, expressing TMEV protein 2C in mammalian cells has been very challenging. We were not able to express TMEV protein 2C to detectable levels. Nevertheless, TMEV has been proven to be an easy to replicate and easy to use virus.

- TMEV protein 2C was localized in infected cells using an anti-TMEV-2C antibody. Tiny dots spread out in the cytoplasm representing newly synthesized protein can be seen early upon infection, which assemble into an ER-like pattern. Protein 2C redistributes to a juxtanuclear location, which represents the viral replication site, and spreads out through the cytoplasm as the viral replication site expands.

- TMEV protein 2C partly overlaps with the Golgi complex during infection, however no co-localization can be observed. This suggests no direct function for protein 2C in the disassembly and disappearance of the Golgi complex.

- TMEV protein 2C interacts with reticulon 3 *in vitro*. RTN3 is an ER-associated protein and the identified interaction may play a role in the intracellular changes in membrane trafficking observed during TMEV infection.

- A previously identified interaction between TMEV protein 2C and AKAP10 could not be confirmed, possibly because of conformational constraints. Two mutations in the AKAP10 binding site, which inhibit the completion of the TMEV infectious cycle, were identified. IAP3 showed a granular pattern spread out in the cytoplasm, which may represent a mitochondrial localization.

- TMEV protein 2C was expressed in *E. coli* as a GST- or a MBP-fusion protein. This allowed us to purify TMEV protein 2C in order to have a polyclonal antibody made against protein 2C. It was however not possible to express protein-complex 2BC in *E. coli*, presumably because of its toxic nature.

- Actin filaments and microtubules undergo drastic rearrangements during TMEV infection. Accumulation of both cytoskeleton components at the cell periphery can be

observed during late stages of infection. TMEV protein 2C is highly similar to katanin, a microtubule-severing protein, suggesting protein 2C may exhibit a similar function in infected cells.

- Endosomes concentrate near the cell membrane during late stages of TMEV infection, suggesting TMEV has a drastic effect on the endocytic pathway.
- PKA redistributes to the verge of the cell during TMEV infection. The possible interaction between protein 2C and AKAP10 may partly cause this displacement.
- The Golgi complex undergoes disassembly during TMEV infection, and eventually completely disappears as confirmed by live imaging of TMEV-infected cells.
- BIG1 seems to locate to the viral replication site during TMEV infection, suggesting it may play a role during replication. The dispersion of the Golgi complex may in part be caused by the activation and displacement of Arf1 by BIG1.

5. References

Agol V.I. (2002) Picornavirus genome: an overview. In *Molecular Biology of Picornaviruses* edited by Semler B.L. and Wimmer E. ASM Press, Washington D.C., USA: 127-148.

Aldabe R., and Carrasco L. (1995) Induction of membrane proliferation by poliovirus proteins 2C and 2BC. *BBRC*, 206: 64-76.

Ali N., and Siddiqui A. (1997) The La antigen binds 59 noncoding region of the hepatitis C virus RNA in the context of the initiator AUG codon and stimulates internal ribosome entry site-mediated translation. *Proc Natl Acad Sci USA*, 94: 2249-2254.

Aminev A.G., Amineva A.P., and Palmenberg A.C. (2003) Encephalomyocarditis viral protein 2A localizes to nucleoli and inhibits cap-dependent mRNA translation. *Virus Res*, 95: 45-57.

Andino R., Rieckhof G.E., and Baltimore D. (1990) A functional ribonucleoprotein complex forms around the 5' end of poliovirus RNA. *Cell*, 63: 369-380.

Andino R., Rieckhof G.E., Achacoso P.L., and Baltimore D. (1993) Poliovirus RNA synthesis utilizes an RNP complex formed around the 5'-end of viral RNA. *EMBO J*, 12: 3587-3598.

Anson D.S. (2004) The use of retroviral vectors for gene-therapy-what are the risks? A review of retroviral pathogenesis and its relevance to retroviral vector-mediated gene delivery. *Genet Vaccines Ther*, 2: 9.

Argos P., Kamer G., Nicklin M.J., and Wimmer E. (1984) Similarity in gene organization and homology between proteins of animal picornaviruses and plant comovirus suggest common ancestry of these virus families. *Nucleic Acids Res*, 12: 7251-7267.

Aridor M., and Balch W.E. (2000) Kinase signaling initiates coat complex II (COPII) recruitment and export from the mammalian endoplasmic reticulum. *J Biol Chem*, 275: 35673-35676.

Armstrong R.N. (1997) Structure, catalytic mechanism, and evolution of the glutathione transferases. *Chem Res Tox*, 10: 2-18.

Babst M., Wendland B., Estepa E.J., and Emr S.D. (1998) The Vps4p AAA ATPase regulates membrane association of a Vps protein complex required for normal endosome fusion. *EMBO J*, 17: 2982-2993.

Bailey C.J., Crystal R.G., and Leopold P.L. (2003) Association of adenovirus with the microtubule organizing center. *J Virol*, 77: 13275-13287.

Bakhshesh M., Groppelli E., Willcocks M.M., Royall E., Belsham G.J., and Roberts L.O. (2008) The Picornavirus Avian Encephalomyelitis virus possesses a Hepatitis C virus-like internal ribosome entry site element. *J Virol*, 82: 1993-2003.

Bakkali Kassimi L., Madec F., Guy M., Boutrouille A., Rose N., and Cruciere C. (2006) Serological survey of encephalomyocarditis virus infection in pigs in France. *Vet Rec*, 159: 511-514.

Baltera R.F., and Tershak D.R. (1989) Guanidine-resistant mutants of poliovirus have distinct mutations in peptide 2C. *J Virol*, 63: 4441-4444.

Baltimore D. (1971) Expression of animal virus genomes. *Bacteriol Rev*, 35: 235-241.

Banerjee R., Echeverri A., and Dasgupta A. (1997) Poliovirus-encoded 2C polypeptide specifically binds to the 3'-terminal sequence of viral negative-strand RNA. *J Virol*, 71: 9570-9578.

Banerjee R., Tsai W., Kim W., and Dasgupta A. (2001) Interaction of poliovirus-encoded 2C/2BC polypeptides with the 3' terminus negative-strand cloverleaf requires an intact stem-loop b. *Virology*, 280: 41-51.

Banerjee R., and Dasgupta A. (2001) Interaction of picornavirus 2C polypeptide with the viral negative-strand RNA. *J Gen Virol*, 82: 2621-2627.

Barco A., and Carrasco L. (1995) A human virus protein, poliovirus protein 2BC, induces membrane proliferation and blocks the exocytic pathway in the yeast *Saccharomyces cerevisiae*. *EMBO J*, 14: 3349-3364.

Barco A., and Carrasco L. (1998) Identification of regions of poliovirus 2BC protein that are involved in cytotoxicity. *J Virol*, 72: 3560-3570.

Battey N.H., James N.C., Greenland A.J., and Brownlee C. (1999) Exocytosis and endocytosis. *Plant Cell*, 11: 643-659.

Beard C.W., and Mason P.W. (2000) Genetic determinants of altered virulence of Taiwanese foot-and-mouth disease virus. *J Virol*, 74: 987-991.

Beijerinck M.W. (1898) Concerning a contagium vivum fluidum as a cause of the spot-disease of tobacco leaves. *Verh Akad Wet Amsterdam*, II: 3-21.

Bejarano E., Cabrera M., Vega L., Hidalgo J., and Velasco A. (2006) Golgi structural stability and biogenesis depend on associated PKA activity. *J Cell Sci*, 119: 3764-3775.

Belov G.A., Fogg M.H., and Ehrenfeld E. (2005) Poliovirus proteins induce membrane association of GTPase ADP-ribosylation factor. *J Virol*, 79: 7207-7216.

Belov G.A., Altan-Bonner N., Kovtunovych G., Jackson C.L., Lippincott-Schwartz J., and Ehrenfeld E. (2007a) Hijacking components of the cellular secretory pathway for replication of poliovirus RNA. *J Virol*, 81: 558-567.

Belov G.A., Habbersett C., Franco D., and Ehrenfeld E. (2007b) Activation of cellular Arf GTPases by poliovirus protein 3CD correlates with virus replication. *J Virol*, 81: 9259-9267.

Belsham G.J. (1993) Distinctive features of foot-and-mouth-disease virus, a member of the picornavirus family-aspects of virus protein-synthesis, protein processing and structure. *Prog Biophys Mol Biol*, 60: 241-260.

Berkova Z., Crawford S.E., Blutt S.E., Morris A.P., and Estes M.K. (2007) Expression of rotavirus NSP4 alters the actin network organization through the actin remodeling protein cofilin. *J Virol*, 81: 3545-3553.

Beske O., Reinchelt M., Taylor M.P., Kirkegaard K., and Andino R. (2007) Poliovirus infection blocks ERGIC-to-Golgi trafficking and induces microtubule-dependent disruption of the Golgi complex. *J Cell Sci*, 120: 3207-3218.

Bienz K., Egger D., Rasser Y., and Bossart W. (1983) Intracellular distribution of poliovirus proteins and the induction of virus-specific cytoplasmic structures. *Virology*, 131: 39-48.

Bienz K., Egger D., and Pasamontes L. (1987) Association of polioviral proteins of the P2 genomic region with the viral replication complex and virus-induced membrane synthesis as visualized by electron microscopic immunocytochemistry and autoradiography. *Virology*, 160: 220-226.

Bienz K., Egger D., Troxler M., and Pasamontes L. (1990) Structural organization of poliovirus RNA replication is mediated by viral proteins of the P2 genomic region. *J Virol*, 64: 1156-1163.

Bienz K., Egger D., Pfister T., and Troxler M. (1992) Structural and functional characterization of the poliovirus replication complex. *Arch Virol*, 136: 147-157.

Bienz K., Egger D., and Pfister T. (1994) Characteristics of the poliovirus replication complex. *Arch Virol*, 136 (suppl. 9): 147-157.

Blyn L.B., Towner J.S., Semler B.L., and Ehrenfeld E. (1997) Requirement of poly(rC) binding protein 2 for translation of poliovirus RNA. *J Virol*, 71: 6243-6246.

Bolten R., Egger D., Gosert R., Schaub G., Landmann L., and Bienz, K. (1998) Intracellular localization of poliovirus plus- and minus-strand RNA visualized by strand-specific fluorescent in situ hybridization. *J Virol*, 72: 8578-8585.

Brockway S.M., Clay C.T., Lu X.T., and Denison M.R. (2003) Characterization of the expression, intracellular localization, and replication complex association of the putative mouse hepatitis virus RNA-dependent RNA polymerase. *J Virol*, 77: 10515-10527.

Burgess J.W., and Yamada E.W. (1987) cAMP-dependent protein kinase isozymes with preference for histone H2B as substrate in mitochondria of bovine heart. *Biochem Cell Biol*, 65: 137-143.

Caliguiri L.A., and Tamm I. (1969) Membranous structures associated with translation and transcription of poliovirus RNA. *Science*, 166: 885-886.

Caliguiri L.A., and Tamm I. (1970a) The role of cytoplasmic membranes in poliovirus biosynthesis. *Virology*, 42: 100-111.

Caliguiri L.A., and Tamm I. (1970b) Characterization of poliovirus-specific structures associated with cytoplasmic membranes. *Virology*, 42: 112-122.

Caliguiri L.A., and Compans R.W. (1973) The formation of poliovirus particles in association with the RNA replication complexes. *J Gen Virol*, 21: 99-108.

Campanella M., de Jong A.S., Lanke K.W.H., Melchers W.J.G., Willems P.H.G.M., Pinton P., Rizzuto R., and van Kuppeveld F.J.M. (2004) The coxsackievirus 2B protein suppresses apoptosis host cell response by manipulating intracellular Ca^{2+} homeostasis. *J Biol Chem*, 279: 18440-18450.

Campbell E.M., Nunez R., and Hope T.J. (2004) Disruption of the actin cytoskeleton can complement the ability of Nef to enhance human immunodeficiency virus type 1 infectivity. *J Virol*, 78: 5745-5755.

Caplow M., and Shanks J. (1996) Evidence that a single monolayer tubulin-GFP cap is both necessary and sufficient to stabilize microtubules. *Mol Biol Cell*, 7: 663-675.

Carrasco L., Guinea R., Irurzun A., and Barco A. (2002) Effects of viral replication on cellular membrane metabolism and function. In *Molecular Biology of Picornaviruses* edited by Semler B.L. and Wimmer E. ASM Press, Washington D.C., USA: 337-354.

Chard L.S., Bordeleau M., Pelletier J., Tanaka J., and Belsham G.J. (2006) Hepatitis C virus-related internal ribosome entry sites are found in multiple genera of the family *Picornaviridae*. *J Gen Virol*, 87: 927-936.

Chardin P., Paris S., Antonny B., Robineau S. Béraud-Dufour S., Jackson C.L., and Chabre M. (1996) A human exchange factor for Arf contains Sec7- and pleckstrin-homology domains. *Nature*, 384: 481-484.

Chen M.S., Huber A.B., van der Haar M.E., Frank M., Schnell L., Spillmann A.A., Christ F., and Schwab M.E. (2000) Nogo-A is a myelin-associated neurite outgrowth inhibitor and an antigen for monoclonal antibody IN-1. *Nature*, 403: 434-439.

Cho M.W., Teterina N., Egger D., Bienz K., and Ehrenfeld E. (1994) Membrane rearrangement and vesicle induction by recombinant poliovirus 2C and 2BC in human cells. *Virology*, 202: 129-145.

Clague M.J. (1998) Molecular aspects of the endocytic pathway. *Biochem J*, 336: 271-282.

Clark A.T., Robertson M.E.M., Conn G.L., and Belsham G.J. (2003) Conserved nucleotides within the J domain of the encephalomyocarditis virus internal ribosome entry site are required for activity and for interaction with eIF4G. *J Virol*, 77: 12441-12449.

Clarke I.N., and Lambden P.R. (2000) Organization and expression of calicivirus genes. *J Infect Dis*, 181: S309-316.

Cohen L., Bénichou D., and Martin A. (2002) Analysis of deletion mutants indicates that the 2A polypeptide of hepatitis A virus participates in virion morphogenesis. *J Virol*, 76: 7495-7505.

Colanzi A., and Corda D. (2007) Mitosis controls the Golgi and the Golgi controls mitosis. *Curr Opin Cell Biol*, 19: 386-393.

Colledge M., and Scott J.D. (1999) AKAPs: from structure to function. *Trends Cell Biol*, 9: 216-221.

Crick F.H., and Watson J.D. (1956) Structure of small viruses. *Nature*, 177: 473-475.

Cuconati A., Xiang W., Lahser F., Pfister T., and Wimmer E. (1998) A protein linkage map of the P2 nonstructural proteins of poliovirus. *J Virol*, 72: 1297-1307.

Cudmore S., Reckmann I., and Way M. (1997) Viral manipulations of the actin cytoskeleton. *Trends Microbiol*, 5: 142-148.

Daecke J., Fackler O.T., Dittmar M.T., and Kräusslich H.G. (2005) Involvement of clathrin-mediated endocytosis in human immunodeficiency virus type 1 entry. *J Virol*, 79: 1581-1594.

Dales S., Eggers H.J., Tamm I., and Palade G.E. (1965) Electron microscopic study of the formation of poliovirus. *Virology*, 26: 379-389.

Damke H., Baba T., van der Bliek A.M., and Schmid S.L. (1995) Clathrin-independent pinocytosis is induced in cells overexpressing a temperature-sensitive mutant of dynamin. *J Cell Biol*, 131: 69-80.

Deitz S.B., Dodd D.A., Cooper S., Parham P., and Kirkegaard K. (2000) MHC I-dependent antigen presentation is inhibited by poliovirus protein 3A. *Proc Natl Acad Sci USA*, 97: 13790-13795.

Delhaye S., van Pesch V., and Michiels T. (2004) The leader protein of Theiler's virus interferes with nucleocytoplasmic trafficking of cellular proteins *J Virol*, 78: 4357-4362.

Dell'Acqua M.L., and Scott J.D. (1997) Protein kinase anchoring. *J Biol Chem*, 272: 12881-12884.

Desai A.B., and Mitchison T.J. (1997) Microtubule dynamics. *Annu Rev Cell Dev Biol*, 13: 83-117.

DeTulleo L., and Kirchhausen T. (1998) The clathrin endocytic pathway in viral infection. *EMBO J*, 17: 4585-4593.

Diefenbach R.J., Miranda-Saksena M., Diefenbach E., Holland D.J., Boadle R.A., Armati P.J., and Cunningham A.L. (2002) Herpes simplex virus tegument protein US11 interacts with conventional kinesin heavy chain. *J Virol*, 76: 3282-3291.

Dimino M.J., Bieszczad R.R., and Rowe M.J. (1981) Cyclic AMP-dependent protein kinase in mitochondria and cytosol from different-sized follicles and corpora lutea of porcine ovaries. *J Biol Chem*, 256: 10876-10882.

Dodd D.A., Giddings T.H., Jr., and Kirkegaard K. (2001) Poliovirus 3A protein limits interleukin-6 (IL-6), IL-8, and beta interferon secretion during viral infection. *J Virol*, 75: 8158-8165.

Doedens J.R., Maynell L.A., Klymkowsky M.W., and Kirkegaard K. (1994) Secretory pathway function, but not cytoskeletal integrity, is required in poliovirus infection. *Arch Virol Suppl*, 9: 159-172.

Doedens J.R., and Kirkegaard K. (1995) Inhibition of cellular protein secretion by poliovirus proteins 2B and 3A. *EMBO J*, 14: 894-907.

Döhner K., Nagel C., and Sodeik B. (2005) Viral stop-and-go along microtubules: taking a ride with dynein and kinesins. *Trends Microbiol*, 13: 320-327.

Donaldson J.G. (2000) Filling in the GAPs in the ADP-ribosylation factor story. *Proc Natl Acad Sci USA*, 97: 3792-3794.

Donnelly M.L.L., Hughes L.E., Luke G., Li X., Mendoza H., ten Dam E., Gani D., and Ryan M.D. (2001) The 'cleavage' activities of FMDV 2A site-directed mutants and naturally-occurring '2A-Like' sequences. *J Gen Virol*, 82: 1027-1041.

Dubuisson J., Penin F., and Moradpour D. (2002) Interaction of hepatitis C virus proteins with host cell membranes and lipids. *Trends Cell Biol*, 12: 517-523.

Dvorak C.M.T., Hall D.J., Hill M., Riddle M., Pranter A., Dillman J., Deibel M., and Palmenberg A.C. (2001) Leader protein of encephalomyocarditis virus binds zinc, is phosphorylated during viral infection, and affects the efficiency of genome translation. *Virology*, 290: 261-271.

Echeverri A., and Dasgupta A. (1995) Amino terminal regions of poliovirus 2C protein mediate membrane binding. *Virology*, 208: 540-553.

Egger D., Pasamontes L., Bolten R., Boyko V., and Biens K. (1996) Reversible dissociation of the poliovirus replication complex: functions and interactions of its components in viral RNA synthesis. *J Virol*, 70: 8675-8683.

Egger D., Teterina N., Ehrenfeld E., and Bienz K. (2000) Formation of the poliovirus replication complex requires coupled viral translation, vesicle production, and viral RNA synthesis. *J Virol*, 74: 6570-6580.

Egger D., Wölk B., Gosert R., Bianchi L., Blum H.E., Moradpour D., and Bienz K. (2002) Expression of hepatitis C virus proteins induces distinct membrane alterations including a candidate viral replication complex. *J Virol*, 76: 5974-5984.

Egger D., and Bienz K. (2005) Intracellular location and translocation of silent and active poliovirus replication complexes. *J Gen Virol*, 86: 707-718.

Eker P., Holm P.K., van Deurs B., and Sandvig K. (1994) Selective regulation of apical endocytosis in polarized Madin-Darby canine kidney cells by mastoparan and cAMP. *J Biol Chem*, 269: 18607-18615.

Elena S.F., and Sanjuán R. (2005) Adaptive value of high mutation rates of RNA viruses: separating causes from consequences. *J Virol*, 79: 11555-11558.

Emini E.A., Schleif W.A., Colonno R.J., and Wimmer E. (1985) Antigenic conservation and divergence between the viral-specific proteins of poliovirus type 1 and various picornaviruses. *Virology*, 140: 13-20.

Ettayebi K., and Hardy M. E. (2003) Norwalk virus nonstructural protein p48 forms a complex with the SNARE regulator VAP-A and prevents cell surface expression of vesicular stomatitis virus G protein. *J Virol*, 77: 11790-11797.

Fauquet C.M., and Fargette D. (2005) International Committee on Taxonomy of Viruses and the 3142 unassigned species. *Virol J*, 2: 64-74.

Fauquet C.M., Mayo M.A., Maniloff J., Desselberger U., and Ball L.A. (2005) Virus Taxonomy: Eight report of the International Committee on Taxonomy of Viruses. Elsevier Academic Press, Burlington, USA.

Fernandez-Vega V., Sosnovtsev S.V., Belliot G., King A.D., Mitra T., Gorbalenya A., and Green K.Y. (2004) Norwalk virus N-terminal nonstructural protein is associated with disassembly of the Golgi complex in transfected cells. *J Virol*, 78: 4827-4837.

Foster L.J., Yeung B., Mohtashami M., Ross K., Trimble W.S., and Klip A. (1998) Binary interactions of the SNARE proteins syntaxin-4, SNAP23, and VAMP-2 and their regulation by phosphorylation. *Biochemistry*, 37: 11089-11096.

Franssen H., Leunissen J., Goldbach R., Lomonossoff G., and Zimmern D. (1984) Homologues sequences in non-structural proteins from cowpea mosaic virus and picornaviruses. *EMBO J*, 3: 855-861.

Franzusoff A., and Schekman R. (1989) Functional compartments of the yeast Golgi apparatus are defined by the Sec7 mutation. *EMBO J*, 8: 2695-2702.

Frolova E., Gorchakov R., Garmashova N., Atasheva S., Vergara L.A., and Frolov I. (2006) Formation of the nsP3-specific protein complexes during Sindbis virus replication. *J Virol*, 80: 4122-4134.

Froshauer S., Kartenbeck J., and Helenius A. (1988) Alphavirus RNA replicase is located on the cytoplasmic surface of endosomes and lysosomes. *J Cell Biol*, 107: 2075-2086.

Gamarnik A.V., and Andino R. (2000) Interactions of viral protein 3CD and poly(rC) binding protein with the 5' untranslated region of the poliovirus genome. *J Virol*, 74: 2219-2226.

Gao X., and Huang L. (1995) Cationic liposome-mediated gene transfer. *Gene Ther*, 2: 710-722.

Garciá-Briones M., Rosas M.F., González-Magaldi M., Martín-Acebes M.A., Sobrino F., and Armas-Portela R. (2006) Differential distribution of non-structural proteins of foot-and-mouth disease virus in BHK-21 cells. *Virology*, 349: 409-421.

Gerber K., Wimmer E., and Paul A.V. (2001) Biochemical and genetic studies of the initiation of human rhinovirus 2 RNA replication: identification of a *cis*-replicating element in the coding sequence of $2A^{pro}$. *J Virol*, 75: 10979-10990.

Ghadge G.D., Ma L., Sato S., Kim J., and Roos R.P. (1998) A protein critical for Theiler's virus-inducedimmune system-mediated demyelinating disease has a cell type-specific antiapoptotic effect and a key role in virus persistence. *J Virol*, 72: 8605-8612.

Gingras A. C., Svitkin Y., Belsham G.J., Pause A., and Sonenberg N. (1996) Activation of the translational suppressor 4E-BP1 following infection with encephalomyocarditis virus and poliovirus. *Proc Natl Acad Sci USA*, 93: 5578-5583.

Girard M., Baltimore D., and Darnell J.E. (1967) The poliovirus replication complex: sites for synthesis of poliovirus RNA. *J Mol Biol*, 24: 59-74.

Giraudo A.T., Beck E., Strebel K., de Mello P.A., La Torre J.L., Scodeller E.A., and Bergmann I.E. (1990) Identification of a nucleotide deletion in parts of polypeptide 3A in two independent attenuated aphthovirus strains. *Virology*, 177: 780-783.

Goodson H.V., Valetti C., and Kreis T.E. (1997) Motors and membrane traffic. *Curr Opin Cell Biol*, 9: 18-28.

Gorbalenya A.E., Blinov V.M., Donchenko A.P., Koonin E.V. (1989) An NTP-binding motif is the most conserved sequence in a highly diverged monopholetic group of proteins involved in positive strand RNA viral replication. *J Mol Evol*, 28: 256-268.

Gorbalenya A.E., and Koonin E.V. (1989) Viral proteins containing the purine NTP-binding sequence pattern. *Nucleic Acids Res*, 17: 84113-8440.

Gorbalenya A.E., Koonin E.V., and Wolf Y.I. (1990) A new superfamily of putative NTP-binding domains encoded by genomes of small DNA and RNA viruses. *FEBS Lett*, 262: 145-148.

Gosert R., Cassinotti P., Siegl G., and Weitz M. (1996) Identification of hepatitis A virus non-structural protein 2B an dits release by the major virus proteinase 3C. *J Gen Virol*, 77: 247-255.

Gouin E., Welch M.D., and Cossart P. (2005) Actin-based motility of intracellular pathogens. *Curr Opin Microbiol*, 8: 35-45.

Gradi A., Svitkin Y.V., Imataka H., and Sonenberg N. (1998) Proteolysis of human eukaryotic translation initiation factor eIF4GII, but not eIF4GI, coincides with the shutoff of host protein synthesis after poliovirus infection. *Proc Natl Acad Sci USA*, 95: 11089-11094.

GrandPré T., Nakamura T., Vartanian T., and Strittmatter S.M. (2000) Identification of the Nogo inhibitor of axon regeneration as a reticulon protein. *Nature*, 403: 439-444.

Greber U.F., and Way M. (2006) A superhighway to virus infection. *Cell*, 124: 741-754.

Green K.Y., Ando T., Balayan M.S., Berke T., Clarke I.N., Estes M.K., Matson D.O., Nakata S., Neill J.D., Studdert M.J., and Thiel H.J. (2000) Taxonomy of the caliciviruses. *J Infect Dis*, 181: S322-330.

Green K.Y., Mary A., Fogg M.H., Weisberg A., Belliot G., Wagner M., Mitra T., Ehrenfeld E., Cameron C.E., and Sosnovtsev S.V. (2002) Isolation of enzymatically active replication complexes from feline calicivirus-infected cells. *J Virol*, 76: 8582-8595.

Grigera P.R., Tisminetzky S.G., Lebendiker M.B., Periolo O.H., and La Torre J.L. (1988) Presence of a 43-kDa host-cell polypeptide in purified aphthovirions. *Virology*, 165: 584-588.

Grimley P.M., Berezesky I.K., and Friedman R.M. (1968) Cytoplasmic structures associated with an arbovirus infection: loci of viral ribonucleic acid synthesis. *J Virol*, 2: 1326-1338.

Grobler D.G., Raath J.P., Braack L.E., Keet D.F., Gerdes G.H., Barnard B.J., Kriek N.P., Jardine J., and Swanepoel R. (1995) An outbreak of encephalomyocarditis-virus infection in free-ranging African elephants in the Kruger National Park. *Onderstepoort J Vet Res*, 62: 97-108.

Gruenberg J. (2001) The endocytic pathway: a mosaic of domains. *Nat Rev Mol Cell Biol*, 2: 721-730.

Grünewald K., Desai P., Winkelr D.C., Heymann J.B., Belnap D.M., Baumeister W., and Steven A.C. (2003) Three-dimensional structure of herpes simplex virus from cryo-electron tomography. *Science*, 302: 1396-1398.

Guinea R., and Carrasco L. (1990) Phospholipid biosynthesis and poliovirus genome replication, two coupled phenomena. *EMBO J*, 9: 2011-2016.

Hansen S.H., Sandvig K., and van Deurs B. (1993) Molecules internalizes by clathrin-independent endocytosis are delivered to endosomes containing transferrin receptors. *J Cell Biol*, 123: 89-97.

Hansen S.H., and Casanova J.E. (1994) Gsα stimulates transcytosis and apical secretion in MDCK cells through camp and protein kinase A. *J Cell Biol*, 126: 677-687.

Harris K.S., Xiang W., Alexander L., Lane W.S., Paul A.V., and Wimmer E. (1994) Interaction of poliovirus polypeptide $3CD^{pro}$ with the 5' and 3' termini of the poliovirus genome. *J Biol Chem*, 269: 27004-27014.

Harrison S.C., Skehel J.J., and Wiley D.C. (1996) Virus structure. In *Fields Virology*, *Third edition* edited by Fields B.N., Knipe D.M., Howley P.M., Chanock R.M., Monath T.P., Melnick J.L., Roizman B., and Straus S.E. Lippincott-Raven Publishers, Philadelphia, USA: 59-100.

Hartman J.J., Mahr J., McNally K., Okawa K., Iwamatsu A., Thomas S., Cheesman S., Heuser J., Vale R.D., and McNally F.J. (1998) Katanin, a microtubule-severing protein, is a novel AAA ATPase that targets to the centrosome using a WD40-containing subunit. *Cell*, 93: 277-287.

Hartman J.J., and Vale R.D. (1999) Microtubule disassembly by ATP-dependent oligomerization of the AAA enzyme katanin. *Science*, 286: 782-785.

Hellen C.U.T., and Wimmer E. (1995) Enterovirus structure and assembly. *In Human enterovirus infection*s edited by Rotbart H.A. ASM Press, Washington D.C., USA: p. 155-174.

Hertzler S., Kalli P., and Lipton H.L. (2001) UDP-galactose transporter is required for Theiler's virus entry into mammalian cells. *Virology*, 286: 336-344.

Higley S., and Way M. (1997) Caracterization of the vaccinia virus F8L protein. *J Gen Virol*, 78: 2633-2637.

Holland J., Spindler K., Horodyski F., Grabau E., Nichol S., and VandePol S. (1982) Rapid evolution of RNA genomes. *Science*, 215: 1577-1585.

Hu W.H., Hausmann O.N., Yan M.S., Walters W.M., Wong P.K., and Bethea J.R. (2002) Identification and characterization of a novel Nogo-interacting mitochondrial protein (NIMP). *J Neurochem*, 81: 36-45.

Huang L.J., Durick K., Weiner J.A., Chun J., and Taylor S.S. (1997) D-AKAP2, a novel protein kinase A anchoring protein with a putative RGS domain. *Proc Natl Acad Sci USA*, 94: 11184-11189.

Huang L.J., Wang L., Durick K., Perkins G., Deerinck T.J., Ellisman M.H., and Taylor S.S. (1999) NH2-terminal targetting motifs direct dual specificity A-kinase-anchoring protein I (D-AKAPI) to either mitochondria or endoplasmic reticulum. *J Cell Biol*, 145: 951-959.

Huber S.A. (1994) VCAM-1 is a receptor for encephalomyocarditis virus on murine vascular endothelial cells. *J Virol*, 68: 3453-3458.

Hughes P.J., and Stanway G. (2000) The 2A proteins of three diverse picornaviruses are related to each other and to the H-rev107 family of proteins involved in the control of cell proliferation. *J Gen Virol*, 81: 201-207.

Hügle T., Fehrmann F., Bieck E., Kohara M., Kräusslich H., Rice G.M., Blum H.E., and Moradpour D. (2001) The hepatitis C virus nonstructural protein 4B is an integral endoplasmic reticulum membrane protein. *Virology*, 284: 70-81.

Hunt S.L., Hsuan J.J., Totty N., and Jackson R.J. (1999) unr, a cellular cytoplasmic RNA-binding protein with five cold-shock domains, is required for internal initiation of translation of human rhinovirus RNA. *Genes Dev*, 13: 437-448.

Irurzun A., Perez L., and Carrasco L. (1992) Involvement of membrane traffic in the replication of poliovirus genomes: effects of brefeldin A. *Virology*, 191: 166-175.

Ivanovsky D. (1892) Concerning the mosaic disease of the tobacco plant. *St Petsb Acad Imp Sci Bul*, 35: 67-70.

Iwahashi J., Kawasaki I., Kohara Y., Gengyo-Ando K., Mitani S., Ohshima Y., Hamada N., Hara K., Kashiwagi T., and Toyoda T. (2002) *Caenorhabditis elegans* reticulon interacts with RME-1 during embryogenesis. *Biochem Biophys Res Commun*, 293: 698-704.

Jackson C.L., and Casanova J.E. (2000) Turning on ARF: the Sec7 family of guanine-nucleotide-exchange factors. *Trends Cell Biol*, 10: 60-67.

Jnaoui K., and Michiels T. (1998) Adaptation of Theiler's virus to L929 cells: mutations in the putative receptor binding site on the capsid map to neutralization sites and modulate viral persistence. *Virology*, 244: 397-404.

Jnaoui K., and Michiels T. (1999) Analysis of cellular mutants resistant to Theiler's virus infection: differential infection of L929 cells by persistent and neurovirulent strains. *J Virol*, 73: 7248-7254.

Joachims M., and Etchison D. (1992) Poliovirus infection results in structural alteration of a microtubule-associated protein. *J Virol*, 66: 5797-5804.

Johannsen E., Luftig M., Chase M.R., Weicksel S., Cahir-McFarland E., Illanes D., Sarracino D., and Kieff E. (2004) Proteins of purified Epstein-Barr virus. *Proc Natl Acad Sci USA*, 101: 16286-16291.

Johnson K.N., and Christian P.D. (1998) The novel genome organization of the insect picorna-like virus *Drosophila* C virus suggests this virus belongs to a previously undescribed virus family. *J Gen Virol*, 79: 191-203.

Jones M.S., Lukashov V.V., Ganac R.D., and Schnurr D.P. (2007) Discovery of a novel human picornavirus from a pediatric patient presenting with fever of unknown origin. *J Clin Microbiol*, 45: 2144-2150.

Kaiser W.J., Chaudhry Y., Sosnovtsev S.V., and Goodfellow I.G. (2006) Analysis of protein-protein interactions in the feline calicivirus replication complex. *J Gen Virol*, 87: 363-368.

Karp G. (2005) Cytoplasmic membrane systems: structure, function, and membrane trafficking. In *Cell and molecular biology. Concepts and experiments, Fourth edition* published by John Wiley & Sons Inc., USA: 279-333.

Keryer G., Skalhegg B.S., Landmark B.F., Hansson V., Jahnsen T., and Tasken K. (1999) Differential localization of protein kinase A type II isozymes in the Golgi-centrosomal area. *Exp Cell Res*, 249: 131-146.

Kilpatrick D.R., and Lipton H.L. (1991) Predominant binding of Theiler's viruses to a 34-kilodalton receptor protein on susceptible cell lines. *J Virol*, 65: 5244-5249.

Kim S.J., Choi W.S., Han J.S., Warnock G., Fedida D., and McIntosh C.H. (2005) A novel mechanism for the suppression of a voltage-gated potassium channel by glucose-dependent insulinotropic polypeptide (GIP): Protein kinase A-dependent endocytosis. *J Biol Chem*, 280: 28692-28700.

King A.M.Q., Brown F., Christian P., Hovi T., Hyypiä T., Knowles N.J., Lemon S.M., Minor P.D., Palmenberg A.C., Skern T. and Stanway G. (2000) Picornaviridae. In *Virus Taxonomy. Seventh report of the International Committee on Taxonomy of Viruses* edited by van Regenmortel M.H.V., Fauquet C.M., Bishop D.H.L., Carstens E.B., Estes M.K., Lemon S.M., Maniloff J., Mayo M.A., McGeoch D.J., Pringle C.R., Wickner R.B. Academic Press, San Diego, USA: p. 657-678.

Klein M., Egger H.J., and Nelsen-Saltz B. (1999) Echovirus 9 strain Barty non-structural protein 2C has NTPase activity. *Virus Res*, 65: 155-160.

Kleitke B., Sydow H., and Wollenberger A. (1976) Evidence for cyclic AMP-dependent protein kinase activity in isolated guinea pig and rat liver mitochondria. *Acta Biol Med Ger*, 35: 9-17.

Klumperman J. (2000) Transport between ER and Golgi. *Curr Opin Cell Biol*, 12: 445-449.

Knowles N.J., Dickinson N.D., Wilsden G., Carra E., Brocchi E., and De Simone F. (1998) Molecular analysis of encephalomyocarditis viruses isolated from pigs and rodents in Italy. *Virus Res*, 57: 53-62.

Knowles N.J., Davies P.R., Henry T., O'Donnell V., Pacheco J.M., and Mason P.W. (2001) Emergence in Asia of foot-and-mouth disease viruses with altered host range: characterization of alterations in the 3A protein. *J Virol*, 75: 1551-1556.

Knox C., Moffat K., Ali S., Ryan M., and Wileman T. (2005) Foot-and-mouth disease virus replication sites form next to the nucleus and close to the Golgi apparatus, but exclude marker proteins associated with host membrane compartments. *J Gen Virol*, 86: 687-696.

Knox C., Miskin J., Rao T.V.S., Wileman T., and Ryan M.D. Picornavirus 2C proteins bind the dual-specificity protein kinase A-anchoring protein D-AKAP2 (AKAP10). *Submitted*.

Kolupaeva V.G., Pestova T.V., Hellen C.U.T., and Shatsky I.N. (1998) Translation eukaryotic initiation factor 4G recognizes a specific structural element within the internal ribosome entry site of encephalomyocarditis virus RNA. *J Biol Chem*, 273: 18599-18604.

Kolupaeva V.G., Lomakin I.B., Pestova T.V., and Hellen C.U.T. (2003) Eukaryotic initiation factors 4G and 4A mediate conformational changes downstream of the initiation codon of the encephalomyocarditis virus internal ribosomal entry site. *Mol Cell Biol*, 23: 687-698.

Komachi K., Redd M.J., and Johnson A.D. (1994) The WD repeats of Tup1 interact with the homeo domain protein alpha 2. *Genes Dev*, 8: 2857-2867.

Komano J., Miyauchi K., Matsuda Z., and Yamamoto N. (2004) Inhibiting the Arp2/3 complex limits infection of both intracellular mature vaccinia virus and primate lentiviruses. *Mol Biol Cell*, 15: 5197-5207.

Kong W.P., and Roos R.P. (1991) Alternative translation initiation site in the DA strain of Theiler's murine encephalomyelitis virus. *J Virol*, 65: 3395-3399.

Koonin E.V., and Dolja V.V. (1993) Evolution and taxonomy of positive-strand RNA viruses: implications of comparative analysis of amino acid sequences. *Crit Rev Biochem Mol Biol*, 28: 375-430. Erratum in: *Crit Rev Biochem Mol Biol*, 28: 546.

Kotsakis A., Pomeranz L.E., Blouin A., and Blaho J.A. (2001) Microtubule reorganization during herpes simplex virus type 1 infection facilitates the nuclear localization of VP22, a major virion tegument protein. *J Virol*, 75: 8697-8711.

Kroemer G. (1999) Mitochondrial control of apoptosis: an overview. *Biochem Soc Symp*, 66: 1-15.

Krogerus C., Egger D., Samuilova O., Hyypiä T., and Bienz K. (2003) Replication complex of human parechovirus 1. *J Virol*, 77: 8512-8523.

Kujala P., Ahola T., Ehsani N., Auvinen P., Vihinen H., and Kääriäinen L. (1999) Intracellular distribution of rubella virus nonstructural protein P150. *J Virol*, 73: 7805-7811.

Kujala P., Ikäheimonen A., Ehsani N., Vihinen H., Auvinen P., and Kääriäinen L. (2001) Biogenisis of the Semliki Forest virus RNA replication complex. *J Virol*, 75: 3873-3884.

Kulinskii V.I., Saatov T.S., Turakulov IaKh, Khalikov S.K., and Zobova N.V. (1981) Study of mitochondrial permeability for labeled cAMP. *Biull Eksp Biol Med*, 91: 427-429.

Kulinskii V.I., and Zobova N.V. (1985) Submitochondrial distribution of cAMP during incubation with rat liver mitochondria. *Biokhimiia*, 50: 1546-1552.

Kusov Y.Y., Probst C., Jecht M., Jost P.D., and Gauss-Muller V. (1998) Membrane association and RNA binding of recombinant hepatitis A virus protein 2C. *Arch Virol*, 143: 931-944.

Laakkonen P., Ahola T., and Kääriäinen L. (1996) The effects of palmytoylation on membrane association of Semliki Forest virus RNA capping enzyme. *J Biol Chem*, 271: 28567-28571.

Lain S., Martin M.T., Riechmann J.L., and Garcia J.A. (1991) Novel catalytic activity associated with positive-strand RNA virus infection: nucleic acid-stimulated ATPase activity of the plum pox potyvirus helicase like protein. *J Virol*, 65: 1-6.

Lama J., and Carrasco L. (1992) Expression of poliovirus nonstructural proteins in Escherichia coli cells. Modification of membrane permeability induced by 2B and 3A. *J Bio. Chem*, 267: 15932-15937.

Lama J., Guinea R., Martinez-Abarca F., and Carrasco L. (1992) Cloning and inducible synthesis of poliovirus non-structural proteins. *Gene*, 117: 185-192.

Lama J., Paul A.V., Harris K.S., and Wimmer E. (1994) Properties of purified recombinant poliovirus protein 3AB as substrate for viral proteinases and as co-factor for RNA polymerase 3Dpol. *J Biol Chem*, 269: 66-70.

Lama J., Sanz M.A., and Carrasco L. (1998) Genetic analysis of poliovirus protein 3A: characterization of a non-cytopathic mutant virus defective in killing Vero cells. *J Gen Virol*, 79: 1911-1921.

Langford G.M. (1995) Actin- and microtubule-dependent organelle motors: inter-relationships between the two motility systems. *Curr Opin Cell Biol*, 7: 82-88.

Lee J.Y., Marshall J.A., and Bowden D.S. (1992) Replication complexes associated with the morphogenesis of rubella virus. *Arch Virol*, 122: 95-106.

Lee J.Y., Marshall J.A., and Bowden D.S. (1994) Characterization of rubella virus replication complexes using antibodies to double-stranded RNA. *Virology*, 200: 307-312.

Lee T.H., and Linstedt A.D. (2000) Potential role for protein kinases in regulation of bi-directional endoplasmic reticulum-to-Golgi transport revealed by protein kinase inhibitor H89. *Mol Biol Cell*, 11: 2577-2590.

Lenk R., and Penman S. (1979) The cytoskeletal framework and poliovirus metabolism. *Cell*, 16: 289-301.

Leong L.E.C., Cornell C.T., and Semler B.L. (2002) Processing determinants and functions of cleavage products of picornavirus polyproteins. In *Molecular Biology of Picornaviruses* edited by Semler B.L. and Wimmer E. ASM Press, Washington D.C., USA: 187-197.

Levine A.J. (1996) The origins of virology. In *Fields Virology*, *Third edition* edited by Fields B.N., Knipe D.M., Howley P.M., Chanock R.M., Monath T.P., Melnick J.L., Roizman B., and Straus S.E. Lippincott-Raven Publishers, Philadelphia, USA: 1-14.

Li J., and Baltimore D. (1990) An intergenic revertant of a poliovirus 2C mutant has an uncoating defect. *J Virol*, 64:1102-1107.

Lipton H.L. (1975) Theiler's virus infection in mice: an unusual biphasic disease process leading to demyelination. *Infect Immun*, 11: 1147-1155.

Lipton H.L. (1978) Characterization of the TO strains of Theiler's mouse encephalomyelitis viruses. *Infect Immun*, 20: 869-872.

Lipton H.L., Friedmann A., Sethi P., and Crowther J.R. (1983) Characterization of Vilyuisk as a picornavirus. *J Med Virol*, 12: 195-203.

Lobert P.E., Escriou N., Ruelle J., and Michiels T. (1999) A coding RNA sequence acts as a replication signal in cardioviruses. *Proc Natl Acad Sci USA*, 96: 11560-11565.

Lodish H., Berk A., Kaiser C.A., Krieger M., Scott M.P., Bretscher A., Ploegh H., and Matsudaira P. (2007) Vesicular traffic, secretion, and endocytosis. In *Molecular Cell Biology, Sixth edition* published by W.H. Freeman and Company, USA: 579-622.

Love D.N., and Sabine M. (1975) Electron microscopic observation of feline kidney cells infected with a feline calicivirus. *Arch Virol*, 48: 213-228.

Lowe M., Nakamura N., and Warren G. (1998) Golgi division and membrane traffick. *Trends Cell Biol*, 8: 40-44.

Luo M., He C., Toth K.S., Zhang C.X., and Lipton H.L. (1992) Three-dimensional structure of Theiler murine encephalomyelitis virus (BeAn strain). *Proc Natl Acad Sci USA*, 89: 2409-2413.

Lustig A., and Levine A.J. (1992) One hundred years of viriology. *J Virol*, 66: 4629-4631.

Mackenzie J.M., Jones M.K., and Westaway E.G. (1999) Markers for trans-Golgi membranes and the intermediate compartment localize to induced membranes with distinct replication functions in flavivirus-infected cells. *J Virol*, 73: 9555-9567.

Magliano D., Marshall J.A., Bowden D.S., Vardaxis N., Meanger J., and Lee J.Y. (1998) Rubella virus replication complexes are virus-modified lysosomes. *Virology*, 240: 57-63.

Marash M., and Gerst J.E. (2001) t-SNARE dephosphorylation promotes SNARE assembly and exocytosis in yeast. *EMBO J*, 20: 411-421.

Martin M.E., Hidalgo J., Rosa J.L., Crottet P., and Velasco A. (2000) Effect of protein kinase A activity on the association of ADP-ribosylation factor 1 to Golgi membranes. *J Biol Chem*, 275: 19050-19059.

Martínez-Menárguez J.A., Prekeris R., Oorschot V.M.J., Scheller R., Slot J.W., Gueze H.J., and Klumperman J. (2001) Peri-Golgi vesicles contain retrograde but not anterograde proteins consistent with the cisternal progression model of intra-Golgi transport. *J Cell Biol*, 155: 1213-1224.

Mason P.W., Bezborodova S.V., and Henry T.M. (2002) Identification and characterization of a *cis*-acting replication element (*cre*) adjacent to the internal ribosome entry site of Foot-and-Mouth Disease virus. *J Virol*, 76: 9686-9694.

Maynell L.A., Kirkegaard K., and Klymkowsky M.W. (1992) Inhibition of poliovirus RNA synthesis by brefeldin A. *J Virol*, 66: 1985-1994.

McNally F.J., and Vale R.D. (1993) Identification of katanin, an ATPase that severs and disassembles stable microtubules. *Cell*, 75: 419-429.

McNally F.J., Okawa K., Iwamatsu A., and Vale R.D. (1996) Katanin, the microtubule-severing ATPase, is concentrated at centrosomes. *J Cell Sci*, 109: 561-567.

Mironov A.A., Beznoussenko G.V., Nicoziani P., Martella O., Trucco A., Kweon H., Di Giandomenico D., Polishchuk R.S., Fusella A., Lupetti P., Berger E.G., Geerts W.J.C., Koster A.J., Burger K.N.J., and Luini A. (2001) Small cargo proteins and large aggregates can traverse the Golgi by a common mechanism without leaving the lumen of cisternae. *J Cell Biol*, 155: 1225-1238.

Mirzayan C., and Wimmer E. (1992) Genetic analysis of an NTP-binding motif in poliovirus polypeptide 2C. *Virology*, 189: 547-555.

Mirzayan C., and Wimmer E. (1994) Biochemical studies on poliovirus polypeptide 2C: evidence for ATPase activity. *Virology*, 199: 176-187.

Mitchison T., and Kirschner M. (1984) Dynamic instability of microtubule growth. *Nature*, 312: 237-242.

Moffat K., Howell G., Knox C., Belsham G.J., Monaghan P., Ryan M.D., and Wileman T. (2005) Effects of foot-and-mouth disease virus nonstructural proteins on the structure and function of the early secretory pathway: 2BC but not 3A blocks endoplasmatic reticulum-to-Golgi transport. *J Virol*, 79: 4382-4395.

Momose F., Kikuchi Y., Komase K., and Morikawa Y. (2007) Visualization of microtubule-mediated transport of influenza viral progeny ribonucleoprotein. *Microbes Infect*, 9: 1422-1433.

Moss J., and Vaughan M. (1998) Molecules and the Arf orbit. *J Biol Chem*, 273: 21431-21434.

Müller G., and Bandlow W. (1987) cAMP-dependent protein kinase activity in yeast mitochondria. *Z Naturforsch*, 42: 1291-1302.

Muniz M., Alonso M., Hidalgo J., and Velasco A. (1996) A regulatory role for cAMP-dependent protein kinase in protein traffic along the exocytic route. *J Biol Chem*, 271:30935-30941.

Muniz M., Martin M.E., Hidalgo J., and Velasco A. (1997) Protein kinase A activity is required for the budding of constitutive transport vesicles from the *trans*-Golgi network. *Proc Natl Acad Sci USA*, 94: 14461-14466.

Murphy F.A. (1996) Virus taxonomy. In *Fields Virology*, *Third edition* edited Fields B.N., Knipe D.M., Howley P.M., Chanock R.M., Monath T.P., Melnick J.L., Roizman B., and Straus S.E. Lippincott-Raven Publishers, Philadelphia, USA: 15-58.

Nakashima N., Sasaki J., and Tariyama S. (1999) Determining the nucleotide sequence and capsid-coding region of himetobi P virus: a member of a novel group of RNA viruses that infect insects. *Arch Virol*, 144: 2051-2058.

Natoni A., Kass G.E.N., Carter M.J., and Roberts L.O. (2006) The mitochondrial pathway of apoptosis is triggered during feline calicivirus infection. *J Gen Virol*, 87: 357-361.

Newlon M.G., Roy M., Hauskens Z.E., Scott J.D., and Jennings P.A. (1997) The A-kinase anchoring domain of type IIα cAMP-dependent protein kinase is highly helical. *J Biol Chem*, 272: 23637-23644.

Newman J.F., and Brown F. (1997) Foot-and mouth disease virus and poliovirus particles contain proteins of the replication complex. *J Virol*, 71: 7657-7662.

Neznanov N., Kondratova A., Chumakov K.M., Angres B., Zhumabayeva B., Agol V.I., and Gudkov A.V. (2001) Poliovirus protein 3A inhibits tumor necrosis factor (TNF)-induced apoptosis by eliminating the TNF receptor from the cell surface. *J Virol*, 75: 10409-10420.

Nie Z., Hirsch D.S., and Randazzo P.A. (2003) Arf and its many interactors. *Curr Opin Cell Biol*, 15: 396-404.

Nigg E.A., Schafer G., Hilz H., and Eppenberger H.M. (1985) Cycli-AMP-dependent protein kinase type II is associated with the Golgi complex and with centrosomes. *Cell*, 41: 1039-1051.

Nilson J., **Stahl S.**, **Lundeberg J.**, **Uhlen M.**, **and Nygren P.A.** (1997) Affinity fusion strategies for detection, purification, and immobilization of recombinant proteins. *Prot Exp Purif*, 11: 1-16.

Nunez J.I., Baranowski E., Molina N., Ruiz-Jarabo C.M., Sanchez C., Domingo E., and Sobrino F. (2001) A single amino acid substitution in nonstructural protein 3A can mediate adaptation of foot-and-mouth disease virus to the guinea pig. *J Virol*, 75: 3977-83.

Oberste M.S., Schnurr D., Maher K., Al-Busaidy S., and Pallansch M. (2001) Molecular identification of new picornaviruses and characterization of a proposed enterovirus 73 serotype. *J Gen Vir*, 82: 409-416.

Oertle T., and Schwab M.E. (2003) Nogo and its partners. *Trends Cell Biol*, 13: 187-194.

Oertle T., Klinger M., Stuermer G.A.O., and Schwab M.E. (2003a) A reticular rhapsody: phylogenetic evolution and nomenclature of the RTN/Nogo gene family. *FASEB J*, 17: 1238-1247.

Oertle T., Huber C., van der Putten H., and Schwab M.E. (2003b) Genomic structure and functional characterisation of the promotersof human and mouse nogo/rtn4. *J Mol Biol*, 325: 299-323.

Ohashi M., and Huttner W.B. (1994) An elevation of cytosolic protein phosphorylation modulates trimeric G-protein regulation of secretory vesicle formation from the trans-Golgi network. *J Biol Chem*, 269: 24897-24905.

Ohsawa K., Watanabe Y., Miyata H., Sato H. (2003) Genetic analysis of a Theiler-like virus isolated from rats. *Comp Med*, 53: 191-196.

Oleszak E.L., Chang J.R., Friedman H., Katsetos C.D., and Platsoucas C.D. (2004) Theiler's virus infection: a model for multiple sclerosis. *Clin Microbiol Rev*, 17: 174-207.

Pacheco J.M., Henry T.M., O'Donnell V.K., Gregory J.B., and Mason P.W. (2003) Role of nonstructural proteins 3A and 3B in host range and pathogenicity of foot-and-mouth disease virus. *J Virol*, 77: 13017-13027.

Padilla P.I., Pacheo-Rodriguez G., Moss J., and Vaughan M. (2003) Nuclear localization and molecular partners of BIG1, a brefeldin A-inhibited guanine nucleotide-exchange protein for ADP-rybosilation factors. *Proc Natl Acad Sci USA*, 101: 2752-2757.

Papa S., Sardanelli A.M., Scacco S., and Technikova-Dobrova Z. (1999) cAMP-dependent protein kinase and phosphoproteins in mammalian mitochondria. An extension of the cAMP-mediated intracellular signal transduction. *FEBS Lett*, 444: 245-249.

Parsley T.B., Towner J.S., Blyn L.B., Ehrenfeld E., and Semler B.L. (1997) Poly (rC) binding protein 2 forms a ternary complex with the 5'-terminal sequences of poliovirus RNA and the viral 3CD proteinase. *RNA*, 3: 1124-1134.

Paul A.V., Molla A., and Wimmer E. (1994) Studies of a putative amphipatic helix in the N-terminus of poliovirus protein 2C. *Virology*, 199: 188-199.

Paul S., and Michiels T. (2006) Cardiovirus leader proteins are functionally interchangeable and have evolved to adapt to virus replication fitness. *J Gen Virol*, 87: 1237-1246.

Pedersen K.W., van der Meer Y., Roos N., and Snijder E.J. (1999) Open reading frame 1a-encoded subunits of the arterivirus replicase induce endoplasmatic reticulum-derived double-membrane vesicles which carry the viral replication complex. *J Virol*, 73: 2016-2026.

Pelham H.R.B. (2001) Traffic through the Golgi apparatus. *J Cell Biol*, 155: 1099-1101.

Peränen J., and Kääriäinen L. (1991) Biogenesis of type I cytopathic vacuoles in Semliki Forest virus-infected BHK-cells. *J Virol*, 65: 1623-1627.

Peränen J., Laakkonen P., Hyvönen M., and Kääriäinen L. (1995) The alphavirus replicase protein nsP1 is membrane-associated and has affinity to endocytic organelles. *Virology*, 208: 610-620.

Pfister T., Pasamontes L., Troxler M., Egger D., and Bienz K. (1992) Immunochemical localization of capsid-related particles in subcellular fractions of poliovirus-infected cells. *Virology*, 188: 676-684.

Pfister T., and Wimmer E. (1999) Characterization of the nucleoside triphosphatase activity of poliovirus protein 2C reveals a mechanism by which guanidine inhibits poliovirus replication. *J Biol Chem*, 274: 6992-7001.

Pfister T., Jones K.W., and Wimmer E. (2000) A cysteine-rich motif in poliovirus protein $2C^{ATPase}$ is involved in RNA replication and binds zinc *in vitro*. *J Virol*, 74: 334-343.

Piccininni S., Varaklioti A., Nardelli M., Dave B., Raney K.D., and McCarthy J.E. (2002) Modulation of the hepatitis C virus RNA-dependent RNA polymerase activity by the non-structural (NS) 3 helicase and the NS4B membrane protein. *J Biol Chem*, 277: 45670-45679.

Pincus S.E., and Wimmer E. (1986) Production of guanidine-resistant and -dependent poliovirus mutants from cloned cDNA: mutations in polypeptide 2C are directly responsible for altered guanidine sensitivity. *J Virol*, 60: 793-796.

Ploubidou A., Moreau V., Ashman K., Reckmann I., González C., and Way M. (2000) Vaccinia virus infection disrupts microtubule organization and centrosome function. *EMBO J*, 19: 3932-3944.

Polatnick J., and Wool S.H. (1982) Localization of foot-and-mouth disease: RNA synthesis on newly formed cellular smooth membranous vacuoles. *Arch Virol*, 71: 207-215.

Porter F.W., Bochkov Y.A., Albee A.J., Wiese C., and Palmenberg A.C. (2006) A picornavirus protein interacts with Ran-GTPase and disrupts nucleocytoplasmic transport. *Proc Natl Acad Sci USA*, 103: 12417-12422.

Prinjha R., Moore S.E., Vinson M., Blake S., Morrow R., Christie G., Michalovich D., Simmons D.L., and Walsh F.S. (2000) Inhibitor of neurite outgrowth in humans. *Nature*, 403: 383-384.

Pritchard A.E., Strom T., and Lipton H.L. (1992) Nucleotide sequence identifies Vilyuisk virus as a divergent Theiler's virus. *Virology*, 191: 469-472.

Qu W., Graves L.M., and Thurman R.G. (1999) PGE(2) stimulates O(2) uptake in hepatic parenchymal cells: involvement of the cAMP-dependent protein kinase. *Am J Physiol*, 277: 1048-1054.

Racaniello V.R. (2001) Picornaviridae: The viruses and their replication. In *Fields Virology*, *Fourth edition* edited by Knipe D.M., Howley P.M., Griffin D.E., Lamb R.A.,

Martin M.A., Roizman B., Straus S.E. Lippincott Williams and Wilkins Publishers, Philadelphia, USA: 685-722.

Radtke K., Döhner K., and Sodeik B. (2006) Viral interactions with the cytoskeleton: a hitchhiker's guide to the cell. *Cell Microbiol*, 8: 387-400.

Rapacciuolo A., Suvarna S., Barki-Harrington L., Luttrell L.M., Cong M., Lefkowitz R.J., and Rockman H.A. (2003) Protein Kinase A and G protein-coupled receptor kinase phosphorylation mediates β-1 adrenergic receptor endocytosis through different pathways. *J Biol Chem*, 278: 35403-35411.

Reddi H.V., Kallio P., and Lipton H.L. (2003) Galactose is needed only for expression of co-receptors used by Theiler's murine encephalomyelitis virus as the virus does not directly bind galactose or use the UDP-galactose transporter as receptor. *J Gen Virol*, 84: 845-849.

Rey O., Canon J., and Krogstad P. (1996) HIV-1 Gag protein associates with F-actin present in microfilaments. *Virology*, 15: 530-534.

Richards O.C., and Ehrenfeld E. (1998) Effects of poliovirus 3AB protein on 3D polymerase-catalyzed reaction. *J Biol Chem*, 273: 12832-12840.

Rieder E., Paul A.V., Kim D.W., van Boom J.H., and Wimmer E. (2000) Genetic and biochemical studies of poliovirus *cis*-acting replication elemet cre in relation to VPg uridylylation. *J Virol*, 74: 10371-10380.

Rindler M.J., Ivanov I.E., and Sabatini D.D. (1987) Microtubule-acting drugs lead to the nonpolarized delivery of the influenza hemagglutinin to the cell surface of polarized Madin-Darby canine kidney cells. *J Cell Biol*, 104: 231-241.

Rios R.M., Celati C.S., Lomann M., Bornens M., and Keryer G. (1992) Identification of a high affinity binding protein for the regulatory subunit RII beta of cAMP-dependent protein kinase in Golgi enriched membranes of human lymphoblasts. *EMBO J*, 11: 1723-1731.

Rodriguez P.L., and Carrasco L. (1993) Poliovirus protein 2C has ATPase and GTPase activities. *J Biol Chem*, 268: 8105-8110.

Rodriguez P.L., and Carrasco L. (1995) Poliovirus protein 2C contains two regions involved in RNA binding activity. *J Biol Chem*, 270: 10105-10112.

Roebroek A.J., van de Velde H.J., Van Bokhoven A., Broers J.L., Ramaekers F.C., and Van de Ven W.J. (1993) Cloning and expression of alternative transcripts of a novel neuroendocrine-specific gene and identification of its 135-kDa translational product. *J Biol Chem*, 268: 13439-13447.

Rogers S.L., and Gelfand V.I. (1998) Myosin cooperates with microtubule motors during organelle transport in melanophores. *Curr Biol*, 8: 161-164.

Roizman B., and Palese P. (1996) Multiplication of viruses: an overview. In *Fields Virology*, *Third edition* edited by Fields B.N., Knipe D.M., Howley P.M., Chanock R.M.,

Monath T.P., Melnick J.L., Roizman B., and Straus S.E. Lippincott-Raven Publishers, Philadelphia, USA: 101-112.

Roos R.P. (2002) Pathogenesis of Theiler's murine encephalomyelitis virus-induced disease. In *Molecular Biology of Picornaviruses* edited by Semler B.L. and Wimmer E. ASM Press, Washington D.C., USA: 427-436.

Roper R.L., Wolffe E.J., Weisberg A., and Moss B. (1998) The envelope protein encoded in the A33R gene is required for formation of actin-containing microvilli and efficient cell-to-cell spread of vaccinia virus. *J Virol*, 72: 4192-4204.

Rossmann M.G. (2002) Picornavirus structure overview. In *Molecular Biology of Picornaviruses* edited by Semler B.L. and Wimmer E. ASM Press, Washington D.C., USA: 27-38.

Rueckert R.R. (1996) *Picornaviridae*: the viruses and their replication. In *Fields Virology*, *Third edition* edited by Fields B.N., Knipe D.M., Howley P.M., Chanock R.M., Monath T.P., Melnick J.L., Roizman B., and Straus S.E. Lippincott-Raven Publishers, Philadelphia, USA: 609-645.

Rust R.C., Landmann L., Gosert R., Tang B.L., Hong W., Hauri H.P., Egger D., and Bienz K. (2001) Cellular COPII proteins are involved in production of the vesicles that form the poliovirus replication complex. *J Virol*, 75: 9808-9818.

Ryan M.D., and Flint M. (1997) Virus-encoded proteinases of the picornavirus super-group. *J Gen Virol*, 78: 699-723.

Ryan M.D., Luke G., Hughes L.E., Cowton V.M., ten Dam E., Li X., Donnelly M.L.L., Mehrotra A., and Gani D. (2002) The aphtho- and cardiovirus "primary" 2A/2B polyprotein "cleavage". In *Molecular Biology of Picornaviruses* edited by Semler B.L. and Wimmer E. ASM Press, Washington D.C., USA: 212-223.

Salonen A., Ahola T., and Kääriäinen L. (2004) Viral RNA replication in association with cellular membranes. *Curr Top Microbiol Immunol*, 285: 139-173.

Sandoval I.V., and Carrasco L. (1997) Poliovirus infection and expression of the poliovirus protein 2B provoke the disassembly of the Golgi complex, the organelle target for the antipoliovirus drug Ro-090179. *J Virol*, 71: 4679-4693.

Sasaki J., Nakashima N., Saito H., and Noda H. (1998) An insect picorna-like virus, Plautia stali intestine virus, has genes of capsid proteins in the 3' part of the genome. *Virology*, 244: 50-58.

Sawicki S.G., Sawicki D.L., and Siddell S.G. (2007) A contemporary view of coronavirus transcription. *J Virol*, 81: 20-29.

Schlegel A., Giddings T.H., Ladinsky M.S., and Kirkegaard K. (1996) Cellular origin and ultrastructure of membranes induced during poliovirus infection. *J Virol*, 70: 6576-6588.

Shah A.M., and Lipton H.L. (2002) Low-neurovirulence Theiler's viruses use sialic acid moieties on N-linked oligosaccharide structures for attachment. *Virology*, 304: 443-450.

Skern T., Hampölz B., Guarné A., Fita I., Bergmann E., Petersen J., and James M.N.G. (2002) Structure and function of picornavirus proteinases. In *Molecular biology of picornaviruses* edited by Semler B.L. and Wimmer E. ASM Press, Washington D.C., USA: 199-212.

Smith D.B., and Johnson K.S. (1988) Single-step purification of polypeptides expressed in *Escherichia coli* as fusions with glutathione-S-transferase. *Gene*, 67:31-40.

Smith G.A., and Enquist L.W. (2002) Break ins and break outs: viral interactions with the cytoskeleton of mammalian cells. *Annu Rev Cell Dev Biol*, 18: 135-161.

Snijder E.J., and Meulenberg J.J.M. (1998) The molecular biology of arteriviruses. *J Gen Virol*, 79: 961-979.

Snijder E.J., van Tol H., Roos N., and Pedersen K.W. (2001) Non-structural proteins 2 and 3 interact to modify host cell membranes during the formation of the arterivirus replication complex. *J Gen Virol*, 82: 985-994.

Snijder E.J., van der Meer Y., Zevenhoven-Dobbe J., Onderwater J.J.M., van der Meulen J., Koerten H.K., and Mommaas A.M. (2006) Ultrastructure and origin of membrane vesicles associated with the severe acute respiratory syndrome coronavirus replication complex. *J Virol*, 80: 5927-5940.

Sosnovtsev S.V., Prikhod'ko E.A., Belliot G., Cohen J.I., and Green K.Y. (2003) Feline calicivirus replication induces apoptosis in cultured cells. *Virus Res*, 94: 1-10.

Springer S, and Schekman R. (1998) Nucleation of COPII vesicular coat complex by endoplasmic reticulum to Golgi vesicle SNAREs. *Science*, 281: 698-700.

Spyrou V., Maurice H., Billinis C., Papanastassopoulou M., Psalla D., Nielen M., Koenen F., and Papadopoulous O. (2004) Transmission and pathogenicity of encaphalomyocarditis virus (EMCV) among rats. *Vet Res*, 35: 113-122.

Stanway G., Hovi T., Knowles N.J., and Hyypiä T. (2002) Molecular and biological basis of picornavirus taxonomy. In *Molecular biology of picornaviruses* edited by Semler B.L. and Wimmer E. ASM Press, Washington D.C., USA: 17-24.

Steiner P., Kulangara K., Sarria J.C., Glauser L., Regazzi R., and Hirling H. (2004) Reticulon 1-C/neuroendocrine-specific protein-C interacts with SNARE proteins. *J Neurochem*, 89: 569-580.

Strauss J.H., and Strauss E.G. (1988) Evolution of RNA viruses. *Ann Rev Microbiol*, 42: 657-683.

Studdert M.J., and O'Shea J.D. (1975) Ultrastructural studies of the development of feline calicivirus in a feline embryo cell line. *Arch Virol*, 48: 317-325.

Suhy D.A., Giddings T.H., Jr., and Kirkegaard K. (2000) Remodeling the endoplasmatic reticulum by poliovirus infection and by individual viral proteins: an autophagy-like origin for virus-induced vesicles. *J Virol*, 74: 8953-8965.

Svitkin Y.V., Gradi A., Imataka H., Morino S., and Sonenberg N. (1999) Eukaryotic initiation factor 4GII (eIF4GII), but not eIF4GI, cleavage correlates with inhibition of host cell protein synthesis after human rhinovirus infection. *J Virol*, 73: 3467-3472.

Svitkin Y.V., Herdy B., Costa-Mattioli M., Gingras A.C., Raught B., and Sonenberg N. (2005) Eukaryotic translation initiation factor 4e availability controls the switch between cap-dependent and internal ribosomal entry site-mediated translation. *Mol Cellular Biol*, 25: 10556-10565.

Swaffield J.C., and Purugganan M.D. (1997) The evolution of the conserved ATPase domain (CAD): reconstructing the history of an ancient protein module. *J Mol Evol*, 45: 549-563.

Tagami S., Eguchi Y., Kinoshita M., Takeda M., and Tsujimoto Y. (2000) A novel protein, RTN-XS, interacts with both Bcl-XL and Bcl-2 on endoplasmic reticulum and reduces their anti-apoptotic activity. *Oncogene*, 19: 5736-5746.

Takeda N., Kuhn R.J., Yang C.F., Takegami T., and Wimmer E. (1986) Initiation of poliovirus plus-strand RNA synthesis in a membrane complex of infected HeLa cells. *J Virol*, 60: 43-53.

Takegami T., Semler B.L., Anderson C.W., and Wimmer E. (1983) Membrane fractions active in poliovirus RNA replication contain VPg precursor polypeptides. *Virology*, 128: 33-47.

Taketomi M., Kinoshita N., Kimura K., Kitada M., Noda T., Asou H., Nakamura T., and Ide C. (2002) Nogo-A expression in mature oligodendrocytes of rat spinal cord in association with specific molecules. *Neurosci Lett*, 332: 37-40.

Takuma T., and Ichida T. (1994a) Catalytic subunit of protein kinase A induces amylase release from streptolysin O-permeabilized parotid acini. *J Biol Chem*, 269: 22124-22128.

Takuma T., and Ichida T. (1994b) Evidence for the involvement of protein phosphorylation in cyclic AMP-mediated amylase exocytosis from parotid acinar cells. *FEBS Lett*, 340: 29-33.

Tang W.F., Yang S.Y., Wu B.W., Jheng J.R., Chen Y.L., Shih C.H., Lin K.H., Lai H.C., Tang P., and Horng J.T. (2007) Reticulon 3 binds the 2C protein of enterovirus 71 and is required for viral replication. *J Biol Chem*, 282: 5888-5898.

Tang Y., Winkler U., Freed E.O., Torrey T.A., Kim W., Li H., Goff S.P., and Morse H.C. 3rd (1999) Cellular motor protein KIF-4 associates with retroviral Gag. *J Virol*, 73: 10508-10513.

Teterina N.L., Kean K.M., Gorbalenya A.E., Agol V.I., and Girard M. (1992) Analysis of the functional significance of amino acid residues in the putative NTP-binding pattern of the poliovirus 2C protein. *J Gen Virol*, 73: 1977-1986.

Teterina N.L., Gorbalenya A.E., Egger D., and Ehrenfeld E. (1997) Poliovirus 2C protein determinants of membrane binding and rearrangements in mammalian cells. *J Virol*, 52: 777-783.

Thiel H.J., and Köning M. (1999) Caliciviruses: an overview. *Vet Microbiol*, 69: 55-62.

Thyberg J., and Moskalewski S. (1999) Role of microtubules in the organization of the Golgi complex. *Exp Cell Res*, 246: 263-279.

Tolskaya E.A., Romanova L.I., Kolesnikova M.S., Gmyl A.P., Gorbalenya A.E., and Agol V.I. (1994) Genetic studies on the poliovirus 2C protein, an NTPase: A plausible mechanism of guanidine effect on the 2C function and evidence for the importance of 2C oligomerization. *J Mol Biol*, 236: 1310-1323.

Toyoda H., Kohara M., Kataoka Y., Suganuma T., Omata T., Imura N., and Nomoto A. (1984) Complete nucleotide sequence of all three poliovirus serotype genomes. Implication for genetic relationship, gene function and antigenic determinants. *J Mol Biol*, 25: 561-585.

Uetz P., Rajagopala S.V., Dong Y., and Haas J. (2007) From ORFeomes to protein interaction maps in viruses. *Genome Res*, 14: 2029-2033.

Vance L.M., Moscufo N., Chow M., and Heinz B.A. (1997) Poliovirus 2C region functions during encapsidation of viral RNA. *J Virol*, 71: 8759-8765.

van de Velde H.J.K., Senden N.H.M., Roskals T.A.D., Broers J.L.V., Ramaekers F.C.S., Roebroek A.J.M., and Van de Ven W.J.M. (1994) NSP-encoded reticulons are neuroendocrine markers of a novel category in human lung cancer diagnosis. *Cancer Res*, 854: 4769-4776.

van der Meer Y., van Tol H., Locker J.K., Snijder E.J. (1998) ORF1a-encoded replicase subunits are involved in the membrane association of the arterivirus replication complex. *J Virol*, 72: 6689-6698.

van der Meer Y., Snijder E.J., Dobbe J.C., Schleich S., Denison M.R., Spaan W.J.M., and Locker J.K. (1999) Localization of mouse hepatitis virus nonstructural proteins and RNA synthesis indicates a role for late endosomes in viral replication. *J Virol*, 73: 7641-7657.

van Eyll O., and Michiels T. (2000) Influence of the Theiler's virus L*protein on macrophage infection, viral persistence, and neurovirulence. *J Virol*, 74: 9071-9077.

van Kuppeveld F.J.M., de Jong A.S., Melchers W.J.G., and Willems P.H.G.M. (2005) Enterovirus protein 2B po(u)res out the calcium: a viral strategy to survive? *Trends Mirobiol*, 13: 41-44.

van Pesch V., van Eyll O., and Michiels T. (2001) The leader protein of Theiler's virus inhibits immediate-early alpha/beta interferon production. *J Virol*, 75: 7811-7817.

van Pesch V., and Michiels T. (2003) Characterization of interferon-alpha 13, a novel constitutive murine interferon-alpha subtype. *J Biol Chem*, 278: 46321-46328.

Wakana Y., Koyama S., Nakajima K., Hatsuzawa K., Nagahama M., Tani K., Hauri H., Melançon P., and Tagaya M. (2005) Reticulon 3 is involved in membrane trafficking between the endoplasmic reticulum and Golgi. *Biochem Biophys Res Commun*, 334: 1198-1205.

Wall M.A., Coleman D.E., Lee E., Iniguez-Lluhi J.A., Posner B.A., Gilman A.G., and Sprang S.R. (1995) The structure of the G protein heterotrimer Giα1β1γ2. *Cell*, 83: 1047-1058.

Walker J.E., Saraste M., Runswick M.J., and Gay N.J. (1982) Distantly related sequences in the α- and β-subunits of ATPase, myosin, kinases and other ATP-requiring enzymes and a common nucleotide-binding fold. *EMBO J*, 1: 945-951.

Wang L., Sunahara R.K., Krumins A., Perkins G., Crochiere M.L., Mackey M., Bell S., Ellisman M.H., and Taylor S.S. (2001) Cloning and mitochondrial localization of full-length D-AKAP2, a protein kinase A anchoring protein. *Proc Natl Acad Sci USA*, 98: 3220-3225.

Waterhouse N.J., and Green D.R. (1999) Mitochondria and apoptosis: HQ or high-security prison? *J Clin Immunol*, 19: 378-387.

Weber S., Granzow H., Weiland F., and Marquardt O. (1996) Intracellular membrane proliferation in E. coli induced by foot-and-mouth disease virus 3A gene products. *Virus Genes*, 12: 5-14.

Weser S., Gerlach M., Kwak D.M.S., Czerwinska M., and Gödecke A. (2006) Detection of TAP-tagged proteins in Western blot, confocal laser scanning microscopy and FACS using the ZZ-domain. *J Biochem Biophys Methods*, 68: 189-194.

Wessels E., Duijsings D., Niu T., Neumann S., Oorschot V.M., de Lange F., Lanke K.H.W., Klumperman J., Henke A., Jackson C.L., Melchers W.J.G., and van Kuppeveld F.J.M. (2006a) A viral protein that blocks Arf1-mediated COPI assembly by inhibiting the guanine nucleotide exchange factor GBF1. *Dev Cell*, 11: 191-201.

Wessels E., Duijsings D., Lanke K.H.W., van Dooren S.H.J., Jackson C.L., Melchers W.J.G., and van Kuppeveld F.J.M. (2006b) Effects of picornavirus 3A proteins on protein transport and GBF1-dependent COP-I recruitment. *J Virol*, 80: 11852-11860.

Wessels E., Duijsings D., Lanke K.H.W., Melchers W.J.G., Jackson C.L., and van Kuppeveld F.J.M. (2007) Molecular determinants of the interaction between

coxsackievirus protein 3A and guanine-nucleotide exchange factor GBF1. *J Virol*, 81: 5238-5245.

Westaway E.G., Mackenzie J.M., Kenney M.T., Jones M.K., and Khromykh A.A. (1997) Ultrastructure of Kunjin virus-infected cells: colocalization of NS1 and NS3 with double-stranded RNA, and NS2B with NS3, in virus-induces membrane structures. *J Virol*, 71: 6650-6661.

Westaway E.G., Mackenzie J.M., and Khromykh A.A. (2002) Replication and gene function in Kunjin virus. *Curr Top Microbiol Immunol*, 267: 323-351.

Westaway E.G., Mackenzie J.M., and Khromykh A.A. (2003) Kunjin RNA replication and applications of Kunjin replicons. *Adv Virus Res*, 59: 99-140.

Willingmann P., Barnert H., Zeichhardt H., and Habermehl K.O. (1989) Recovery of structurally intact and infectious poliovirus type 1 from HeLa cells during receptor-mediated endocytosis. *Virology*, 168: 417-420.

Wolffe E.J., Katz E., Weisberg A., and Moss B. (1997) The A34R glycoprotein is required for induction of specialized actin-containing microvilli and efficient cell-to-cell transmission of vaccinia virus. *J Virol*, 71: 3904-3915.

Wölk B., Sansonno D., Krausslich H.G., Dammacco F., Rice C.M., Blum H.E., and Moradpour D. (2000) Subcellular localization, stability, and trans-cleavage competence of the hepatitis C virus NS3-NS4A complex expressed in tetracycline-regulated cell lines. *J Virol*, 74: 2293-2304.

Woodman P.G., Mundy D.I., Cohen P., and Warren G. (1992) Cell-free fusion of endocytic vesicles is regulated by phosphorylation. *J Cell Biol*, 116: 331-338.

Xiang Y., Seemann J., Bisel B., Punthambaker S., and Wang Y. (2007) Active ADP-ribosylation factor-1 (ARF1) is required for mitotic Golgi fragmentation. *J Biol Chem*, 282: 21829-21837.

Yamaga A.K., and Ou J. (2002) Membrane topology of the hepatitis C virus NS2 protein. *J Biol Chem*, 277: 33228-33234.

Yamasaki K., Weihl C.C., and Roos R.P. (1999) Alternative translation initiation of Theiler's murine encephalomyelitis virus. *J Virol*, 73: 8519-8526.

Yang Y., Rijnbrand R., McKnight K.L., Wimmer E., Paul A., Martin A., and Lemon S.M. (2002) Sequence requirements for viral RNA replication and VPg uridylylation directed by the internal *cis*-acting replication element (*cre*) of Human Rhinovirus type 14. *J Virol*, 76: 7485-7494.

Yip T.T., Nakagawa Y., and Porath J. (1989) Evaluation of the interaction of peptides with Cu(II), Ni(II), and Zn(II) by high-performance immobilized metal ion affinity chromatography. *Anal Biochem*, 183: 159-171.

Zeichhardt H., Wetz K., Willingmann P., and Habermehl K.O. (1985) Entry of poliovirus type 1 and mouse Elberfeld (ME) virus into Hep-2 cells: receptor mediated endocytosis and endosomal or lysosomal uncoating. *J Gen Virol*, 66: 483-492.

Zhou L., Luo Y., Wu Y., Tsao J., and Luo M. (2000) Sialylation of the host receptor may modulate entry of demyelinating persistent Theiler's virus. *J Virol*, 74: 1477-1485.

Zhu B., Cai G., Hall E.O., and Freeman G.J. (2007) In-Fusion™ assembly: seamless engineering of multidomain fusion proteins, modular vectors, and mutations. *BioTechniques*, 43: 354-359.